The background of the cover is a grayscale histological image, likely a hematoxylin and eosin (H&E) stained section of tissue. It shows a complex arrangement of glandular or ductal structures, some of which appear irregular and crowded, characteristic of neoplastic tissue. The overall texture is granular and detailed, with various shades of gray representing different cellular components and extracellular matrix.

Optical cancer screening and multiple primary tumors in the upper aerodigestive tract

Oisín Bugter

Optical cancer screening and multiple primary tumors in the upper aerodigestive tract

Oisín Bugter

Optical Cancer Screening and Multiple Primary Tumors in the Upper Aerodigestive Tract

Printing of this thesis was financially supported by the SBOH.

ISBN: 978-94-6419-235-3.

Printing by Gildeprint.

© Oisín Bugter 2021.

All rights reserved. No part of the material protected by this copyright notice may be reproduced or utilized in any form or by any other means, electronic or mechanical, including photocopying, recording or by any other information storage and retrieval system, without prior permission of the copyright owner.

Optical cancer screening and multiple primary tumors in the upper aerodigestive tract

Optische kankerscreening en multiple primaire tumoren in de bovenste tractus aerodigestivus

Thesis

to obtain the degree of Doctor from the
Erasmus University Rotterdam
by command of the
rector magnificus
Prof.dr. F.A. van der Duijn Schouten
and in accordance with the decision of the Doctorate Board.

The public defence shall be held on
July 2nd 2021 at 10.30 AM

by

Oisín Bugter

born in Amsterdam, the Netherlands.

Erasmus University Rotterdam



Doctoral Committee

Promotor: Prof. dr. R.J. Baatenburg de Jong

Other members: Prof. dr. S. Sleijfer
Prof. dr. C. Verhoef
Prof. dr. A.M. Rijs

Copromotors: Dr. D.J. Robinson
Dr. J.A.U. Hardillo

Table of contents

Chapter 1	General introduction	9
Chapter 2	Multiple primary tumors	
a	Survival of head and neck cancer patients with metachronous multiple primary tumors is surprisingly favorable	27
b	A cause-specific Cox model for second primary tumors in head and neck cancer patients: a RONCDOC study	43
Chapter 3	Electron microscopy and field cancerization	
	Early upper aerodigestive tract cancer detection using electron microscopy to reveal chromatin packing alterations in buccal mucosa cells	59
Chapter 4	Optical Screening study	
a	Optical pre-screening for laryngeal cancer using reflectance spectroscopy of the buccal mucosa	81
b	Optical detection of field cancerization in the buccal mucosa of patients with esophageal cancer	101
c	Optical detection of field cancerization in the buccal mucosa of patients with lung cancer	115
Chapter 5	Endoscopic screening: two systematic reviews	
a	Early detection of esophageal second primary tumors using Lugol chromoendoscopy in patients with head and neck cancer: a systematic review and meta-analysis	129
b	Screening for head and neck second primary tumors in patients with esophageal squamous cell cancer: a systematic review and meta-analysis	147

Chapter 6	LIGHT study	
	Detecting head and neck lymph node metastases with light reflectance spectroscopy: a pilot study	161
Chapter 7	General discussion	175
Chapter 8	Short version	
a	English summary	189
b	Nederlandse samenvatting	197
	Addendum	
	List of abbreviations and acronyms	207
	Affiliations of contributing authors	210
	PhD portfolio	212
	List of publications	214
	Dankwoord	216
	About the author	219

Chapter I

General introduction

Tumors of the upper aerodigestive tract

The head and neck (HN) region, esophagus and lungs are often referred to with the umbrella term upper aerodigestive tract (UADT). In the embryologic development of a human these organs all develop from a structure known as the early foregut.[1] The early foregut separates in the respiratory tract (larynx and lungs) and digestive tract (pharynx and esophagus) within the first two months of development.[2] There is no single universal definition of the UADT.[3] Most often it encompasses the mucosal head and neck region, the esophagus, and the trachea. For the purpose of this thesis, we also include the entire respiratory tract as is done by other researchers. Due to the shared origin, neoplastic diseases that develop in the UADT share many characteristics.

Head and neck cancer

Head and neck cancer has an increasing incidence worldwide.[4] In 2018, the European incidence of head and neck tumors (lip, oral cavity, larynx, nasopharynx, oropharynx, hypopharynx, and salivary glands) was more than 160.000, with more than 70.000 related deaths (Figure 1).[5] In the Netherlands, 3.163 new HN tumors were diagnosed in the same year and 919 patients died of the consequences. Most HN tumors are squamous cell carcinoma's.[6] The main risk factors for their development are tobacco use and alcohol consumption.[4, 6, 7] Head and neck squamous cell carcinomas (HNSCC) typically develop in the 6th decade of life and are predominant in males.[7] A recent increase in the incidence of oropharyngeal tumors has been linked to the oncogenic virus human papillomavirus (HPV).[4] Affected HPV positive HNSCC patients tend to be younger, non-smokers and with a history of multiple sexual partners.[7]

Patients with early-stage HNSCCs have a high chance of adequate and curative treatment. Unfortunately, the majority of patients are diagnosed with tumors in advanced stages of development. This is partly explained by the late onset of clinical symptoms (*i.e.*, hoarseness, sore throat, and pain) and sometimes also by patient delay. The most important factor that guides therapeutic decision making in newly diagnosed patients is accurate staging of the tumor.[7] Staging methods generally include examination by a head and neck surgeon, flexible pharyngo-laryngoscopy, and radiological assessment of the primary tumor (CT or MRI, or both) and neck (CT, MRI and/or ultrasound).[8] Chest imaging is also routinely performed to detect the presence of lung metastases or a second primary tumor (SPT).[7] Depending on the TNM stage and primary tumor site, patients are treated with various combinations of surgery, radiation therapy, and chemotherapy.[4] Patients with early-stage disease are generally treated with surgery or radiation therapy with curative intent.[7]

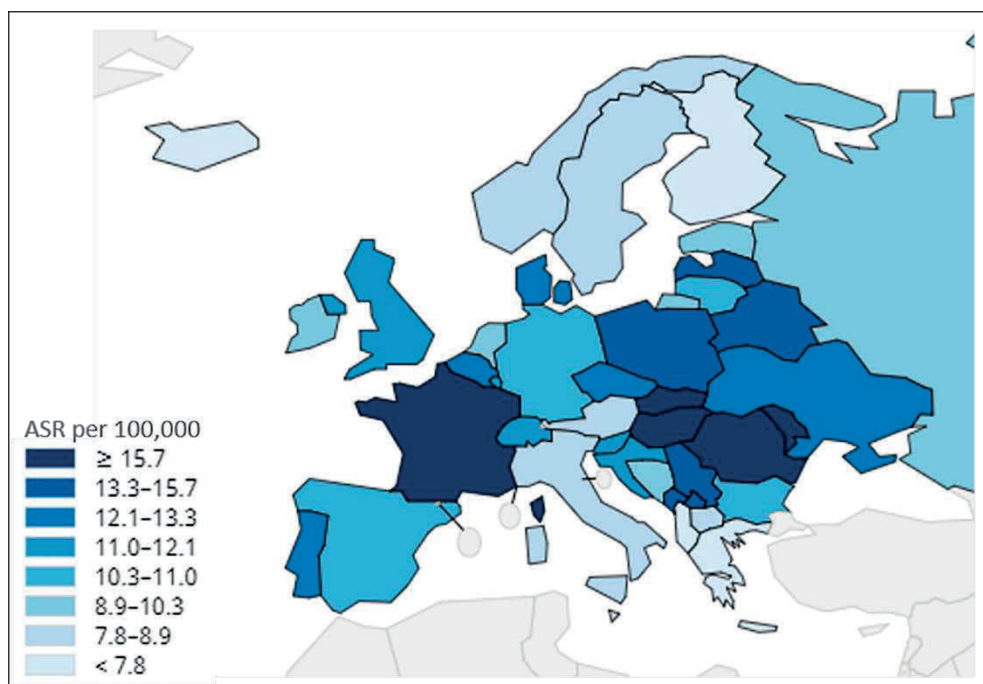


Figure I. Estimated age-standardized incidence rates (World) in 2018, head and neck cancer, both sexes, all ages. Figure derived from Global Cancer Observatory (GCO), <https://gcoiarcfr/>.

Elective neck dissection of the ipsilateral cervical lymph nodes (LN) in the clinically uninvolved neck remains a standard procedure in patients with a high risk for occult neck lymphadenopathy.[9] For locally advanced HNSCC (stage III or IV), surgery with radiotherapy and chemo-radiation therapy are the main means for treatment. A substantial survival advancement in the treatment of HNSCC has been the introduction of concurrent administration of chemotherapy and radiotherapy.[4, 7]

Due to advancements in diagnostics and treatment, the 5-year survival of HNSCC patients has improved from 55% in 1992-1996 to 66% in 2002-2006.[10] This still relatively low survival rate might be explained by patient delay prior to diagnosis, high tumor stages at diagnosis and a high incidence of tumor recurrence.[7, 11-14] In addition, patients with HNSCC are characterized by excess mortality after cure for their cancer.[15] Reasons may be other (smoking and alcohol related) comorbidities.[16] Another factor negatively affecting survival is the development of more than one primary tumor. Patients treated for HNSCCs have a high tendency to develop multiple primary tumors (MPT).[12] Multiple primary tumors are squamous cell tumors which develop synchronously or metachronously with the index tumor.[17, 18] It has to be noted that they are not the same as a residual/

recurrent tumors, which occur at the same site as the index tumor. The predominant location of occurrence of MPTs is the HN region. However, they also develop in associated organs such as the lungs and esophagus.[12, 19, 20]

Lung and esophageal cancer

Lung cancer remains the leading cause of cancer deaths.[21, 22] It shares its main risk factor, tobacco use, with HN cancer.[23] Approximately 85% of lung cancers are non-small cell lung cancer (NSCLC). Of all NSCLCs about 40% are adenocarcinomas, 25% squamous cell carcinomas and the remaining are other subtypes. Patients with early-stage lung tumors can benefit from complete surgical resection or curative radiotherapy, whereas treatment of patients with high-stage tumors is often non curative. However, an increasing percentage of them can benefit from molecular targeted therapies.[22] The 5-year survival rate of patients with early stage lung tumors is considerably higher (52%) than that of the total lung cancer population (15%).[24]

Esophageal tumors also show a similarity to head and neck and lung tumors. The vast majority of esophageal tumors are squamous cell carcinoma (ESCC) or adenocarcinoma (EAC). In developed counties, EAC is the predominant subtype of esophageal cancer.[25] Alcohol consumption and tobacco use are the main risk factors for the development of ESCC.[25] For EAC, white race, male sex, gastroesophageal reflux disease, and obesity are also known risk factors.[26] Unfortunately, about 60% of patients are diagnosed with an incurable locally advanced or metastatic EC.[27] This is in part the reason why the overall 5-year survival is around 15%-25%.[25] Early diagnosis and treatment of (pre)cancerous lesions could greatly improve the overall patient outcome.[28]

Upper aerodigestive tract cancer screening

Patients with early tumors have a significant better disease specific survival rate than patients with advanced tumors.[29] Unfortunately, diagnosis in advanced development stages is, as mentioned above, the case with the majority of tumors in the UADT. This highlights the need of a reliable detection method to facilitate early tumor detection.[30] UADT tumors appear well suited to population screening because of (a) the association of identifiable risk factors, (b) the ability to diagnose early tumors with a clinical examination, (c) the survival advantage of early diagnosis, and (d) the significant morbidity and mortality associated with the disease.[31]

Head and neck cancer

Most efforts made to screen for HN tumors have focused on manual and visual examination or flexible pharyngo-laryngoscopy at an outpatients clinic.[31] They also have an emphasis

on ‘easy reachable’ tumors in the oral cavity and on LN metastases.[32-35] Although some of these studies show promising results, their approaches are often time consuming and have a low sensitivity for early-stage tumors and for tumors beyond the oral cavity (*i.e.*, the pharynx and larynx). Also, the large population of persons at risk for head and neck cancer makes it challenging to develop a cost-effective program. To date there is a dearth of reliable and practical screening methods for HNSCC.

Lung and esophageal cancer

Considerably more studies have been performed to study lung cancer screening. Very recently, the long awaited results of the NELSON trial were published.[36] This randomized controlled trial investigated whether low-dose CT screening could reduce lung cancer mortality among former and current smokers. It showed that volume CT lung-cancer screening, with low rates of follow-up procedures for test results suggestive of lung cancer, resulted in substantially lower lung-cancer mortality than no screening among high-risk persons.

In developed countries most esophageal cancer screening is focused on the development of EAC in patients with Barrett’s esophagus.[25] However, screening other persons at risk (*e.g.*, patients with previous HN cancer) for *both* EAC and ESCC might also prove to be beneficial.[25] Endoscopy, the gold standard for diagnosing (pre-)cancerous esophageal lesions, has undergone major improvements over the last decades.[37] Image-enhanced endoscopy, which includes dye-based techniques, has been proposed as a more accurate screening tool than conventional white-light endoscopy.[37-39] Lugol’s stain is the most promising. When used during flexible esophageal endoscopy it has a high diagnostic accuracy to detect early stage esophageal lesions.[40] Asian screening studies have found percentages of up to 20% dysplastic lesions and invasive carcinoma’s in asymptomatic persons.[41] It is not known yet whether these results can be applied to a Western population. Our study in Chapter 5a will address this question.

Field cancerization

A new line in cancer screening research is focused on field cancerization (FC). Field cancerization is also referred to as “field effect” or “field carcinogenesis”. Field cancerization is described as an altered field in which the epithelium has multiple independent foci of abnormal tissue that can subsequently give rise to (pre-)malignant lesions.[42] These foci are seen as collection of cells that have gained some but not all the phenotypic alterations required for a malignancy.[43] It could thus be seen as a development stage before the histological detectable dysplasia. There are several theories that explain the occurrence of FC and consequently the possible development of a malignancy.[42, 44] One is the

polyclonal theory, which states that multiple squamous cell lesions occur independently of each other. This is due to exposure to carcinogens which leads to multiple genetic abnormalities in the entire tissue field. The other theory states that multiple lesions arise from a monoclonal origin due to the migration of altered or even dysplastic cells by a) migration of malignant cells through the saliva or by b) intra-epithelial migration of the initially transformed cells. These FC theories may also give a better understanding to the occurrence of MPTs.

There is evidence that FC occurs throughout the body in different tissue types and organs (e.g., colon, stomach, esophagus, mammae, lung, and skin) including the upper aerodigestive tract, which includes the oral cavity.[43] The oral cavity is a predominant and prevalent sites of development of (pre-) malignancies, since it comes into direct contact with many carcinogens.[44] The current challenge lies in a reliable and useful method to detect FC in the oral cavity. A number of biomarkers have been suggested to occur early in pre-dysplastic (i.e., FC) mucosa. They include altered epithelial cell proliferation, cell apoptosis, gene expression, and rate of methylation.[42, 45] Since these alterations occur a sub diffractive lengths scale of less than 200 nm, they are not visible with confocal microscopy. Optical techniques could potentially be the solution to this issue.

This premise is based on the fact that the spatial variation of the concentration of intracellular solids (e.g., proteins, DNA, RNA, lipids) gives rise to spatial fluctuations in the refractive index of the tissue.[46] Due to the optical diffraction limit, it requires nanoscale-sensitive optical spectroscopy, or microscopy techniques that utilize different illumination sources with a wavelength smaller than light, such as neutrons and electrons.[47, 48]

Biomedical optics

Biomedical optics is a study of the interaction between light and (human) tissue. Light possesses energy and is capable of interacting with biological cells, tissues, and organs. Such interactions can be used to probe the state of such tissues for analytical purposes. The science of light generation, manipulation, transmission, and measurement is known as photonics. The application of photonic technologies and principles to medicine and life sciences is known as biophotonics (Figure 2).[49] Many biophotonics applications make use of optical fibers to transport and collect the light to and from the desired measurement location. Optical fibers are thin, flexible, dielectric (non-conductive), and in most cases non-invasive (Figure 3). These properties also allow them to be introduced into the body for endoscopic measurements. The majority of applications for medical purposes use the distribution of light within tissue. This distribution is determined by the optical properties of the tissue: absorption and scattering.[50]

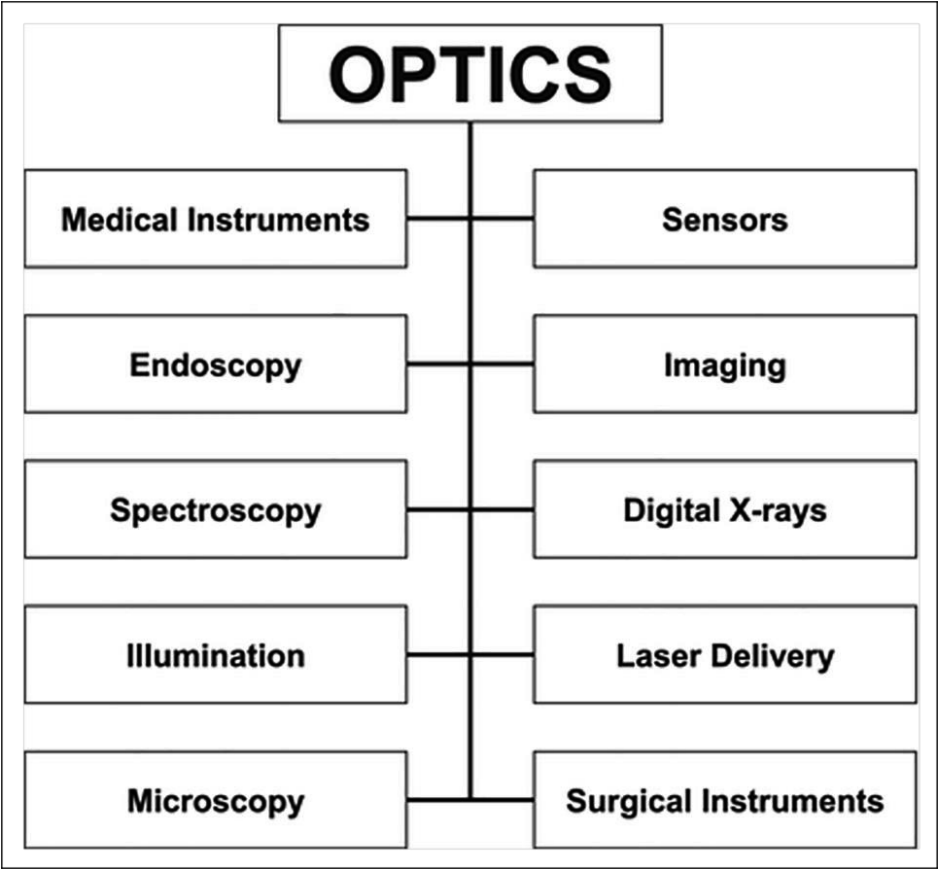


Figure 2. Applications of optics in medicine. Figure derived from Méndez, Optics in Medicine. In: Al-Amri M., El-Gomati M., Zubairy M. (eds) Optics in Our Time. Springer. 2016.

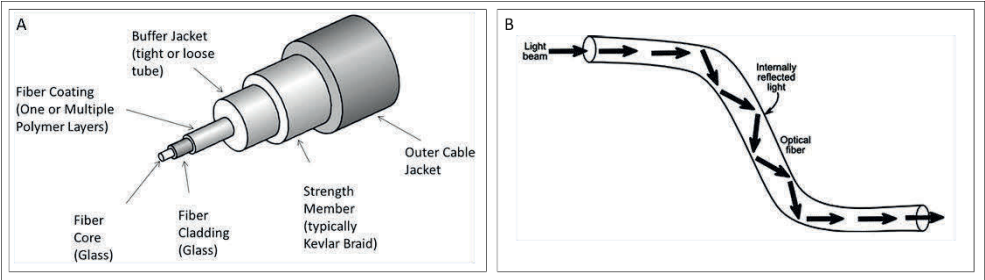


Figure 3. A) Schematic of an optical fiber. B) An optical fiber is able to guide light through the principle of total internal reflection. This allows the transmission of light shape taken by the optical fiber. Figure derived from Méndez, Optics in Medicine. In: Al-Amri M., El-Gomati M., Zubairy M. (eds) Optics in Our Time. Springer. 2016.

Absorption

Absorption of light (photons) happens in chromophores which are present in tissue (or exogenous administered). The predominant chromophores in humans in the visible light wavelength region are oxy- and deoxyhemoglobin. Absorption spectroscopy is the measurement of absorption of light in tissue as a function of the wavelength. The absorption spectrum is the variation of the intensity of light absorption. It is primarily determined by the molecular composition of the measured tissue.

Scattering

Molecules which are exposed to light are not only able to absorb photons, but they can also scatter in different directions. This physical process is called scattering. In human tissue scattering centers are grouped together and photons may scatter multiple times. This is known as multiple scattering. Multiple scattering can be modeled as a more deterministic process because the combined results of a large number of scattering events tend to average out. This is exemplified by a light beam passing through thick fog. Due to the highly scattering nature of tissue a proportion of photons will be back-scattered from the surface of the illuminated tissue. The back-scattered, or reflected, photons have travelled a distance through the tissue and contain spectral information on the various structures it consists of. The distribution of scattered light provides valuable information about the (nano)structure of tissue.

Reflectance spectroscopy

Reflectance spectroscopy enables the measurement of both concentration of tissue chromophores and ultrastructural information related to scattering of the tissue.[51] Optical spectra acquired from tissue contain the combined effects of all tissue optical properties, and are also dependent on illumination and detection geometry. Tissue optical properties are characterized by the absorption coefficient (μ_a) and the scattering coefficient (μ_s), which are the inverse of the mean free paths between absorption and scattering events, respectively, and the scattering phase function (PF), which describes the angular distribution of scattering events.

The tissue absorption coefficient μ_a [mm^{-1}] can be accurately quantified from a measurement without prior knowledge of the tissue scattering properties.[52] μ_a can then be further decomposed into the constituent absorption spectra of known tissue chromophores. This enables accurate measurement of the concentration of chromophores and of physiological parameters such as microvascular blood oxygen saturation, blood volume fraction and mean vessel diameter. These parameters have the potential to be used to differentiate between tissues with and without FC.[53]

Scattering in tissue results from variations in refractive index between the various cell and tissue components and their surroundings. At large source-detector separations, light transport can be considered diffuse and is therefore only dependent on the absorption coefficient (μ_a) and the reduced scattering coefficient (μ_s'), given by $\mu_s' = \mu_s(1-g_1)$, where $g_1 = \cos(\theta)$ is the first moment of the scattering phase function (PF), also called the scattering anisotropy. At large source-detector distances, light transport is insensitive to the exact shape of the PF.[54] This is not the case for small source-detector distances such as in SFR spectroscopy. They contain contributions from non-diffuse photons, making the collected intensity dependent on both μ_s and the exact form of the PF.

Single-fiber reflectance spectroscopy

Single fiber reflectance spectroscopy (SFR) has previously been developed by our group. In SFR spectroscopy one fiber serves as both source and detector. One advantage of this geometry is that SFR is sensitive to superficial tissues and their microvasculature, which are susceptible to early changes in morphology such as FC. SFR spectroscopy allows us to determine tissue absorption without prior knowledge of the scattering coefficient.

SF reflectance spectra are analyzed using a mathematical model that describes the wavelength-dependent effects of absorption and scattering on the reflectance intensity collected from tissue. The model is given as follows

$$R_{SF} = \left[\alpha_1 \left(\frac{\lambda}{\lambda_0} \right)^{\alpha_2} \right] e^{-\mu_a^{tissue} \langle LSF \rangle} \quad (1)$$

Here, the term in square brackets is a background scattering model that follows Mie theory dependence, with fitted parameters describing the Mie amplitude (α_1) and Mie slope (α_2). Attenuation due to absorption within the tissue is modeled using the modified Beer-Lambert law and is a function of both the tissue absorption coefficient μ_a^{tissue} and the SF photon path length (LSF).

We showed that the photon path length is dependent on μ_a , the reduced scattering coefficient μ_s' , and the fiber diameter d_{fiber} , and is given as a model structure that requires specification of μ_s' at one wavelength. Because it is not possible to accurately measure μ_s' with just one SFR measurement, we have to assume that μ_s' at 800nm = 1mm⁻¹, and the background scattering model estimates the wavelength-dependent change in μ_s' .

The error introduced to parameter estimates due to this assumption was quantified by varying the assumed μ_s' (800nm) across a wide range that is representative of biological tissue, with resulting changes to the estimates of ρ , StO₂, d_v , and Mie slope of 20%,

respectively. While these results indicate the error is small, it is desirable to not require the assumption within the model.

Failure to account for PF effects for small source-detector separations will introduce errors into optical property estimates as described. The Legendre moments of the PF can be utilized to characterize the effect of large angle scattering events on the collected reflectance signal. This is done by introducing a parameter $\gamma = 1 - g_2 / 1 - g_1$ that includes information about the first two moments of the PF, given as g_1 and g_2 , respectively. These first two moments correspond to the mean and the variance of the distribution of the angular scattering events specified by the PF.

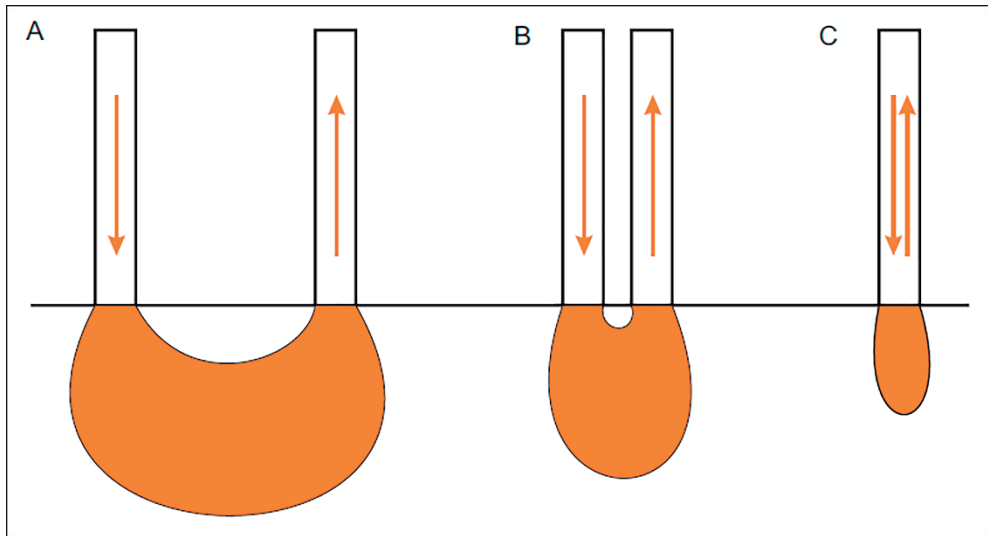


Figure 4. Probe designs. A) large source-detector separation, B) small source-detector separation, C) single fiber probe. From U.A. Gamm, Quantification of Tissue Scattering Properties by Use of Fiber Optic Spectroscopy, Introduction. 2013

Multidiameter single-fiber reflectance spectroscopy

For this purpose, SFR is further extended to encompass multidiameter single-fiber reflectance (MDSFR) spectroscopy in order to extract the exact scattering properties of tissue. In MDSFR spectroscopy two or more fiber diameters are used on the same tissue location to determine μ_s' and γ .

Our group has developed semi-empirical models for the collected SFR in the absence of absorption, R_{SF}^0 [%], and the effective photon path length for SFR, $\langle L_{SFR} \rangle$ [mm], based on experimentally validated Monte Carlo simulations.[51] The tissue absorption coefficient can be determined from a single SFR measurement using a modified Beer–Lambert law

relationship (Eq. 1) with the model for effective SFR path length and using the model for R_{SF}^0 ,

$$R_{SF}^0 = \eta_{lim} \left(1 + p_6 e^{-p_4 \mu_s' d_f} \right) \left[\frac{\mu_s' d_f^{p_5}}{p_4 + (\mu_s' d_f)^{p_5}} \right], \quad (2)$$

with a background scattering model.

In this equation R_{SF}^0 is the reflectance in the absence of absorption. R_{SF}^0 is measured during spectroscopy as the number of reflected photons as a function of the wavelength combined with prior knowledge of the absorption spectra of the known chromophores. η_{lim} is the collection efficiency at the diffusion limit. This is given as 2.7% for a fiber numerical aperture of 0.22 in a medium of refractive index 1.38. As this is a property of the optical fiber it is a known value. d_f is the diameter of the fiber. It is also a known value which can be altered by changing the fibers. p_4 , p_5 , and p_6 are fitted parameters. The fitted parameters have been previously determined by computer simulations of the SFR covering a wide range of the parameters d_f , μ_s' , μ_a , g , and γ . p_4 , p_5 , and p_6 are specifically sensitive to the phase function parameter, γ , where p_4 , p_5 , and $p_6 = 2.3 \text{ l}\gamma^2$, 0.57γ , and $0.63 \text{ l}\gamma^2$ respectively. Gamma and μ_s' are unknown parameters.

Equations that have more than one unknown (in this case two) can be solved using simultaneous equations. These can be created by performing reflectance measurements with two (or more) fiber diameters. In this way we can perform absolute quantification of μ_s' and γ over the measured wavelength range.

The MDSFR spectroscopy device and the spectral analysis are thoroughly described in Chapter 4 and 6. MDSFR spectroscopy uses a bundle of 19 fibers for both light delivery and collection. Each fiber in the bundle is trifurcated at the proximal end to enable light *delivery* from a halogen lamp, light *delivery* from two LEDs, and light *collection* to the spectrometer. The fibers are bundled into three concentric groups of one, six and twelve fibers. They are polished at an angle of 15 degrees at the fiber tip to avoid collection of specular reflection. Three computer-controlled shutters and a series of fiber-optic interconnects enable illumination and spectroscopic detection of independent fiber groups. This allows single fiber reflectance (SFR) measurement with a diameter of 200, 600 and 1000 μm without moving the probe. In this device we choose to use 3 fiber diameters. Less fiber diameters would make the model less stable and more fiber diameters would not be very advantageous to the model, but would be less cost effective. The maximal sampling depth of MDSFR spectroscopy is approximately 500 μm . For the analysis of the spectra, the tissue absorption properties are first were calculated using the individual SFR spectra of the 200, 600, and

1000 μm fibers. Next, the tissue scattering properties μ_s' (mm^{-1}) and γ (-) are determined by combining the absorption-corrected spectra of multiple fiber diameters. Finally, four physiological parameters were extracted from the 1000 μm SFR fit.

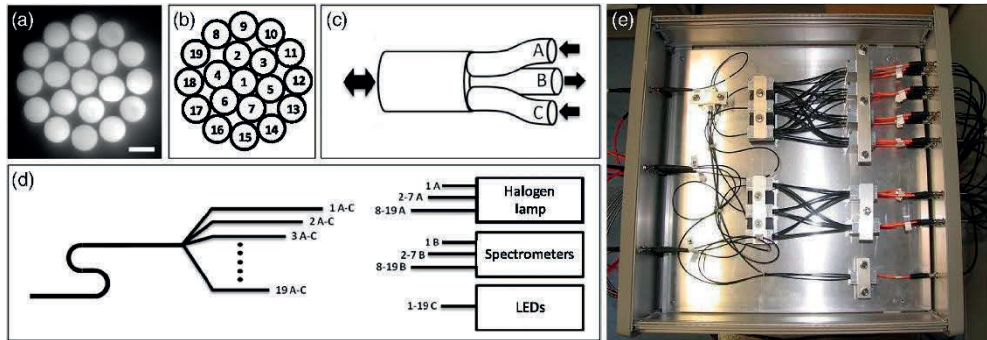


Figure 5. A schematic representation of the MDSFR device with numbering of the fiber cores, trifurcation at the proximal end of each fiber in the bundle, and the fiber tree. (e) A photograph of the fiber tree. Figure derived from Hoy et al., Method for rapid..., J Biomed Opt, 2013.

Electron microscopy

Although optical techniques are very promising, they have some limitations.[55] First, they do not allow direct nanoscale visualization of the structures they are sensitive to FC. Second, conventional optical property measurements do not isolate optical properties to small structures (e.g., organelles) within intact tissue, because the optical properties are usually averaged over a relatively large measurement volume. Lastly, many optical property extraction methods are based on approximated scattering phase function models, which make the measured optical properties vulnerable to the accuracy of the chosen model. Overcoming these limitations becomes crucial when trying to improve techniques using optical properties as diagnostic markers.

The development of nanoscale imaging techniques such as electron microscopy (EM) provides a way to overcome this challenge.[55] Electron microscopy (EM) is a technique to assess and also visualize the nano-anatomy of tissue, in our case buccal mucosa. The basic principle of EM to produce a magnified image of a thinly sliced prepared sample is similar to conventional light microscope. However, with EM the light source is replaced by a beam of fast-moving electrons that pass through the tissue sample which has been placed in a vacuum chamber. The lenses are replaced by a series of coil-shaped electromagnets through which the electron beam travels. The image is then magnified by the coils and focused onto an imaging device. In a way the electrons in EM act as particles of light, photons. However,

electrons they have a wavelength that is several hundred times smaller than photons, which allows EM to produce images with a much higher degree of detail.[56]

Electron microscopy image analysis allows quantification of the organization of cellular structures that are responsible for light scattering. A promising target to analyze is the quantification of chromatin organization in the cell nucleus. Little is yet known about chromatin organization in the earliest stage of cancer progression.[57] In Chapter 3 we aimed to analyze the chromatin organization of cells within in field of tumors and of cells outside this field. In Chapter 4 we performed spectroscopic measurements on the same tissue types. A logic hypothesis is that a change in nuclear organization would also change the intensity of light scattering.

Scope of this thesis

The goal of this thesis was to study the feasibility of a novice optical device to screen for HN, lung, and esophageal cancer. We also studied HNSCC patients with multiple primary tumors and investigated whether screening for MPTs in a high-risk population is warranted. In *Chapter 2*, we analyzed the incidence and survival rate of head and neck cancer patient that developed multiple primary tumors (MPT). We looked at MPTs occurring in the head and neck region, lungs, and esophagus and tried to identify risk factors for their development. In *Chapter 3*, we literally took a closer look at FC. Electron microscopy images were analyzed to detect nano-structural changes that could indicate the presence of FC. In *Chapter 4* we investigated a potential new optical method, MDSFR spectroscopy, to detect FC in the buccal mucosa of cancer patients. It could represent a first step towards the development of a non-invasive pre-screening method. We studied this method in patients with head and neck, lung, and esophageal cancer. In *Chapter 5*, we took the results from previous chapters and studied the literature to check whether there was sufficient evidence to screen head and neck cancer patients for unknown second primary tumors in the esophagus using modern endoscopic techniques. This study was also repeated vice versa: screening esophageal cancer patients for second primary head and neck tumors. In *Chapter 6* we investigated if SFR spectroscopy could be used to detect lymph node metastases *in vivo*. In the final *Chapter 7* the most important result and conclusions of the presented research are discussed including the future perspective of FC detection in the broader scope of cancer screening.

References

1. Metzger R, et al. - Embryology of the early foregut. - *Semin Pediatr Surg* 2011.
2. Kluth D, et al. - The embryology of the foregut. - *Semin Pediatr Surg* 2003.
3. National Collaborating Centre for C - - 2016.
4. Marur S, et al. - Head and Neck Squamous Cell Carcinoma: Update on Epidemiology, Diagnosis, and Treatment. - *Mayo Clin Proc* 2016.
5. Global Cancer Observatory (GCO). <https://gco.iarc.fr/>.
6. Mifsud M, et al. - Evolving trends in head and neck cancer epidemiology: Ontario, Canada 1993-2010. - *Head Neck* 2017.
7. Argiris A, et al. - Head and neck cancer. - *Lancet* 2008.
8. Baatenburg de Jong RJ, et al. - Assessment of cervical metastatic disease. - *ORL J Otorhinolaryngol Relat Spec* 1993.
9. de Bree R, et al. - Advances in diagnostic modalities to detect occult lymph node metastases in head and neck squamous cell carcinoma. - *Head Neck* 2015.
10. Pulte D, et al. - Changes in survival in head and neck cancers in the late 20th and early 21st century: a period analysis. - *Oncologist* 2010.
11. McGurk M, et al. - Delay in diagnosis and its effect on outcome in head and neck cancer. - *Br J Oral Maxillofac Surg* 2005.
12. Priante AV, et al. - Second primary tumors in patients with head and neck cancer. - *Curr Oncol Rep* 2011.
13. Leon X, et al. - Can cure be achieved in patients with head and neck carcinomas? The problem of second neoplasm. - *Expert Rev Anticancer Ther* 2001.
14. Seiwert TY, et al. - State-of-the-art management of locally advanced head and neck cancer. - *Br J Cancer* 2005.
15. van der Schroeff MP, et al. - Prognosis: a variable parameter: dynamic prognostic modeling in head and neck squamous cell carcinoma. - *Head Neck* 2012.
16. Datema FR, et al. - Impact of comorbidity on short-term mortality and overall survival of head and neck cancer patients. - *Head Neck* 2010.
17. Warren S, et al. - Multiple primary malignant tumors: A survey of the literature and a statistical study. - *American Journal of Cancer* 1932.
18. Hong WK, et al. - Prevention of second primary tumors with isotretinoin in squamous-cell carcinoma of the head and neck. - *N Engl J Med* 1990.
19. de Vries N, et al. - Dubbel-tumoren bij patiënten met een plaveiselcelcarcinoom van het slijmvlies in het hoofd-halsgebied. Double tumors in patients with a mucosal squamous cell carcinoma in the head and neck region. - *Ned Tijdschr geneesk* 1985.
20. De Felice F, et al. - Follow-Up in Head and Neck Cancer: A Management Dilemma. - *Advances in Otolaryngology* 2015.
21. Duma N, et al. - Non-Small Cell Lung Cancer: Epidemiology, Screening, Diagnosis, and Treatment. - *Mayo Clin Proc* 2019.
22. Hirsch FR, et al. - Lung cancer: current therapies and new targeted treatments. - *Lancet* 2017.
23. Malhotra J, et al. - Risk factors for lung cancer worldwide. - *Eur Respir J* 2016.
24. Siegel RL, et al. - Cancer statistics, 2015. - *CA Cancer J Clin* 2015.
25. Domper Arnal MJ, et al. - Esophageal cancer: Risk factors, screening and endoscopic treatment in Western and Eastern countries. - *World J Gastroenterol* 2015.
26. Huang FL, et al. - Esophageal cancer: Risk factors, genetic association, and treatment. - *Asian J Surg* 2018.
27. Kollarova H, et al. - Epidemiology of esophageal cancer--an overview article. - *Biomed Pap Med Fac Univ Palacky Olomouc Czech Repub* 2007.
28. Pennathur A, et al. - Esophageal carcinoma. - *Lancet* 2013.
29. Hall SF, et al. - Using TNM staging to predict survival in patients with squamous cell carcinoma of head & neck. - *Head Neck* 1999.
30. Whang SN, et al. - Recent Progress in Therapeutic Treatments and Screening Strategies for the Prevention and Treatment of HPV-Associated Head and Neck Cancer. - *Viruses* 2015.
31. Gogarty DS, et al. - Conceiving a national head and neck cancer screening programme. - *J Laryngol Otol* 2016.
32. Hapner ER, et al. - Results of a large-scale head and neck cancer screening of an at-risk population. - *J Voice* 2011.
33. Nunn H, et al. - Oral cancer screening in the Bangladeshi community of Tower Hamlets: a social model. - *Br J Cancer* 2009.

34. O'Sullivan EM - Prevalence of oral mucosal abnormalities in addiction treatment centre residents in Southern Ireland. - *Oral Oncol* 2011.
35. Sankaranarayanan R, et al. - Effect of screening on oral cancer mortality in Kerala, India: a cluster-randomised controlled trial. - *Lancet* 2005.
36. de Koning HJ, et al. - Reduced Lung-Cancer Mortality with Volume CT Screening in a Randomized Trial. - *N Engl J Med* 2020.
37. Chung CS, et al. - Image-enhanced endoscopy for detection of second primary neoplasm in patients with esophageal and head and neck cancer: A systematic review and meta-analysis. - *Head Neck* 2016.
38. Kaltenbach T, et al. - American Gastroenterological Association (AGA) Institute technology assessment on image-enhanced endoscopy. - *Gastroenterology* 2008.
39. Blanchard D, et al. - Guidelines update: Post-treatment follow-up of adult head and neck squamous cell carcinoma: Screening for metastasis and metachronous esophageal and bronchial locations. - *Eur Ann Otorhinolaryngol Head Neck Dis* 2015.
40. Makuuchi H, et al. - Endoscopic screening for esophageal cancer in 788 patients with head and neck cancers. - *Tokai J Exp Clin Med* 1996.
41. Lao-Sirieix P, et al. - Screening for oesophageal cancer. - *Nat Rev Clin Oncol* 2012.
42. Angadi PV, et al. - Oral field cancerization: current evidence and future perspectives. - *Oral Maxillofac Surg* 2012.
43. Curtius K, et al. - An evolutionary perspective on field cancerization. - *Nat Rev Cancer* 2018.
44. Mohan M, et al. - Oral field cancerization: an update on current concepts. - *Oncol Rev* 2014.
45. Damania D, et al. - Nanocytology of rectal colonocytes to assess risk of colon cancer based on field cancerization. - *Cancer Res* 2012.
46. Subramanian H, et al. - Optical methodology for detecting histologically unapparent nanoscale consequences of genetic alterations in biological cells. - *Proc Natl Acad Sci U S A* 2008.
47. Gerchman S, et al. - Chromatin higher-order structure studied by neutron scattering and scanning transmission electron microscopy. - 1987.
48. Le Gros MA, et al. - Soft X-ray tomography reveals gradual chromatin compaction and reorganization during neurogenesis in vivo. - 2016.
49. Méndez A - Optics in Medicine. In: Al-Amri M., El-Gomati M., Zubairy M. (eds) *Optics in Our Time*. - Springer 2016.
50. Krafft C - Modern trends in biophotonics for clinical diagnosis and therapy to solve unmet clinical needs. - *J Biophotonics* 2016.
51. Hoy CL, et al. - Method for rapid multidiameter single-fiber reflectance and fluorescence spectroscopy through a fiber bundle. - *J Biomed Opt* 2013.
52. Kanick SC, et al. - Method to quantitate absorption coefficients from single fiber reflectance spectra without knowledge of the scattering properties. - *Opt Lett* 2011.
53. Kanick SC, et al. - Characterization of mediastinal lymph node physiology in vivo by optical spectroscopy during endoscopic ultrasound-guided fine needle aspiration. - *J Thorac Oncol* 2010.
54. van Leeuwen-van Zaane F, et al. - In vivo quantification of the scattering properties of tissue using multi-diameter single fiber reflectance spectroscopy. - *Biomed Opt Express* 2013.
55. Wu W, et al. - Using electron microscopy to calculate optical properties of biological samples. - *Biomed Opt Express* 2016.
56. Gordon RE - Electron microscopy: a brief history and review of current clinical application. - *Methods Mol Biol* 2014.
57. Rizvi MA, et al. - Nuclear blebbing of biologically active organoselenium compound towards human cervical cancer cell (HeLa): In vitro DNA/HSA binding, cleavage and cell imaging studies. - 2015.

Chapter 2a

Multiple primary tumors: incidence and survival rates

Survival of head and neck cancer patients with metachronous multiple primary tumors is surprisingly favorable

Oisín Bugter; Rens van Iwaarden; Emilie Dronkers; Martine de Herdt; Marjan Wieringa; Gerda Verduijn; Marc Mureau; Ivo ten Hove; Esther van Meerten; José Hardillo; Robert Baatenburg de Jong

Head & Neck, Apr 2019, PMID: 30593712

Abstract

Background. The objectives of this study are to determine the incidence and survival rate of patients with head and neck squamous cell carcinoma (HNSCC) with multiple primary tumors (MPT) in the HN-region, lung, or esophagus.

Methods. Patient and tumor specific data of 1372 patients with HNSCC were collected from both the national cancer registry and patient records to ensure high-quality double-checked data.

Results. The total incidence of MPTs in the HN-region, lung, and esophagus in patients with HNSCC was 11% (149/1372). Patients with lung MPTs and esophageal MPTs had a significant worse 5-year survival than patients with HN-MPTs (29%, 14%, and 67%, respectively, $P < 0.001$). The 5-year survival rate for synchronous HN MPTs was only 25%, whereas it was surprisingly high for patients with metachronous HN MPT (85%, $P < 0.001$).

Conclusions. One of 10 patients with HNSCC develop MPTs in the HN-region, lung, or esophagus. The 5-year survival of patients with metachronous HN MPTs was surprisingly favorable.

Introduction

Head and neck cancer (lip, oral cavity, naso-, oro- and hypopharynx, and larynx) has an increasing incidence with 686,000 new cases and 404,000 associated mortalities worldwide in 2012.[1] The majority of head and neck tumors are squamous cell carcinoma (HNSCC).[2] Due to advances in surgical and radio- and chemotherapy techniques, the 5-year survival of HNSCC patients has improved from 55% in 1992-1996 to 66% in 2002-2006.[3] This relatively low survival rate could be explained by high tumor stages at diagnosis, patient delay prior to diagnosis, and a high incidence of tumor recurrence.[4-7] Another important factor affecting survival might be the development of multiple primary tumors (MPT's) in the head and neck region (HN-region), but also in associated organs such as the lung and esophagus.[5, 8]

Multiple primary tumors are squamous cell tumors which develop at or after diagnosis of the index tumor.[9, 10] Patients with second (SPT), third, fourth or even more primary tumors are defined as patients with MPT's. Multiple primary tumors are not the same as a residual/ recurrent tumors, which occur at the same site as the index tumor. For patients with an index HNSCC, MPT's most frequently occur in the HN-region, lung, or esophagus.[5, 11]

The concept that explains the occurrence of MPT's is field cancerization (FC). Field cancerization implies that tumors do not arise as an isolated tumor, but occur in a field of pre-neoplastic squamous cells that have an anaplastic tendency. This tendency gives rise to a multifocal development of tumors at various rates within the field[12]. For HNSCC patients, this FC is thought to extend as far as the lung and esophagus.[13] There are several theories that explain FC. The first is the polyclonal theory, which states that multiple precursor fields arise under the influence of carcinogenic agents.[12] The other theories are based on monoclonal concepts with a spread of dysplastic cells, which give rise to new fields in which MPT's may develop.[14]

The incidence of MPT's in HNSCC patients is reported to range from 9.4-14.4%.[5] Most second primary tumors (SPT's) occur in the HN-region (40-59%), lung (31-37%), and esophagus (9-44%).[5] The overall survival rate of patients who develop MPT's is lower than the survival of patients with only a single primary tumor.[6] A major decrease of 5-year overall survival rates from 69% to 32% has been reported for patients with metachronous MPT's compared to patients without MPT's.[15, 16] It has even been suggested that MPT's could have a worse effect on the survival of HNSCC patients than residual/ recurrent tumors of the index tumor.[5, 17]

In the literature, there is limited information available on the incidence and impact of MPT's on the survival of HNSCC patients with a Caucasian ethnicity. Most studies on this topic have been performed in Asia and therefore the results may not be generalizable for HNSCC patients in Western countries, since tumor incidences vary widely.[18] Subsequently, incidence and survival rates of patients with MPT's could be under- or overestimated. Also, cohorts that include a large number of patients are scarce.

The main objective of this study is to describe the incidence of MPT's in a large Dutch cohort of HNSCC patients. The second objective is to analyze the effect of MPT's on the survival rates of HNSCC patients.

Materials and methods

This paper was written according to the STROBE guidelines for reporting observational studies.[19] It was approved by the medical ethics committee of the Erasmus MC (MEC-2016-751).

Subjects

Patients were selected from the Rotterdam Oncology Documentary (RONCDOC), which is a database that comprises all head and neck cancer patients treated at the Erasmus MC Cancer Institute since 1995. We included all 1372 patients who had been diagnosed with a head and neck squamous cell carcinoma (lip, oral cavity, naso- oro- and hypopharynx, larynx, sinonasal cavity) as index tumor between 1 January 2008 and 31 December 2011. The final date of follow-up was 14 August 2017. No patients were excluded. Patients were divided into three groups: patients who developed a second primary tumor in the 1) head and neck region, 2) lung, or 3) esophagus.

Data collection

Patient, tumor and therapy data were acquired from the Netherlands Comprehensive Cancer Organization (a national cancer registry where all histologically proven cancers in the Netherlands are registered – irrespective of the hospital where the cancer is diagnosed) and merged with data from the patient records of the Erasmus MC Cancer Institute. Subsequently, the data were manually checked for each patient using available data from the patient records. If there was any doubt about the validity of the data collected, the patient was discussed by the research staff until a consensus was reached. A log was kept in which the inclusion of patients was recorded. This led to a high degree of classification accuracy and low risk of selection bias. The following data were collected: date of birth and death, last follow up date, comorbidity, prior malignancies, tobacco and alcohol consumption, body

mass index (BMI), clinical and histopathologic TNM and tumor stage, type and intention of therapy, and location and time to occurrence of MPT's.

Multiple primary tumors were defined according to the Warren & Gates and Hong et al. criteria, which state that: the MPT 1) must be diagnosed as malignant on histologic examination, 2) must be histologically distinct from the index tumor and thus not a metastasis, 3) has to be at least 2 cm from site of the index tumor or the tumor has to occur > 3 years after the diagnoses of the index tumor.[9, 10] Patients with second, third, fourth or even more primary tumors (> 1 primary tumor) were identified as patients with MPT's. A second primary tumor (SPT) is thus a first MPT. A MPT was defined as synchronous if the tumor developed < 6 months after the diagnosis of the index tumor and as metachronous if it developed after ≥ 6 months.

Table 1. Patient characteristics

Number of patients	149	
Follow-up , mean months (SD)	51.9 (27.9)	
Male sex , n (%)	111 (74.5)	
Age , mean yr (SD)	63.1 (8.8)	
Smoking status , n (%) / median PY (IQR)		
Current smoker	114 (76.5) /	42 (33-59)
Previous smoker	27 (18.1) /	40 (25-50)
Non-smoker	7 (4.7) /	0 (0-0)
Missing	1 (0.7)	
Alcohol consumption , n (%) / median UPW (IQR)		
Current drinker	114 (76.5) /	28 (14-42)
Previous drinker	22 (14.8) /	28 (14-42)
Non-drinker	12 (8.0) /	0 (0-0)
Missing	1 (0.7)	
Comorbidity* , n (%)		
None	39 (26.2)	
Mild	57 (38.2)	
Moderate	31 (20.8)	
Severe	22 (14.8)	
Body mass index , n (%)		
Underweight (< 18.5)	10 (6.7)	
Normal weight (18.5-24.9)	78 (52.3)	
Overweight (25.0 – 29.9)	47 (31.5)	
Obese (≥ 30)	9 (6.2)	
Missing	5 (3.3)	

n = number, yr = year, SD = standard deviation, PY = pack-years, UPW = units per week. * Comorbidity measured by Adult Comorbidity Evaluation 27.

A distinct differentiation should be made between MPT's and residual/recurrent tumors, which occur at the same site and share the same histopathology as the index tumor. Residual tumors develop < 6 months after the index tumor and recurrent tumors ≥ 6 months, but

< 3 years. A tumor developed at the same site as and ≥ 3 years after the index tumor was considered to be a MPT.

Comorbidities were scored with the Adult Comorbidity Evaluation-27 (ACE-27).[20] The intention of therapy was scored as curative or palliative based on the Dutch guidelines for the treatment of HNSCC, lung carcinoma, and esophagus carcinoma.[21] Height and weight were used to calculate the body mass index (BMI). Patients were categorized in underweight (BMI < 18.5), normal weight (BMI 18.5-24.9), overweight (BMI 25-29.9), and obese (BMI ≥ 30). Tobacco and alcohol use was registered as current-, previous- or non-smoker/drinker. For tobacco use the number of pack years was registered and for alcohol use the number of units per week.

Statistical analysis

If quantitative variables were normally distributed, the results are expressed as mean values and standard deviation (SD), otherwise median and inter quartile range (IQR) is used. Categorical data are reported as frequencies and percentages and differences between groups were analyzed using the chi-squared test. A Kaplan-Meier survival analysis was used for survival analyses and the log-rank test to compare the survival distributions of two groups of patients. The 5-year survival from the date of diagnosis of the index tumor was analyzed and, additionally, the 3-year survival rate from the date of diagnosis of the SPT. The survival rate was analyzed separately for patients with synchronous an metachronous SPT's. A complete case analysis was used to handle missing data. However, all data on the outcomes of interest (incidence and survival) were complete. Statistical analysis was performed using SPSS version 21.0 (IBM Corp., Armonk, NY, USA).

Results

General patient- and index tumor characteristics

A total of 149 patients with multiple primary tumors and a head and neck squamous cell carcinoma as index tumor were identified in our cohort. Their baseline characteristics are shown in detail in Table 1. The mean duration of follow-up was 51.9 months (SD 27.9). One hundred eleven patients (74.5%) were male and the mean age was 63.1 years (SD 8.8). The majority of patients was a current smoker (114 [76.5%]). This group had a median number of 42.0 pack years (IQR 33.0-58.8). The majority of patients was also current alcohol abusers (114 [76.5%]), who had a median alcohol consumption of 28 units per week (IQR 14-42). There were 110 patients (73.8%) with mild to severe comorbidity.

Table 2. Characteristics of index tumor (n = 149)

Tumor location, n (%)	
Lip	2 (1.3)
Oral cavity	46 (30.9)
Oropharynx	40 (26.8)
Hypopharynx	11 (7.4)
Supraglottic	28 (18.8)
Glottis	18 (12.1)
Sinonasal cavity	4 (2.7)
Tumor stage, n (%)	
0 (CIS)	6 (4.0)
I	39 (26.2)
II	34 (22.8)
III	26 (17.4)
IV	43 (28.9)
Missing	1 (0.7)
Therapy, n (%)	
Surgery	36 (24.1)
Radiotherapy	52 (34.9)
Chemotherapy	0 (0.0)
Surgery + RT	32 (21.5)
RT + CT	20 (13.4)
Surgery + RT + CT	5 (3.4)
No Therapy	4 (2.7)
Intention of the therapy, n (%)	
Curative therapy	141 (94.6)
Palliative therapy	8 (5.4)
Residual tumors, n (%)	0 (0.0%)
Recurrent tumors, n (%)	12 (8.1%)

CIS = carcinoma in situ, RT = radiotherapy, CT = chemotherapy.

Table 2 provides a detailed overview of the characteristics of the HNSCC index tumor. Most tumors were in the oral cavity (46 [30.9%]), followed by the oropharynx (40 [26.8%]), and the supraglottic region (28 [18.8%]). The tumor stage ranged from 0 (carcinoma in situ) to stage IV. Radiotherapy was the most frequent used therapy (52 patients [34.9%]), whilst 36 patients (24.2%) received surgery. Thirty-two patients (21.5%) received surgery with adjuvant radiotherapy. Twenty patients (13.4%) received a combination of radio- and chemotherapy. Recurrences of the index tumor occurred in 12 (8.1%) of the 149 cases. No residual tumors were detected.

MPT incidence and time to occurrence

Figure 1 presents the distribution of the MPT development during follow up. A total of 1372 patients with an HNSCC index tumor was diagnosed at the Erasmus MC Cancer Institute between 2008 and 2011. The total incidence of MPT's in HNSCC patients was 10.9% (n = 149). The second primary tumor of these patients was located in the head and neck region

in 5.5% of the cases ($n = 75$), in the lung in 4.9 % of the cases ($n = 63$), and in the esophagus in 0.8% ($n = 11$). Of these patients with a SPT, 19.5% (29/147) also developed a third primary tumor (TPT). Seven patients with TPT's (24.1%) even developed more than three primary tumors.

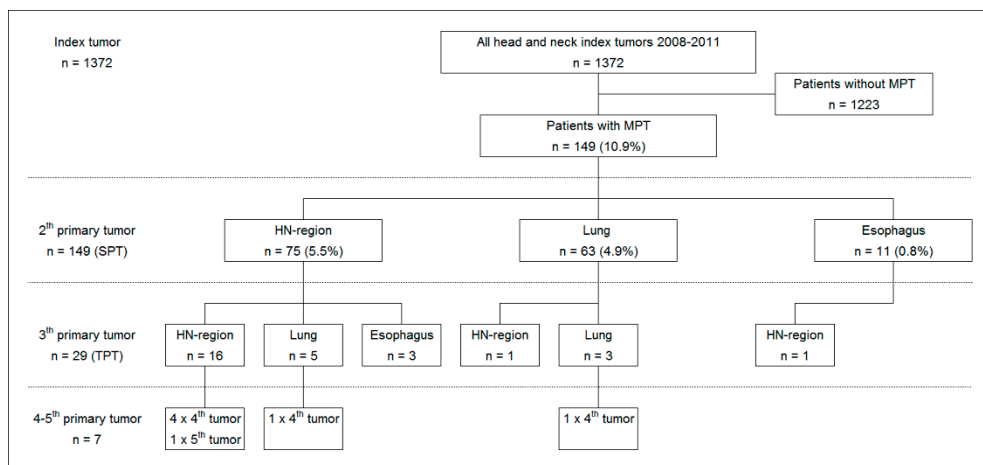


Figure 1. Flowchart presents the distribution of the multiple primary tumor development in head and neck cancer patients. MPT = multiple primary tumor, HN = head and neck, SPT = second primary tumor, TPT = third primary tumor.

The median time to occurrence of all SPT's was 22.9 months (IQR 2.1-47.4). The head and neck-SPT's (HN-SPT's) were synchronous in 23 cases (30.7%), with a median time to occurrence of 0.1 months (0.0-0.9). Fifty-two HN-SPT cases (69.3%) were metachronous, with a median time to occurrence of 41.7 months (IQR 19.0-58.0). The index tumors of patients with metachronous HN-SPT's were more often advanced (stage III and IV) than synchronous HN-SPT's (56.5% vs. 26.9%). The SPT's in the lung were synchronous in 18 cases (28.6%) and had a median time to occurrence of 1.8 months (IQR 1.0-2.7). Forty-five lung-SPT's (71.4%) occurred metachronously and had a median time to occurrence of 37.1 months (IQR 22.7-55.0). Almost a quarter ($n = 3$) of the SPT's in the esophagus developed synchronously and the other 72.7% ($n = 8$) metachronously. The median time to occurrence from the index tumor to the third primary tumor was 34.5 months (IQR 11.2-60.0)

Survival analysis

The survival of all 149 patients with MPT's was analyzed. Their overall 5-year survival, measured from the occurrence of the index tumor, was 46.8%. The 5-year survival of patients who developed an HN-SPT (67.3%) was better than patients who had a lung-SPT (28.6%, $p < 0.001$), or an esophageal-SPT (13.6%, $p < 0.001$) (Figure 2).

Figure 3A shows that patients with synchronous HN-SPT's had a worse 5-year survival rate (24.5%) than patients with metachronous HN-SPT's (84.6%, $p < 0.001$). The 5-year survival of patients with a synchronous SPT in the lung (16.7%) was also worse than those with metachronous lung-SPT's (33.3%, $p = 0.003$). Patients with metachronous lung-SPT's had a lower a 5-year survival rate than patients with metachronous HN-SPT's ($p < 0.01$). On the other hand, the survival of patients with a synchronous SPT in the lung and HN-region was not significantly different ($p = 0.189$).

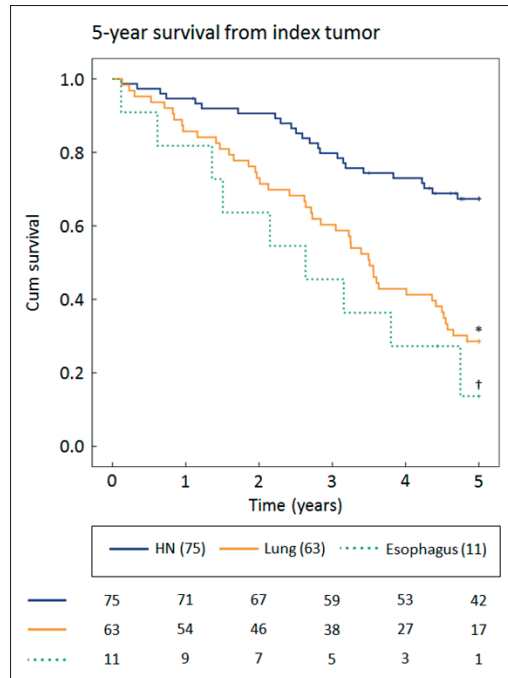


Figure 2. The 5-year survival from the diagnosis of the head and neck index tumor for patients with second primary tumors in the head and neck region, the lung, and the esophagus. HN = head and neck. Numbers at the bottom of the figure represent patients at risk. * $p < 0.001$ compared to HN, † $p < 0.001$ compared to HN. P-values calculated with log-rank test.

The median survival of patients with synchronous HN-SPT's was 3.2 years (IQR 1.1-4.4), while it was 6.1 years (IQR 4.8-7.5) for metachronous cases. The median survival of patients with synchronous lung-SPT's was 1.6 years (IQR 0.7-3.5) and 4.0 years (IQR 2.7-5.9) for patients with metachronous lung-SPT's. Due to the limited number of patients with an esophageal-SPT, we were not able to analyze differences between metachronous and synchronous SPT's in this group.

Figure 3B shows the 3-year survival rate, measured from the moment the SPT was diagnosed. This was the same for patients with a synchronous (59.8%) and metachronous

HN-SPT (62.8%). A difference was seen in the group of patients with lung-SPT. Patients with metachronous lung-SPT's had a worse 3-year survival rate (9.9%) than patients with synchronous lung-SPT's (33.3%, $p = 0.048$). Metachronous lung-SPT's were more often diagnosed in a high stage (III and IV) of development (34 [75.6%]) than synchronous lung-SPT's (9 [50.0%], $p = 0.049$) and also more often than metachronous HN-SPT's (21 [40.4%], $p < 0.001$).

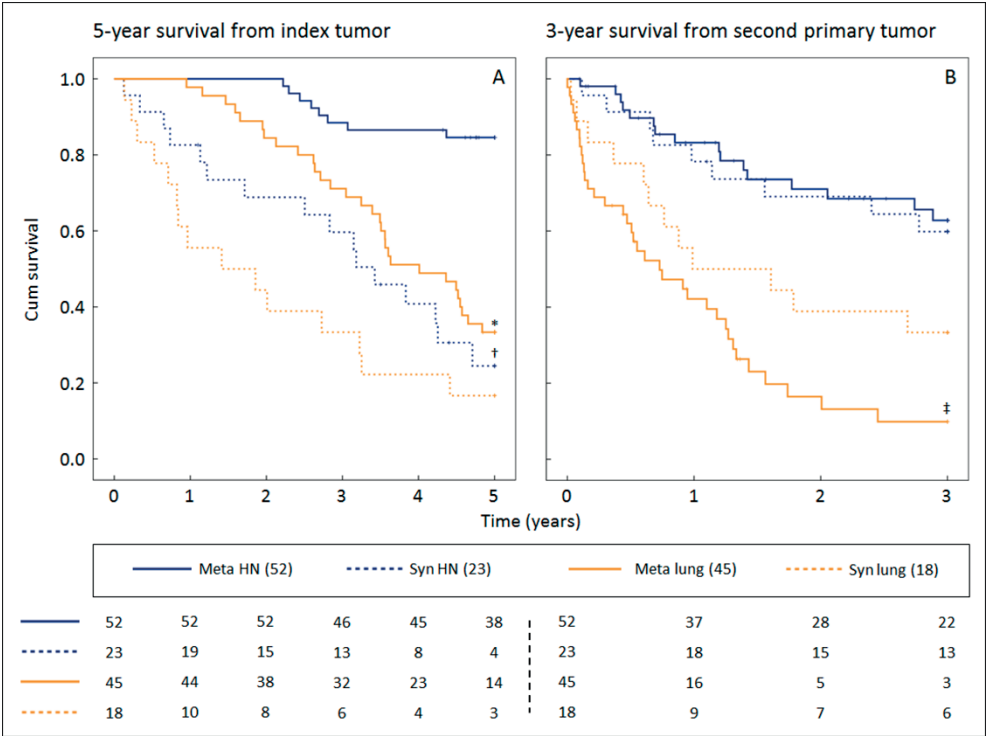


Figure 3. A) The 5-year survival from the diagnosis of the head and neck index tumor for patients with syn- and metachronous second primary tumors in the head and neck region and the lung. **B)** The 3-year survival from the diagnosis of the second primary tumor for the same patients. Syn = synchronous, Meta = metachronous, HN = head and neck. Numbers at the bottom of the figure represent patients at risk. * $p < 0.001$ compared to meta HN, † $p < 0.001$ compared to meta HN, ‡ $p = 0.048$ compared to syn lung. P-values calculated with log-rank test.

Discussion

This study showed that one out of ten head and neck squamous cell carcinoma patients develop at least one multiple primary tumor in the head and neck region, lung or esophagus. We acquired our results by using high quality, double checked data obtained from the national cancer registry and the patients records. Surprisingly, MPT's develop as frequently

in lung (4.9%) as in the HN-region (5.3%). The 5-year survival rate of all patients was 47%. This is lower than the 66% stated in the literature.[3, 22] Patients with MPT's which were synchronous or in the lung or esophagus had the worst survival. On the other hand, patients with metachronous head and neck-SPT's had a surprisingly high 5-year survival rate of 85%.

We showed that the 5-year survival rate of HNSCC patients with a synchronous HN-SPT was significantly worse than patients with a metachronous HN-SPT. This finding is similar to the results of two previous studies.[23, 24] This could be explained by the higher percentage of high-stage tumors (stage III and IV) in the synchronous HN-SPT group (56%) compared to the metachronous HN-SPT group (40%). However, this difference was not significantly different, $p = 0.196$. Another explanation is that the development of a synchronous MPT in the HN-region limits the treatment options of the index tumor. Panosetti et al. showed that treatment protocols of the index tumor need to be adjusted when a synchronous SPT is diagnosed.[23] The treatment strategy had to be adjusted in 50% of HNSCC patients with a synchronous HN-SPT. Subsequently, this adjustment caused a decline in the 5-year survival rate from 18% to 8%.

The location of the SPT was also of significant influence on the survival. Although the incidence of SPT's in the HN-region and lung were almost the same in the present study, the 5-year survival of patients who developed a SPT in the lung (29%) was significantly worse than of patients with HN-SPT's (67%). The survival rate of patients with esophageal-SPT's was even lower (14%). These findings are in line with the results of other studies.[15, 25]

Interestingly, the 3-year survival rate, measured from the occurrence of the SPT, was the same for patients with syn- and metachronous HN-SPT's (61% vs. 63%). On the other hand, it was significantly lower for patients with lung-SPT's: 33% for synchronous and 10% for metachronous MPT's. The difference between the 5-year survival (from the index tumor) and 3-year survival (from the SPT) of metachronous SPT's could be explained by the long median time to occurrence. This indicates that syn- and metachronous SPT's have a similar mortality and that the time to occurrence of an SPT is what dictates patient survival. The first 6 months after the index tumor are important for the prediction of survival of an individual patient. Patients who developed a SPT within this period (synchronous) have a significant worse survival 5-year survival rate, measured from the index tumor, than patients who stayed free of an SPT for the first 6 months (metachronous).

The majority of metachronous lung-SPT's were diagnosed in stage III or IV (76%). This could be an explanation of the lower survival rate in this group compared to patients with synchronous lung-SPT's or metachronous HN-SPT's. Many patients with high-stage lung tumors are incurable and if treatment is available, it often induces severe comorbidity.[26]

To our knowledge, all current follow-up protocols for HNSCC patients lack an active screening for MPT's in the lung, despite the evident negative effect of lung-MPT's on patient survival and the similar incidence as HN-MPT's. Screening for lung-MPT's could be considered because of the low survival rate of affected patients and the high percentage of high-stage lung-MPT's.[24, 27]

Several studies also advocate the use of surveillance and screening for esophageal-MPT's.[28] A French multi-centered study investigated the use of endoscopy of the esophagus in the work-up of HNSCC patients to screen for MPT's. They found an 8-times higher percentage of 6.8% esophageal carcinoma and high-grade dysplasia than the 0.8% in our study.[29] A study by De Vries et al. also showed high percentages of esophageal-MPT's in a cohort of Dutch HNSCC patients.[8] Several Asian studies have even shown esophageal-MPT incidences of up to 41%.[30-33] Therefore, we believe our incidence of esophageal-MPT's is an underestimation of the actual incidence. This discrepancy between the literature and our findings could indicate that many esophageal-MPT's are never diagnosed, despite the fact that diagnosis of early stage esophageal-MPT's could improve the outcome of HNSCC patients.[34] It is even suggested that early esophageal-MPT diagnosis and treatment could give these patients a similar prognosis as patients who did not developed an esophageal-MPT.[35] These findings suggest that endoscopic screening for esophageal-MPT's in the work-up of HNSCC patients might cause a health benefit.

We showed an increasing risk to develop a MPT in patients who already have a MPT. The incidence increased from 11% for a SPT in patients with a HSNCC index tumor up to 24% for a 4th primary tumor in patients with three primary tumors. These findings are in line with the multifocal development of tumors within a precursor field, stated by the field cancerization theory.[12] Other literature showed that a continuous exposure to carcinogenic agents like smoking and alcohol and possibly radiotherapy treatment also increases the risk to develop a MPT.[36] The increasing incidence and the field cancerization theory combined give rise to the question whether patients with MPT can be completely cured.

No residual tumors were detected in this cohort and the rate of recurrent tumors was 8.1%. This is relatively low, compared to a recent review, that reported local residual/recurrence rates varying from 10-50%, depending on the location and stage of the primary tumor.[11] This could be explained by the fact that all our patients have MPT's. Lester et al. stated that 85% of all recurrences appear after 13-31 months.[37] In comparison, the median time to occurrence of all SPT's in the present study was 23 months (IQR 2-47). This could mean that a selection of our patients might have died as a consequence of a MPT before a recurrence could have developed. It could also indicate that

less recurrences were diagnosed because diagnostics and treatment were focused on the MPT.

There are limitations to the present study that might have had an influence on the results we obtained. One is the relatively small number of patients with esophageal-MPT's. This prevented us to perform a detailed survival analysis in this group of patients. Another limitation is the absence of a control group of HNSCC patients who did not develop a MPT. Consequently, we had to compare the survival of our patients with MPT's with previously reported data of HNSCC patients without MPT's. This also prohibited us to compare the difference in effect on survival between MPT's and residual/ recurrent tumors and to identify risk factors and risk profiles for the occurrence of MPT's. It could also be argued to exclude patients with tumors with a known low risk to develop multiple primary tumors (HPV-negative oropharyngeal and sinonasal tumors). However, they were a minority of our total study population. Another point of concern is the fact that the distinction between a lung-MPT and a distant lung metastasis is challenging. Ideally, identification of genetic relation between both tumors. In this study, loss-of-heterozygosity analysis was performed in most cases of lung cancer. However some exceptions were made for patients with 1) lung tumors that developed > 5 years after the index HNSCC tumor and 2) patients who were treated with a palliative intent because of stage-IV lung tumors. Despite these limitations, our protocolled method of data collection and large total cohort size, made it possible to draw reliable conclusions from our results.

Conclusion

In conclusion, about one in ten head and neck squamous cell carcinoma patients developed multiple primary tumors in the head and neck region, lung, or esophagus. This could be explained by the field cancerization theory. Multiple primary tumors had a negative effect on the survival, which was most pronounced in patients with MPT's which were synchronous or in the lung or esophagus. Patients with metachronous MPT in the HN-region had a surprisingly good 5-year survival rate. Screening and a better follow-up might be considered to increase the overall survival of HNSCC patients, because of the high incidence and the negative effect on survival. This specifically applies to MPT's which develop in the lung and esophagus. Future goals of research are to compare HNSCC patients with and without MPT's and identify risk factors and risk profiles for their development.

References

1. Ferlay J, et al. - Cancer incidence and mortality worldwide: sources, methods and major patterns in GLOBOCAN 2012. - *Int J Cancer* 2015.
2. Leon Barnes JWE, Peter Reichart, David Sidransky: WHO pathology and genetics of head and neck tumours. In.; 2003
3. Pulte D, et al. - Changes in survival in head and neck cancers in the late 20th and early 21st century: a period analysis. - *Oncologist* 2010.
4. McGurk M, et al. - Delay in diagnosis and its effect on outcome in head and neck cancer. - *Br J Oral Maxillofac Surg* 2005.
5. Priante AV, et al. - Second primary tumors in patients with head and neck cancer. - *Curr Oncol Rep* 2011.
6. Leon X, et al. - Can cure be achieved in patients with head and neck carcinomas? The problem of second neoplasm. - *Expert Rev Anticancer Ther* 2001.
7. Seiwert TY, et al. - State-of-the-art management of locally advanced head and neck cancer. - *Br J Cancer* 2005.
8. de Vries N, et al. - Dubbeltumoren bij patiënten met een plaveiselcelcarcinoom van het slijmvlies in het hoofd-halsgebied. Double tumors in patients with a mucosal squamous cell carcinoma in the head and neck region. - *Ned Tijdschr geneesk* 1985.
9. Warren S, et al. - Multiple primary malignant tumors: A survey of the literature and a statistical study. - *American Journal of Cancer* 1932.
10. Hong WK, et al. - Prevention of second primary tumors with isotretinoin in squamous-cell carcinoma of the head and neck. - *N Engl J Med* 1990.
11. De Felice F, et al. - Follow-Up in Head and Neck Cancer: A Management Dilemma. - *Advances in Otolaryngology* 2015.
12. Mohan M, et al. - Oral field cancerization: an update on current concepts. - *Oncol Rev* 2014.
13. Heroiu Cataloiu AD, et al. - Multiple cancers of the head and neck. - *Maedica (Buchar)* 2013.
14. Angadi PV, et al. - Oral field cancerization: current evidence and future perspectives. - *Oral Maxillofac Surg* 2012.
15. Chen MC, et al. - Impact of second primary esophageal or lung cancer on survival of patients with head and neck cancer. - *Oral Oncol* 2010.
16. Jung YS, et al. - Metachronous Second Primary Malignancies after Head and Neck Cancer in a Korean Cohort (1993-2010). - *PLoS One* 2015.
17. Chuang SC, et al. - Risk of second primary cancer among patients with head and neck cancers: A pooled analysis of 13 cancer registries. - *Int J Cancer* 2008.
18. Gupta B, et al. - Global Epidemiology of Head and Neck Cancers: A Continuing Challenge. - *Oncology* 2016.
19. von Elm E, et al. - The Strengthening the Reporting of Observational Studies in Epidemiology (STROBE) statement: guidelines for reporting observational studies. - *Ann Intern Med* 2007.
20. Piccirillo JF, et al. - Prognostic importance of comorbidity in a hospital-based cancer registry. - *Jama* 2004.
21. Leemans CR, et al. - Richtlijn Hoofd-halstumoren. 2012. - <http://richtlijndatabasen/richtlijn/hoofd-halstumoren>
22. Braakhuis BJ, et al. - Incidence and survival trends of head and neck squamous cell carcinoma in the Netherlands between 1989 and 2011. - *Oral Oncol* 2014.
23. Panosetti E, et al. - Site and incidence of multiple cancers in patients with squamous cell carcinomas of the upper aerodigestive tract. - *Laryngorhinootologie* 1990.
24. Di Martino E, et al. - Survival in second primary malignancies of patients with head and neck cancer. - *J Laryngol Otol* 2002.
25. Dequanter D, et al. - Second primary lung malignancy in head and neck cancer patients. - *Eur Ann Otorhinolaryngol Head Neck Dis* 2011.
26. Yoon SM, et al. - Therapeutic management options for stage III non-small cell lung cancer. - *World J Clin Oncol* 2017.
27. van der Haring IS, et al. - Second primary tumours after a squamous cell carcinoma of the oral cavity or oropharynx using the cumulative incidence method. - *Int J Oral Maxillofac Surg* 2009.
28. De Monès E, et al. - Initial staging of squamous cell carcinoma of the oral cavity, larynx and pharynx (excluding nasopharynx). Part 2: Remote extension assessment and exploration for secondary synchronous locations outside of the upper aerodigestive tract. 2012 SFORL guidelines. - *Eur Ann Otorhinolaryngol Head Neck Dis* 2013.
29. Dubuc J, et al. - Endoscopic screening for esophageal squamous-cell carcinoma in high-risk patients: a prospective study conducted in 62 French endoscopy centers. - *Endoscopy* 2006.
30. Lee YC, et al. - Transnasal endoscopy with narrow-band imaging and Lugol staining to screen patients with head and neck cancer whose condition limits oral intubation with standard endoscope (with video). - *Gastrointest Endosc* 2009.
31. Morimoto M, et al. - Significance of endoscopic screening and endoscopic resection for esophageal cancer in patients with hypopharyngeal cancer. - *Jpn J Clin Oncol* 2010.

32. Wang WL, et al. - The benefit of pretreatment esophageal screening with image-enhanced endoscopy on the survival of patients with hypopharyngeal cancer. - *Oral Oncol* 2013.
33. Muto M, et al. - Association between aldehyde dehydrogenase gene polymorphisms and the phenomenon of field cancerization in patients with head and neck cancer. - *Carcinogenesis* 2002.12376487
34. Kominek P, et al. - Chromoendoscopy to detect early synchronous second primary esophageal carcinoma in patients with squamous cell carcinomas of the head and neck? - *Gastroenterology research and practice* 2013.
35. Lim H, et al. - Clinical significance of early detection of esophageal cancer in patients with head and neck cancer. - *Gut Liver* 2015.
36. Atienza JA, et al. - Incidence of second primary malignancies in patients with treated head and neck cancer: a comprehensive review of literature. - *Curr Med Res Opin* 2012.
37. Lester SE, et al. - "When will I see you again?" Using local recurrence data to develop a regimen for routine surveillance in post-treatment head and neck cancer patients. - *Clin Otolaryngol* 2009.

Chapter 2b

Multiple primary tumors: risk factors

A cause-specific Cox model for second primary tumors in head and neck cancer patients: a RONCDOC study

Oisín Bugter* & Rens van Iwaarden*; Nikki van Leeuwen; Daan Nieboer; Emilie Dronkers; José Hardillo; Robert Baatenburg de Jong

* Authors contributed equally to his work.

Head & Neck, Jun 2021, PMID: 33655596

Abstract

Background. The aim of this study was to identify risk factors for the development of second primary tumors (SPT) in the head and neck region, lungs, and esophagus in patients with head and neck cancer.

Methods. We collected data from 1581 patients. A cause specific Cox model for the development of an SPT was fitted, accounting for the competing risks residual/recurrent tumor and mortality.

Results. Of all patients, 246 (15.6%) developed SPTs. Analysis showed that tobacco and alcohol use, comorbidity and the oral cavity subsite were risk factors for SPTs. The C-index, the discriminative accuracy, of the model for SPT was 0.65 (95% CI 0.61 – 0.68).

Conclusions. Our results show that there is potential to identify patients that have an increased risk to develop an SPT. This might increase their survival chances and quality of life. More research is needed to provide HN clinicians with definitive recommendations.

Introduction

Each year in the Netherlands, approximately 2.500 patients are diagnosed with head and neck squamous cell carcinoma (HNSCC) of the oral cavity, pharynx and larynx.[1] At present, these patients have a low to moderate 5-year survival rate of 45-69% depending on the subsite of the tumor.[1] Low survival rates can be explained by the high incidence of tumor recurrence, advanced tumor stages at diagnosis, and patient delay.[2-4] However, part of the mortalities are not caused by the index tumor, but by the occurrence of a second primary tumor (SPT).[2] Addressing, diagnosing and treating more SPTs might be of substantial benefit for HNSCC patients.

Second primary tumors in patients with HNSCC occur most frequently in the head and neck (HN) region, the lungs and the esophagus.[2] They can develop alongside the index tumor or during follow-up and are not the same as a residual/recurrent tumors or metastases.[5, 6] The frequent occurrence of SPTs in HNSCC patients can be explained by the concept of field cancerization (FC).[7] This concept implies that tumors occur in a field of pre-neoplastic squamous cells that have an anaplastic tendency. This tendency could give rise to multifocal development of primary tumors at various rates within the field.

At present, there is limited evidence available on factors that increase the risk of SPT development in patients with an HNSCC index tumor. Some studies have suggested old age, tobacco and alcohol use, and the subsite of the index tumor to be independent risk factors for SPTs.[8, 9] A tendency for SPTs to develop along the respiratory axis (lungs) in patients with an index laryngeal tumor and along the digestive axis (esophagus) for patients with hypopharyngeal index tumors has also been noted.[10] Consequently, tobacco use is associated with increased risk for lung SPTs and alcohol use for SPTs in the esophagus.[11] However, most data is derived from small studies performed in Asia. It is unclear if these results can be extrapolated to a Western population. Also, most studies do not account for competing risks (e.g., a patient that dies shortly after treatment will not develop an SPT).

The objective of the present study is to identify risk factors and develop a prediction model for the development of SPTs in the HN region, lungs, and esophagus in a large cohort of patients with HNSCC. If risk factors are identified they may help to personalize follow-up strategies with regards to screening for SPTs. Possibly, subgroups of HN cancer patients can be identified that are more prone to the development of an SPT. This approach the potential to diagnose more SPTs in early stage of development and thereby potentially increase the overall survival rate and quality of life of HNSCC patients.

Materials and Methods

This study was approved by the medical ethics committee of the Erasmus MC (MEC-2016-751). The manuscript was written according to the STROBE guidelines for reporting observational studies.[12]

Subjects

Patients were selected from the Rotterdam Oncology Documentary (RONCDOC). The RONCDOC is a database that comprises HN cancer patients treated at the Erasmus MC Cancer Institute. We analyzed 1774 patients who had been diagnosed with a HNSCC (oral cavity, naso- oro- and hypopharynx, and larynx) between 1 January 2006 and 31 December 2011. The end date was chosen to allow long term follow up of all patients. The patients included were divided into two groups: patients who developed an SPT and a control group with only one HNSCC. The SPT group was further subdivided in three groups: patients with a HN, lung, or esophagus SPT. We excluded patients with prior malignancies in the HN region, lungs, or esophagus and patients who were treated with palliative intent (most often because of distance metastases).

Data collection

Patient, tumor and therapy data were acquired from both the Netherlands Comprehensive Cancer Organization (IKNL) and from the electronic patient records of the Erasmus MC Cancer Institute.[13] Subsequently, the data of each included patient were manually checked for inconsistencies between the two sources and missing data. Data was revised or supplemented when needed. In the case of doubt about the validity of the patient data, the specific patient was discussed by the research staff until a consensus was reached. A log was kept in which the inclusion of patients was recorded. This led to a high degree of classification accuracy and low risk of selection bias. The following patient data were collected: date of birth and death, last follow up date, comorbidity, prior malignancies, tobacco and alcohol consumption, anemia, and weight loss. The following tumor and therapy data were collected for the index tumor and the SPT: subsite, date of diagnosis, clinical and histopathologic TNM-classification, tumor stage, and type and intention of therapy. Data on patient follow-up was obtained using the electronic patient records and the Dutch Civil Registry. Final date of follow-up was defined as the final date the patient was confirmed to be alive. The minimum follow-up was 5 years.

Definitions

Second primary tumors were defined according to the Warren & Gates and the updated Hong et al. criteria, which state that: the SPT 1) must be diagnosed as malignant, 2) must be histologically distinct from the index tumor, and 3) has to be at least 2 cm from site of the

index tumor or has to occur > 3 years after the diagnoses of the index tumor.[5, 6] These criteria were used to distinguish SPTs from metastases and residual/recurrent tumors. The latter occur at the same site and share the same histopathology as the index tumor. Residual tumors develop < 6 months after the index tumor and recurrent tumors between 6 months and 3 years. A tumor that developed at the same site as but ≥ 3 years after the index tumor was considered to be an SPT. An SPT was defined as synchronous if the tumor developed < 6 months after the diagnosis of the index tumor and as metachronous if it developed after ≥ 6 months. Comorbidities were scored with the Adult Comorbidity Evaluation-27 (ACE-27).[14] The ACE-27 is a validated evaluation form which can be used to identify important medical comorbidities and grade their severity. The intention of therapy was scored as curative or palliative based on the Dutch guidelines for the treatment of HNSCC, lung carcinoma, and esophagus carcinoma.[15] Tobacco and alcohol use was registered as never, past, and current smoker/drinker. For tobacco use the number of pack years (PY) was registered and for alcohol use the number of units per week. Anemia was defined as hemoglobin levels < 8.5 mmol/L for males and < 7.5 mmol/L for females. Weight loss was defined as the percentage of weight patients lost within 6 months prior to diagnosis of the index tumor. It was categorized as mild (< 5%), moderate (≥ 5 and < 10%), and severe ($\geq 10\%$). The candidate predictors for our model were age, sex, tobacco use (in PY), alcohol use (in U/W), cT, cN, comorbidity (ACE-27), subsite of the index tumor, and therapy of the index tumor.

Statistical analysis

Statistical analyses were performed using IBM SPSS (version 21.0) and R Statistical Software (version 3.6.2). Continuous data were expressed as mean values and standard deviation (SD). Categorical data were presented as frequencies and percentages. Differences between groups were analyzed using the χ^2 -test or the Fisher's exact-test (categorical data) and the independent students t-test (continuous data). Data was missing for the variables related to tobacco and alcohol use, anemia, weight loss, TNM-classification, tumor stage, and therapy. To handle the missing data, multiple imputation was performed 5 times using package *mice* in R.[16] Cause-specific Cox regression analysis was used to estimate the hazard ratios (HRs) of the candidate predictors to develop an SPT. Competing risks are present when an individual is at risk for more than one event and the occurrence of one of these competing events will prevent the event of interest from ever happening. In the present study, mortality and the occurrence of a residual/recurrent tumor were identified as competing events with the occurrence of an SPT. We performed three separate Cox models, one for our primary outcome (SPT), one for the competing risk mortality and one for the competing risk the occurrence of a residual/recurrent tumor. Consequently, these three models were combined in one cause-specific Cox model. This final model can be used to calculate the

Table 1. Baseline patient characteristics and univariable analysis between control and SPT group (n = 1581)

Variable	Control group	SPT + group	P-value	SPT + sub-groups						Missing N (%)
				HN	P-value	Lungs	P-value	Esoph.	P-value	
N total	1335	246		141		82		23		-
Male sex, n (%)	986 (74)	174 (70)	0.308	92 (65)	0.028*	64 (78)	0.400	18 (78)	0.633	-
Age, mean (SD)	64 (11)	63 (9)	0.099	62 (9)	0.065	63 (9)	0.638	63 (8)	0.834	-
Tobacco use, n (%)			0.011*		0.238		0.028*		0.190	9 (1)
Never	167 (13)	19 (8)		15 (11)		4 (45)		0 (0)		
Past	370 (28)	56 (23)		31 (22)		18 (22)		7 (30)		
Current	791 (60)	169 (69)		93 (67)		60 (73)		16 (70)		
PY, mean (SD)	33 (27)	41 (34)	0.001*	32 (22)	0.635	53 (46)	<0.0001*	48 (23)	0.023*	338 (21)
Alcohol use, n (%)			0.001*		0.061		0.047*		0.008*	14 (0.9)
Never	271 (21)	25 (10)		17 (12)		8 (10)		0 (0)		
Past	111 (8)	24 (10)		13 (9)		6 (7)		5 (22)		
Current	940 (71)	196 (80)		110 (79)		68 (83)		18 (78)		
U/W, mean (SD)	20 (26)	30 (39)	<0.0001*	27 (29)	0.004*	34 (55)	<0.0001*	32 (15)	0.002*	167 (11)
Comorbidity, n (%)			0.089		0.764		0.016*		0.009*	3 (0.2)
None	438 (33)	61 (25)		44 (31)		13 (16)		4 (17)		
Mild	462 (35)	98 (40)		52 (38)		34 (42)		11 (48)		
Moderate	309 (23)	59 (24)		34 (24)		23 (28)		2 (9)		
Severe	124 (9)	27 (11)		10 (7)		11 (14)		6 (26)		
Anemia, n (%)	195 (15)	30 (13)	0.327	20 (15)	0.948	7 (9)	0.125	3 (13)	0.759	79 (5)
Weight loss, n (%)			0.942		0.899		0.925		0.682	332 (21)
< 5%	794 (75)	136 (74)		77 (78)		44 (73)		15 (79)		
≥ 5% and < 10%	146 (14)	27 (15)		16 (15)		8 (13)		3 (16)		
≥ 10%	124 (12)	22 (12)		13 (12)		8 (13)		1 (5)		

SPT = second primary tumor, HN = head and neck, PY = pack year, U/W = alcohol units per week. Comorbidity was scored by the ACE-27. P-values compared to the control group were calculated with student t-test (continuous data) and χ^2 -test (categorical data), * p-value < 0.05.

absolute risk for the development of SPTs taking into account the two competing risks. The absolute risk for the development of an STP, accounting for mortality and a recurrent tumor, for a few example patients were calculated.[17] Backward stepwise selection was used in the multivariable analysis to define the final Cox models, using Akaike Information Criterion ($p < 0.157$) as a cut-off score. The concordance probability (C-index) was assessed to evaluate the model's discriminative performance. In survival analysis, a pair of patients is called concordant if the risk of the event predicted by a model is lower for the patient who experiences the event at a later time point. The C-index is the frequency of concordant pairs among all pairs of subjects.

Table 2. Baseline index tumor characteristics and univariable analysis of control and SPT group (n = 1581)

Variable	Control group	SPT + group	P-value	SPT + sub-groups						Missing
				HN	P-value	Lungs	P-value	Esoph.	P-value	
N total	1335	246	-	141	-	82	-	23	-	-
Subsite, n (%)			0.002*		<0.0001*		0.286		0.386	0 (0)
Oral cavity	381 (29)	87 (35)		60 (43)		23 (28)		4 (17)		
Nasopharynx	29 (2)	1 (0)		0 (0)		1 (1)		0 (0)		
Oropharynx	294 (22)	70 (29)		38 (27)		26 (32)		6 (26)		
Hypopharynx	106 (8)	18 (7)		10 (7)		4 (5)		4 (17)		
Larynx	525 (39)	70 (29)		33 (23)		28 (34)		9 (39)		
cT, n (%)			0.394		0.015*		0.433		0.733	5 (0)
CIS	15 (1)	6 (2)		6 (4)		0 (0)		0 (0)		
1	378 (29)	66 (27)		45 (32)		17 (21)		4 (17)		
2	400 (30)	82 (33)		46 (33)		29 (35)		7 (30)		
3	274 (21)	48 (20)		22 (16)		20 (24)		6 (26)		
4	263 (20)	6 (18)		22 (16)		16 (20)		6 (26)		
cN, n (%)			0.568		0.502				0.967	11 (1)
0	869 (66)	165 (67)		99 (70)		51 (62)	0.723	15 (65)		
1	155 (12)	34 (14)		18 (13)		13 (16)		3 (13)		
2	287 (22)	45 (18)		23 (16)		17 (21)		5 (22)		
3	13 (1)	2 (1)		1 (1)		1 (1)		0 (0)		
Tumor stage, n (%)			0.399		0.022*		0.440		0.885	17 (1)
0	15 (1)	6 (2)		6 (4)		0 (0)		0 (0)		
I	310 (24)	57 (23)		39 (28)		14 (17)		4 (17)		
II	277 (21)	55 (22)		30 (21)		20 (24)		5 (22)		
III	255 (19)	51 (21)		25 (18)		20 (24)		6 (26)		
IV	462 (35)	76 (31)		40 (29)		28 (34)		8 (35)		
Therapy, n (%)			0.653		0.157		0.626		0.268	15 (1)
Radiotherapy	426 (32)	73 (30)		38 (27)		30 (37)		5 (22)		
Surgery + RT	401 (30)	68 (28)		39 (28)		21 (26)		8 (35)		
Surgery	258 (20)	54 (22)		40 (29)		12 (15)		2 (9)		
RT + CT	191 (15)	43 (18)		21 (15)		16 (20)		6 (26)		
Surg + RT + CT	43 (3)	7 (3)		2 (1)		3 (4)		2 (9)		
Chemotherapy	2 (0)	0 (0)		0 (0)		0 (0)		0 (0)		
RT, n (%)	1061 (80)	191 (78)	0.397	100 (71)	0.013*	70 (85)	0.262	21 (91)	0.187	15 (1)

SPT = second primary tumor, HN = head and neck, PY = pack year, RT = radiotherapy, CT = chemotherapy. P-values compared to the control group were calculated with χ^2 -test (categorical data), * p-value < 0.05.

Results

Of the initial 1774 HNSCC patients, 193 patients were excluded because of prior malignancies in the HN region, lungs or esophagus or because they were not treated with curative intent. The remaining 1581 patients were included in this study. Of them, 246 (15.6%) developed an SPT. The SPTs developed in the HN region in 141 cases (8.9%), in the lungs in 82 cases (5.2%) and in the esophagus in 23 cases (1.4%). The median follow-up was 4.96 years (IQR 2.05- 6.90).

Patient and tumor characteristics of the SPT and control group are presented in Table 1 and 2. After univariable analysis, the following variables were significantly different between the SPT group and controls: tobacco use (status and PY), alcohol use (status and U/W), and the subsite of the index tumor. For patients with HN SPTs, the baseline characteristics differed on the variables sex, alcohol use (U/W), the subsite, cT-classification, and tumor stage of the index tumor, and surprisingly whether patient had received radiotherapy (RT) as part of their treatment ($p = 0.013$). For lung SPT patients, tobacco use (status and PY), alcohol use (status and U/W), and comorbidity were significantly different between patient with lung SPTs and non-SPT controls. The group of patients with esophageal SPTs was too small to make reliable conclusions.

The mean amount of PYs was higher in the SPT group (41 [SD 34]) than in the controls (33 [SD 27], $p < 0.001$). Alcohol use was also significantly higher in the group of patients that developed an SPT. Patients with SPTs were more often current smokers ($p < 0.001$) and used more units of alcohol per week (30 [SD 39] vs. 20 [SD 26], $p < 0.001$).

Multivariable Cox regression analysis was performed for the primary outcome SPT and competing risks mortality and the occurrence of a residual/recurrent tumor, after establishing the univariable relationship between the tumor-and patient-specific variables as mentioned above (Table 3 and Appendix 1). Data on tobacco use and the amount of PY was missing in 338 cases (21.4%). Alcohol consumption was unknown in 167 cases (10.5%) and for three patients (0.002%) there was not enough data to calculate the comorbidity index.

Patients that developed SPTs smoked more tobacco. The HR per pack year was 1.007 (95% CI 1.004-1.011, $p = 0.097 \cdot 10^{-3}$). A similar result showed for alcohol use: the HR per unit per week was 1.006 (95% CI 1.004-1.09, $p = 0.005 \cdot 10^{-3}$). Patients with no comorbidity on the ACE-27 index were less likely to develop an SPT. The HRs for mild, moderate and severe comorbidity were 1.568, 1.435, and 1.854 respectively. Finally, the results showed that patients with laryngeal tumors developed less SPTs than patients with oral cavity tumors (p

= 0.002). The cT and cN classification, age, and therapy of the index tumor did not significantly contribute to the model for SPT.

Table 3. Hazard Ratios from the cause-specific Cox regression analysis of risk factors for the development of SPTs

Variable	HR	(95% CI)	P-value	Missings (%)
Tobacco (PY)	1.007	(1.004-1.011)	0.097·10 ^{-3*}	21.4
Alcohol (U/W)	1.006	(1.004-1.009)	0.005·10 ^{-3*}	10.5
Comorbidity				<0.1
None	1.000	Reference		
Mild	1.568	(1.138-2.159)	0.006*	
Moderate	1.435	(0.998-2.062)	0.051	
Severe	1.854	(1.165-2.950)	0.009*	
Subsite				0.0
Oral cavity	1.000	Reference		
Nasopharynx	0.190	(0.026-1.368)	0.099	
Oropharynx	1.018	(0.739-1.402)	0.915	
Hypopharynx	0.740	(0.437-1.252)	0.261	
Larynx	0.707	(0.441-0.835)	0.002*	

HR = hazard ratio, CI = confidence interval, PY = pack year, U/W = units per week. Comorbidity was scored by the ACE-27. * p-value < 0.05.

The C-index of the overall prediction model for SPTs was 0.65 (95% CI 0.61 – 0.68). The absolute risks for the development of an SPT based on the cause specific Cox model, accounting for competing risks of ten randomly selected patients was presented in Table 4.

Discussion

In this study we developed a model for the development of SPTs in a large population of consecutive HNSCC patients. A total of 246 (15.6%) patients of our population developed an SPT. The majority occurred in the HN region, followed by the lungs and esophagus. These values are in accordance with the findings from previous studies.[2] Our prediction model showed that tobacco and alcohol use, comorbidity and the location of the index tumor predicted the occurrence of an SPT. A better understanding of which subpopulation of HNSCC patients have an increased SPT risk, could guide clinicians in their decisions regarding length of follow up and active SPT screening.

SPT risk factors

Our results showed a strong association between the use of tobacco and alcohol and the occurrence of SPTs. The SPT risk significantly increased with every consumed pack year or unit alcohol per week at the moment of diagnosis of the index tumor. Some studies did not find this association.[18, 19] While others only found an increased risk for severe alcohol users (> 3 units/day).[8] It is thought that the continuation of tobacco and alcohol after treatment increases the risk for the occurrence of an SPT. While our study did not address the continuation of tobacco and alcohol use, Do et al. showed an increased risk for the development of SPT in patients who continued these habits.[20] Hence, it could be wise to counsel and help patients to break these patterns of behavior.

Our study suggests that patients with comorbidity have a higher risk to develop an SPT than patients without a systemic disease. While comorbidity is a known prognostic factor for the overall survival of a HN cancer patient, there is, to our knowledge, no literature that evaluates the association between comorbidity and the development of SPTs.[21] It is not understood why the presence of comorbidity at the time of diagnosis of the index tumor, is associated with the risk to develop an SPT in the follow-up period.

Table 4. Patient characteristics and absolute risk for a second primary tumor in ten randomly selected patients.

Patient	PY	U/W	ACE-27	Location	cT	cN	Age	Therapy	AbsRisk
1	24	2	None	Nasoph.	2	2	56	Surg + CRT	0,050
2	40	35	Moderate	Larynx	1	0	89	RT	0,080
3	75	2	None	Larynx	0	0	83	RT	0,083
4	0	28	None	Oral	1	1	44	Surgery	0,095
5	20	0	Mild	Hypoph.	3	1	73	RT	0,095
6	50	63	None	Hypoph.	3	2	49	Surg + CRT	0,101
7	25	42	Mild	Hypoph.	3	2	62	Surg + CRT	0,111
8	50	84	Moderate	Oral	1	3	57	Surg + CRT	0,112
9	40	42	Moderate	Hypoph.	2	0	63	RT	0,173
10	60	112	Mild	Hypoph.	3	1	49	Surg + CRT	0,293

PY = pack years, U/W = alcohol units per week, ACE-27 = comorbidity score, AbsRisk = absolute risk, surg = surgery, CRT = chemoradiotherapy, RT = radiotherapy.

Some researchers found a higher risk for the development of SPTs in patients with regional lymph node metastases (N+ status) of the index tumor.[18, 19] In this study univariate analysis showed a significant difference in the cT-classification and tumor stage of patients a SPT in the HN region compared to the control group. However multivariate analysis showed no association between the cT- or cN-classification or tumor stage of the index tumor and the development of an SPT. This could be explained by the fact that an SPT is looked upon as an individual malignant entity, which is not related to the index tumor.[5]

A potentially interesting finding in our univariable analysis is that patients that developed a HN SPT more frequently received RT as (a part of the) therapy of their index tumor. This group includes patients that received only RT and patients received RT in combination with surgery and/or chemotherapy. This might be because RT treatment is often given to patients with more developed tumors. However, cT and cN classification did not prove to be predictive factors for SPT development. It could also suggest that RT increases the risk of developing an SPT within the RT field, as has been suggested by other researchers. Gao et al. reported that RT carried a 68% excess risk of developing an SPT in the HN region in patients who survived more than 5 years after laryngeal cancer.[22] A large retrospective study of more than 30.000 oral cavity HNSCC also showed that patients treated with radiation only or radiation with surgery had higher risks of developing an SPT, than patients treated with surgery only.[23] According to Rennemo et al. RT does seem to delay the occurrence of an SPT within the mucosa exposed to irradiation, with many SPTs occurring late during follow-up.[24]

Screening and follow-up

The incidence of esophageal SPTs in the present study (1.5%) falls in the incidence range of 1-6%, which were reported in other retrospective non-screening studies.[25] This study also showed an incidence of 15% in studies that actively screen for esophageal SPTs with Lugol chromoendoscopy. Lugol is a stain that is sprayed on the esophageal mucosa. Mucosal areas that are void of Lugol's stain are associated with dysplasia. The discrepancy between incidences of retrospective studies and screening studies could partially be explained by the differences between Western and Asian populations, since the majority of screening studies are performed in Asian populations. However, it is also possible that the stated incidence in non-screening studies underestimates the true incidence of esophageal SPTs in HNSCC patients. In that case it might be useful to screen HNSCC patients with Lugol chromoendoscopy to diagnose more esophageal SPTs.

Crippen et al. showed an average time to diagnosis of lung SPT of 6.7 years, with only 18% of the cases diagnosed in the first five years.[26] They also concluded that HN cancer patients in all subsites had a significantly higher relative risk of a lung SPT than the standard population. Additionally, Pagedar et al. reported that patients with low stage lung SPTs (after an index HN tumor) had a worse survival rate than patients with an index lung tumor and no SPT.[27] Combining the long time to occurrence and low survival rate of affected patients, screening for lung SPTs in patients treated for HNSCC does not seem to have a positive effect on their overall survival. Defining a subpopulation in which lung SPT screening is advantageous based on the subsite of the index HNSCC tumor proved to be difficult. A study by Lee et al. found that patients with index laryngeal tumors were most prone to develop SPTs.[8] These findings are in conflict with our results. We found a significant lower

risk for patients with a laryngeal tumor to develop an SPT in the HN-region, lungs or esophagus compared to patients with an index tumor in the oral cavity. Cloos et al. discussed the difference between tumors in different HN subsites.[28] They argue that this difference might be explained by the different embryogenetic development of the subsites and their different mucosal exposure to tobacco and alcohol.

Our cause-specific Cox regression analysis showed a moderate capability to predict the development of SPTs. Tobacco and alcohol use, comorbidity, and subsite in the oral cavity are the highest risk factors. Another study by Brands et al. concluded in their review that patients with oral squamous cell carcinoma have a lifelong risk for a SPT.[29] They discuss the benefit of routine follow-up and weigh the extra anxiety patients without new disease will experience against the possible gain of quality of life and survival of patients with an SPT. The risk model we have developed here might aid in a stricter selection of HNSCC patients who need to undergo long time follow-up of SPTs. We believe an increased awareness of the occurrence of lung and esophageal SPTs in HN cancer patients could lead to earlier SPT diagnosis. For example, a patient that experiences dysphagia after RT treatment for a HN tumor could suffer from (long-term) post-radiation complication, but their symptoms might also be caused by a esophageal SPT. In this case, an endoscopy might be warranted. Our results also show that, for example, patients with oral or oropharyngeal tumors are more prone to develop SPTs than patients with laryngeal tumors. Clinicians should be extra aware of possible SPTs in these subgroups of patients. Diagnosing SPTs at an earlier stage of development will of course increase the quality of life of patients compared to diagnosis at an later stage.

Limitations

Our study has some limitations that may have influenced our results. First, the number of patients with a lung or esophagus SPT was limited in this study. As a result, it was not possible to determine the risk factors for SPTs in these subsites. Second, it remained challenging to determine whether a lung malignancy is an SPT or a metastasis from the index HN tumor. Ideally, the genetics of both tumors should be determined. In this study loss of heterozygosity analysis was performed in most squamous cell carcinoma in the lungs. However, exceptions were made for patients with lung carcinoma which developed more than five years after the index tumor and for patients who were treated with a palliative intent. Finally, we might not have analyzed all possible risk factors that include the human papilloma and Epstein-Barr virus, which are known to be related to tumor development. Since we collected all our data at the moment of diagnosis of the index tumor, we were also not able to determine the risk of continuation of tobacco and alcohol use within our population. Despite these possible limitations, we managed to conduct a study with high quality data and data analysis that produced reliable and clinically useful results.

Conclusion

In this work, we identified that tobacco and alcohol use, comorbidity and the oral cavity subsite were the most pronounced risk factors for the development of an SPT for HNSCC patients. Despite our high-quality data and correction for competing risks in our prediction model for the development of SPTs, it should be further developed to allow clinical use. More research with larger groups per SPT subsite (HN region, lungs, or esophagus) is needed to provide HN clinicians with definitive recommendations regarding the follow-up of their patients and potential SPT screening regimes.

References

1. - Nederlandse Kankerregistratie, beheerd door IKNL (Netherlands Comprehensive Cancer Organization) © June 2018. <https://www.cijfersoverkanker.nl>. -
2. Priante AV, et al. - Second primary tumors in patients with head and neck cancer. - *Curr Oncol Rep* 2011.
3. McGurk M, et al. - Delay in diagnosis and its effect on outcome in head and neck cancer. - *Br J Oral Maxillofac Surg* 2005.
4. Seiwert TY, et al. - State-of-the-art management of locally advanced head and neck cancer. - *Br J Cancer* 2005.
5. Warren S, et al. - Multiple primary malignant tumors: A survey of the literature and a statistical study. - *American Journal of Cancer* 1932.
6. Hong WK, et al. - Prevention of second primary tumors with isotretinoin in squamous-cell carcinoma of the head and neck. - *N Engl J Med* 1990.
7. Mohan M, et al. - Oral field cancerization: an update on current concepts. - *Oncol Rev* 2014.
8. Lee DH, et al. - Second cancer incidence, risk factor, and specific mortality in head and neck squamous cell carcinoma. - *Otolaryngol Head Neck Surg* 2013.
9. Atienza JA, et al. - Incidence of second primary malignancies in patients with treated head and neck cancer: a comprehensive review of literature. - *Curr Med Res Opin* 2012.
10. Chu PY, et al. - Different patterns of second primary malignancy in patients with squamous cell carcinoma of larynx and hypopharynx. - *Am J Otolaryngol* 2010.
11. Dikshit RP, et al. - Risk factors for the development of second primary tumors among men after laryngeal and hypopharyngeal carcinoma. - *Cancer* 2005.
12. von Elm E, et al. - The Strengthening of Reporting of Observational Studies in Epidemiology (STROBE) statement: guidelines for reporting observational studies. - *Ann Intern Med* 2007.
13. - Netherlands Comprehensive Cancer Organization (IKNL) <https://www.iknl.nl/en>. -
14. Piccirillo JF, et al. - Prognostic importance of comorbidity in a hospital-based cancer registry. - *Jama* 2004.
15. Leemans CR, et al. - Richtlijn Hoofd-halstumoren. 2012. - <http://richtlijndatabasen/richtlijn/hoofd-halstumoren>
16. van Buuren S - <https://stefvanbuuren.name/fimd/>. -
17. Gerds TA, et al. - Absolute risk regression for competing risks: interpretation, link functions, and prediction. - *Stat Med* 2012.
18. Feng Z, et al. - Second primary cancer after index head and neck squamous cell carcinoma in Northern China. - *Oral Surg Oral Med Oral Pathol Oral Radiol* 2017.
19. Ko HH, et al. - Factors influencing the incidence and prognosis of second primary tumors in patients with oral squamous cell carcinoma. - *Head Neck* 2016.
20. Do KA, et al. - Second primary tumors in patients with upper aerodigestive tract cancers: joint effects of smoking and alcohol (United States). - *Cancer Causes Control* 2003.
21. Datema FR, et al. - Impact of comorbidity on short-term mortality and overall survival of head and neck cancer patients. - *Head Neck* 2010.
22. Gao X, et al. - Second primary cancers in patients with laryngeal cancer: a population-based study. - *Int J Radiat Oncol Biol Phys* 2003.
23. Hashibe M, et al. - Radiotherapy for oral cancer as a risk factor for second primary cancers. - *Cancer Lett* 2005.
24. Rennemo E, et al. - Reduced risk of head and neck second primary tumors after radiotherapy. - *Radiother Oncol* 2009.
25. Bugter O, et al. - Early detection of esophageal second primary tumors using Lugol chromoendoscopy in patients with head and neck cancer: A systematic review and meta-analysis. - *Head Neck* 2019.
26. Crippen MM, et al. - Second primary lung malignancy following head and neck squamous cell carcinoma. - *Laryngoscope* 2019.
27. Pagedar NA, et al. - Second Primary Lung Cancer After Head and Neck Cancer: Implications for Screening Computed Tomography. - *Ann Otol Rhinol Laryngol* 2015.
28. Cloos J, et al. - Increased mutagen sensitivity in head-and-neck squamous-cell carcinoma patients, particularly those with multiple primary tumors. - *Int J Cancer* 1994.
29. Brands MT, et al. - Time patterns of recurrence and second primary tumors in a large cohort of patients treated for oral cavity cancer. - *Cancer Med* 2019.

Chapter 3

Electron microscopy and field cancerization

Early upper aerodigestive tract cancer detection using electron microscopy to reveal chromatin packing alterations in buccal mucosa cells

Oisín Bugter, MD* & Yue Li*; Anouk Wolters; Vasundhara Agrawal; Amil Dravid; Andrew Chang; Jose Hardillo; Ben Giepmans; Robert Baatenburg de Jong; Arjen Amelink; Vadim Backman; Dominic Robinson

* Authors contributed equally to this work.

Accepted at Microscopy and Microanalysis, May 2021

Abstract

Background. A profound characteristic of field cancerization is alterations in chromatin packing. This study aimed to quantify these alterations using electron microscopy image analysis of buccal mucosa cells of laryngeal, esophageal, and lung cancer patients.

Methods. Analysis was done on normal-appearing mucosa, believed to be within the cancerization field, and not tumor itself. Large-scale electron microscopy (nanotomy) images were acquired of cancer patients and controls. Within the nuclei, the chromatin packing of euchromatin and heterochromatin was characterized. Further, the chromatin organization was quantified through chromatin packing density scaling.

Results. A significant difference was found between the cancer and control groups in the chromatin packing density scaling parameter for length scales below the optical diffraction limit (200 nm) in both the euchromatin ($p = 0.002$) and the heterochromatin ($p = 0.006$).

Conclusions. The chromatin packing scaling analysis also indicated that the chromatin organization of cancer patients deviated significantly from the control group. They might allow for novel strategies for cancer risk stratification and diagnosis with high sensitivity. This could aid clinicians in personalizing screening strategies for high-risk patients and follow-up strategies for treated cancer patients.

Introduction

Head and neck (HN), esophageal, and lung cancer are all frequently occurring types of tumors [1-3]. They are often referred to as upper aerodigestive tract (UADT) tumors. Worldwide, an estimated more than three million new cases were diagnosed in 2018, and more than two million patients died of the consequences[4]. These three tumor types share the two most important risk factors for their development: smoking and for the HN region and esophagus also alcohol [5-7]. Tobacco and alcohol use cause physiological and mutagenic effects on the exposed mucosa of the UADT. Unfortunately, a large percentage of UADT tumors are diagnosed in advanced stages of development, often limiting the treatment options and survival chances of diseased patients [3, 8, 9]. Diagnosing more tumors in an early stage of development could have a significant positive impact [3, 10, 11]. Patients with early-stage UADT tumors could benefit from complete surgical resection or curative radiotherapy, whereas treatment of patients with high-stage tumors is sometimes not with curative intent [9].

Early tumor detection by screening asymptomatic high-risk patients holds the potential to increase the survival rate of lung cancer patients substantially. Upper aerodigestive tract tumors, in theory, appear ideally suited to such screening because of (a) the association of identifiable risk factors, (b) the survival advantage of early diagnosis, (c) the significant morbidity and mortality associated with the disease. At present, there are no national screening programs for HN, esophageal, or lung cancer in Western countries. Some issues screening initiatives are facing is the low sensitivity for early-stage tumors, the substantial population of at-risk persons, and the risk of overdiagnosing due to false-positive results [7, 12].

A novel yet effective approach to cancer screening is focused on detecting changes in apparently histologically normal tissue described as field cancerization (FC). Field carcinogenesis is the notion that a multitude of physiological and nanoscale architectural alterations affect an entire organ or tract before ultimately resulting in a focal neoplasm in one area of the organ [13]. There is evidence that FC of HN, lung, and esophageal cancers encompasses the entire UADT [14]. This concept is supported by the high incidence of second primary tumors in patients with UADT tumors [15, 16]. The FC tissue alterations occur superficially in the epithelial layer, the basal membrane, and the vascularized papillary layer of the lamina propria. They include alterations in the microvasculature and the tissue nanoscale architecture, such as the organization of the chromatin, the cytoskeleton, and the size and structure of cell nuclei and organelle [17, 18]. Accurate detection of FC could potentially be used to pre-screen for UADT tumors [14, 19, 20]. Optical techniques have proven to be sensitive to detect the changes in the nano-organization of tissue [21]. The

detection of FC could potentially be used as a risk-stratification method to decrease the population size of persons at risk for UADT tumors.

A technique to assess and visualize the nano-anatomy of tissue, in our case, buccal mucosa, is electron microscopy (EM). One of the downsides of EM imaging at high resolution is typically a small field of view of a given tissue sample, which makes it difficult to correlate changes at high magnification to a wide tissue scale. To tackle this problem, we applied large-scale EM (nanotomy), which allows for ultrastructural examination of tissue, cells, organelles, and macromolecules in a single data set [22, 23]. A nanotomy data set combines thousands of conventional EM images. Moreover, the software allows zooming in and out of the image from a total overview to nanoscale resolution in a ‘Google Earth’ approach. Using this technique, large areas of tissue are scanned and presented online. A significant advantage of nanotomy over conventional EM is unbiased data acquisition, presentation, and sharing at high resolution [22, 23].

A promising target to analyze as a possible alteration due to FC is the quantification of chromatin organization in the cell nucleus. As the carrier of genetic information, chromatin forms and regulates the nano-environment in which transcription happens [24]. Higher-order chromatin organization is essential in regulating gene transcription, and abnormalities in such an organization are associated with a variety of diseases, including neurological disorders, autoimmune diseases, and cancer. While nuclear blebbing and chromatin condensation (> 200 nm) has been identified by optical microscopy as a hallmark for carcinogenesis, little is known about chromatin organization before this stage of progression of cancer at an even smaller length scale [25]. Due to the optical diffraction limit of approximately 200 nm, it requires super-resolution optical microscopy, nanoscale-sensitive optical spectroscopy, or microscopy techniques that utilize different illumination sources with a wavelength smaller than light, such as neutrons, electrons, and x-ray [26, 27].

High-resolution electron tomography experiments with DNA-specific staining showed that chromatin consists of disordered polymers with a diameter ranging from 5-24 nm with a differential packing density throughout the nucleus [28]. A classical polymer is expected to exhibit self-similar, fractal behavior across all length scales, and the fractal dimension is determined by the balance between polymer-polymer and polymer-solvent interaction as well as constraint-processes such as, in the case of chromatin, loop formation in part driven by extrusion, transcriptional, and lamin-associated processes [29, 30]. For chromatin, it has been reported that the chromatin polymer forms spatially segregated packing domains with sub-Mb genomic size, sub-200 nm physical size, and internal fractal structure [31, 32]. The packing configuration plays an important role in regulating gene transcription by dictating chromatin accessibility and the diffusion rate of transcriptional reactants such as

transcription factors [33, 34]. Importantly, shown through computational modeling, optical studies, and EM studies, the fractal dimension of chromatin packing domains has a non-monotonic relationship with active transcription. It also plays a critical role in the regulation of transcriptional plasticity of cells and their access to the genomic landscape [33]. A mass fractal can be characterized by a power-law spatial autocorrelation function (ACF), $ACF \sim r^{(D-3)}$, with D being the fractal dimension. Previous work has shown that the chromatin of more aggressive tumors exhibits an increase in the fractal dimension of the chromatin [35].

In this work, we analyzed normal-appearing buccal mucosa from patients with tumors elsewhere in the UADT (larynx, esophagus, and lungs). We hypothesized that the ACF and the fractal dimension D of patients with cancer differs from the control group. In order to utilize the large-scale EM data, we developed a novel convolutional neural network (CNN) to segment the nucleus from the tissue bed in gray-scale images. We further quantified the fractal dimension D of the euchromatin and the heterochromatin independently to investigate ultrastructural alterations in the buccal mucosa cells of patients with UADT cancers and control subjects. If proven that cancer patients have an altered chromatin packing in the mucosa adjacent to their tumor, this may be a step towards the development of novel and sensitive tools for cancer screening.

Materials and Methods

Subjects

This study was approved by the Medical Ethics Committee of the Erasmus MC (MEC-2017-551). Patients were recruited from the departments of 'Otorhinolaryngology and Head and Neck Surgery', 'Gastroenterology and Hepatology', and 'Pulmonology' of the Erasmus MC Cancer Institute. Patients with UADT malignancies and non-oncologic control patients were included. In this study, we also include the lungs under the 'umbrella term' UADT. The oncologic group consisted of patients with primary and untreated HN (all laryngeal cancer), esophageal, and lung cancer (all subsites and stages). The non-oncologic control group consisted of patients with chronic rhinosinusitis with or without nasal polyps, chronic obstructive pulmonary disease, or gastrointestinal diseases. The absence of occult, unexpected malignancies in this group was confirmed using an endoscopic examination or imaging. Patients with a medical history of malignancies were excluded. All patients signed an informed consent form before enrollment in this study. Patient and tumor-specific data such as date of birth, sex, substance abuse, tumor stage, and tumor type were collected using the electronic medical patient record.

Biopsy procedure

The buccal mucosa biopsies were performed at the outpatient clinics. The biopsies were performed on normal-appearing mucosa and at least 5 cm from the primary tumor. First, local buccal mucosa anesthesia was given with a submucosal injection of approximately 1 mL xylocaine 2% - adrenaline 1:80.000. Second, the buccal mucosa was slightly turned 'inside out' manually to have optimal visualization to perform a 2 mm Ø punch biopsy. The sample was cut from the subcutaneous tissue with a curved iris scissor without lifting the sample with a pair of forceps or tweezers. In this way no external pressure was applied on the biopsy, maintaining the mucosa organization as optimally as possible before placing the biopsy in a fixative. Finally, the pressure was applied to the biopsy location with a singular gauze for approximately 1 minute. Sutures were not needed.

Sample preparation, image acquisition, and automated annotation

The sample preparation and image acquisition protocols were described in detail previously [22]. In short, fresh buccal mucosa samples were immediately fixated in small vials in 3 mL solution of 0.5% paraformaldehyde, 2% glutaraldehyde, and 0.1 M sodium cacodylate (pH 7.4) and stored at 4 °C. They were washed in 0.1 M sodium cacodylate and postfixed in 1% osmium tetroxide and 1.5% potassium ferrocyanide. The samples were dehydrated in ethanol by incubations in increasing ethanol concentrations. They were then embedded in epoxy resin and sectioned with a diamond knife to ultrathin sections of ~ 80 nm. Sections were mounted on formvar coated copper grids and stained with 2% uranyl acetate in water and Reynold lead citrate.

Image acquisition was performed with a Supra 55-VM scanning EM (Carl Zeiss AG, Oberkochen, Germany) with ATLAS software (Fibics Incorporated, Ottawa, Canada). We used scanning EM with an external scan generator capable of acquiring multiple large fields of view at high resolution using scanning transmission EM detection. One image generated this way is equivalent to the fields of view of ~ 100 transmission EM images, which significantly reduces the amount of stitching needed. Samples were recorded at a 2.5 nm pixel size. Scans were stitched, and raw data sets were rendered as HTML files.

Nucleus segmentation using a convolutional neural network (CNN)

The CNN employed to segment the nucleus from the large-scale STEM images in this work was initially trained with TEM cheek cell electron micrographs by Dravid (Figure 1).[36] The CNN model is based on the Deep Residual U-Net, a residual learning framework for substantially deeper networks. It has shown significant success in segmentation tasks such as road extraction.[37] The Deep Residual U-net relies on an encoder-decoder structure proposed in the original U-Net encoder-decoder model, whereby an image is down-sampled to its features of interest via the left branch of the model as seen in Figure 1a, and then up-

the opposite pattern: 256, 128, then 64 filters. Overall, these convolutions learn features of the input TEM image that will contribute to the segmentation.

The network was trained for 30 epochs. By the end of every epoch, each training example has been fed into the network. Based on these training examples, the network adjusts the parameters of the internal operations in order to learn a better mapping between each micrograph and its corresponding segmentation. Multiple epochs, or passes through the entire dataset, are required for the optimization process to iteratively adjust the parameters. The number of epochs was set to 30 in order for the model to learn an effective mapping but avoid a neural network's tendency to "memorize" non-generalizable oddities specific to the training examples. This phenomenon, known as "overfitting", occurs when training for too many epochs. Two input micrographs were fed in simultaneously at a time to train the model faster than with one input. However, the amount of video memory limits how many inputs could be processed at a time to two. The Adam optimization algorithm was then employed to adjust the parameters in order to converge to an optimal segmentation model [40]. The learning rate was set to 10^{-5} to control the magnitude of each optimization step and the standard binary cross-entropy loss function was used for monitoring the effect of this optimization process on adjusting the model's performance.

Accuracy was evaluated using the dice coefficient, which compares which pixels were correctly predicted to be the nucleus between the original input and generated segmentation mask. Using 300 training examples, an accuracy of 96% was achieved. This was implemented in the Keras library with a Tensorflow backend on a machine equipped with an NVIDIA GTX 1080, Core i7 CPU, and 32 GB of RAM.

The electron micrographs containing cheek buccal mucosa cells were manually selected for downstream nucleus segmentation. Limited by the available RAM, the images were first downsized by a factor of 4 before feeding them to the CNN. The output masks were upsampled to recover the original resolution. Active contour algorithm (Matlab, MathWorks) was used to refine the boundary of the nucleus mask based on the morphological features in the original EM images.

Spatial autocorrelation function

STEM images of ~ 80 nm thin sections were used in the analysis of chromatin packing density alterations between cancer patients and controls. The bright-field contrast in STEM attenuates following Beer's law,

$$I(x, y) = I_0 e^{-\sigma \rho(x, y) t}. \quad (1)$$

Where $I(x, y)$ is the STEM bright-field image intensity distribution, I_0 is the incident beam intensity, σ is the absorption coefficient of the biological sample to the incident beam, $\rho(x, y)$ is the density distribution, and t is the section thickness. In our experiment, I_0 and t were controlled to be constant for all images, and we assumed that the biological sample has a relative constant σ given current resolution. As a result, only the chromatin density $\rho(x, y)$ contributes to the final image intensity $I(x, y)$. To obtain the density fluctuation function, $\rho_\Delta(x, y)$, we took the negative logarithm of the STEM images and then subtracted the mean value from the image. At the same time, the incident beam intensity I_0 is canceled out.

Next, the two-dimensional ACF was calculated from the density fluctuation obtained from the STEM images using the Wiener- Khinchine relation:

$$B_\rho(x, y) = F^{-1}\{|F(\rho_\Delta(x, y))|^2\} \quad [35]. \quad (2)$$

Where F^{-1} and F is the inverse Fourier, and the Fourier transform, respectively, and the ρ_Δ represents the fluctuations in the chromatin density. To minimize the noise, a rotational average of $B_\rho(x, y)$ was taken to obtain the final form of the ACF, $B_\rho(r)$, representing the correlation of chromatin density as a function of spatial separation r . Notice that mathematically, a fractal structure can be characterized by a power-law ACF, $B_\rho(r) \sim r^{D-3}$, with D being the fractal dimension. To analyze the chromatin packing structure from the experimental ACF obtained, we fit the ACF to the Whittle-Matérn (WM) family of correlation functions [41]. WM is defined as the product of a power law and a modified Bessel function of the second kind ($K_{\frac{D-3}{2}}$) of the order $\frac{D-3}{2}$.

$$B_\rho(r) = A_\rho \left(\frac{r}{l_n}\right)^{\frac{D-3}{2}} K_{\frac{D-3}{2}}\left(\frac{r}{l_n}\right). \quad (3)$$

In (3), A_ρ , l_n , and D are fitting parameters. A_ρ is the density fluctuation amplitude; l_n is correlation length indicating the characteristic length of chromatin heterogeneity; the dimension D controls the shape of ACF, such that $D \rightarrow \infty$ for Gaussian; $D = 4$ for exponential; $3 < D < 4$ for stretched exponential; and $D < 3$ for power-law shape of the ACF. Particularly, when $D < 3$, the biological medium can be considered a mass fractal and D takes the special meaning of the fractal dimension.

Each nucleus was segmented using the CNN. As heterochromatin and euchromatin are genetically distinct and have a different affinity to osmium and uranyl/lead staining, they were segmented from the nucleus using automated grayscale thresholding. In special cases where the chromatin in the cell nucleus was composed primarily of the euchromatin, we did not

conduct ACF analysis for the heterochromatin, as the resulting ACF would not have been representative of the true statistics of the chromatin packing. Mean ACF was calculated from all the cells of the same patient for both euchromatin and heterochromatin. For each mean ACF, the D value for euchromatin and heterochromatin was obtained by WM fitting from $r = 79$ nm to $r = 200$ nm in correspondence to the section thickness. In particular, the fitting range of D is constrained by $\frac{5}{3} \leq D \leq 4$, the boundary values represent physiological values for reported in published work [35]. In addition, the D value was also calculated for each cell. Overall, 253 cells from 20 patients were analyzed (control: $N_{\text{patient}} = 6$, $N_{\text{cell}} = 68$; lung cancer: $N_{\text{patient}} = 1$, $N_{\text{cell}} = 10$; esophagus cancer: $N_{\text{patient}} = 6$, $N_{\text{cell}} = 78$; HN cancer: $N_{\text{patient}} = 7$, $N_{\text{cell}} = 97$). Figure 2 summarizes the methods utilized for the image analysis and evaluating D.

Statistical analysis

The quantitative variables were non-normally distributed and thus the values were expressed as the median and interquartile range (IQR). Differences between groups were analyzed with the Mann-Whitney U test. Categorical data were reported as frequencies and percentages and differences between groups were analyzed using the chi-squared test or Fisher's exact test. For ACF analysis, a two-sample Kolmogorov-Smirnov (K-S) test was performed to evaluate the difference of ACF values between the control and cancer groups, as the K-S test is sensitive not only the median of the ACFs but also to the shape, which is characteristic of the underlying structure of chromatin packing. For D values calculated from mean ACFs per patient, a two-sided Wilcoxon rank-sum test was employed. For D values calculated from individual ACF per cell, student t-test was used. Statistical analysis was performed using SPSS (IBM Corp., Armonk, NY, USA) and MATLAB (MathWorks, Natick, MA, USA). The cut-off for significance was set at $p < 0.05$.

Results

Large-scale EM datasets for buccal mucosa biopsies

Normal appearing buccal mucosa biopsies from twenty patients were included in this study: 14 patients with cancer (7 HN, 6 esophageal, and 1 lung cancer) and 6 non-oncologic controls. Their baseline characteristics are presented in Table I. There was a non-significant difference in the percentage of males between the cancer and control groups (66.7% and 78.6%). The median age between the cancer and control groups was also similar (69.0 [IQR 66.0-72.8] vs. 62.0 [IQR 57.2-74.5] years). Only the HN cancer group had a significantly higher amount of pack years than the control group. Six patients (42.9%) of the cancer group had a stage I, two patients (14.3%) a stage II, five patients (35.7%) a stage III, and one patient (7.1%) a stage IV carcinoma.

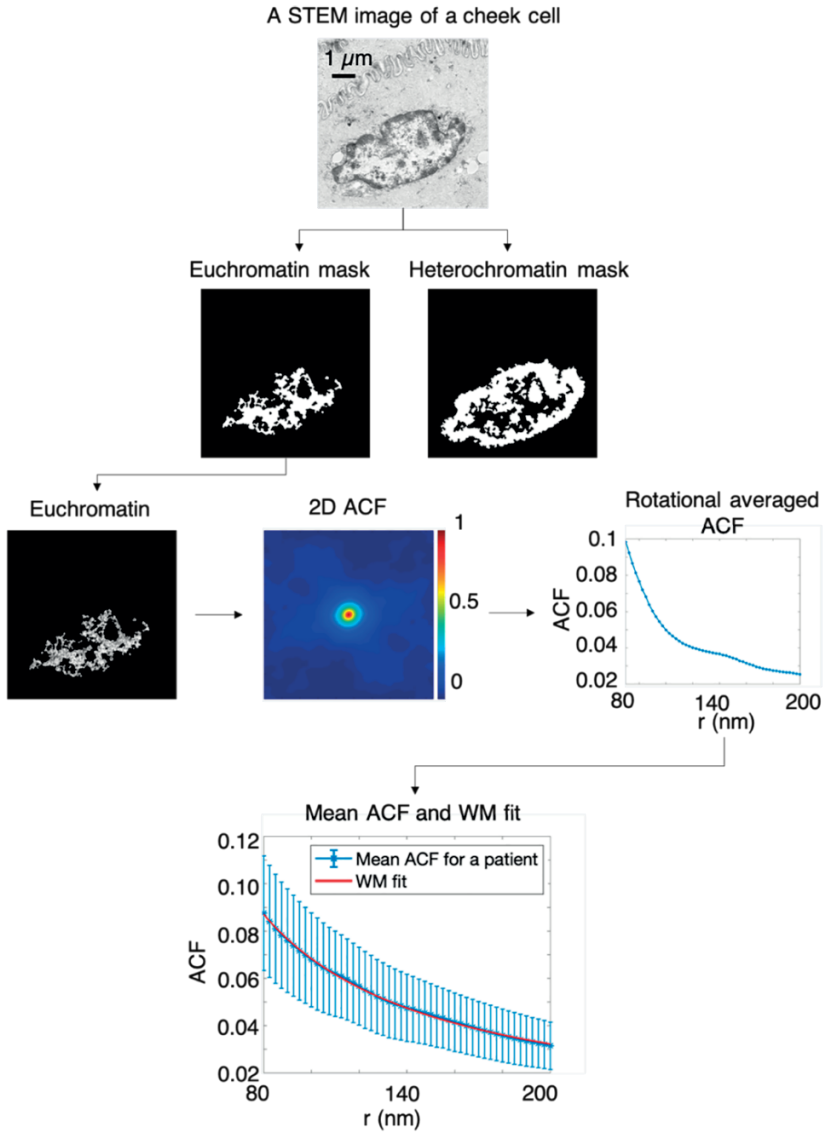


Figure 2. Workflow of obtaining chromatin packing D from a STEM image of a cheek cell. The nucleus is segmented using the CNN trained specifically for this task with electron micrographs. The masks for euchromatin and heterochromatin are further created from the mask for the nucleus using automatic grayscale intensity thresholding. While the heterochromatin is mainly located in the periphery of the nucleus, some penetrates the nuclear interior space. On the other hand, the euchromatin primarily distributes in the interior of the nucleus. 2D ACF is calculated for both euchromatin and heterochromatin separately, and the rotational average is employed to remove the noise from the ACF curve. Mean ACF is obtained by averaging ACFs of individual cells for each patient, and WM fitting is used to quantify chromatin packing in terms of D. The fitting range is from $r = 80$ nm to $r = 200$ nm, as the section has a finite thickness of 80 nm, and the ACF curve is smoothed for length scales below 80 nm due to projection.

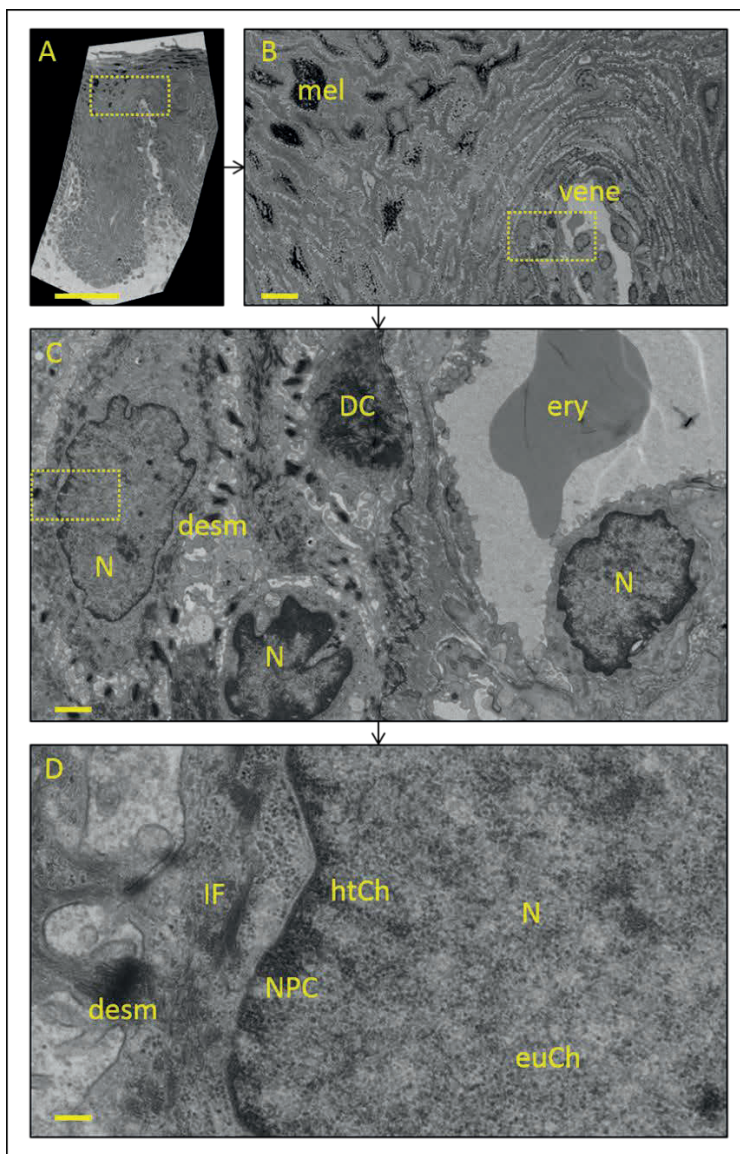


Figure 3. Nanotomography of buccal mucosa of an esophageal cancer patient. A large area of 0.2x0.4mm is recorded at 2.5 nm pixel size. This allows to compare histological known landmarks up to macromolecular complexes. (A) Overview allows to discriminate layers of the epithelium of the mucosa: stratum basale; stratum spinosum; stratum intermedium; stratum superficiale (for reference to the different layers see Sokol et al.[42]) (B) Zooming in allows to recognize a vein, melanocytes (mel) and other mesoscale structures. (C) Further zooming discloses other cell types such as an erythrocyte (ery); organelles such as nuclei (N), desmosomes (desm), as well as a desmosome cluster (DC). At the maximum resolution macromolecules such as intermediate filaments (IF), nuclear pore complexes (NPC) as well as euchromatin (euCh) and heterochromatin (htCh) can be identified. Note that this is a poor presentation of the data present: all data is available at high resolution in zoomable datasets via <http://nanotomography.org/OA/index.html>. The dataset used for this figure is 2016-194. Bars: 100, 10, 1, 0.2 μm.

Table 1. Baseline characteristics of included patients.

	Control (n = 6)	Cancer (n = 14)	P-value	Tumor sublocations of cancer group					
				HN (n = 7)	P-value	Esoph. (n = 6)	P-value	Lung (n = 1)	P-value
Male, n (%)	4 (66.7)	11 (78.6)	0.613	7 (100.0)	0.192	4 (66.7)	1.000	0 (0.0)	0.429
Age, median (IQR)	62.0 (57.2-74.5)	69.0 (66.0-72.8)	0.284	69.2 (66.3-73.2)	0.568	70.1 (66.3-75.5)	0.200	64.3 -	0.617
Smoking			0.067		0.099		0.059		0.459
Never	3 (50.0)	1 (7.1)		-		1 (16.7)		-	
Past	1 (16.7)	8 (57.1)		3 (42.9)		5 (83.3)		-	
Current	2 (33.3)	5 (35.7)		4 (57.1)		0 (0.0)		1 (100.0)	
Smoking PY, median (IQR)	6.3 (0.0-28.5)	30.0 (11.9-36.3)	0.081	35.0 (30.0-40.0)	0.031*	21.2 (7.5-30.6)	0.413	24.0 -	0.604
Tumor stage, n (%)									
I		6 (42.9)		5 (71.4)		1 (16.7)		0	
II		2 (14.3)		0		1 (16.7)		1 (100.0)	
III		5 (35.7)		2 (28.6)		3 (50.0)		0	
IV		1 (7.1)		0		1 (16.7)		0	
Tumor type, n (%)									
PCC		12 (85.7)		7 (100.0)		3 (50.0)		1 (100.0)	
Adeno		2 (14.3)		0		3 (50.0)		0	

HN = head and neck, esoph. = esophagus IQR = interquartile range, PY = pack years, SCC = squamous cell carcinoma. P-value are compared to the control group. * = p-value < 0.05.

The large-scale EM datasets of the buccal mucosa biopsies are available to view online at <http://nanotomy.org/OA/index.html>. The nanotomy images show the non-keratinizing epithelial layer of the buccal mucosa and the superficial part of the lamina propria including the capillaries. The basal layer is located in between the two layers (Figure 3).

Nucleus segmentation pipeline with a pre-trained CNN

Figure 1 showcases the implemented Residual U-Net architecture. A 640x640x1 grayscale EM image with a cheek cell nucleus is downsampled through convolutions within each residual block, ResBloc (Figure 1b) is employed to obtain a smaller-scale image consisting of the features of interest that can benefit the accuracy of the model. The right side of the model CNN consists of upsampling operations, which restore the size of the image. The skip connections pass fine details, which are lost through downsampling, over to the right side of the network to relay the structure of the STEM micrograph in the final binary segmentation mask.

Characterizing chromatin packing using ACF for cheek cells in control and cancer groups
We utilized the grayscale image intensity in the STEM micrographs to characterize the spatial heterogeneity of chromatin density distribution. We quantified the relative magnitudes and

length scales of all spatial fluctuations in the degree of chromatin compaction via its ACF, $B_p(r)$. Upon comparison of chromatin density correlation between the controls and cases representing various cancers, we have found a qualitative difference in chromatin packing at subdiffractive length scales (Figure 4a-b). Using K-S tests, we confirmed that the ACFs for overall control ($n = 6$) and cancer group ($n = 14$) are statistically significantly different ($p < 0.001$) for both the euchromatin and the heterochromatin at all length scales. The mean ACFs for individual diagnostic groups are shown Figure 4c-d.

Quantifying chromatin packing alterations using packing scaling factor D

We further quantified the chromatin packing scaling D below the optical diffraction limit in terms of D by fitting the ACFs to WM-family of functionals (Figure 5). The fitting range was chosen to be from 80 nm to 200 nm (optical diffraction limit). As the resin sections for STEM imaging have a similar finite thickness of around 80 nm, the ACF will overestimate the correlation of chromatin density fluctuation below this length scale due to the projection average. For the overall control group, we obtained a median D value of 1.77 (IQR 1.67 – 1.90) for the euchromatin and 2.24 (IQR 1.67 – 2.41) for the heterochromatin. For the overall cancer group, we obtained a median D value of 2.24 (IQR 2.12 – 2.48) for the euchromatin, and 3.00 (IQR 2.52 – 4) for the heterochromatin. We employed Wilcoxon rank-sum to quantify the alteration in D distribution for the control and the cancer group, and obtained significant statistical difference for both the euchromatin ($p = 0.002$) and the heterochromatin ($p = 0.006$). Particularly, $5/3 < D < 3$ is indicative of underlying mass-fractal chromatin structure, $D > 3$ suggests a non-fractal distribution of chromatin density that is consistent with a stretched exponential function. Significantly, we observed that cancer patients showed an increase in median packing scaling D by 26.6% for the euchromatin, and by 33.9% for the heterochromatin. In addition, the median value of D for the heterochromatin of the cancer patients equals 3, suggesting a fundamental alteration in chromatin packing, which can have a substantial effect in regulating gene transcription and phenotypic plasticity [34]. Since a small number of patients were employed in the analysis, we further quantified the chromatin packing scaling for every cell within each group, and evaluated the statistical difference between control patients and cancer patients (Figure 5e-f). Overall, we observed a significant difference between chromatin packing scaling for the control group ($n = 76$) and the cancer group ($n = 219$) in both the euchromatin ($p = 0.010$) and the heterochromatin ($p = 0.007$).

Discussion

This study is, to our knowledge, the first to utilize large-scale EM images to investigate FC tissue changes associated with cancer of the UADT. Our aim was to investigate whether these changes could be used to discriminate cancer patients from controls. Utilizing spatial

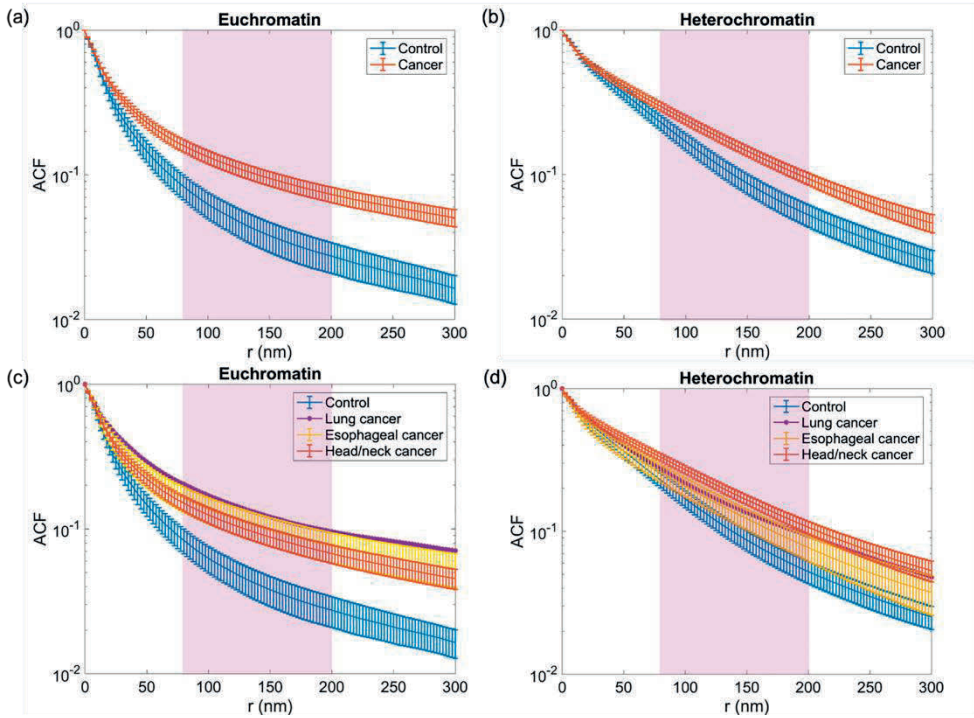


Figure 4. Differentiation of control versus cancer cells based on chromatin packing alterations using ACF analysis. ACFs for the euchromatin (a) and the heterochromatin (b) for the all control (blue) and the all cancer (red) group show distinct chromatin packing within $80 \text{ nm} < r < 200 \text{ nm}$ (purple shaded region) with $p < 0.001$. The breakdown of ACFs by diagnosis is shown in (c) for the euchromatin and (d) for the heterochromatin. The ACFs were calculated from averaging the mean ACFs per patient, and the error bars represent the standard error.

correlation function analysis, we characterized chromatin packing below the optical diffraction limit and identified significant changes between for control and cancer groups in both the euchromatin and the heterochromatin contents. Moreover, we showed that the difference in fractal dimensions calculated from the spatial correlation function agrees with the well-known hallmarks of cancer but manifested at a much smaller length scale. These results highlight that the alterations in chromatin observed in the field of a tumor represent an early-stage event of carcinogenesis.

Elevated D is a hallmark of cancer cells and has been reported through multiple lines of work using Partial Wave Spectroscopic (PWS) microscopy in colorectal, lung, and breast cancers [43, 44]. From a theoretical perspective, the spatial arrangement of chromatin packing affects large scale gene expression patterns through a number of physical regulators, such as chromatin volume concentration, accessible surface area, and chromatin packing scaling D [34, 45]. Particularly, chromatin with an increased D in the tumor field can select

for a higher transcriptional and adaptive potential. This ability, in turn, may facilitate the prognosis of tumor cells independent of tumor type, stage, demographic factors, and molecular transformations [34]. Recently, utilizing EM, Cherkezyan and Stypula et al. reported the existence of significant alterations in chromatin packing in the colorectal cancer field in both human and animal models [35]. They identified a profound shift of chromatin organization: the chromatin of cancer subjects had chromatin with a higher fractal dimension or, in some cases, adopted a non-fractal configuration, while the control subjects had a normal fractal chromatin structure. In the same vein, optical nanosensing showed an increase in the fractal dimension of chromatin in the field cancerization associated with a variety of malignancies [46]. In the present study, we have also identified similar alterations in chromatin packing comparing the cancer group with the control group.

A previous series of studies by our group had the same aim as the present study: discriminating cancer patients from controls by detecting FC tissue changes [47-49]. In these studies, *in vivo* multidiameter single-fiber reflectance (MDSFR) spectroscopy measurements were performed on the buccal mucosa of a larger cohort of UADT cancer patients, including the twenty included in the present study. This provides an opportunity to compare the EM images analysis results with the scattering results from optical spectroscopy. A logical hypothesis would be that an increased D in cell nuclei will correlate with an increased power of scattering of light during spectroscopic measurements. Though not significantly different, we indeed found a tendency for the scattering power of μ_s' to be higher for cancer patients. Possibly, this difference was not significant because, although the patients included were the same, the measured tissue volumes were not. In the EM study, the cell nuclei were segmented and isolated, while in the spectroscopic studies the optical properties of the complete cells of the mucosal top layer were averaged. By studying the ultrastructural changes in chromatin organization, it is possible to detect initial stages of various kinds of cancers. It is important to note that in this work, instead of a single cancer model, we assessed three types of cancers and their controls: head/neck, esophageal, and lung cancer. The direction of alterations in chromatin packing in terms of D is consistent for all cancer groups compared to the control group. This probably reflects the fact that these three organs that encompass the UADT all have their embryological origin in the early foregut [50]. The UADT also encompasses the oral cavity which is a predominant and prevalent site of development of (pre)malignancies, because it comes into direct contact with many carcinogens.

Although not explored in this work, there are several implications of an increasing D in chromatin packing in FC. Besides buccal mucosa cells investigated in this work, there is a plethora of different types of cells along the spectrum of differentiation within buccal mucosa imaged in the large-scale EM dataset. A similar trend in chromatin packing for basal and

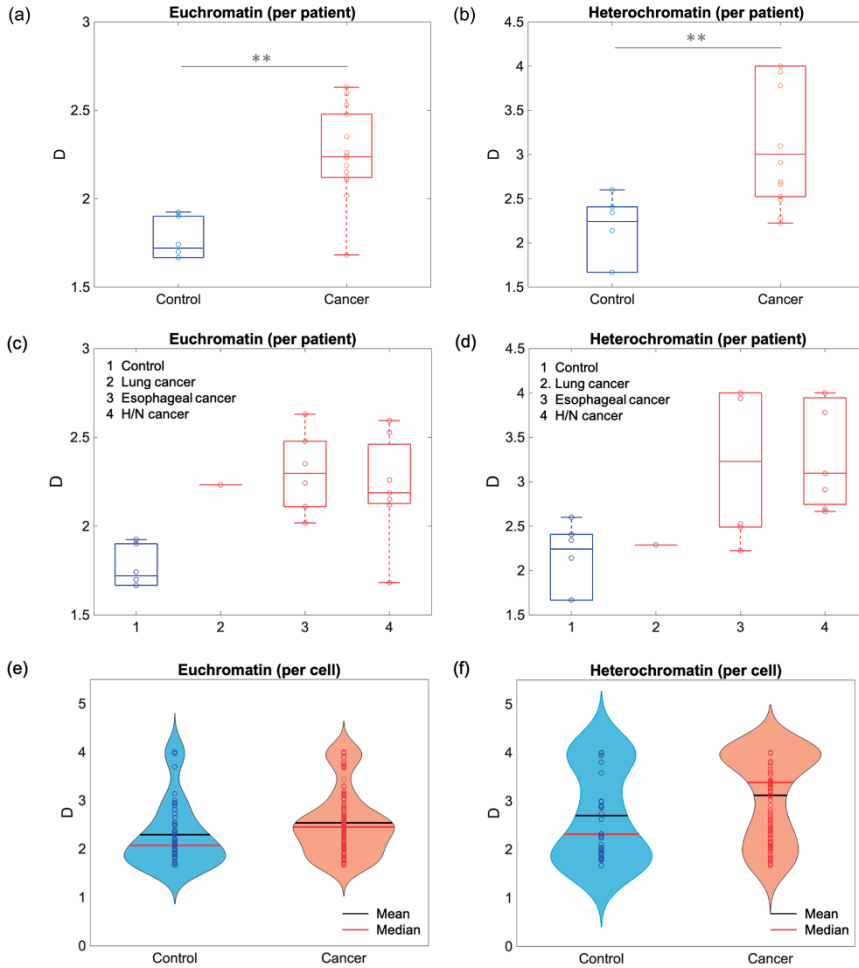


Figure 5. Quantifying chromatin packing alterations using packing scaling D . Mean ACF per patient was employed in calculating D within the length scales under the diffraction limit. For all control and cancer patients, the difference in D is statistically significant for the euchromatin (a) with p -value = 0.002 and the heterochromatin (b) with p -value = 0.005. For each diagnostics category, the head/neck cancer shows a significant difference compared to the control group, while the esophageal only exhibits moderate difference for the euchromatin (c) with p -value = 0.015 for H/N cancer and p -value = 0.004 for esophageal cancer and the heterochromatin (d) with p -value = 0.003 for H/N cancer and p -value = 0.037 for esophageal cancer. Chromatin packing scaling distribution calculated from each cell for (e) the euchromatin and (f) the heterochromatin. The black line denotes the mean value and the red line represents the median value

pickle layers is expected. Therefore, this dataset gives us the opportunity to study the effects of differentiation progression on higher-order chromatin organization. It is expected that as the phenotypic plasticity decreases during differentiation, the chromatin packing scaling would also decrease. Although the CNN was trained to segment the nucleus of epithelial

cells, transfer learning can be implemented to tune the CNN to adapt quickly to other types of cells.

The clinical applicability of the method and results described in the present study will probably not be in the shape of a diagnostic tool for routine use. At present the analysis is too time consuming and not cost effective. However, our findings did confirm the presence of ultrastructural field effect changes in the buccal mucosa of patients with distant UADT tumors and that these changes can be used to differentiate them from non-oncologic controls. This paves the way for existing optical techniques, like MDSFR spectroscopy or PWS microscopy to utilise and quantify these changes so that they may be applied in clinical practice. These techniques are easy-to-use, fast and non-invasive and might be used to screen for distant tumors or aid surgeons in achieving adequate tumor resection margins.

There are several limitations to our study design that should be considered. First, the number of patients included was limited, and more patients need to be recruited to validate our current findings. This was especially true for the lung cancer group with only one patient. Second, the segmentation of the euchromatin and the heterochromatin relies solely on the EM image intensity. Labeling molecular markers, such as histone modifications, are required for a more rigorous and accurate separation of those two compartments. The resin sections of tissue biopsy in our study have a finite thickness of ~ 80 nm, and projections instead of 3D tomography of the sections were used. Due to the intensity averaging along the z-direction, the ACFs calculated from the projection images do not reflect the chromatin packing at length scales below the thickness of the section, and therefore, restricted our analysis to larger length scales. In order to investigate the chromatin alterations at a finer scale, future studies can incorporate thinner sections or electron tomography.

Conclusion

We identify significant quantitative nanoscale alterations in chromatin packing in FC for UADT cancers. Through large-scale EM datasets and high-throughput image processing using CNN, we confirm that the ultrastructural field effect changes of the nuclear organization are a hallmark of cancer. We propose that the CNN segmentation pipeline and the downstream nanoscale nuclear abnormalities identified here can be employed as biomarkers for FC. The large-scale EM nanotome data sets combined with semi-automated data analysis might overcome previous clinical applicability issues, such as the long duration of the analysis. Optical techniques like MDSFR spectroscopy or PWS microscopy could also utilize the abnormalities in chromatin packing for the diagnosis and risk stratification of cancer.

References

1. Ferlay J, et al. - Cancer incidence and mortality worldwide: Sources, methods and major patterns in GLOBOCAN 2012. - *Int J Cancer* 2015.
2. Torre LA, et al. - Global cancer statistics, 2012. - *CA Cancer J Clin* 2015.
3. Siegel RL, et al. - Cancer statistics, 2015. - *CA Cancer J Clin* 2015.
4. Global Cancer Observatory (GCO). <https://gco.iarc.fr/>.
5. Marur S, et al. - Head and Neck Squamous Cell Carcinoma: Update on Epidemiology, Diagnosis, and Treatment. - *Mayo Clin Proc* 2016.
6. Malhotra J, et al. - Risk factors for lung cancer worldwide. - *Eur Respir J* 2016.
7. Domper Arnal MJ, et al. - Esophageal cancer: Risk factors, screening and endoscopic treatment in Western and Eastern countries. - *World J Gastroenterol* 2015.
8. Kollarova H, et al. - Epidemiology of esophageal cancer--an overview article. - *Biomed Pap Med Fac Univ Palacky Olomouc Czech Repub* 2007.
9. Horeweg N, et al. - The importance of screening for lung cancer. - *Expert Rev Respir Med* 2014.
10. Pennathur A, et al. - Oesophageal carcinoma. - *Lancet* 2013.
11. Hall SF, et al. - Using TNM staging to predict survival in patients with squamous cell carcinoma of head & neck. - *Head Neck* 1999.
12. de Koning HJ, et al. - Reduced Lung-Cancer Mortality with Volume CT Screening in a Randomized Trial. - *N Engl J Med* 2020.
13. Roy HK, et al. - Optical detection of buccal epithelial nanoarchitectural alterations in patients harboring lung cancer: implications for screening. - *Cancer Res* 2010.
14. Kopelovich L, et al. - Surrogate anatomic/functional sites for evaluating cancer risk: an extension of the field effect. - *Clin Cancer Res* 1999.
15. Krishnatreya M, et al. - Synchronous primary cancers of the head and neck region and upper aero digestive tract: Defining high-risk patients. - *Indian J Cancer* 2013.
16. van de Ven S, et al. - Screening for head and neck second primary tumors in patients with esophageal squamous cell cancer: A systematic review and meta-analysis. - *United European Gastroenterol J* 2019.
17. Subramanian H, et al. - Nanoscale cellular changes in field carcinogenesis detected by partial wave spectroscopy. - *Cancer Res* 2009.
18. Evers D, et al. - Optical spectroscopy: current advances and future applications in cancer diagnostics and therapy. - *Future Oncol* 2012.
19. Sidransky D - The oral cavity as a molecular mirror of lung carcinogenesis. - *Cancer Prev Res (Phila)* 2008.
20. Angadi PV, et al. - Oral field cancerization: current evidence and future perspectives. - *Oral Maxillofac Surg* 2012.
21. Roy HK, et al. - Nanocytology for field carcinogenesis detection: novel paradigm for lung cancer risk stratification. - *Future Oncol* 2011.
22. Kuipers J, et al. - Large-scale Scanning Transmission Electron Microscopy (Nanotomy) of Healthy and Injured Zebrafish Brain. - *J Vis Exp* 2016.
23. de Boer P, et al. - Large-scale electron microscopy database for human type I diabetes. - *Nat Commun* 2020.
24. Phillips-Cremins JE, et al. - Architectural protein subclasses shape 3D organization of genomes during lineage commitment. - 2013.
25. Rizvi MA, et al. - Nuclear blebbing of biologically active organoselenium compound towards human cervical cancer cell (HeLa): In vitro DNA/HSA binding, cleavage and cell imaging studies. - 2015.
26. Gerchman S, et al. - Chromatin higher-order structure studied by neutron scattering and scanning transmission electron microscopy. - 1987.
27. Le Gros MA, et al. - Soft X-ray tomography reveals gradual chromatin compaction and reorganization during neurogenesis in vivo. - 2016.
28. Ou HD, et al. - ChromEMT: Visualizing 3D chromatin structure and compaction in interphase and mitotic cells. - 2017.
29. De Gennes P-G, et al.: Scaling concepts in polymer physics. Cornell university press; 1979.
30. Flory PJJToCP - The configuration of real polymer chains. - 1949.
31. Virk RKA, et al. - Disordered chromatin packing regulates phenotypic plasticity. - *Science Advances* 2020.
32. Huang K, et al. - Physical and data structure of 3D genome. - *Science Advances* 2020.
33. Li Y, et al. - Nanoscale Chromatin Imaging and Analysis (nano-ChIA) platform bridges 4-D chromatin organization with molecular function. - 2020.
34. Virk R, et al. - Disordered Chromatin Packing Regulates Ensemble Gene Expression and Phenotypic Plasticity. - 2020.

35. Cherkezyan L, et al. - Nanoscale changes in chromatin organization represent the initial steps of tumorigenesis: a transmission electron microscopy study. - 2014.
36. Dravid AJMT - Employing deep networks for image processing on small research datasets. - 2019.
37. Zhang Z, et al. - Road extraction by deep residual u-net. - 2018.
38. Ronneberger O, et al.: U-net: Convolutional networks for biomedical image segmentation. In International Conference on Medical image computing and computer-assisted intervention. Springer; 2015: 234-41.
39. He K, et al.: Deep residual learning for image recognition. In Proceedings of the IEEE conference on computer vision and pattern recognition. 2016: 770-8.
40. Kingma DP, et al. - Adam: A method for stochastic optimization. - 2014.
41. Rogers JD, et al. - Modeling light scattering in tissue as continuous random media using a versatile refractive index correlation function. - Selected Topics in Quantum Electronics, IEEE Journal of 2014.
42. Sokol E, et al. - Large-Scale Electron Microscopy Maps of Patient Skin and Mucosa Provide Insight into Pathogenesis of Blistering Diseases. - J Invest Dermatol 2015.
43. Gladstein S, et al. - Correlating colorectal cancer risk with field carcinogenesis progression using partial wave spectroscopic microscopy. - 2018.
44. Subramanian H, et al. - Partial-wave microscopic spectroscopy detects subwavelength refractive index fluctuations: an application to cancer diagnosis. - 2009.
45. Huang K, et al. - Physical and data structure of 3D genome. - 2020.
46. Bauer GM, et al. - The transformation of the nuclear nanoarchitecture in human field carcinogenesis. - Future Science OA 2017.
47. Bugter O, et al. - Optical pre-screening for laryngeal cancer using reflectance spectroscopy of the buccal mucosa. - Biomed Opt Express 2018.
48. Bugter O, et al. - Optical detection of field cancerization in the buccal mucosa of patients with esophageal cancer. - Clin Transl Gastroenterol 2018.
49. Bugter O, et al. - Towards the Optical Detection of Field Cancerization in the Buccal Mucosa of Patients with Lung Cancer. - Transl Oncol 2019.
50. Metzger R, et al. - Embryology of the early foregut. - Semin Pediatr Surg 2011.

Chapter 4a

Optical Screening study: head and neck

Optical pre-screening for laryngeal cancer using reflectance spectroscopy of the buccal mucosa

Oisín Bugter; Jose Hardillo; Robert Baatenburg de Jong; Arjen Amelink; Dominic Robinson

Biomedical Optics Express, Sep 2018, PMID: 30319894

Abstract

Background. A new approach in early cancer detection focusses on detecting field cancerization (FC) instead of the tumor itself. The aim of the current study is to investigate whether reflectance spectroscopy can detect FC in the buccal mucosa of patients with laryngeal cancer.

Methods. The optical properties of the buccal mucosa of patients were measured with multidiometer single-fiber reflectance spectroscopy.

Results. The blood oxygen saturation and blood volume fraction were significantly lower in the buccal mucosa of laryngeal cancer patients than in non-oncologic controls. The data of these two parameters were combined to form a single 'biomarker α ', which optimally discriminates these two groups. Alpha was lower in the laryngeal cancer group (0.28) than the control group (0.30, $p = 0.007$). Alpha could identify oncologic patients with a sensitivity of 78% and a specificity of 74%.

Conclusions. These results might be the first step toward optical pre-screening for laryngeal cancer.

Introduction

Head and neck cancer (lip, oral cavity, nasopharynx, other pharynx and larynx) is the 7th most frequent type of cancer worldwide. There were an estimated 686,000 new cases and 404,000 associated mortalities in 2012. Males are more often affected than females with a ratio of 3:1 [1]. The epidemiology of head and neck cancer varies greatly depending on geographic region and level of exposure to risk factors [1, 2]. The main risk factors are smoking and alcohol use, which cause physiological and mutagenic effects on the exposed mucosa of the upper aerodigestive tract (UADT). They have a synergetic effect and account for about 75% of all head and neck tumors [2, 3].

One of the most important prognostic factors for head and neck cancer is TNM-stage [4-6]. Early tumors have a significant better disease specific survival rate than advanced tumors [7]. However, the majority of head and neck squamous cell carcinomas (HNSCC) are discovered at late stages of tumor progression. This highlights the need of a reliable detection method to facilitate early HNSCC detection [8]. Head and neck cancer appears ideally suited to screening because of (a) the significant morbidity and mortality associated with the disease, (b) the survival advantage of early diagnosis, (c) the association of identifiable risk factors, and (d) the ability to diagnose early tumors with a clinical examination [9]. All HNSCC population (pre-)screening methods so far have relied on visual and manual examination of patients and have focused mainly on oral cavity tumors and lymph node metastases [10-13]. Although these studies show promising results, their approaches are time consuming and have a low sensitivity for early stage tumors and for tumors beyond the oral cavity, i.e., the pharynx and larynx. This leaves us, at present, without a reliable and practical screening method for HNSCC.

A promising new approach to cancer screening is focused on detecting field cancerization (FC). Field cancerization is the notion that a multitude of physiological and nanoscale architectural alterations affect an entire organ or tract before ultimately resulting in a focal neoplasm in one area of the organ [14]. These mucosal changes occur superficially in the epithelial layer, the basal membrane, and the vascularized papillary layer of the lamina propria. There is evidence that FC of head and neck, lung and esophageal cancers encompasses the entire UADT [15]. Accurate detection of FC in an easy accessible location of the UADT such as the buccal mucosa could potentially be used to screen for distant HNSCC [15, 16]. There are several tissue alterations related to FC. Specifically, alterations in cells due to changes in their microvasculature and nanoscale architecture have been linked to FC. Optical techniques, such as reflectance spectroscopy, have the potential to be sensitive to these sub-diffractive length scale alterations caused by FC [17, 18].

Reflectance spectroscopy enables the measurement of both concentration of tissue chromophores and ultrastructural information related to scattering of the tissue [19]. Optical spectra acquired from tissue contain the combined effects of all tissue optical properties and are also dependent on illumination and detection geometry. The measurement of individual tissue optical properties and tissue components are still a major challenge. Single-fiber reflectance (SFR) spectroscopy can be used to address this challenge. In SFR, the illumination and detection are performed by the same optical fiber. This results in measurements of shallow tissue depths on the order of the fiber diameter. This shallow measuring depth is well matched with dimensions of the mucosa in which the FC changes occur [20, 21]. Additionally, measurements are also sensitive to the scattering phase function [22]. As such, SFR spectroscopy may be well suited for detection of ultrastructural changes of FC.

It has been shown that the tissue absorption coefficient μ_a [mm^{-1}] (in this article, all wavelength-dependent variables are presented in boldface) can be accurately quantified from an SFR measurement without prior knowledge of the tissue scattering properties [23]. μ_a can then be further decomposed into the constituent absorption spectra of known tissue chromophores. This enables accurate measurement of the concentration of chromophores and of physiological parameters such as microvascular blood oxygen saturation, blood volume fraction and mean vessel diameter. These parameters could be used to differentiate between tissue with and without FC [24].

SFR is also sensitive to the scattering phase function. We previously showed that it is possible to quantify the reduced scattering coefficient, $\mu_s' = \mu_s \cdot (1 - g_1)$ [mm^{-1}], and the phase function parameter, $\gamma = (1 - g_2) / (1 - g_1)$ [-], by acquiring multiple SFR measurements with different fiber diameters [25, 26]. Quantitative measurements of μ_s' and γ could provide insight into the tissue ultrastructure because the scattering phase function is directly related to the tissue refractive index correlation function [27]. However, sequential placement of multiple optical fibers to conduct multi-diameter single fiber reflectance (MDSFR) spectroscopy is known to cause errors. To solve this problem, our group has previously demonstrated a MDSFR device, which uses a 19-core fiber bundle. This allows for multiple single-fiber measurement of different diameters without moving the fiber tip [19].

Recently, the use of MDSFR spectroscopy to detect FC in the buccal mucosa of patients with esophageal cancer was investigated [28]. The objective was to differentiate between patients with esophageal cancer and non-oncologic controls based on the MDSFR measurements at a distant, but accessible site. The median value of the optical biomarker σ , a combination of two scattering parameters, was increased in patients with esophageal squamous cell carcinoma compared to control patients (2.07 vs. 1.8, $p = 0.022$). This finding

might be the first step towards non-invasive, optical buccal mucosa screening for esophageal cancer using FC detection. In similar approaches progress has been made with the use of low-coherence enhanced backscattering (LEBS) spectroscopy. This has been applied to detect FC of colorectal, pancreatic, and lung tumors [29-31]. For patients with lung cancer, LEBS spectroscopy of the buccal mucosa was able to identify patients with tumors with a promising sensitivity of 79% and specificity of 83% [29].

The present study describes the first attempt to develop a non-invasive, easy-to-use pre-screening method for laryngeal cancer based on detecting FC with the use of fiber-optic spectroscopy. Our aim is to assess whether detection of FC in the buccal mucosa using MDSFR spectroscopy is feasible to identify patients with laryngeal cancer. If proven feasible, this technology could serve as a basis for the development of a patient-friendly pre-screening tool of a selected high-risk population.

Materials and methods

Subjects and examination procedure

The Medical Ethics Committee of the Erasmus Medical Center approved this case-control study (MEC-2015-356). Patients were recruited from the outpatient clinic of the department of Otorhinolaryngology and Head and Neck Surgery of the Erasmus Medical Center Cancer Institute between January 2016 and February 2017. Clinical parameters such as sex, age, medical history, smoking (pack years), and TNM-stage of tumor were recorded using the electronic medical record (CSC-iSOFT, Virginia, USA). Patients were divided into an oncologic group and a non-oncologic control group. The oncologic group consisted of patients with primary and untreated laryngeal SCC. They were referred to our clinic for diagnosis and treatment of their tumor. Tumors of all TNM-stages were included. The head and neck squamous cell carcinomas were confirmed by laryngoscopy, CT-scan and histopathology. The non-oncologic control group consisted of patients with chronic rhinosinusitis with or without nasal polyps and patients treated for cholesteatoma. The absence of an occult, unexpected HNSCC was confirmed by laryngoscopy. All included patients were smokers or ex-smokers. Patients with a medical history of lung or esophageal cancer were excluded from both groups. The study size estimation was based on the optical buccal mucosa differences between lung cancer and control patients of a previous study [14]. All patients signed an informed consent form before inclusion in this study.

Optical measurements of the buccal mucosa were performed at the outpatients clinic. All measurements were done by a single investigator (OB). The probe tip was gently placed in contact with the buccal mucosa, after disinfection of the fiber bundle with Tristel Trio (Tristel Solutions Ltd, Snailwell, UK). Five consecutive MDSFR spectra were acquired per

patient at a single site without moving the probe tip, with a total duration of forty seconds (Fig. 1). Measurements were performed in the exact same way in the oncologic and non-oncologic group.

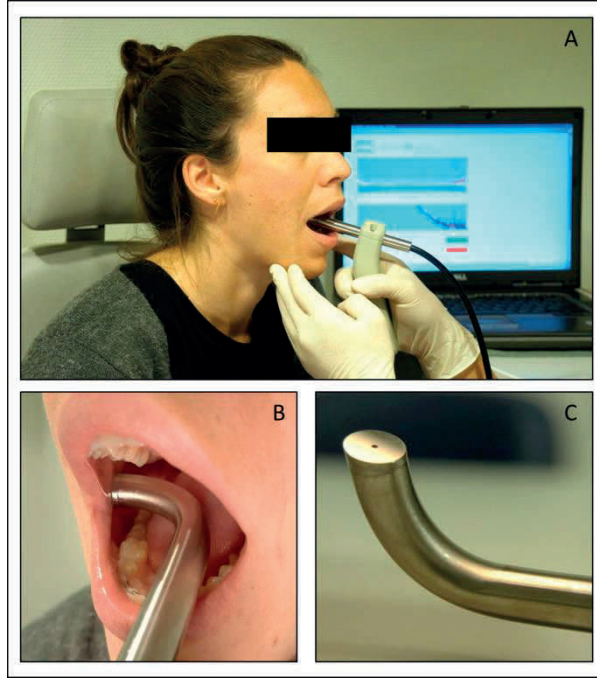


Figure 1. Multidiameter single-fiber reflectance spectroscopy measurement. Subject is a volunteer who gave written consent to use and publish her image. A) Overview of setup with patient, probe, and laptop for data storage. B) Placement of probe tip on the buccal mucosa. C) Close-up of probe tip.

MDSFR model for extraction of optical properties

We have previously described the MDSFR model for extraction of optical properties in detail [19]. In summary, our group has developed semi-empirical models for the collected SFR in the absence of absorption, R_{SF}^0 [%], and the effective photon path length for SFR, $\langle L_{SFR} \rangle$ [mm], based on experimentally validated Monte Carlo simulations [20, 32, 33]. The tissue absorption coefficient can be determined from a single SFR measurement using a modified Beer–Lambert law relationship

$$R_{SF} = R_{SF}^0 e^{-\mu_a \langle L_{SFR} \rangle}, \quad (1)$$

with the model for effective SFR path length

$$\frac{\langle L_{\text{SFR}} \rangle}{d_f} = \frac{C_{\text{PF}} p_1}{(\mu_s')^{p_2} [p_3 + (\mu_a d_f)^{p_3}]}, \quad (2)$$

and using the model for R_{SF}^0 ,

$$R_{\text{SF}}^0 = \eta_{\text{lim}} \left(1 + p_6 e^{-p_4 \mu_s' d_f} \right) \left[\frac{\mu_s' d_f^{p_5}}{p_4 + (\mu_s' d_f)^{p_5}} \right], \quad (3)$$

with a background scattering model [34]. In the above equations, η_{lim} is the collection efficiency at the diffusion limit. This is given as 2.7% for a fiber numerical aperture of 0.22 in a medium of refractive index 1.38 [35]. The parameters $[C_{\text{PF}}, p_1, p_2, p_3]$ and $[p_4, p_5, p_6]$ are fitted parameters, which were previously determined by Monte Carlo simulations of the SFR covering the parameter ranges of $d_f = [0.2\text{-}1.0]\text{mm}$, $\mu_s' = [0.3\text{-}3.6]\text{mm}^{-1}$, and $\mu_a = [0\text{-}3.0]\text{mm}^{-1}$ using modified and unmodified Henyey–Greenstein phase functions with $g_i = [0.8, 0.9, 0.95]$ and $\gamma = [1.4\text{-}1.9]$ [20, 22]. The values $[0.944, 1.54, 0.18, 0.64]$ for $[C_{\text{PF}}, p_1, p_2, p_3]$ and the values $[6.82, 0.969, 1.55]$ for $[p_4, p_5, p_6]$ were found to minimize the residual error between the SFR model and the simulations [20, 22].

Recently, we have demonstrated that $[p_4, p_5, p_6]$ are specifically sensitive to the phase function parameter, γ , where $[p_4, p_5, p_6] = [2.31\gamma^2, 0.57\gamma, 0.631\gamma^2]$ [32]. As a result, successive SFR measurements with at least two fiber diameters enable simultaneous solution of Eq. (3) for absolute quantification of μ_s' and γ over the measured wavelength range [25, 26].

Design of the MDSFR device

The optical properties of the buccal mucosa were measured using a custom made MDSFR device, which has been described in detail in a previous paper [19]. In short, MDSFR uses a 19-core fiber bundle of individual 200 μm fibers for both light delivery and collection (Fig. 2). At the proximal end of the fiber bundle each fiber is trifurcated to be connected to a) a fiber delivering light from a halogen lamp in the visible to near-infrared wavelength range (400-900 nm), b) a fiber delivering light from a 365 nm and 405 nm LED and c) a fiber collecting light returning from the tissue and delivering it to the spectrometer. At the distal end of the fiber bundle, which is placed in contact with the buccal mucosa, the fibers are bundled into three concentric groups comprised of one, six and twelve fibers. They are polished at an angle of 15 degrees to minimize the collection of specular reflections. The

most distal part of the fiber bundle was encased in a 12 mm diameter curved metal housing for the optimal application on buccal mucosa (Fig. 1). A series of fiber optic interconnects and three computer-controlled shutters enables illumination and spectroscopic detection of the center fiber, the middle ring, and the outer ring of fibers, independently. In this way, a sequential co-axial single fiber reflectance (SFR) measurement of 200, 600 and 1000 μm can be made without moving the probe. The entire device is installed on a portable medical cart that is approved to be used in the outpatients clinic.

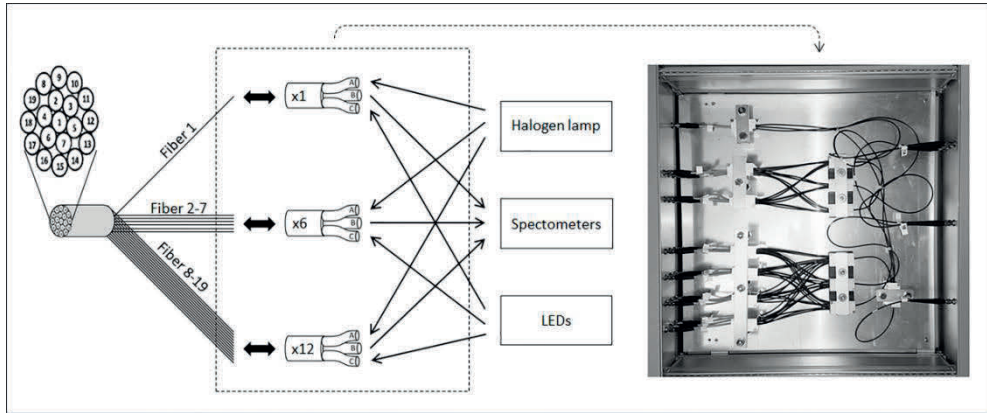


Figure 2. A schematic representation of the MDSFR device with numbering of the fiber cores, trifurcation at the proximal end of each fiber in the bundle, and the fiber tree. A photograph of the fiber tree is added on the right.

System calibration

MDSFR system calibration is important for quantitative estimation of optical properties. The calibration procedure to account for the spectral illumination, transmission and detection efficiencies of the measurement system was described in detail previously [19]. In short, the MDSFR system merges spectra from different fibers and spectrometers to create measurements with varying effective fiber diameters. Correct merging of spectrometer channels requires correction for differences in spectral sensitivity and transmission efficiency between channels. This can be achieved by comparing the spectra measured by each channel under uniform illumination. This is accomplished by inserting the probe into an integrating sphere and illuminating the sphere with the halogen lamp through a side port. The spectra acquired from the center fiber ($I_{\text{center}}^{\text{int.sphere}}$ [counts/s]) and middle ring of fibers ($I_{\text{middle}}^{\text{int.sphere}}$) are then normalized by the spectrum acquired from the outer ring of fibers ($I_{\text{outer}}^{\text{int.sphere}}$). These spectra are used to arrive at wavelength-dependent weighting coefficients (W_{center} [-] and W_{middle}) for the two innermost channels:

$$W_{\text{center}} = \frac{1}{12} \frac{I_{\text{outer}}^{\text{int.sphere}}}{I_{\text{outer}}^{\text{int.sphere}}} \quad (4)$$

and

$$W_{\text{middle}} = \frac{6}{12} \frac{I_{\text{outer}}^{\text{int.sphere}}}{I_{\text{outer}}^{\text{int.sphere}}} \cdot \quad (5)$$

The weighting coefficients are calculated relative to the outer channel because this channel has the largest detection area and thus the largest signal-to-noise ratio. During an MDSFR measurement, the spectra from each channel are combined using these weighting coefficients into effective single-fiber spectra with three different effective diameters, where

$$I_{\text{small}}^{\text{eff}} = I_{\text{center}} \quad , \quad (6)$$

$$I_{\text{med}}^{\text{eff}} = W_{\text{center}} I_{\text{center}} + W_{\text{middle}} I_{\text{middle}} \quad , \quad (7)$$

and

$$I_{\text{large}}^{\text{eff}} = W_{\text{center}} I_{\text{center}} + W_{\text{middle}} I_{\text{middle}} + I_{\text{outer}} \quad . \quad (8)$$

These spectra are then calibrated to account for the spectral illumination and transmission efficiencies and the spectrometer sensitivity for each effective fiber diameter. This calibration is achieved by acquiring MDSFR spectra from a water sample and from an Intralipid based scattering optical phantom. The spectrum acquired from the water sample ($I_{\text{water}}^{\text{eff}}$) originates from back reflections within the system and is subtracted from every measurement, while the spectra acquired from the Intralipid scattering phantom ($I_{\text{cal}}^{\text{eff}}$) is compared with the absolute reflectance for this phantom ($R_{\text{cal}}^{\text{sim}}$), which has been simulated for each effective fiber diameter using a Monte Carlo model. The resulting measurement is calibrated into absolute reflectance (R_{SF}), where

$$R_{\text{SF}} = R_{\text{cal}}^{\text{sim}} \frac{I_{\text{meas}}^{\text{eff}} - I_{\text{water}}^{\text{eff}}}{I_{\text{cal}}^{\text{eff}} - I_{\text{water}}^{\text{eff}}} \quad . \quad (9)$$

Eq. (9) is used to calibrate the reflectance spectra from each effective fiber diameter independently, where the measured spectra, I^{eff} , are given by Eqs. (6), (7), or (8), depending on the effective diameter.

A system validation was also performed to prove that the merged spectra acquired from the individual fibers are equivalent to the SFR spectra measured by a single solid-core fiber [19].

Spectral analysis

The complete analysis of spectra is well described in previous papers [24, 36, 37]. In short, the SFR spectra were analyzed using a mathematical model that describes the wavelength-dependent effects of scattering and absorption on the reflectance intensity collected by the device following Eqs. (1-3). For the background scattering model we use a power law dependence, with fitted parameters describing the scattering amplitude (α_1) and scattering slope (α_2). For the tissue absorption we assume the presence of blood and bilirubin. The summed contribution of the chromophores oxygenated and deoxygenated hemoglobin (HbO₂ and Hb, respectively) and albumin-bound bilirubin is given as follows:

$$\mu_a^{\text{tissue}} = \rho C_v \left(\text{StO}_2 \cdot \mu_a^{\text{HbO}_2} + (1 - \text{StO}_2) \cdot \mu_a^{\text{Hb}} \right) + \mu_a^{\text{bil}} \cdot [\text{BIL}]_{\text{tis}} \quad (10)$$

Here ρ is the blood volume fraction (BVF), StO_2 is the microvascular saturation, $\mu_a^{\text{HbO}_2}$ is the specific absorption coefficient of oxygenated hemoglobin, μ_a^{Hb} is the specific absorption coefficient of deoxygenated hemoglobin, and μ_a^{bil} and $[\text{BIL}]_{\text{tis}}$ are the specific absorption coefficient and concentration of albumin-bound bilirubin, respectively. The basis spectra for these 3 chromophores were reported in [37, 38]. Within tissue, blood (and in turn Hb and HbO₂) is located within the vasculature. This heterogeneous distribution affects the spectral shape of the absorption detected by reflectance spectroscopy; an effect that is characterized by the C_v term, which is given as:

$$C_v = \frac{\left\{ 1 - \exp \left(- \left(\text{StO}_2 \cdot \mu_a^{\text{HbO}_2} + (1 - \text{StO}_2) \cdot \mu_a^{\text{Hb}} \right) \cdot D_v \right) \right\}}{\left\{ \left(\text{StO}_2 \cdot \mu_a^{\text{HbO}_2} + (1 - \text{StO}_2) \cdot \mu_a^{\text{Hb}} \right) \cdot D_v \right\}} \quad (11)$$

and includes an estimate of the average vessel diameter (D_v).

Statistical analysis

Outcome parameters were calculated by taking an average of the five buccal mucosa measurements taken per patient weighted by the individual confidence intervals of the fitted parameters. Ten result parameters were analyzed: StO_2 , BVF, VD, $[\text{BIL}]_{\text{tis}}$, μ_s' at 450 nm, μ_s' at 800 nm, μ_s' power law scattering parameter, γ at 450 nm, γ at 800 nm, and average γ . Our quantitative variables were not normally distributed due to the relative small groups. We thus report our results as median value and interquartile range (IQR). Differences between the oncologic and non-oncologic group were analyzed using the Mann-Whitney U test. Qualitative data were reported as counts and frequencies, and differences between groups were analyzed using the χ^2 -test. To optimally identify HNSCC patients, a linear discriminant analysis was used in SPSS to create biomarker α . We included all significantly different parameters with the 'stepwise method'. This analysis shows the relative contribution of these parameters to the differentiation between cancer patients and controls, which allows the most optimal merge into combined biomarker α . A ROC-curve of α was created to perform a sensitivity and specificity analysis. There were no missing data. Statistical analysis was performed using SPSS version 21 (IBM Co., Armonk, NY, USA) and the cut off point for significance was a p-value < 0.05.

Results

Forty-six patients were included in this study: 23 head and neck squamous cell carcinoma patients and 23 non-oncologic control patients (Table 1). The male to female ratio in the HNSCC group was 6.7:1 and 3.6:1 in the control group ($p = 0.437$). The median age at time of measurement was the same for HNSCC group and the control group (68.2 [IQR 56.7-73.1] vs. 67.8 [61.9-70.1], $p = 0.575$). The median amount of pack years was 35.0 (20.0-45.0) in the HSNCC and 30 (17.5-50.0) in the control group ($p = 0.895$).

The HNSCC group consisted of 18 patients with a glottic tumor and five with a supraglottic tumor. Five tumors were carcinomas in situ. Eight tumors were staged T1, three T2, seven T3, and zero T4. The majority of the tumors (20 [87.0%]) had not metastasized. Three tumors had metastasized to regional lymph nodes. They were all staged N1. There were no patients with distant metastases in this cohort.

The intra-patient variation of the five consecutive measurements varied between 3 and 22% deviation from the mean for the ten parameters. The variations the absorption outcome parameters StO_2 , BVF, VD and $[\text{BIL}]_{\text{tis}}$ were 6, 21, 18, and 22% respectively. In the scattering parameters intra-patient variations ranged from 7-15% in the μ_s' parameters and from 3-5% in the γ parameters.

Table 1. Patient demographics

	HNSCC group (n = 23)	Control group (n = 23)	P-value
Male sex (%)	86.9	78.3	0.437
Age, year (median [IQR])	68.2 (56.7-73.1)	67.8 (61.9-70.1)	0.575
Smoking, PY (median [IQR])	35.0 (20.0-45.0)	30.0 (17.5-50.0)	0.895

HNSCC = head and neck squamous cell carcinoma, PY = pack year, IQR = interquartile range. P-values calculated with χ^2 test (sex) and Mann-Whitney U test (age and smoking).

Table 2. Results of MDSFR physiological parameters

Parameter (median [IQR])	HNSCC group (n = 23)	Control group (n = 23)	P-value
StO₂ (%)	73.1 (72.0-79.1)	78.4 (72.9-81.7)	0.038*
BVF (%)	2.61 (2.00-3.40)	3.19 (2.80-3.62)	0.024*
VD (mm)	0.05 (0.04-0.07)	0.06 (0.04-0.07)	0.410
[BIL]_{tis} ($\mu\text{mol/L}$)	6.96 (4.10-8.42)	6.20 (4.48-8.05)	0.913

IQR = interquartile range, HNSCC = head and neck squamous cell carcinoma, StO₂ = blood oxygen saturation, BVF = blood volume fraction, VD = vessel diameter, [BIL]_{tis} = tissue bilirubin concentration. * = p-value < 0.05. P-values calculated with Mann-Whitney U test.

Two physiological parameters, StO₂ and BVF, recovered from MDSFR measurements on the buccal mucosa, were significantly different between the HNSCC and the control group. Table 2 shows the group values of all four physiological parameters. The remaining 6 parameters, all based on scattering contrast, were not significantly different between cancer and control groups and are therefore not shown in Table 2. Figure 3 shows representative MDSFR spectra from the three fiber diameters of (A) an HNSCC patient and (B) a control patient. The median StO₂ was lower in the HNSCC group (73.3% [72.0-79.1]) than the control group (79.4% [72.9-81.7], $p = 0.030$). The same was true for the median value of BVF (2.6% [2.0-3.4] vs. 3.2% [2.8-3.6], $p = 0.020$). This decrease was more pronounced in patients with tumors of higher T-stages (Fig. 4). The scattering parameters were not able to differentiate between the HNSCC group and the control group.

Based on a linear discriminant analysis of all the parameters, the StO₂ and BVF parameters were combined into biomarker α . Alpha was significantly lower in the HNSCC group than in the control group (0.28 [0.27-0.29] vs. 0.30 [0.28-0.33], $p = 0.007$). Biomarker α had the potential to distinguish patients with a HNSCC from healthy controls with a sensitivity of 78.3%, a specificity of 73.9%, and an area under the curve of 73.0% (Fig. 5).

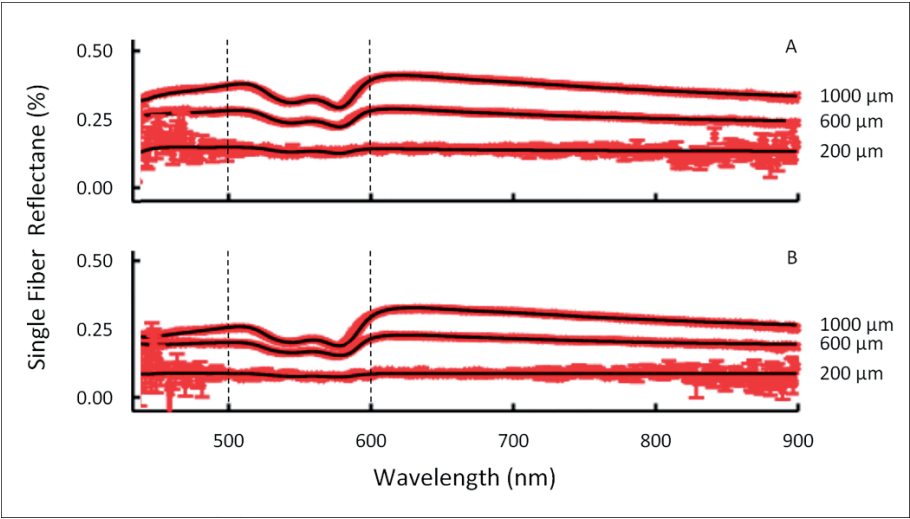


Figure 3. Example of spectra acquired from the buccal mucosa of A) a patient with a laryngeal tumor and B) a non-oncologic control. The three lines per patient represent the spectra derived from the effective 200, 600 and 1000 μm fiber diameters. Patient A features a lower absorption coefficient in the wavelength region from 500-600 nm (indicated by vertical dashed lines). The spectrum from patient A correlates with a lower blood oxygen saturation and blood volume fraction and consequently a lower value of biomarker α than patient B.

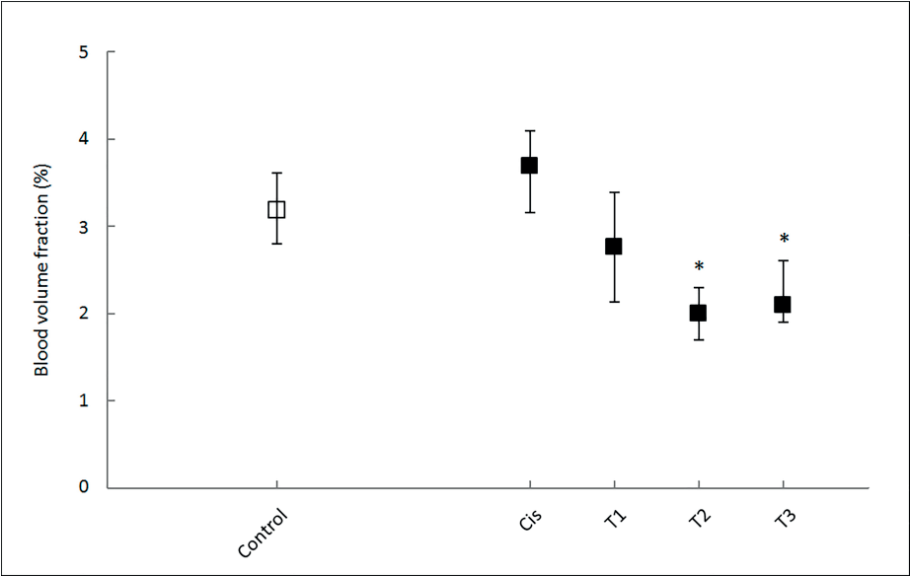


Figure 4. Values of BVF split up per T-stage versus non-oncologic control group. Median values are plotted in squares. Error bars represent interquartile range. * = p-value < 0.05. P-values calculated with Mann-Whitney U test. Cis = carcinoma in situ, T1-3 = T-stage I-3.

Discussion

In this study we have, for the first time, demonstrated that the optical properties of the buccal mucosa of patients with laryngeal cancer were significantly different than controls. The differences in optical properties were related to differences in the microvascular blood oxygen saturation and blood volume, possibly related to field cancerization. Measurements were performed with an easy-to-use, non-invasive fiber-optic technology: multidiameter single-fiber reflectance spectroscopy.

Our findings represent a first step towards the use of MDSFR spectroscopy on the buccal mucosa as a pre-screening tool for HNSCC. MDSFR spectroscopy has the potential to be used in a large scale community based testing of high risk patients. In such a scenario, patients with a positive test will be referred to a head and neck oncology center to undergo additional tests (e.g., complete clinical examination, laryngoscopy, and CT-scan) to confirm a HNSCC.

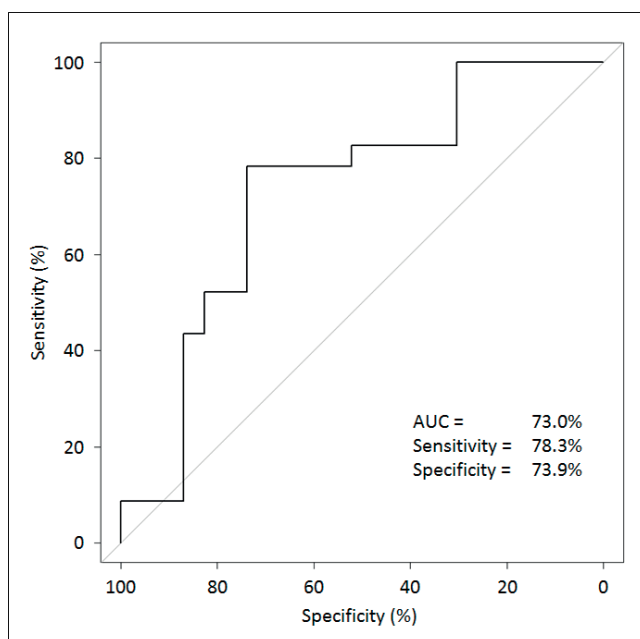


Figure 5. ROC curve of biomarker α (composed of BVF and StO₂). AUC = area under the curve.

In a recent study, we investigated if the current approach of performing MDSFR spectroscopy of the buccal mucosa could also be used in patients with esophageal squamous cell carcinoma cancer [28]. Interestingly, the parameters that were found to be

discriminative differed between laryngeal and esophageal cancer patients. The present study found that the physiological parameters (blood oxygen saturation and blood volume fraction) were altered, while μ_s' , a scattering parameter, was altered in the buccal mucosa of esophageal cancer patients. The mechanisms behind this difference are not yet fully understood. A possibility is that the FC has a distinct physiological and architectural signature between different types of distant malignancy. However, this hypothesis has to be tested.

The sensitivity and specificity of MDSFR pre-screening for laryngeal cancer (78% and 74%) found in the present study are similar to those of a recent optical screening study for lung cancer (79% and 83%) [29]. This study investigated whether low-coherence enhanced backscattering spectroscopy of the buccal mucosa could predict the presence of a distal lung tumor. Despite the use of reflectance spectroscopy in both studies, the discriminatory parameters were also of different optical origin. Similar to our esophagus study, LEBS screening for lung cancer found differences in light scattering, while the present study found differences in light absorption: the microvascular StO_2 and BVF were lowered in patients with HNSCC. Interestingly, these results suggest a decrease in microvasculature in FC. This contradicts the general notion that a local increase of microvasculature occurs in a tumor.

While we have not yet fully elucidated the mechanisms underlying the altered physiological parameters in the buccal mucosa of HNSCC patients, it is interesting to speculate on potential reasons of the lower values of StO_2 and BVF. The decrease in BVF could be caused by hemolysis in the HNSCC that leads to heme accumulation and upregulation of heme oxygenase (HO). In this scenario a local increase will also increase circulating levels of HO. Activity of HO will then increase circulating levels of vasoactive metabolites such as carbon monoxide. Heme itself also has a major impact on vascular tone via multiple mechanisms (including NOS, COX, CYP450, and sGC) [39]. The combination of both pathways has complex effects on the vascular tone. This could, in principle, lead to buccal vasoconstriction and reduced BVF in patients with HNSCC. An additional result of our study supports this hypothesis: the decreased BVF was more pronounced in advanced tumors than early stage tumors. A final possibility is that the actual BVF is not decreased but that we measure a lower value due to an increased thickness of the epithelial layer. Buccal mucosa is a multi-layered tissue; if the non-vascularized epithelial layer is thickened it is possible that MDSFR spectroscopy will interrogate a smaller volume of the vascularized lamina propria, thus resulting in an apparently low BVF. The low StO_2 values may be an indication of oxidative stress in the buccal mucosa of HNSCC patients.

A possible limitation of this study is the relatively small number of patients per group. This prevented us from splitting our cohort in a training a validation set to test the discriminative

power of biomarker α . It could also cause an underestimation of p-values and a less 'smooth' ROC-curve. Another potential issue is that we did not account for all patients characteristics that could potentially have an influence on the optical properties of the buccal mucosa. While we did account for the most important risk factor, smoking, we did not do so for alcohol use.

The HNSCC group in this study consisted of laryngeal tumors. This subsite was chosen since it is the most distant from the buccal mucosa. The aim of this study was, however, to demonstrate the feasibility of a screening method for all HNSCC locations. We will further investigate this in a following study. We also plan to investigate whether the approach described in this study is applicable to screen for lung cancer. All tumors of the UADT have a similar etiology and share smoking and alcohol use as their two major risk factors, which can be explained by their shared embryologic origin [40]. Previously reported analogous studies have shown that reflectance spectroscopy has the potential to screen for lung and esophageal cancer [29, 30].

Conclusion

In conclusion, our results demonstrate that the buccal mucosa of patients with laryngeal cancer is altered, possibly by field cancerization. Multidiameter single-fiber reflectance spectroscopy measurements showed that the blood oxygen saturation and blood volume fraction was decreased in HNSCC patients. Our biomarker α was able to differentiate between HNSCC patients and controls with a sensitivity of 78% and a specificity of 74%. This shows promise for the use of MDSFR spectroscopy of the buccal mucosa to pre-screen high risk patients. Diagnosing non-symptomatic, early stage tumors could significantly decrease the associated morbidity and improve the survival and quality of life of HNSCC patients.

References

1. Ferlay J, et al. - Cancer incidence and mortality worldwide: Sources, methods and major patterns in GLOBOCAN 2012. - *Int J Cancer* 2015.
2. Pezzuto F, et al. - Update on Head and Neck Cancer: Current Knowledge on Epidemiology, Risk Factors, Molecular Features and Novel Therapies. - *Oncology* 2015.
3. Mehanna H, et al. - Head and neck cancer--Part 1: Epidemiology, presentation, and prevention. - *Bmj* 2010.
4. Mehanna H, et al. - Head and neck cancer--Part 2: Treatment and prognostic factors. - *Bmj* 2010.
5. Datema FR, et al. - Impact of comorbidity on short-term mortality and overall survival of head and neck cancer patients. - *Head Neck* 2010.
6. Baatenburg de Jong RJ, et al. - Prediction of survival in patients with head and neck cancer. - *Head Neck* 2001.
7. Hall SF, et al. - Using TNM staging to predict survival in patients with squamous cell carcinoma of head & neck. - *Head Neck* 1999.
8. Whang SN, et al. - Recent Progress in Therapeutic Treatments and Screening Strategies for the Prevention and Treatment of HPV-Associated Head and Neck Cancer. - *Viruses* 2015.
9. Gogarty DS, et al. - Conceiving a national head and neck cancer screening programme. - *J Laryngol Otol* 2016.
10. Hapner ER, et al. - Results of a large-scale head and neck cancer screening of an at-risk population. - *J Voice* 2011.
11. Nunn H, et al. - Oral cancer screening in the Bangladeshi community of Tower Hamlets: a social model. - *Br J Cancer* 2009.
12. O'Sullivan EM - Prevalence of oral mucosal abnormalities in addiction treatment centre residents in Southern Ireland. - *Oral Oncol* 2011.
13. Sankaranarayanan R, et al. - Effect of screening on oral cancer mortality in Kerala, India: a cluster-randomised controlled trial. - *Lancet* 2005.
14. Roy HK, et al. - Optical detection of buccal epithelial nanoarchitectural alterations in patients harboring lung cancer: implications for screening. - *Cancer Res* 2010.
15. Kopelovich L, et al. - Surrogate anatomic/functional sites for evaluating cancer risk: an extension of the field effect. - *Clin Cancer Res* 1999.
16. Sidransky D - The oral cavity as a molecular mirror of lung carcinogenesis. - *Cancer Prev Res (Phila)* 2008.
17. Subramanian H, et al. - Nanoscale cellular changes in field carcinogenesis detected by partial wave spectroscopy. - *Cancer Res* 2009.
18. Evers D, et al. - Optical spectroscopy: current advances and future applications in cancer diagnostics and therapy. - *Future Oncol* 2012.
19. Hoy CL, et al. - Method for rapid multidiameter single-fiber reflectance and fluorescence spectroscopy through a fiber bundle. - *J Biomed Opt* 2013.
20. Kanick SC, et al. - Monte Carlo analysis of single fiber reflectance spectroscopy: photon path length and sampling depth. - *Phys Med Biol* 2009.
21. Prestin S, et al. - Measurement of epithelial thickness within the oral cavity using optical coherence tomography. - *Head Neck* 2012.
22. Kanick SC, et al. - Measurement of the reduced scattering coefficient of turbid media using single fiber reflectance spectroscopy: fiber diameter and phase function dependence. - *Biomed Opt Express* 2011.
23. Kanick SC, et al. - Method to quantitate absorption coefficients from single fiber reflectance spectra without knowledge of the scattering properties. - *Opt Lett* 2011.
24. Kanick SC, et al. - Characterization of mediastinal lymph node physiology in vivo by optical spectroscopy during endoscopic ultrasound-guided fine needle aspiration. - *J Thorac Oncol* 2010.
25. Gamm UA, et al. - Measurement of tissue scattering properties using multi-diameter single fiber reflectance spectroscopy: in silico sensitivity analysis. - *Biomed Opt Express* 2011.
26. Gamm UA, et al. - Quantification of the reduced scattering coefficient and phase-function-dependent parameter gamma of turbid media using multidiameter single fiber reflectance spectroscopy: experimental validation. - *Opt Lett* 2012.
27. Turzhitsky V, et al. - A predictive model of backscattering at subdiffusion length scales. - *Biomed Opt Express* 2010.
28. Bugter O, et al. - Optical detection of field cancerization in the buccal mucosa of patients with esophageal cancer. - *Clin Transl Gastroenterol* 2018.
29. Radosevich AJ, et al. - Buccal spectral markers for lung cancer risk stratification. - *PLoS One* 2014.
30. Konda VJ, et al. - Nanoscale markers of esophageal field carcinogenesis: potential implications for esophageal cancer screening. - *Endoscopy* 2013.

31. Roy HK, et al. - Association between rectal optical signatures and colonic neoplasia: potential applications for screening. - *Cancer Res* 2009.
32. Kanick SC, et al. - Method to quantitatively estimate wavelength-dependent scattering properties from multidiameter single fiber reflectance spectra measured in a turbid medium. - *Opt Lett* 2011.
33. Kanick SC, et al. - Empirical model of the photon path length for a single fiber reflectance spectroscopy device. - *Opt Express* 2009.
34. Stegehuis PL, et al. - Toward optical guidance during endoscopic ultrasound-guided fine needle aspirations of pancreatic masses using single fiber reflectance spectroscopy: a feasibility study. - *J Biomed Opt* 2017.
35. Bargo PR, et al. - Collection efficiency of a single optical fiber in turbid media. - *Appl Opt* 2003.
36. Middelburg TA, et al. - Correction for tissue optical properties enables quantitative skin fluorescence measurements using multi-diameter single fiber reflectance spectroscopy. - *J Dermatol Sci* 2015.
37. Amelink A, et al. - Effect of hemoglobin extinction spectra on optical spectroscopic measurements of blood oxygen saturation. - *Opt Lett* 2009.
38. Kanick SC, et al. - Integration of single-fiber reflectance spectroscopy into ultrasound-guided endoscopic lung cancer staging of mediastinal lymph nodes. - *J Biomed Opt* 2010.
39. Fredenburgh LE, et al. - Haeme oxygenase signalling pathway: implications for cardiovascular disease. - *Eur Heart J* 2015.
40. Metzger R, et al. - Embryology of the early foregut. - *Semin Pediatr Surg* 2011.

Chapter 4b

Optical Screening study: esophagus

Optical detection of field cancerization in the buccal mucosa of patients with esophageal cancer

Oisín Bugter; Manon Spaander; Marco Bruno; Robert Baatenburg de Jong; Arjen Amelink;
Dominic Robinson

Clinical and Translational Gastroenterology, Apr 2018, PMID: 29712897

Abstract

Introduction. Esophageal cancer is an increasingly common type of neoplasm with a very poor prognosis. This prognosis could improve with more early tumor detection. We have previously shown that we can use an optical spectroscopy to detect field cancerization in the buccal mucosa of patients with laryngeal cancer. The aim of this prospective study was to investigate whether we could detect field cancerization of buccal mucosa of patients with esophageal squamous cell carcinoma (ESCC) and esophageal adenocarcinoma (EAC).

Methods. Optical measurements were performed *in vivo* using a novel optical technique: multidiameter single-fiber reflectance (MDSFR) spectroscopy. MDSFR spectra were acquired by a handheld probe incorporating three fiber diameters. Multiple absorption and scattering parameters that are related to the physiological and ultrastructural properties of the buccal mucosa were derived from these spectra. A linear discriminant analysis of the parameters was performed to create a combined biomarker σ to discriminate oncologic from non-oncologic patients.

Results. Twelve ESCC, 12 EAC and 24 control patients were included in the study. The median value of our biomarker σ was significantly higher in patients with ESCC (2.07 [1.93-2.10]) than control patients (1.86 [1.73-1.95], $p = 0.022$). After cross-validation σ was able to identify ESCC patients with a sensitivity of 66.7% and a specificity of 70.8%. There were no significant differences between the EAC group and the control group.

Conclusions. Field cancerization in the buccal mucosa can be detected using optical spectroscopy in ESCC patients. This may be the first step towards non-invasive ESCC cancer screening.

Introduction

Esophageal cancer (EC) is an increasingly common type of neoplasm with a very poor prognosis. Worldwide, an estimated 450,000 new EC cases and 400,000 deaths occurred in 2012, making it the 8th most common type of cancer.[1] The vast majority of EC are squamous cell carcinoma (ESCC) or adenocarcinoma (EAC). Early diagnosis and treatment of (pre)cancerous lesions could greatly improve the overall patient outcome.[2] Unfortunately, about 60% of patients are diagnosed with an incurable locally advanced or metastatic EC.[3]

A promising new approach for cancer detection is focused on field cancerization (FC). Field cancerization is the notion that the initial tissue changes that lead to a neoplasm, do not only occur in the tumor site itself, but instead affect an entire organ or tract.[4] These tissue changes include alterations in the microvasculature and the tissue nanoscale architecture, such as the organization of the cytoskeleton and the size and structure of cell nuclei and organelles.[5, 6] In the case of EC, it is presumed that FC encompasses the entire upper aerodigestive tract. This is supported by the high incidence of second primary tumors in patients with esophageal, but also head and neck and lung, carcinoma.[7] Optical techniques, such as reflectance spectroscopy, have the potential to detect tissue changes caused by FC. Accurate optical detection of FC in an easily accessible, non-invasive anatomic location, such as the buccal mucosa, could potentially be used to detect distant EC.[4, 8, 9]

A number of studies investigated similar approaches for early tumor detection. The first study analysed cells of the cytologically normal proximal esophagus of patients with distal EAC *ex vivo* with partial wave spectroscopy.[10] Esophageal adenocarcinoma patients were shown to have a 1.8-times higher ($p = 0.01$) disorder strength, a parameter that is closely related to FC, than non-oncologic controls. A different *ex vivo* optical technique was used to detect FC in rectal mucosa biopsies to diagnose colorectal neoplasia.[11] This could predict the presence of an advanced adenoma with a promising sensitivity of 100% and a specificity of 80%. An final interesting study used a new *in vivo* optical technique to detect FC in the buccal mucosa of lung cancer patients.[12] Their optical biomarker was able to predict the presence of lung cancer with a sensitivity of 79% and a specificity of 83%. These studies illustrate the promise of optical detection of FC at a distant anatomic site than the actual malignancy.

Our group has recently developed a novel optical technique, multidiameter single-fiber reflectance (MDSFR) spectroscopy, which enables non-invasive quantification of the optical properties of tissue using a simple fiber-optic probe. MDSFR spectroscopy combines data from multiple single fiber reflectance (SFR) spectra. One SFR spectrum contains the

combined information on how much light has been absorbed and scattered in tissue. From such a reflectance spectrum, the tissue absorption coefficient (μ_a) can be quantified. Spectral deconvolution of μ_a yields measurements of several physiological parameters. Successive SFR measurements with two or more fiber diameters enables the quantification of two scattering parameters, γ and μ_s' , that are influenced by the angular scattering probability (phase function).[13-15] γ and μ_s' are closely related to the nanoscale architecture of tissue.[16] In a previous study, we used MDSFR spectroscopy to detect FC in the buccal mucosa of patients with laryngeal cancer.[17] The blood oxygen saturation and blood volume fraction were lower in the buccal mucosa of patients with cancer than the control group. The combined parameter α was able to predict the presence of a tumor with a sensitivity of 78% and a specificity of 74%.

This study describes the first attempt to use reflectance spectroscopy of the buccal mucosa to assess if FC is present in EC. Again, we do this by measuring the optical properties of the buccal mucosa of patients with and without cancer. Differences in the values of our absorption and scattering parameters could indicate the presence of FC. The presence of FC may then be used to identify patients with EC. If proven feasible, this study would be the first step toward implementing this method as a detection tool for EC.

Methods

Subjects and examination procedure

This prospective study was approved by the Medical Ethics Committee of the Erasmus MC Cancer Institute. Patients were recruited from the outpatient clinic of the Gastroenterology and Hepatology department between December 2015 and January 2017. Clinical parameters such as: gender, age, medical history, smoking (pack-years) and TNM-stage of tumor were collected using the electronic medical record (CSC-iSOFT, Virginia, USA). The oncologic group of patients consisted of patients with primary and untreated esophageal squamous cell carcinoma and esophageal adenocarcinoma. Tumors of all TNM-stages were included. The esophageal squamous cell carcinoma and esophageal adenocarcinoma were confirmed by an endoscopic examination and histopathology. The non-oncologic control group consisted of patients that underwent endoscopic examination for a variety of complaints, e.g., gastro-esophageal reflux, dysphagia and abdominal pain. The absence of an occult, unexpected malignancy or Barrett's esophagus was confirmed during the endoscopic examination. Patients with a medical history of head and neck or lung cancer were excluded from all study groups. Informed consent forms were signed before inclusion in this study by all patients.

The multi diameter single fiber reflectance measurements of the buccal mucosa were performed before the endoscopic examination (Figure 1). All measurements were done by a single investigator (OB). The probe tip was gently placed in contact with the buccal mucosa, after disinfecting the fiber bundle with Tristel Trio (Tristel Solutions Ltd, Snailwell, UK). Five consecutive MDSFR measurements were performed without moving the probe tip. The total duration of these measurements was approximately forty seconds.

Multidiameter single-fiber reflectance device

The absorption and scattering properties of the buccal mucosa were quantified with a custom made MDSFR spectroscopy device. In a previous paper, we have described it in detail.[18] In summary, MDSFR spectroscopy uses one fiber bundle for both light delivery and collection. The fiber has 19 cores of 200 μm fibers. Each fiber in the fiber bundle is trifurcated at the proximal end into a fiber delivering light from a halogen lamp, a fiber

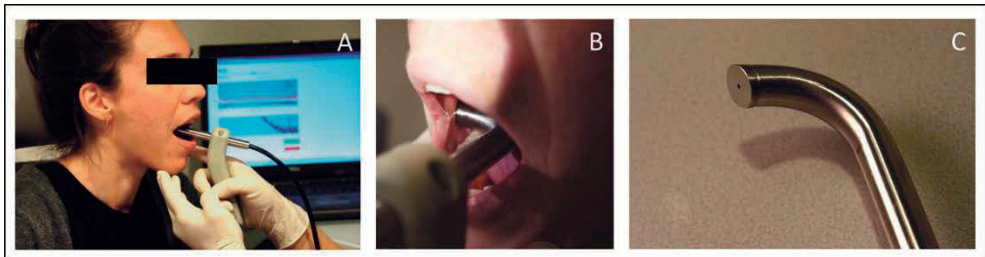


Figure 1. Application of the multidiameter single-fiber reflectance spectroscopy probe on the buccal mucosa. A) Overview picture with in the background spectra on laptop. B) Detail of probe contact with buccal mucosa. C) Detail of probe tip angled at 15 degrees.

delivering light from a 365 nm and 405 nm LED, and a fiber collecting light to the spectrometer. At the fiber tip, the fibers are bundled into three concentric groups comprising one, six and twelve fibers. To avoid collection of specular reflection, they are polished at an angle of 15 degrees. The last 10 cm of the fiber bundle is at the distal end encased in a 12 mm diameter curved metal housing. This metal housing ensures optimal application on buccal mucosa (Figure 1). A series of fiber optic interconnects and three computer-controlled shutters enable illumination and spectroscopic detection of independent fiber groups. This allows sequential single fiber reflectance (SFR) measurement of 200, 600 and 1000 μm to be made without moving the probe. Additional fluorescence measurements are made by illuminating all fibers in the bundle by the 365 nm LED and consecutively the 405 nm LED. The entire device is portable and approved for use in the outpatients clinic. A detailed description of the calibration procedure has been described previously.[18]

The nature of FC requires that the tissue optical properties are measured superficially. The maximal sampling depth of MDSFR spectroscopy (500 μm) is well matched with the thickness of the epithelial layer of the buccal mucosa (250-350 μm) and the underlying vascularized layer of the lamina propria (300-350 μm). [19, 20]

Spectral analysis

A previous paper by our group describes the complete analysis of spectra in detail. [21] First, the individual SFR spectra of the 200, 600, and 1000 μm fibers are used to calculate the tissue absorption properties. The absorption-corrected spectra of multiple fiber diameters were then combined to determine the tissue scattering properties: μ_s' (mm^{-1}), and γ (-). Next, we can extract four physiological parameters from the 1000 μm SFR fit: microvascular blood oxygen saturation (StO_2 (%)), blood volume fraction (BVF (%)), mean vessel diameter (VD (mm)) and tissue bilirubin concentration ($[\text{BIL}]_{\text{tis}}$ ($\mu\text{mol/L}$)). Finally, the intrinsic fluorescence is calculated from the raw fluorescence spectrum using the optical properties that are previously measured with MDSFR spectroscopy. This quantity is given by the product of the absorption coefficient of the tissue fluorophores at the excitation wavelength $\mu_{a,x}^f$ and their quantum efficiency across the emission spectrum Q (-).

Table 1. Patient characteristics

	Controls (n = 24)	ESCC (n = 12)	EAC (n = 12)
Male gender n (%)	10 (42)	7 (59)	11 (92)*
Age median (IQR)	61 (55-69)	70 (64-74)†	68 (65-72)†
Smoking PY median (IQR)	4 (0-30)	28 (6-30)#	16 (6-34)
Smoking status n (%)			
Never	11 (46)	2 (17)†	3 (25)
Past	9 (38)	6 (50)	7 (58)
Current	4 (17)	4 (33)	2 (17)

ESCC = esophageal squamous cell carcinoma. EAC = esophageal adenocarcinoma. IQR = inter quartile range. PY = pack-year. * = p-value < 0.05 compared to controls. † = p-value < 0.1 compared to controls. # = p-value is NOT significantly different ($p = 0.182$). P-values calculated with χ^2 test (gender and smoking status) and Mann-Whitney U test (age and smoking PY).

Statistical analysis

The optical parameters were calculated by averaging the five buccal mucosa measurements taken per patient weighted by the individual confidence intervals of the fitted parameters. Twelve parameters were analysed: StO_2 , BVF, VD, $[\text{BIL}]_{\text{tis}}$, μ_s' at 450 and 800 nm, μ_s' power law scattering parameter, γ at 450 and 800 nm, average γ and intrinsic fluorescence under 365 nm and 405 nm excitation. Our quantitative variables were not normally distributed.

We thus report our results as median value and interquartile range (IQR). Differences between two groups were analysed using the t-test (normally distributed data) or the Mann-Whitney U test (non-normally distributed data). Qualitative data was reported as counts and percentages, and differences between groups were analysed using the chi-squared test or the Fisher's exact test. Binary logistic regression was used to investigate if the outcome parameters could predict the presence of a malignancy. The age at measurement was included in the analysis as a covariate. We standardized our data to a standard normal distribution ($x_{\text{new}} = (x - \mu) / \text{sd}$) where μ is the mean and sd is the standard deviation of parameter x to compute a biomarker to identify EC patients. A linear discriminant analysis of the parameters was performed to create a combined biomarker σ . A ROC-curve of σ was created to perform a sensitivity and specificity analysis. A leave-one-out cross-validation was performed to test the robustness of σ . There was no missing data. Statistical analysis was performed using SPSS version 21 (IBM Co., Armonk, NY, USA) and the cut off point for significance was $p < 0.05$.

Results

Forty-eight patients were included in this study: 12 patients with esophageal squamous cell carcinoma, 12 patients with esophageal adenocarcinoma and 24 control patients (Table 1). The percentage of males was higher in both the ESCC 7/12 (58.3%) and EAC group 11/12 (91.7%), than in the controls 10/24 (41.7%), $p = 0.004$. The median age of the patients was 69.9 (64.1-74.8) years in the ESCC group and 68.3 (64.8-71.8) years in the EAC group. This was higher than the 61.2 (54.9-69.0) years in the control group. The median amount of pack-years was 27.5 (6.3-30.0), 16.5 (6.3-33.8) and 4.0 (0.0-30.0) in the ESCC, EAC and control group respectively.

Table 2 shows the TNM-classification and location of the ESCC and EAC. T-stage was equally divided over the two types of EC. ESCC were staged as T1 in two (16.7%), T3 in nine (75.0%), and T4 in one (8.0%) cases and EAC were staged as T1 in two (16.7%), T2 in one (8.3%), and T3 in nine (75.0%) cases. Most tumors were not metastasized to regional lymph nodes, N0 in 8 (66.6%) patients in ESCC group and four (33.3%) patients in EAC group. Tumors were staged N1 and N2 in two (16.7%) cases in the ESCC group and in four (33.3%) cases in the EAC group. Distant metastasis (M1) was found in one ESCC and one EAC patient. ESCC was located in the upper, middle and lower esophagus in two (16.7%) six (50.0%) and four (33.3%) cases. All EAC tumors were located in the lower esophagus.

The intra-patient variation of the five consecutive measurements varied between 3.7 and 24.8% deviation from the mean for the twelve MDSFR parameters. This variation was similar to measurements in two previous studies.[17, 22] μ_s' at 450 nm varied 9.6%, at 800 nm

8.6%, and the average μ_s' parameter varied 17.9%. The values of the three γ -parameters varies from 3.7 to 5.2%. The absorption parameters StO_2 , BVF, VD and $[BIL]_{tis}$ varied slightly more with intra-patient variations 8.0, 22.5, 18.2 and 24.8% respectively.

Table 2. TNM-classification and location of ESCC and EAC tumors

	ESCC (n (%))	EAC (n (%))
T-stage		
I	2 (17)	2 (17)
II	-	1 (8)
III	9 (75)	9 (75)
IV	1 (8)	-
N-stage		
0	8 (67)	4 (33)
I	2 (17)	4 (33)
II	2 (17)	4 (33)
III	-	-
M-stage		
0	11 (92)	11 (92)
I	1 (8)	1 (8)
Location		
Upper	2 (17)	-
Middle	6 (50)	-
Lower	4 (33)	12 (100)

ESCC = esophageal squamous cell carcinoma (n = 12). EAC = esophageal adenocarcinoma (n = 12). - = 0 cases.

Based on a linear discriminant analysis of all the MDSFR parameters, μ_s' at 450 nm and μ_s' at 800 nm were combined into biomarker σ . μ_s' at 450 nm and μ_s' at 800 nm were the only two parameters that were significantly different between the ESCC group and the controls. All other parameters showed no significant difference between these two groups. Sigma had a 4% bigger area under the curve than μ_s' at 450 nm alone. It also significantly increased the sensitivity/specificity ratio.

Figure 2 shows that biomarker σ was significantly higher in patients with ESCC than non-oncologic controls: 2.07 (1.93-2.10) vs. 1.86 (1.73-1.95), $p = 0.022$. Logically, individual values of μ_s' at 450 nm ($p = 0.033$) and 800 nm ($p = 0.029$) were also higher in the ESCC group than the control group (Figure 2). Figure 3 shows a ROC-curve of σ for the ESCC group with an area under the curve of 75.7% (95% CI: 57.4-94.0). Biomarker σ was able to differentiate patients with ESCC from controls with a sensitivity of 66.7% and a specificity of 83.3%. A leave-one-out cross-validation was performed to test the robustness of sigma

to predict patients with ESCC. This slightly decreased the diagnostic performance to a sensitivity of 66.7% and a specificity of 70.8%. Interestingly, there was no correlation between smoking (pack years) and biomarker sigma ($r^2 = 0.0275$ and standard error of estimate = 0.1826).

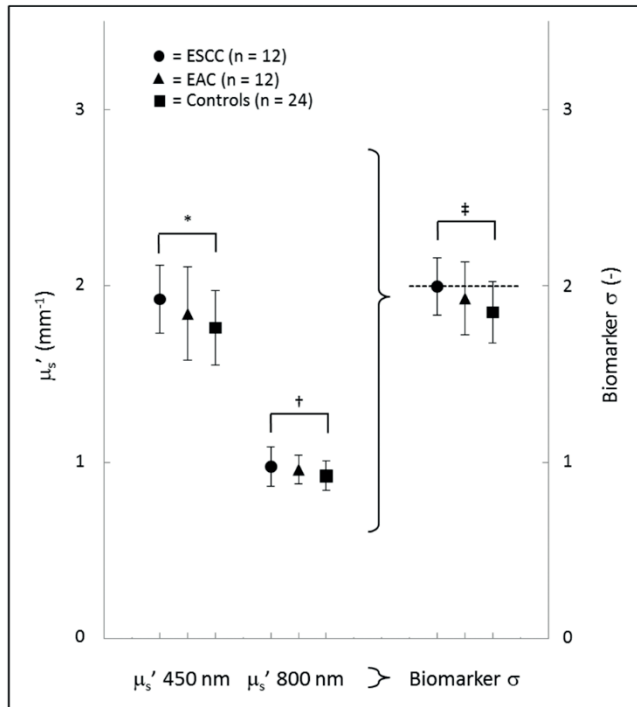


Figure 2. Values of μ_s' at 450 nm and 800 nm and biomarker σ (combination of μ_s' at 450 nm and 800 nm). Circles, triangles, and squares represent means and error bars represent standard deviation. ESCC = esophageal squamous cell carcinoma, EAC = esophageal adenocarcinoma. * $p = 0.030$, † $p = 0.045$ and ‡ $p = 0.012$. P-values were calculated with a binary logistic regression with 'age' as a covariate.

There were no significant differences in all parameters between the EAC group and the control group.

Discussion

This study demonstrates that field cancerization is present in the buccal mucosa of patients with esophageal squamous cell carcinoma and that it can be detected using optical spectroscopy. Multiple absorption and scattering parameters were measured with

multidiameter single-fiber reflectance spectroscopy. We found that our biomarker σ which is a combination of μ_s' at 450 and 800 nm, was significantly higher in patients with ESCC than in non-oncologic controls. Sigma was able to identify patients with ESCC with a sensitivity of 67% and a specificity of 70.8%. Unfortunately, σ could not distinguish patients with esophageal adenocarcinoma from controls.

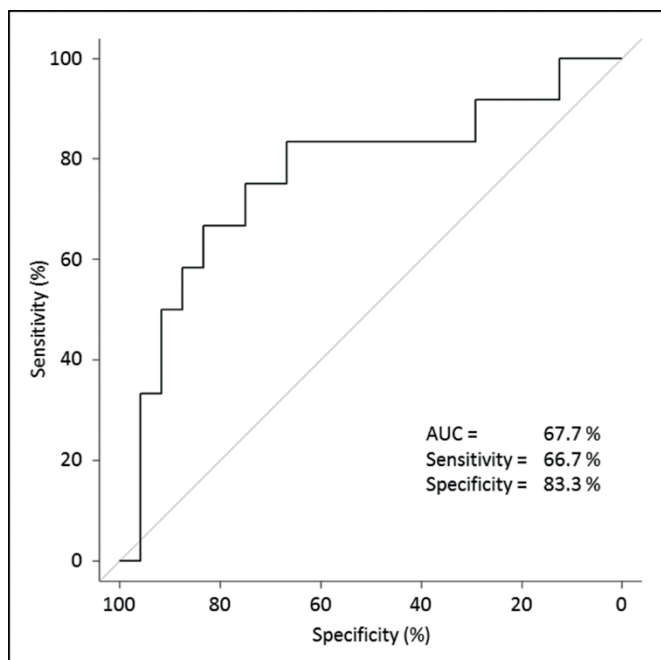


Figure 3. ROC curve of biomarker σ (composed of μ_s' at 450 and 800 nm). AUC = area under the curve.

Our main result showed the first proof that the buccal mucosa of patients with ESCC is altered. The increase of scattering parameter μ_s' indicates that alterations in the nano-architecture of the buccal mucosa have occurred. Studies have shown that an increase in scattering events correlates with increase of the local density of macromolecules and changes in their organization.[23] These alterations are key elements of FC.[24] Our findings confirm the results of a similar study that used *in vivo* low-coherence enhanced backscattering spectroscopy of the buccal mucosa to identify patients with lung cancer.[12] Their results also suggest that it is possible to detect nano-architectural changes in the buccal mucosa in patients with a tumor of the upper aerodigestive tract. Their biomarker was able to identify patients with lung cancer with a promising sensitivity of 79% and a specificity of 83% in their testing set. In a recent study, utilizing MDSFR in patients with head and neck squamous cell carcinoma cancer, we found that the physiological parameters

(blood oxygen saturation and blood volume fraction) were altered instead of scattering parameters such as μ_s' . [17] It is not yet fully understood how this can be explained, since laryngeal and esophageal cancer patients share the same risk factors. It might be that the FC has a different signature for different types of malignancies. However, this hypothesis has to be tested.

The results of the present study are promising with regard to the use of MDSFR spectroscopy as an innovative tool for early cancer detection. We chose a threshold that resulted in a higher specificity than sensitivity. This will result in a lower number of false positives and thus a lower number of falsely diagnosed patients. On the other hand, this will result in a relative high number of false negatives, which means that the test will miss some patients with malignancies. [25] A cost-effectiveness analysis will have to be performed in a later stage to decide the appropriate threshold and applicability of σ for detecting ESCC.

Our approach, using MDSFR spectroscopy of the buccal mucosa to identify patients with esophageal cancer was more effective for ESCC than EAC. This difference is expected because FC in tissue partly develops due to exposure to carcinogens. The carcinogens of ESCC and EAC differ. As such, the main risk factors for ESCC are smoking and alcohol use, while the main risk factor for EAC is gastric reflux. This also explains why all EAC were located in the lower esophagus, whereas most ESCC were located in the upper and middle esophagus (Table 2). However, evidence for FC of EAC was recently shown in a study in which cytologically normal proximal esophageal squamous cells were obtained by brushings during endoscopy. The disorder strength of these samples was significantly higher in patients with distal EAC ($p < 0.01$) and patients with distal Barrett's esophagus ($p < 0.01$) than healthy controls. This indicates that proximal squamous cells might undergo changes that are caused by distal EAC or Barrett's esophagus. [10] An important issue to address while discussing an EC detection tool is that although ESCC is the predominant histological type of EC worldwide, this is not the case in many developed countries. In developed countries the incidence of EAC has been exceeding that of SCC for some time with percentages reported of up to 80%. This highlights the need for a screening method for EAC in the 'western world'. Unfortunately MDSFR buccal mucosa spectroscopy did not show to be effective for EAC based on our results. It might however show value in high ESCC incidence regions in Asia. [2]

In the present study we did not fully investigate the effect of smoking. Smoking is known to cause mucosal changes, some of which can lead to FC. [9] The exact relationship between smoking induced mucosal changes and FC is unknown, e.g., patient A with 20 PY could have extensive FC while patient B with the same amount of PY has normal mucosa. This is underlined by the fact that the lifetime risk of smokers to develop for instance lung cancer

is only 10%.[26] Ideally, in the present study, the amount of pack years and distribution of current-, past-, and non-smokers should have been matched between the EC group and the controls. Although these differences in our study were not significantly different, they were not matched. This could have positively influenced our discriminative power to identify ESCC patients (Figure 3). Also due to the small number of patients per group we were not able to take the amount of pack years into our multivariate analysis of σ . However we were able to do this in a previous study in which we tested the discriminative power of α to identify laryngeal cancer patients.[17] In that study smoking pack years did influence the results, but not to a significant degree. Therefore, we believe that optical detection of FC still shows promise for detecting ESCC patients.

There are a number of other potential limitations that should be considered. One is the relatively small number of patients per group, which might have had an influence in multiple ways: a) it prevents us from making definitive statements about the discriminative power of the optical detection of FC, b) it could lead to an underestimation of the significance of differences between groups (p-value), c) we were not able to test the discriminative power of σ on an independent training-set, and d) we were only able to correct our statistical analysis for one covariate: age. However, age was also the only borderline significantly different baseline patient characteristic. Another possible limitation is that the investigator who performed the measurements (OB) was not blind to the oncologic status of the patients. A final point of attention is the fact that the majority of patients in this cohort had advanced tumors (T3). For a screening tool that ultimately has an effect on patient survival the test performance characteristics should be tested and found adequate in patients with early esophageal cancer, preferably T1 or T2. Survival in these patients is significantly better.

Conclusion

In conclusion, we have demonstrated that the reduced scattering coefficient, μ_s' , is increased in the buccal mucosa of patients with ESCC. This increase could be used to discriminate between patients with and without ESCC based on an optical measurement of the buccal mucosa. To our knowledge, this is the first proof of the concept that it is possible to detect ESCC by detecting FC in the buccal mucosa. A larger study is now needed before definitive conclusions on the potential role of MDSFR spectroscopy detecting for ESCC can be drawn.

References

1. Torre LA, et al. - Global cancer statistics, 2012. - *CA Cancer J Clin* 2015.
2. Pennathur A, et al. - Oesophageal carcinoma. - *Lancet* 2013.
3. Kollarova H, et al. - Epidemiology of esophageal cancer--an overview article. - *Biomed Pap Med Fac Univ Palacky Olomouc Czech Repub* 2007.
4. Kopelovich L, et al. - Surrogate anatomic/functional sites for evaluating cancer risk: an extension of the field effect. - *Clin Cancer Res* 1999.
5. Subramanian H, et al. - Nanoscale cellular changes in field carcinogenesis detected by partial wave spectroscopy. - *Cancer Res* 2009.
6. Evers D, et al. - Optical spectroscopy: current advances and future applications in cancer diagnostics and therapy. - *Future Oncol* 2012.
7. Krishnatreya M, et al. - Synchronous primary cancers of the head and neck region and upper aero digestive tract: Defining high-risk patients. - *Indian J Cancer* 2013.
8. Sidransky D - The oral cavity as a molecular mirror of lung carcinogenesis. - *Cancer Prev Res (Phila)* 2008.
9. Angadi PV, et al. - Oral field cancerization: current evidence and future perspectives. - *Oral Maxillofac Surg* 2012.
10. Konda VJ, et al. - Nanoscale markers of esophageal field carcinogenesis: potential implications for esophageal cancer screening. - *Endoscopy* 2013.
11. Roy HK, et al. - Association between rectal optical signatures and colonic neoplasia: potential applications for screening. - *Cancer Res* 2009.
12. Radosevich AJ, et al. - Buccal spectral markers for lung cancer risk stratification. - *PLoS One* 2014.
13. Gamm UA, et al. - Quantification of the reduced scattering coefficient and phase-function-dependent parameter gamma of turbid media using multidiameter single fiber reflectance spectroscopy: experimental validation. - *Opt Lett* 2012.
14. Gamm UA, et al. - Measurement of tissue scattering properties using multi-diameter single fiber reflectance spectroscopy: in silico sensitivity analysis. - *Biomed Opt Express* 2011.
15. Kanick SC, et al. - Method to quantitatively estimate wavelength-dependent scattering properties from multidiameter single fiber reflectance spectra measured in a turbid medium. - *Opt Lett* 2011.
16. Radosevich AJ, et al. - Ultrastructural alterations in field carcinogenesis measured by enhanced backscattering spectroscopy. - *J Biomed Opt* 2013.
17. Bugter O, et al. - Optical Screening for Laryngeal Cancer Using Reflectance Spectroscopy of the Buccal Mucosa. - Submitted at *Head&Neck* october 2017
18. Hoy CL, et al. - Method for rapid multidiameter single-fiber reflectance and fluorescence spectroscopy through a fiber bundle. - *J Biomed Opt* 2013.
19. Prestin S, et al. - Measurement of epithelial thickness within the oral cavity using optical coherence tomography. - *Head Neck* 2012.
20. Kanick SC, et al. - Monte Carlo analysis of single fiber reflectance spectroscopy: photon path length and sampling depth. - *Phys Med Biol* 2009.
21. Middelburg TA, et al. - Correction for tissue optical properties enables quantitative skin fluorescence measurements using multi-diameter single fiber reflectance spectroscopy. - *J Dermatol Sci* 2015.
22. Brooks S, et al. - Sources of variability in the quantification of tissue optical properties by multidiameter single-fiber reflectance and fluorescence spectroscopy. - *J Biomed Opt* 2015.
23. Roy HK, et al. - Nanocytology for field carcinogenesis detection: novel paradigm for lung cancer risk stratification. - *Future Oncol* 2011.
24. Backman V, et al. - Light-scattering technologies for field carcinogenesis detection: a modality for endoscopic prescreening. - *Gastroenterology* 2011.
25. Maxim LD, et al. - Screening tests: a review with examples. - *Inhal Toxicol* 2014.
26. Alberg AJ, et al. - Epidemiology of lung cancer: ACCP evidence-based clinical practice guidelines (2nd edition). - *Chest* 2007.

Chapter 4c

Optical Screening study: lungs

Towards the optical detection of field cancerization in the buccal mucosa of patients with lung cancer

Oisín. Bugter; Sigrid van Brummelen; Cor van der Leest; Joachim Aerts; Alexander Maat; Robert Baatenburg de Jong; Arjen Amelink; Dominic Robinson

Translational Oncology, Dec 2019, PMID: 31473370

Abstract

Introduction. An increase in detection of early-stage asymptomatic lung tumors could increase the overall survival rate of lung cancer patients. A new approach to cancer (pre-) screening focusses on detecting field cancerization instead of the tumor itself. The objective of this study was to investigate the use of optical spectroscopy to detect field cancerization in the buccal mucosa of lung cancer patients.

Methods. Optical buccal mucosa measurements were performed in lung cancer patients and controls using multidiameter single-fiber reflectance spectroscopy. We analyzed whether the measured optical parameters could distinguish lung cancer patients from controls.

Results. Twenty-three lung cancer patients, 24 chronic obstructive pulmonary disease (COPD) control patients, and 36 non-COPD controls were included. The majority of tumors were non-small-cell lung carcinomas (96%) and classified as stage I (48%). The tissue scattering properties μ_s' and γ at 800 nm and the tissue bilirubin concentration were all near-significantly different ($p = 0.072$, 0.058 , and 0.060 , respectively) between the lung cancer and COPD group. μ_s' at 800 nm had a sensitivity of 74% and a specificity of 63%. The microvascular blood oxygen saturation of the lung cancer patients was also higher than the COPD patients (78% vs. 62%, $p = 0.002$), this is probably a consequence of the systemic effect of COPD.

Conclusions. We have demonstrated that μ_s' at 800 nm is increased in the buccal mucosa of patients with lung cancer compared to controls with COPD. This might be an indication of field cancerization in the oral cavity of patients with lung cancer.

Introduction

Lung cancer is a major public health problem because of its high incidence and high mortality. It is the worldwide leading cause of cancer related death.[1] This high mortality is partly caused by the fact that early-stage lung cancer often causes no clinical symptoms.[2] As a result lung cancer is commonly diagnosed in more advanced stages of development with regional and distant metastases.[1] Patients with early-stage lung tumors can benefit from complete surgical resection or curative radiotherapy, whereas treatment of patients with high-stage tumors is often not curative.[2] This results in a substantially higher 5-year survival of 52% for patients with early-stage tumors than the 5-year survival of 15% of the total lung cancer population.[1]

Early detection by screening asymptomatic high-risk patients holds the potential to substantially increase the survival rate of lung cancer patients. At present, most scientific research has focused on low-dose computed tomography (LDCT).[3] The largest randomized controlled trial on the effectiveness of LDCT-screening for lung cancer showed a 20% lung cancer mortality reduction compared to using chest radiography.[4] The awaited mortality outcome results of the Dutch-Belgian randomized lung cancer screen trial (NELSON trial) are thought to replicate this reduction.[5] A recent systematic review recommended to LDCT-screen adults between 55 and 74 years who are at high risk for lung cancer.[6] However, they also warn of the potential harm of screening: false-positive results, adverse effects of invasive follow-up testing, and overdiagnosis.

A novel strategy for lung cancer (pre-)screening is focused on field cancerization (FC). The goal of this type of screening is not to detect the tumor itself but instead detect local tissue changes caused by FC. These superficial tissue changes are caused by accumulating exposure to carcinogens and include alterations in the microvasculature and the tissue nanoscale architecture, such as the organization of the cytoskeleton and the size and structure of cell nuclei and organelles.[7, 8] An alternative theory states that multiple fields arise due to the migration of dysplastic and altered cells. Either by migration of malignant cells through the saliva (micro metastasis) or intra-epithelial migration of the progeny of initially transformed malignant cells.[9, 10] The FC of lung cancer is assumed to consist of the entire upper airway including the main bronchi, trachea and even the, easily accessible, oral cavity.[11] Most research on FC lung cancer screening is done on airway tissue gene expression.[3] However, this is an expensive and time consuming method. Optical reflectance spectroscopy has been proposed as a fast and easy-to-use alternative technique to detect FC and possibly use for cancer screening.[7]

The approach to pre-screen for lung cancer has been investigated by Roy et al. by optical measurements of the buccal mucosa.[12, 13] In a first *ex vivo* study they showed the proof of concept that buccal optical spectroscopy may potentially work as a pre-screening tool for lung cancer.[12] In a second *in vivo* study an optical fiber was used to interrogate the buccal mucosa with the aim to detect FC changes.[13] Their optical biomarker was able to predict the presence of lung cancer with a sensitivity of 79% and a specificity of 83%. However, 50% of the control patients in the validation set were non-smokers, which may have influenced the study outcome.

Our research group has developed a novel optical technique: multidiameter single-fiber reflectance (MDSFR) spectroscopy.[14] It enables fast, non-invasive measurements of how much light has been absorbed and scattered in tissue. Spectral deconvolution of the tissue absorption coefficient yields measurements of four physiological parameters. Repeated measurements with different diameters enables the quantification of two scattering parameters: the reduced scattering coefficient μ_s' and the phase function parameter γ . These scattering parameters are closely related to the nanoscale architecture of tissue and thus to FC changes. In two previous studies, our group used MDSFR spectroscopy to detect FC in the buccal mucosa of patients with esophageal and laryngeal cancer.[15, 16] These results show the promise of the use of MDSFR spectroscopy as a cancer pre-screening tool. In laryngeal cancer patients, the blood oxygen saturation and blood volume fraction were lowered in the buccal mucosa of the oncologic patients.[16] The combined parameter α , encompassing StO_2 and BVF, was able to predict the presence of a laryngeal tumor with a sensitivity of 78% and a specificity of 74%. In esophageal cancer patients the μ_s' at 450 and 800 nm was increased in the buccal mucosa of the oncologic group, indicating changes in the nanoscale architecture possibly related to FC.[15]

The present study reports the first attempt to use MDSFR spectroscopy in the buccal mucosa of lung cancer patients to investigate if FC changes can be detected. This was accomplished by comparing the buccal mucosa optical properties of patients with and without lung cancer. We hypothesize that the values of the optical parameters will be different between these groups. This could indicate the presence of FC and thus a, distant, lung tumor. If proven feasible, this technique might be used as a pre-screening tool for a high-risk population and possibly reduce lung cancer mortality by diagnosing more early-stage tumors.

Materials and Methods

Subjects and examination procedure

This prospective study was approved by the Medical Ethics Committees of the Erasmus MC Cancer Institute (MEC-2015-256) and the Franciscus Gasthuis & Vlietland. Patients were recruited from the outpatient clinic of the Pulmonology department of the Franciscus Gasthuis & Vlietland and the outpatient clinic of the Thoracic Surgery department of the Erasmus MC Cancer Institute between November 2016 and February 2018. Clinical parameters such as: sex, age, medical history, smoking (never/past/current and pack-years) and TNM-stage of tumor were collected using the electronic medical record (CSC-iSOFT, Virginia, USA). The oncologic group of patients consisted of patients with primary and untreated lung cancer. Patients with non-small cell lung cancer (NSCLC) and patients with small cell lung cancer (SCLC), tumor stages (I-IV), were included. The lung tumors were confirmed by imaging techniques or histopathology. The two non-oncologic control groups consisted of patients with chronic obstructive pulmonary disease (COPD) and non-COPD smoking patients with a variety of other non-oncologic diseases (e.g., chronic rhinosinusitis,

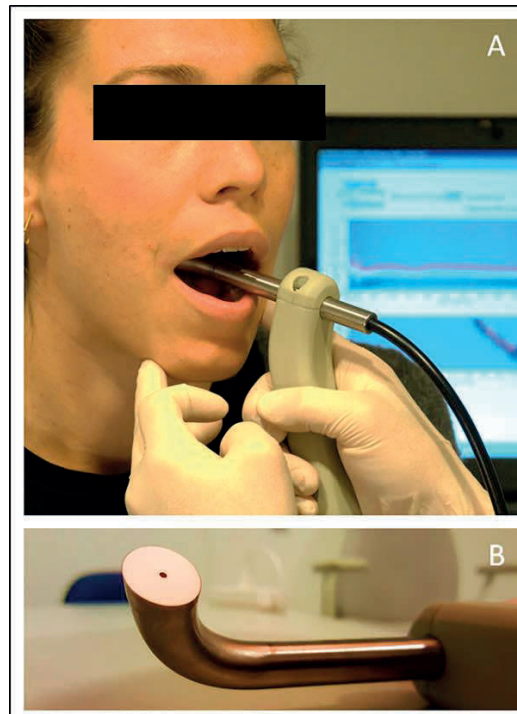


Figure 1. Multidiameter single-fiber reflectance spectroscopy probe on the buccal mucosa. A) Overview picture with in the background spectra on laptop. B) Detail of probe tip angled at 15 degrees.

cholesteatoma, gastro-esophageal reflux, dysphagia, and abdominal pain). The absence of an occult, unexpected malignancy in the lungs was confirmed by CT imaging < 1 year prior to inclusion in the study in the COPD group. Patients with a medical history of head and neck or esophageal cancer were excluded from this study. Informed consent forms were signed before inclusion in this study by all patients.

The multi diameter single fiber reflectance *in vivo* measurements of the buccal mucosa were performed at the outpatient clinic (Figure 1). A single investigator (OB) performed all measurements. After disinfecting the fiber bundle with Tristel Trio (Tristel Solutions Ltd, Snailwell, UK), the probe tip was gently placed in contact with the buccal mucosa. Five consecutive MDSFR measurements were performed with the probe-tip on the same place on the mucosa. In total, the measurements take approximately forty seconds.

Study samples

Eighty-three patients were included in this study: 23 patients with lung cancer, 24 control patients with COPD, and 36 non-COPD control patients (Table 1). The percentage of males was 56.5% in the lung cancer group, 41.7% in the COPD group ($p = 0.308$), and 75.0% in the non-COPD control group ($p = 0.138$). The median age of the patients was 69.1 (IQR 64.3-73.7) years in the lung cancer group. This was higher than the COPD control group (62.0 [IQR 51.8-65.6], $p = 0.001$) and the non-COPD control group (65.0 [IQR 58.3-69.1], $p = 0.042$). There was no significant difference in smoking status or smoking pack years between the lung cancer and both control groups.

Table 1. Baseline characteristics of lung cancer, COPD control and non-COPD control patients

	Lung cancer	COPD control	P-value	Non-COPD control	P-value
N	23	24		36	
Male sex, n (%)	13 (56.5)	10 (41.7)	0.308	27 (75.0)	0.138
Age, median (IQR)	69.1 (64.3-73.68)	62.0 (51.8-65.6)	0.001*	65.0 (58.3-69.1)	0.042*
Smoking, n (%)			0.555		0.266
Never	1 (4.3)	0 (0.0)		0 (0.0)	
Past	13 (56.5)	13 (54.2)		26 (72.2)	
Current	9 (39.1)	11 (45.8)		10 (27.8)	
Smoking, PY, median (IQR)	36.0 (20.0-50.0)	37.5 (25.5-45.8)	0.594	30.0 (15.0-49.0)	0.539

PY = pack years. P-values calculated with chi-square test (sex and smoking status) and Mann-Whitney U test (age and smoking pack years). * = p -value < 0.005.

Table 2 shows the tumor stage and type of the lung cancer group. Most tumors were stage I (12, 52.2%). Four tumors were stage II (17.4%), 4 tumors were stage III (17.4%) and 3 tumors were stage IV (13.1%). The majority of tumors were NSCLC of which 12 were squamous cell carcinoma's, 8 were adenocarcinoma's and 2 were undifferentiated large cell carcinoma. One patient (4.3%) had a SCLC.

Table 2. Tumor stage and type of lung cancer group

Tumor stage, n (%)	
I	12 (52.2)
II	4 (17.4)
III	4 (17.4)
IV	3 (13.0)
Tumor type, n (%)	
NSCLC	22 (95.7)
- Squamous cell carcinoma	- 12 (52.2)
- Adenocarcinoma	- 8 (34.8)
- Unknown	- 2 (8.7)
SCLC	1 (4.3)

NSCLC = non-small cell lung cancer; SCLC = small cell lung cancer.

Multidiameter single-fiber reflectance device

The buccal mucosa *in vivo* measurements were performed with a custom made MDSFR spectroscopy device, which was described in detail in a previous paper.[14] In summary, MDSFR spectroscopy uses a bundle of 19 fibers for both light delivery and collection. Each fiber of 200 μm in the bundle is trifurcated at the proximal end to enable light delivery from a halogen lamp, light delivery from a 365 nm and 405 nm LED, and light collection to the spectrometer. The fibers are bundled into three concentric groups of one, six and twelve fibers. They are polished at an angle of 15 degrees at the fiber tip to avoid collection of specular reflection. The last 10 cm of the fiber bundle towards the fiber tip is encased in a 12 mm diameter curved metal housing, for optimal application on buccal mucosa (Figure 1). Three computer-controlled shutters and a series of fiber-optic interconnects enable illumination and spectroscopic detection of independent fiber groups. This allows single fiber reflectance (SFR) measurement of 200, 600 and 1000 μm without moving the probe. The sampling diameter (over which parameters are averaged) is 1000 μm . The sampling depth is of the order of 500 μm (half the maximum fiber diameter). The MDSFR spectroscopy device is easily portable and has been approved to be used in the clinic. A detailed description of the system calibration and validation has been described previously.[14]

The maximal sampling depth of MDSFR spectroscopy is approximately 500 μm . For the buccal mucosa this seems to be well matched for the superficial occurrence of FC. The epithelial layer of the buccal mucosa is 250-350 μm thick and the, vascularized, lamina propria is 300-350 μm thick.[17, 18]

Spectral analysis

The complete analysis of spectra is described in detail in a previous paper by our group.[19] First, the tissue absorption properties were calculated using the individual SFR spectra of

the 200, 600, and 1000 μm fibers. Next, the tissue scattering properties μ_s' (mm^{-1}) and γ (-), that are influenced by the angular scattering probability (phase function), were determined by combining the absorption-corrected spectra of multiple fiber diameters. Finally, four physiological parameters were extracted from the 1000 μm SFR fit: microvascular blood oxygen saturation (StO_2 [%]), blood volume fraction (BVF [%]), mean vessel diameter (VD [mm]) and tissue bilirubin concentration ($[\text{BIL}]_{\text{tis}}$ [$\mu\text{mol/L}$]).

Statistical analysis

The optical parameters were calculated by averaging the five buccal mucosa measurements taken per patient. Ten parameters were analyzed: StO_2 , BVF, VD, $[\text{BIL}]_{\text{tis}}$, μ_s' at 450 and 800 nm, γ at 450 and 800 nm, and average γ . Our sample size was calculated based on a study that tried to differentiate lung cancer patients from controls with *ex vivo* optical measurements of buccal mucosa cells. The difference in mean of their optical parameter was 2.3 with a standard deviation of 1.0. It was hypothesized that standard deviation of our measurements would be higher (2.1) because they were performed in a heterogeneous *in vivo* environment. The number of patients required in each group would therefore be ≥ 23 (power = 0.8 and alpha = 0.01). Continuous data were reported as median value and interquartile range (IQR) (non-normally distributed data and $n < 30$ per group) and differences between two groups were analyzed using a binary logistic regression, with age at measurement as a covariate. Categorical data were reported as counts and percentages, and differences between groups were analyzed using the chi-squared test or the Fisher's exact test when appropriate. Binary logistic regression (with age as covariate) was used to investigate if the outcome parameters were significantly different between the two groups. The sensitivity and specificity of optical parameters to predict patients with lung cancer were calculated using an ROC-curve. There were no missing data. Statistical analysis was performed using SPSS version 21 (IBM Co., Armonk, NY, USA) and the cut off point for significance was $p < 0.05$.

Results

Table 3 presents the results of the buccal mucosa *in vivo* measurements of the lung cancer patients and the two control groups. The StO_2 in the buccal mucosa of the lung cancer patients was 77.5% (IQR 70.8-82.1), which was significantly higher than in the COPD control group (62.3% [IQR 57.6-68.3], $p = 0.002$). The $[\text{BIL}]_{\text{tis}}$, μ_s' at 800 nm, and γ at 800 nm parameters were all near-significantly different between the lung cancer and COPD control group. μ_s' at 800 nm was also significantly lower in the non-COPD control group (1.00 [IQR 0.93-1.05] vs. 1.04 [IQR 0.98-1.13], $p = 0.015$). On the other hand, the BVF was higher in the non-COPD control group (3.25 [IQR 2.73-3.61]) than in the lung cancer group (2.50 [IQR 1.70-3.30]).

Table 3. Optical properties of buccal mucosa measurements

Parameter (Median [IQR])	Lung cancer (n = 23)	COPD control (n = 24)	P-value	Non-COPD (n = 36)	P-value
StO ₂ (%)	77.5 (70.8-82.1)	62.3 (57.6-68.3)	0.002*	75.9 (70.3-81.3)	0.553
BVF (%)	2.50 (1.70-3.30)	2.30 (1.73-3.68)	0.701	3.25 (2.73-3.61)	0.043*
VD (mm)	0.04 (0.03-0.06)	0.05 (0.04-0.08)	0.651	0.05 (0.04-0.06)	0.579
[BIL] _{tis} (μmol/L)	7.30 (4.89-9.88)	9.59 (6.69-11.6)	0.060†	6.70 (4.70-8.39)	0.523
μ _s ' at 800 nm (mm ⁻¹)	1.04 (0.98-1.13)	0.96 (0.90-1.04)	0.072†	1.00 (0.93-1.05)	0.015*
μ _s ' at 450 nm (mm ⁻¹)	1.82 (1.61-2.10)	1.84 (1.65-2.11)	0.968	1.84 (1.69-2.06)	0.790
γ at 800 nm (-)	1.64 (1.60-1.74)	1.63 (1.57-1.68)	0.058†	1.65 (1.60-1.71)	0.784
γ at 450 nm (-)	1.65 (1.59-1.72)	1.68 (1.56-1.74)	0.585	1.68 (1.61-1.73)	0.064†
γ average (-)	1.65 (1.60-1.75)	1.66 (1.60-1.72)	0.157	1.67 (1.62-1.74)	0.880

IQR = interquartile range, StO₂ = blood oxygen saturation, BVF = blood volume fraction, VD = vessel diameter, [BIL]_{tis} = tissue bilirubin concentration, μ_s' = reduced scattering coefficient, γ = phase function parameter. P-values were calculated with binary logistic regression, with age at measurement as a covariate. * = p-value < 0.05, † = p-value < 0.10.

Figure 2 shows the discriminative power of two buccal mucosa parameters, StO₂ and μ_s' at 800 nm, that differentiate the best between lung cancer patient and controls. Compared to the COPD group, StO₂ could predict the presence of a lung tumor with a sensitivity of 78.3%, a specificity of 79.2% and an area under the curve (AUC) of 86.5% (95% CI 76.1-96.9). μ_s' at 800 nm had a lower discriminative power between the same two groups with a sensitivity of 73.9%, a specificity of 62.5% and an AUC of 69.2% (95% CI 53.9-84.6). The results of μ_s' at 800 nm compared to the non-COPD group were similar with a sensitivity of 65.2%, a specificity of 67.7% and an AUC of 66.4% (95% CI 51.6-81.2). Combining multiple parameters did not results in a higher discriminative power.

Discussion

In this study, we attempted to detect FC in the buccal mucosa of lung cancer patients. For this purpose we used MDSFR, which was hypothesized to be sensitive to the sub-diffraction length tissue changes caused by FC. Measurements were performed on oncologic patients and matched controls. Several buccal mucosa optical parameters showed significant differences between the lung cancer and control groups.

Our primary interest lay in the comparison of the lung cancer and COPD patients, since we hypothesized that the patients in these groups would be as homogeneous as possible. Also COPD is closely linked with lung cancer at a molecular level.[20] One notable result of the present study is that the buccal mucosa StO₂ was significantly lower in the COPD patients, but not in the non-COPD control group. However, this is probably not the result of FC but

a consequence of a systemic decrease in StO_2 due to COPD. Therefore, we believe that measuring the buccal mucosa StO_2 for screening purposes is not appropriate.

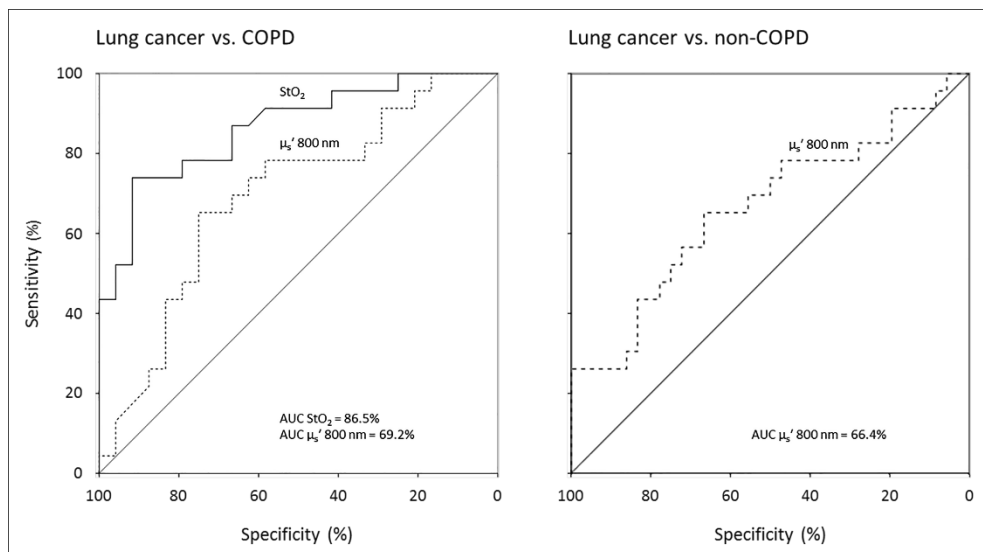


Figure 2. ROC curves of blood oxygen saturation (solid line) and μ_s' at 800 nm (dashed lines) for predicting the presence of cancer between the lung cancer and the two control groups. AUC = area under the curve.

Interestingly, the scattering parameter μ_s' at 800 nm was also near-significantly higher in the lung cancer group than the COPD patients and significantly higher than in the, larger, non-COPD group. An increase in μ_s' means that the photons that enter the mucosa undergo more scattering events. This indicates that the buccal mucosa of lung cancer patients has undergone some form of transformation, that might be the result of FC.[21] An increase of scatter events is correlated with an increase of the local density of macromolecules and changes in their organization.[22]

Our findings confirm the results of a study with a very similar study design that used low-coherence enhanced backscattering spectroscopy (LEBS).[13] The LEBS biomarker was also increased in lung cancer patients, indicating buccal mucosa transformation due to FC. However, the discriminative power of the LEBS power was higher than μ_s' at 800 nm with a sensitivity, specificity, and AUC of 79%, 83%, 89%, respectively. It is unclear how this difference might be explained. Two possible explanations are that their validation control group consisted of 33% non-smokers and that Radosevich et al. included 53% high-stage tumors (stage III and IV), compared to 30% in the present study.

The discriminative power of our optical method was lower for patients with lung cancer than for patients with head and neck or esophageal squamous cell carcinoma, which we have investigated in two earlier studies.[15, 16] This might be explained by the distance from the buccal mucosa to the tumor, which is the longest for lung cancer. To our knowledge, there are no studies that investigated optical methods to detect FC closer to the lung tumor (e.g., larynx, trachea, or bronchi). However, this would increase the complexity of the screening method, since it would require endoscopy

There are some limitations of our study design that should be considered. One is the relative small number of patients per group. This might have led to an underestimation of the significance of the differences between groups (p-value) and it prevented us from testing the discriminative power of our optical parameters on an independent training set. Another limitation is that the different groups were not optimally matched. Age at measurement proved to be lower in both control groups than the lung cancer group. However, we corrected for this difference in our statistical analysis.

Conclusion

In conclusion, we have demonstrated that μ_s' at 800 nm is increased in the buccal mucosa of patients with lung cancer compared to controls with and without COPD. This increase could be an indication of FC in the oral cavity of patients with lung cancer. A study with a larger study population is needed to investigate whether MDSFR spectroscopy of the buccal mucosa could function as a (pre)screening tool for lung cancer.

References

1. Siegel RL, et al. - Cancer statistics, 2015. - CA Cancer J Clin 2015.
2. Horeweg N, et al. - The importance of screening for lung cancer. - Expert Rev Respir Med 2014.
3. Spira A, et al. - Update in Lung Cancer 2014. - Am J Respir Crit Care Med 2015.
4. National Lung Screening Trial Research T, et al. - Reduced lung-cancer mortality with low-dose computed tomographic screening. - N Engl J Med 2011.
5. Ru Zhao Y, et al. - NELSON lung cancer screening study. - Cancer Imaging 2011.
6. Lewin G, et al. - Recommendations on screening for lung cancer. - Cmaj 2016.
7. Subramanian H, et al. - Nanoscale cellular changes in field carcinogenesis detected by partial wave spectroscopy. - Cancer Res 2009.
8. Evers D, et al. - Optical spectroscopy: current advances and future applications in cancer diagnostics and therapy. - Future Oncol 2012.
9. Mohan M, et al. - Oral field cancerization: an update on current concepts. - Oncol Rev 2014.
10. Angadi PV, et al. - Oral field cancerization: current evidence and future perspectives. - Oral Maxillofac Surg 2012.
11. Kopelovich L, et al. - Surrogate anatomic/functional sites for evaluating cancer risk: an extension of the field effect. - Clin Cancer Res 1999.
12. Roy HK, et al. - Optical detection of buccal epithelial nanoarchitectural alterations in patients harboring lung cancer: implications for screening. - Cancer Res 2010.
13. Radosevich AJ, et al. - Buccal spectral markers for lung cancer risk stratification. - PLoS One 2014.
14. Hoy CL, et al. - Method for rapid multidiameter single-fiber reflectance and fluorescence spectroscopy through a fiber bundle. - J Biomed Opt 2013.
15. Bugter O, et al. - Optical detection of field cancerization in the buccal mucosa of patients with esophageal cancer. - Clin Transl Gastroenterol 2018.
16. Bugter O, et al. - Optical pre-screening for laryngeal cancer using reflectance spectroscopy of the buccal mucosa. - Biomed Opt Express 2018.
17. Prestin S, et al. - Measurement of epithelial thickness within the oral cavity using optical coherence tomography. - Head Neck 2012.
18. Kanick SC, et al. - Monte Carlo analysis of single fiber reflectance spectroscopy: photon path length and sampling depth. - Phys Med Biol 2009.
19. Middelburg TA, et al. - Correction for tissue optical properties enables quantitative skin fluorescence measurements using multi-diameter single fiber reflectance spectroscopy. - J Dermatol Sci 2015.
20. Durham AL, et al. - The relationship between COPD and lung cancer. - Lung Cancer 2015.
21. Backman V, et al. - Light-scattering technologies for field carcinogenesis detection: a modality for endoscopic prescreening. - Gastroenterology 2011.
22. Roy HK, et al. - Nanocytology for field carcinogenesis detection: novel paradigm for lung cancer risk stratification. - Future Oncol 2011.

Chapter 5a

Endoscopic screening: esophageal SPTs in head and neck cancer patients

Early detection of esophageal second primary tumors using Lugol chromoendoscopy in patients with head and neck cancer: a systematic review and meta-analysis

Oisín Bugter; Steffi van de Ven; Jose Hardillo; Marco Bruno; Arjun Koch; Robert Baatenburg de Jong

Head & Neck, Apr 2019, PMID: 30593712

Abstract

Background. Early detection of esophageal secondary primary tumors (SPT) in head and neck squamous cell carcinoma (HNSCC) patients could increase patient survival. The purpose of this study was to determine the diagnostic yield of esophageal SPTs using Lugol chromoendoscopy.

Methods. A systematic review of all available databases was performed to find all Lugol chromoendoscopy screening studies.

Results. Fifteen studies with a total of 3386 patients were included. The average yield of esophageal-SPTs in HNSCC patients was 15%. The prevalence was the highest for patients with an index hypopharyngeal (28%) or oropharyngeal (14%) tumor. The esophageal-SPTs were classified as high-grade dysplasia in 49% of the cases and as invasive carcinoma's in 51%.

Conclusions. Our results show that 15% of the HNSCC patients that underwent Lugol chromoendoscopy were diagnosed with an esophageal-SPT. Based on these results there is enough evidence to perform Lugol chromoendoscopy, especially in an Asian patient population.

Introduction

Part of the mortality of patients treated for head and neck squamous cell carcinoma (HNSCC) is caused by the occurrence of second primary tumors (SPT).[1] Risk factors for their development include alcohol and tobacco use, age, and the sub-location of the index tumor (e.g., hypopharynx).[2] Most SPTs in HNSCC patients occur in the head and neck region, esophagus, and lungs.[1, 3-6] The risk of esophageal-SPTs after HNSCC treatment is an 8- to 22-fold greater than in the general population.[7-9] These SPTs are often diagnosed in advanced stages, which leads to a very low 5-year survival rate for affected patients.[6, 10-12] The prevalence of esophageal-SPTs in patients with HNSCC is estimated to range from 0-22%.[13]

The occurrence of esophageal-SPTs in HNSCC patients is often explained by field cancerization of the entire upper aerodigestive tract.[14, 15] The theory of field cancerization states that the mucosal field around the index tumor possesses subtle histologic and genetic changes that increase the risk of syn- and metachronous malignancies. These subtle tissue changes are thought to be the effect of exposure to accumulating carcinogens (e.g., alcohol and tobacco).[10]

Early diagnosis and treatment of an esophageal-SPT may improve the overall outcome of HNSCC patients.[5, 10, 16] It has even been suggested that its treatment will affect patient survival more than the index HNSCC tumor.[5] Esophageal carcinomas can remain asymptomatic for a long time during development. A result of this is that many patients SPTs only seek medical attention when the tumor is in advanced stages development.[17] Routine screening of the esophagus in the work-up and follow-up of HNSCC patients could potentially detect more early-stage esophageal-SPTs.[18-20]

The diagnosis of esophageal-SPTs may impact the management of both tumors.[13] Early-stage esophageal-SPTs may benefit from less invasive endoscopic resection, which can be performed without compromising the treatment of the HNSCC.[21] However, advanced esophageal-SPTs are often diagnosed metachronously and will typically be managed by chemoradiotherapy and surgery.[22] The treatment of the index HNSCC could also hinder that of the esophageal cancer due to treatment sequelae or restrictions to therapeutic options. When possible, personalized treatment should be focused on both tumors.[22, 23]

Endoscopic techniques to screen the esophagus have undergone major improvements over the last decades.[10] White-light endoscopy is deemed to be insufficient for the detection of superficial cancerous lesions in asymptomatic patients.[9, 10] However, studies with image-enhanced endoscopy, which includes Lugol's stain, have shown very promising results.

Lugol's stain isolates abnormal 'mucosal islands' within otherwise normal esophageal tissue, enabling targeted biopsy.[9] Lugol chromoendoscopy has a high diagnostic accuracy. When combined with narrow band imaging (NBI), it is reported to have a sensitivity of 94.7% and a specificity of 90.4% to detect early stage esophageal lesions.[24, 25]

Based on these results many clinics in Asia implemented esophageal-SPT screening in HNSCC patients.[10] Recently, the French Society of Otorhinolaryngology recommended routine flexible white-light esophageal endoscopy in the workup of patients with oro- and hypopharyngeal HNSCC or chronic alcohol use.[13] The addition of Lugol stain was recommended. They also suggested to perform routine screening for metachronous esophageal-SPTs in the follow-up of HNSCC patients.[9]

Esophageal Lugol chromoendoscopy is not widely used in the management of HNSCC patients in the Western world. We performed a systematic review on studies that used Lugol chromoendoscopy to detect esophageal-SPTs in HNSCC patients. Our main objective was to investigate the yield of Lugol chromoendoscopy for head and neck cancer patients in general, but also for specific head and neck sub-locations. A second aim was to investigate whether current data from non-Asian patient populations provide enough evidence to justify Lugol chromoendoscopy screening for esophageal-SPTs in patients with HNSCC in the Western world.

Materials and Methods

Literature search and selection criteria

We searched the Embase, Medline (including PubMed), Web of Science, Cochrane, and Google Scholar databases for relevant studies. The search was performed in April 2017 without a limit on publication date. The following keywords were used for the search: 'second/ multiple primary tumor', 'esophageal cancer', and 'head and neck cancer'. We limited our search to studies written in English and on humans. Duplicate studies were removed. The remaining citations were reviewed (by OB) bases on title and abstract and in second stage on full text. We included studies that investigated the use of Lugol chromoendoscopy to detect esophageal second primary tumors in HNSCC patients. We excluded studies primarily designed as case reports or reviews. The next paragraph presents our full electronic search strategy for the Embase database (see e-content I in the Supplement for full search strategy).

('second cancer'/exp OR 'multiple cancer'/de OR (((Metachronous OR Synchronous OR Second* OR Multiple OR double OR triple OR quadruple OR quintuple OR subsequen* OR Simultan*) NEAR/6 (tumo* OR primary OR malignan* OR carcin* OR neoplas* OR

cancer*)):ab,ti) AND ('esophagus tumor'/exp OR 'esophagus'/exp OR 'esophagus examination'/exp OR (esophag* OR oesophag* OR (upper NEXT/3 (aerodigest* OR digest*)):ab,ti) AND ('head and neck tumor'/exp OR 'larynx tumor'/exp OR (('head'/exp OR neck/exp) AND 'primary tumor'/de) OR (((lip OR mouth OR oral OR nose OR nasal OR tongue OR tonsil OR nasopharynx* OR oropharynx* OR hypopharynx* OR pharynx* OR larynx* OR head OR neck) NEAR/10 (tumo* OR primary OR malignan* OR carcin* OR neoplas* OR cancer* OR primar*)):ab,ti) AND [english]/lim NOT ([animals]/lim NOT [humans]/lim).

Assessment of study quality

The methodological quality and risk of bias of the selected Lugol chromoendoscopy screening studies was tested (by OB) with the Methodological Index for Non-Randomized Studies (MINORS).[26] Its relevance to the current topic was determined using a three-criterion checklist, including 1) impact factor of publishing journal and thus an indication of quality of peer-review, 2) data on the prevalence of esophageal-SPT per head and neck sub-location, and 3) clarity of the text (Table 1). The total score of both the MINORS scale and relevance criteria was used as a quality score. Based on this score, the quality was classified as low (total score ≤ 10 points), medium (total score 11-14 points) or high (total score ≥ 15 points). Studies of medium and high quality were included for further analysis and low-quality studies were excluded.

Table 1. Relevance criteria

Criteria	Score		
	0	1	2
Impact factor	< 2	2-3.9	≥ 4
Sub-location	No	-	Yes
Text clarity	Low	Medium	High

Data extraction

Data from all included studies were extracted onto record forms (by OB) and results were summarized as a Preferred Reporting Items for Systematic Reviews and Meta-Analyses (PRISMA) check list and flow chart.[27] The total prevalence of diagnosed esophageal-SPTs were recorded as primary outcome. An esophageal-SPT was defined as an esophageal lesion classified as category 4 and 5: high-grade dysplasia or carcinoma. When possible three secondary outcomes were recorded : (a) the SPT prevalence per sub-location of the index head and neck tumor (oral cavity, oropharynx, hypopharynx, larynx, nasopharynx and other) and per tumor stage (0 to 4) of the index tumor; (b) whether the SPTs were diagnosed synchronously (≤ 6 months after diagnosis of index tumor, in some cases simultaneously) or metachronously (> 6 months after diagnosis of index tumor); and (c) in which stage of

development the SPTs were according to the Vienna classification of gastrointestinal epithelial neoplasia.[28] Finally, first author, country of study population, year of publication, study design, and population size were also recorded.

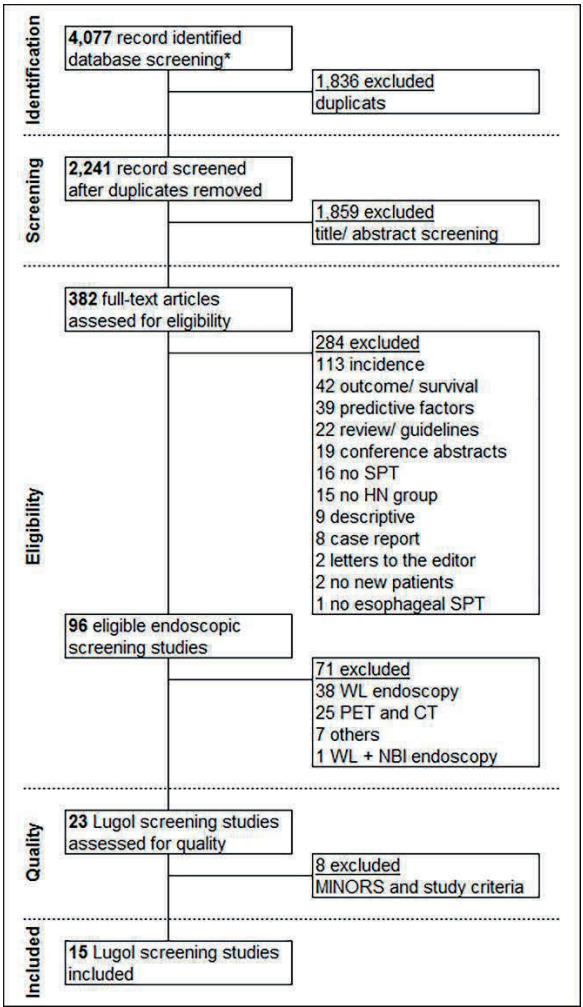


Figure 1. Study selection process. * = Embase, Medline, Web of Science, Cochrane, and Google Scholar; WL = white light; SPT = multiple primary tumor; NBI = narrow band imaging; HN = head and neck.

Statistical analysis

Data were reported as counts and percentages. The SPT prevalence was calculated for each study as the total number of detected SPTs divided by the total population that was screening in the particular study. In studies where the Standard Error (SE) was not reported,

we calculated it from the prevalence using the following formula: $SE = \sqrt{p(1-p)/n}$; where, p = prevalence and n = total number of patients with ESCC that were screened for head and neck SPTs. Review Manager software (version 5.3) was used for meta-analysis. Random effects model was used to calculate the pooled prevalence. I^2 was used to evaluate the level of heterogeneity between studies. Subgroup analyses were performed for specific head and neck cancer sub-locations.

Results

Study selection, quality assessment, and characteristics

Results of our search query for eligible, qualitative Lugol chromoendoscopy screening studies are presented in Figure 1. The search identified 4077 citations. After removing duplicates 2241 citations were reviewed. Based on review of title and abstract, 1859 citations were excluded. The remaining 382 studies were reviewed for their eligibility by reviewing the full text. This revealed 96 studies that screened a population of HNSCC patients for esophageal second primary tumors. Reasons for exclusion of other studies are mentioned in Figure 1. Review of the 96 screening studies resulted in the selection of 23 Lugol chromoendoscopy screening studies (Table 2).[21, 22, 25, 29-48] Most other screening studies were performed with only white-light endoscopy (e.g., 'triple-endoscopy) or with the use of PET/CT.

The combined quality score of the MINORS- and relevance-criteria qualified 15 studies as medium or high quality and these were included in the present review.[21, 22, 25, 29-40] The remaining studies of low quality were excluded. The methodological quality assessment using MINORS resulted in scores ranging from 6 to 11 points, (median 8 and maximal possible score 16). The relevance criteria score ranged from between 0 to 5 points (median 3 and maximal possible score 6).

Twelve of the studies included (80%) were performed in Asia (Korea, Japan, and Taiwan) and the remaining three in Switzerland, France, and Brazil. Nine studies were performed within the last decade and all studies within the last two decades. Most studies collected data prospectively (13, 87%). The study populations ranged from 40 to 676 patients (median 171) and the total number of patients was 3386. All studies used similar methods by applying 10-40 mL of 0.8-3.0% Lugol's solution on the esophageal mucosa.

Prevalence

The average prevalence of esophageal-SPTs in HNSCC patients of the 15 included studies was 15.2% (413/ 3386, 95% CI: 11.4-19.0) (Figure 2). The three studies with the highest

prevalence included only or mostly patients with a hypopharyngeal index tumor.[21, 22, 33] Two Japanese studies only included patients with oral cavity tumors.[30, 39] The average esophageal-SPT prevalence of the 12 Asian studies was 17.7% (358/2627, 95% CI: 12.7-22.7). This was higher than the average of the three non-Asian studies: 6.0% (55/759, 95% CI: 2.3-9.7).

Table 2. Characteristics and MINORS + relevance scores of all 23 Lugol chromoendoscopy screening studies.

Authors	Country	Year	Design	N	Score			Quality
					MINORS	Relevance	Total	
Included studies								
Gong et al. [29]	Korea	2016	Pro	458	10	5	15	High
Wang, C.H. et al. [25]	Taiwan	2014	Pro	294	11	3	14	Medium
Wang, W.L. et al. [22]	Taiwan	2013	Pro	180	9	5	14	Medium
Ikawa et al. [30]	Japan	2012	Pro	171	8	4	12	Medium
Wang, W.L. et al. [31]	Taiwan	2011	Pro	315	11	5	16	High
Morimoto et al. [21]	Japan	2010	Pro	64	7	4	11	Medium
Fukuhara et al. [32]	Japan	2010	Pro	157	8	4	12	Medium
Lee et al. [33]	Taiwan	2009	Pro	44	11	4	15	High
Boller et al. [34]	Switzerland	2009	Pro	40	11	3	14	Medium
Dubuc et al. [35]	France	2006	Pro	393	10	3	13	Medium
Hashimoto et al. [36]	Brazil	2005	Pro	326	10	4	14	Medium
Muto, M. et al. [37]	Japan	2002	Pro	78	9	4	13	Medium
Tanabe et al. [38]	Japan	2001	Retro	134	8	3	11	Medium
Fukuzawa et al. [39]	Japan	1999	Pro	56	7	4	11	Medium
Horiuchi et al. [40]	Japan	1998	Retro	676	7	4	11	Medium
Excluded studies								
Laohawiriyakamol et al. [41]	Thailand	2014	Pro	89	10	0	10	Low
Komínek et al. [42]	Czech R.	2013	Pro	132	9	0	9	Low
Chow et al. [43]	China	2009	Retro	118	7	2	9	Low
Muto, M. et al. [44]	Japan	2002	Retro	389	6	1	7	Low
Tincani et al. [45]	Brazil	2000	Pro	60	7	0	7	Low
Ina et al. [46]	Japan	1994	Pro	127	7	2	9	Low
Chisholm et al. [47]	China	1992	Pro	37	7	0	7	Low
Shiozaki et al. [48]	Japan	1990	Pro	178	7	2	9	Low

N = number of head and neck cancer patients included, Pro = prospective, Retro = retrospective, Year = year of publication

Prevalence per sub-location

Nine Asian studies reported data of esophageal-SPTs per sub-location of the index HNSCC (Figure 30).[21, 22, 29-32, 38-40] The prevalence of esophageal-SPTs was the highest in patients with hypopharyngeal index tumors, followed by patients with oropharyngeal, oral cavity, laryngeal and nasopharyngeal tumors. The average prevalence of esophageal lesions in patients with hypopharyngeal tumors of seven studies was 28.0% (161/574, 95% CI: 22.5-33.5)). Five studies reported an average of 14.0% (35/308, 95% CI: 5.4-22.5) esophageal-SPTs in patients with oropharyngeal tumors. The diagnostic yield of Lugol chromoendoscopy in patients with oral cavity tumors was 7.2% (47/637, 95% CI: 3.2-11.2). For patients with laryngeal index tumors the rate of esophageal-SPTs was 3.4% (19/474, 95% CI: 1.8-5.4). Four studies reported only 2 esophageal-SPTs in 109 patients with nasopharyngeal tumors and none were found in patients with other index tumors (e.g., glandular tumors).

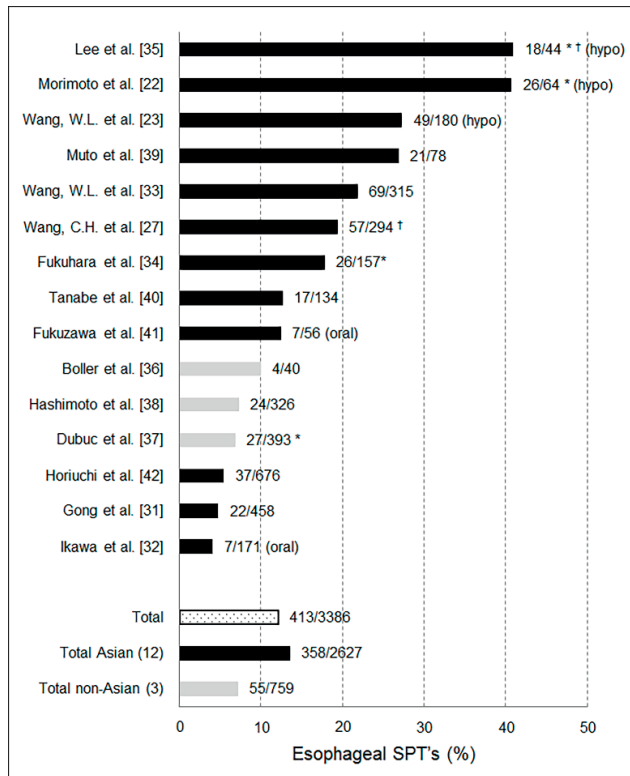


Figure 2. Overview of prevalence of esophageal-SPTs of 15 Lugol chromoendoscopy screening studies. hypo = study included only patients with hypopharyngeal tumors; oral = study included only patients with oral cavity tumors; SPT = multiple primary tumor; * = both syn- and metachronous screening; † = transnasal Lugol chromoendoscopy. Error bars represent 95% confidence intervals.

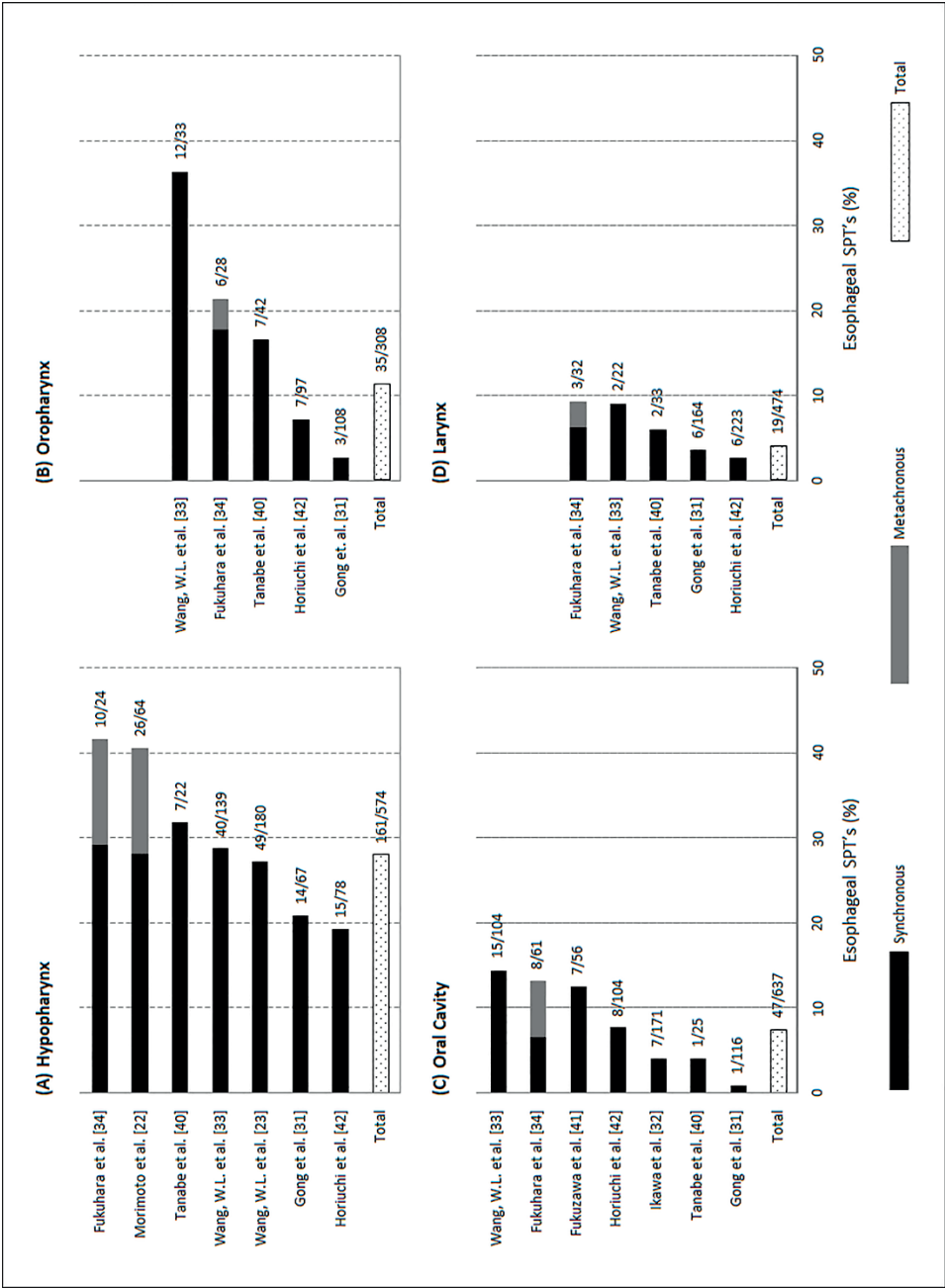


Figure 3. Overview of prevalence of esophageal-SPTs per sub-location of index head and neck squamous cell carcinoma: (A) hypopharynx, (B) oropharynx, (C) oral cavity, and (D) larynx. Nine Asian studies with sub-location specific data. Fukuhashi et al. and Morimoto et al. screened both syn- and metachronously. Error bars represent 95% confidence intervals

Time to diagnosis

Most studies only performed endoscopic screening of the esophagus in the work-up of the index HNSCC tumor and thus only diagnosed synchronous, or even simultaneous, esophageal-SPTs. Four studies performed both syn- and metachronous esophageal endoscopies.[21, 32, 33, 35] Morimoto et al. performed at diagnosis of the HNSCC and annually during follow-up.[21] Eighteen (69.2%) of all SPTs were diagnosed synchronously and 8 (30.8%) metachronously. Fukuhara et al. found a similar distribution between synchronously diagnosed SPTs ($n = 17$ [60.7%]) and those that were diagnosed metachronously ($n = 9$ [32.1%]).[32] The two other studies also metachronous endoscopies, but did not separately mention the syn- or metachronous diagnostic yield of Lugol chromoendoscopy.[33, 35]

Vienna classification

Eight studies differentiated between esophageal-SPTs classified as category 4 (high-grade dysplasia) or 5 (carcinoma).[21, 25, 29, 31, 33-36] The remaining studies either did not mention the category or only mentioned category 5. Almost half of all esophageal-SPTs found in these eight studies (48.6%, range 22.2-100.0) were category 4 lesions, high-grade dysplasia. That was approximately the same for Asian (43.3%, $n = 5$) and non-Asian (57.4%, $n = 3$) studies. Three of these seven studies also differentiated the esophageal carcinoma's in low- (stage I and II) and high-stage (stage III and IV) esophageal tumors.[21, 29, 31] Their combined data shows that 53.9% (41/76) of all esophageal carcinoma's were classified as low-stage and 46.1% (35/76) as high-stage.

Prevalence per index tumor stage

Three Asian studies also reported the prevalence of esophageal-SPTs in HNSCC patients per tumor stage of the index tumor.[21, 29, 39] There were a total of five (3.1%, 95% CI: 0.3-5.8) esophageal-SPTs in 150 patients with stage I HNSCC, 28.8% (95% CI: -5.7-63.3) esophageal-SPTs in patients with stage II HNSCC, 5.34% (95% CI: 1.1-9.6) esophageal-SPTs in stage III HNSCC, and 22.5% (95% CI: -2.3-47.3) in patients with a stage IV index HNSCC.

Discussion

To our knowledge, this is the first systematic review on the diagnostic yield of Lugol chromoendoscopy for esophageal second primary tumors in patients with head and neck squamous cell carcinoma. Our main findings show that on average 15% of the primary HNSCC patients that underwent Lugol chromoendoscopy were diagnosed with an esophageal-SPT. We found that the prevalence was the highest for patients with hypopharyngeal index tumors.

There is a large discrepancy between the prevalence of esophageal-SPTs in HNSCC patients found with Lugol chromoendoscopy screening (15%, 95% CI: 11-19) and the prevalence of retrospective non-screening studies (1-6%).[6, 7, 49-53] This was also noted by Wang, W.L. et al.[31] This discrepancy could indicate that without an active screening programme esophageal-SPTs are underdiagnosed in patients with HNSCC.[7] Multiple studies state that the occurrence of esophageal-SPTs negatively influences patient survival, especially in patients with advanced esophageal-SPTs.[23, 54-56] Some researchers even claim that SPTs are the leading cause of treatment failure and death in HNSCC patients.[31]

The hypopharynx, and in particular involvement of the piriform sinus, is a well-known risk factor for the development of esophageal-SPTs.[57-60] The results from the present review also SPTs underlined this. Wang, W.L. et al. compared two hypopharyngeal HNSCC cohorts: before and after implementing pretreatment Lugol chromoendoscopy esophagus screening.[22] Active esophageal screening tripled the amount of diagnosed esophageal-SPTs (5.3% vs. 15.3%). The present study also found esophageal-SPTs in 11% of oropharyngeal cancer patients, which is also a known sub-location to be at risk factor for the development of an esophageal-SPT.[60, 61] However, the two largest studies in this review with specific oropharynx data by Horiuchi et al. and Gong et al. found relatively low prevalence of esophageal-SPTs (7.2% and 2.8%) in this sub-group of patients.

The finding that up to a third of all esophageal-SPTs found in the studies by Morimoto et al. and Fukuhara et al. were diagnosed metachronously during follow-up, could indicate that the results of the other synchronous studies underestimate the true prevalence of esophageal-SPTs.[21, 32] It is also an indication that esophageal screening of HNSCC patients should also be performed in the follow-up of the index tumor. However, the optimal esophageal screening schedule has yet to be defined.

Approximately 50% of the esophageal lesions found in this review were classified as high-grade dysplasia. Of the remaining lesions classified as invasive carcinoma, about half were early-stage. This is similar to findings from other researchers.[22, 29, 38] Wang, W.L. et al. showed that an active screening protocol diagnosed more HGD lesions and early-stage carcinoma's, which significantly reduced the mortality rate of affected patients.[22] This is possibly the result of adjustments of the treatment strategy aimed at treating two instead of one tumor and less invasive endoscopic treatment of the esophageal lesions. Multiple studies claim that treatment of the esophageal-SPT increases the survival, especially in patients with early-stage tumors.[23, 54-56]

Five of the included studies in this review used NBI in addition to Lugol chromoendoscopy.[22, 25, 29, 31, 33] Wang, C.H. et al. concluded that this combination of

both techniques has the highest diagnostic accuracy to detect esophageal lesions: a sensitivity of 95%, a specificity of 90%, and an accuracy of 91% (95% CI 88-94).[25] Several other researchers have investigated the use of full-body ^{18}F -FDG-PET/CT. They reported a considerably lower diagnostic esophageal-SPT yield that ranged from 0.43% to 4.85%.[62-66] As Kondo et al. also mentioned that PET/CT seems to be an inferior technique for detection of esophageal-SPTs because it is not sensitive for early tumors.[62]

Two of the studies included in this review performed transnasal Lugol chromoendoscopy.[25, 33] Tumor-related airway obstruction or post-radiation trismus sometimes make the oropharyngeal passage difficult to reach with conventional endoscopes. The transnasal route bypasses this problem. Transnasal Lugol chromoendoscopy has the additional advantage that it can be performed in unsedated patients and that it even has a higher completion rate than conventional endoscopy.[67] SPTs

The prevalence of SPTs after HNSCC in the existing literature varies greatly geographically. In Asia, second primary gastrointestinal tract malignancies are more common after index HNSCC than in the Western world.[2] It is thought that Asians have a higher exposure to risk factors such as smoking and alcohol use. Other risk factor such as hot beverage drinking and betel quid chewing and genetic susceptibility have also been suggested to play a part.[68] As a result, the literature on this topic, including the studies of this review, are mostly from Asian countries. In the present review only three studies were non-Asian. This prohibits us to draw bold conclusions and extrapolate results on the usefulness of Lugol chromoendoscopy in a non-Asian patient population, as also stated by Morimoto et al.[21]

Another limitation is the quality of the included studies. Since the quality of a review greatly relies on the quality of the included data, we excluded studies of low quality. Although the remaining 15 studies were all similar in methodology and research question, there was some heterogeneity among the studies in the sub-sites of the index HNSCC tumors that were included. This might have had an influence on the average prevalence of all studies. However, the four largest studies ($n = 326$ -676) with the highest weight on the average fortunately included all sub-locations. A final potential limitation is that the study selection and quality assessment was performed by one reviewer. The overall study quality could have benefited from a an assessment by two independent reviewers.

Conclusion

In conclusion, this review has shown that the prevalence of esophageal second primary tumors in head and neck cancer patients is high, especially for patients with a hypo- and oropharyngeal index tumor. A large percentage of esophageal lesions were found in early

stage of development. Literature shows that this group of patients could significantly benefit from dual tumor treatment, resulting in an increased 5-year survival rate. Based on our results there appears to be strong evidence to perform Lugol chromoendoscopy screening in an Asian patient population. More screening studies are needed to confirm the same for the Western world and Lugol chromoendoscopy holds the potential to increase the overall survival rate of head and neck cancer patients, due a lowered SPT-specific mortality.

References

1. Priante AVM, et al. - Second primary tumors in patients with head and neck cancer. - *Curr Oncol Rep* 2011.
2. Atienza JAS, et al. - Incidence of second primary malignancies in patients with treated head and neck cancer: A comprehensive review of literature. - *Curr Med Res Opin* 2012.
3. Shaha AR, et al. - Synchronicity, multicentricity, and metachronicity of head and neck cancer. - *HEAD NECK SURG* 1988.
4. Morris LGT, et al. - Anatomic sites at elevated risk of second primary cancer after an index head and neck cancer. - *Cancer Causes Control* 2011.
5. Bradley PJ, et al. - Searching for metachronous tumours in patients with head and neck cancer: The ideal protocol! - *Curr Opin Otolaryngol Head Neck Surg* 2010.
6. Tiwana MS, et al. - Incidence of second metachronous head and neck cancers: Population-based outcomes over 25 years. - *Laryngoscope* 2014.
7. Schotborgh C, et al. - High incidence of a second primary esophageal squamous cell carcinoma in patients with previous head-and-neck cancer: A nationwide population-based study. - *Gastroenterology* 2011.
8. Morris LGT, et al. - Second primary cancers after an index head and neck cancer: Subsite-specific trends in the era of human papillomavirus - Associated oropharyngeal cancer. - *J Clin Oncol* 2011.
9. Blanchard D, et al. - Guidelines update: Post-treatment follow-up of adult head and neck squamous cell carcinoma: Screening for metastasis and metachronous esophageal and bronchial locations. - *Eur Ann Otorhinolaryngol Head Neck Dis* 2015.
10. Chung CS, et al. - Image-enhanced endoscopy for detection of second primary neoplasm in patients with esophageal and head and neck cancer: A systematic review and meta-analysis. - *Head Neck* 2016.
11. Dhooge IJ, et al. - Multiple primary malignant tumors in patients with head and neck cancer: Results of a prospective study and future perspectives. - *Laryngoscope* 1998.
12. Paniello RC, et al. - Practice patterns and clinical guidelines for posttreatment follow-up of head and neck cancers: a comparison of 2 professional societies. - *Arch Otolaryngol Head Neck Surg* 1999.
13. De Monès E, et al. - Initial staging of squamous cell carcinoma of the oral cavity, larynx and pharynx (excluding nasopharynx). Part 2: Remote extension assessment and exploration for secondary synchronous locations outside of the upper aerodigestive tract. 2012 SFORL guidelines. - *Eur Ann Otorhinolaryngol Head Neck Dis* 2013.
14. Sabharwal R, et al. - Genetically altered fields in head and neck cancer and second field tumor Review. - *South Asian j cancer* 2014.
15. Angadi PV, et al. - Oral field cancerization: current evidence and future perspectives. - *Oral Maxillofac Surg* 2012.
16. León X, et al. - Second neoplasm in patients with head and neck cancer. - *Head Neck* 1999.
17. Alsop BR, et al. - Esophageal Cancer. - *Gastroenterol Clin North Am* 2016.
18. Stoeckli SJ, et al. - Role of routine panendoscopy in cancer of the upper aerodigestive tract. - *Otolaryngol Head Neck Surg* 2001.
19. Heroiu Cataloiu AD, et al. - Multiple cancers of the head and neck. - *Medica* 2013.
20. Argiris A, et al. - Epidemiology, staging, and screening of head and neck cancer. - *Cancer Treat Res* 2003.
21. Morimoto M, et al. - Significance of endoscopic screening and endoscopic resection for esophageal cancer in patients with hypopharyngeal cancer. - *Jpn J Clin Oncol* 2010.
22. Wang WL, et al. - The benefit of pretreatment esophageal screening with image-enhanced endoscopy on the survival of patients with hypopharyngeal cancer. - *Oral Oncol* 2013.
23. Saeki H, et al. - The treatment outcomes of synchronous and metachronous esophageal squamous cell carcinoma and head and neck squamous cell carcinoma. - *Esophagus* 2012.
24. Makuuchi H, et al. - Endoscopic screening for esophageal cancer in 788 patients with head and neck cancers. - *Tokai J Exp Clin Med* 1996.
25. Wang CH, et al. - Use of transnasal endoscopy for screening of esophageal squamous cell carcinoma in high-risk patients: Yield rate, completion rate, and safety. - *Dig Endosc* 2014.
26. Slim K, et al. - Methodological index for non-randomized studies (minors): development and validation of a new instrument. - *ANZ J Surg* 2003.
27. Moher D, et al. - Preferred reporting items for systematic reviews and meta-analyses: the PRISMA statement. - *J Clin Epidemiol* 2009.
28. Schlemper RJ, et al. - The Vienna classification of gastrointestinal epithelial neoplasia. - *Gut* 2000.
29. Gong EJ, et al. - Routine endoscopic screening for synchronous esophageal neoplasm in patients with head and neck squamous cell carcinoma: a prospective study. - *Dis Esophagus* 2016.

30. Ikawa H, et al. - Upper gastrointestinal tract cancers as double-cancers in elderly patients with oral squamous cell carcinoma. - *Bull Tokyo Dent Coll* 2012.
31. Wang WL, et al. - Risk factors for developing synchronous esophageal neoplasia in patients with head and neck cancer. - *Head Neck* 2011.
32. Fukuhara T, et al. - Characteristics of esophageal squamous cell carcinomas and lugol-voiding lesions in patients with head and neck squamous cell carcinoma. - *J Clin Gastroenterol* 2010.
33. Lee YC, et al. - Transnasal endoscopy with narrow-band imaging and Lugol staining to screen patients with head and neck cancer whose condition limits oral intubation with standard endoscope (with video). - *Gastrointest Endosc* 2009.
34. Boller D, et al. - Lugol chromoendoscopy combined with brush cytology in patients at risk for esophageal squamous cell carcinoma. - *Surg Endosc Interv Tech* 2009.
35. Dubuc J, et al. - Endoscopic screening for esophageal squamous-cell carcinoma in high-risk patients: a prospective study conducted in 62 French endoscopy centers. - *Endoscopy* 2006.
36. Hashimoto CL, et al. - Lugol's dye spray chromoendoscopy establishes early diagnosis of esophageal cancer in patients with primary head and neck cancer. - *The American journal of ...* 2005.
37. Muto M, et al. - Association between aldehyde dehydrogenase gene polymorphisms and the phenomenon of field cancerization in patients with head and neck cancer. - *Carcinogenesis* 2002.12376487
38. Tanabe H, et al. - Alcohol consumption as a major risk factor in the development of early esophageal cancer in patients with head and neck cancer. - *Intern Med* 2001.
39. Fukuzawa K, et al. - High incidence of synchronous cancer of the oral cavity and the upper gastrointestinal tract. - *Cancer Lett* 1999.
40. Horiuchi M, et al. - Survival benefit of screening for early esophageal carcinoma in head and neck cancer patients. - *Dig Endosc* 1998.
41. Laohawiriyakamol S, et al. - Evaluating synchronous esophageal cancer in head and neck cancer patients using Lugol dye chromoendoscopy. - *J Med Assoc Thailand* 2014.
42. Kominek P, et al. - Chromoendoscopy to detect early synchronous second primary esophageal carcinoma in patients with squamous cell carcinomas of the head and neck? - *Gastroenterol Res Pract* 2013.
43. Chow TL, et al. - Prediction of simultaneous esophageal lesions in head and neck squamous cell carcinoma: A multivariate analysis. - *Arch Otolaryngol Head Neck Surg* 2009.
44. Muto M, et al. - Association of multiple Lugol-voiding lesions with synchronous and metachronous esophageal squamous cell carcinoma in patients with head and neck cancer. - *Gastrointest Endosc* 2002.
45. Tincani AJ, et al. - Diagnosis of superficial esophageal cancer and dysplasia using endoscopic screening with a 2% lugol dye solution in patients with head and neck cancer. - *Head Neck* 2000.
46. Ina H, et al. - The frequency of a concomitant early esophageal cancer in male patients with oral and oropharyngeal cancer. Screening results using Lugol dye endoscopy. - *Cancer* 1994.
47. Chisholm EM, et al. - Lugol's iodine dye-enhanced endoscopy in patients with cancer of the oesophagus and head and neck. - *EUR J SURG ONCOL* 1992.
48. Shiozaki H, et al. - Endoscopic screening of early esophageal cancer with the Lugol dye method in patients with head and neck cancers. - *CANCER* 1990.
49. Herranz Gonzalez-Botas J, et al. - Second primary tumours in head and neck cancer. - *Acta Otorrinolaringol Esp* 2016.
50. Andersen AR, et al. - Secondary oesophageal or gastric cancer in patients treated for head and neck squamous cell carcinoma. - *Dan Med J* 2016.
51. Krishnatreya M, et al. - Synchronous primary cancers in the head and neck region and upper aero digestive tract: Role of triple endoscopy. - *Indian J Cancer* 2015.
52. Lee DH, et al. - Second Cancer Incidence, Risk Factor, and Specific Mortality in Head and Neck Squamous Cell Carcinoma. - *Otolaryngology-Head and Neck Surgery* 2013.
53. Kim E, et al. - Incidence of esophageal cancers among oral cavity and pharynx cancer patients: A review of the SEER database (1973-2007). - *J Clin Oncol* 2011.
54. Park JW, et al. - Clinical outcomes of synchronous head and neck and esophageal cancer. - *Radiat Oncol J* 2015.
55. Lim H, et al. - Clinical significance of early detection of esophageal cancer in patients with head and neck cancer. - *Gut Liver* 2015.
56. Graff P, et al. - Management of Patients with Head and Neck Tumours Presenting at Diagnosis with a Synchronous Second Cancer at Another Anatomic Site. - *Clin Oncol* 2011.
57. Liu WS, et al. - Secondary primary cancer in patients with head and neck carcinoma: the differences among hypopharyngeal, laryngeal, and other sites of head and neck cancer. - *Eur J Cancer Care (Engl)* 2014.
58. Yamamoto E, et al. - Site specific dependency of second primary cancer in early stage head and neck squamous cell carcinoma. - *Cancer* 2002.

59. Kim dH, et al. - Clinical significance of intensive endoscopic screening for synchronous esophageal neoplasm in patients with head and neck squamous cell carcinoma. - *Scand J Gastroenterol* 2014.
60. Hung SH, et al. - Routine endoscopy for esophageal cancer is suggestive for patients with oral, oropharyngeal and hypopharyngeal cancer.[Erratum appears in *PLoS One*. 2017 Jan 20;12 (1):e0170866; PMID: 28107467]. - *PLoS ONE* 2013.
61. Su YY, et al. - Effect of routine esophageal screening in patients with head and neck cancer. - *JAMA Otolaryngol Head Neck Surg* 2013.
62. Kondo N, et al. - Diagnostic sensitivity of 18fluorodeoxyglucose positron emission tomography for detecting synchronous multiple primary cancers in head and neck cancer patients. - *Eur Arch Oto-Rhino-Laryngol* 2012.
63. Wallowy P, et al. - 18F-FDG PET for detecting metastases and synchronous primary malignancies in patients with oral and oropharyngeal cancer. - *NuklearMedizin* 2009.
64. Liu FY, et al. - Synchronous malignancies in patients with squamous cell carcinomas of the oral cavity. - *Eur J Nucl Med Mol Imaging* 2011.
65. Krabbe CA, et al. - FDG-PET and detection of distant metastases and simultaneous tumors in head and neck squamous cell carcinoma: A comparison with chest radiography and chest CT. - *Oral Oncol* 2009.
66. Chan SC, et al. - 18F-FDG PET/CT and 3.0-T whole-body MRI for the detection of distant metastases and second primary tumours in patients with untreated oropharyngeal/hypopharyngeal carcinoma: A comparative study. - *Eur J Nucl Med Mol Imaging* 2011.
67. Roof SA, et al. - Transnasal esophagoscopy in modern head and neck surgery. - *Current Opinion in Otolaryngology & Head and Neck Surgery* 2015.
68. Zhang HZ, et al. - Epidemiologic differences in esophageal cancer between Asian and Western populations. - *Chin J Cancer* 2012.

Chapter 5b

Endoscopic screening: head and neck SPTs in esophageal cancer patients

Screening for head and neck second primary tumors in patients with esophageal squamous cell cancer: a systematic review and meta-analysis

Steffi van de Ven; Oisín Bugter; Jose Hardillo; Marco Bruno; Robert Baatenburg de Jong; Arjun Koch

United European Gastroenterology Journal, Dec 2019, PMID: 31839955

Abstract

Background. Esophageal squamous cell carcinomas (ESCCs) are often accompanied by head and neck second primary tumors (HNSPTs). The prognosis of patients with an additional HNSPT is worse compared to patients with only ESCC. Therefore, early detection of HNSPTs may improve the overall outcome of patients with ESCC. The purpose of this study was to investigate the yield of endoscopic screening for HNSPTs in patients with primary ESCC.

Methods. We conducted a systematic literature search of all available databases. Studies were included if ESCC patients were endoscopically screened for HNSPT. The primary outcome was the pooled prevalence of HNSPTs.

Results. Twelve studies, all performed in Japan, were included in this systematic review with a total of 6483 patients. The pooled prevalence of HNSPTs was 6.7% (95% CI: 4.9-8.4). The overall heterogeneity was high across the studies ($I^2 = 89.0\%$, $p < 0.001$). Most HNSPTs were low-stage (85.3%) and located in the hypopharynx (60.3%). The proportion of synchronous (48.2%) and metachronous (51.8%) HNSPTs was comparable.

Conclusions. Based on our results, HNSPT screening could be considered in patients with primary ESCC. All studies were performed in Japan, it is therefore not clear if this this consideration applies to the Western world.

Introduction

Both esophageal and head and neck (HN) cancer are common malignancies worldwide.[1, 2] Esophageal squamous cell carcinoma (ESCC) is the most common histologic type in the esophagus.[3] Patients with ESCC, frequently develop second primary tumors (SPTs) in the upper aerodigestive tract. Most often in the HN region, but also in the esophagus and lungs.[4, 5] The presence of SPTs can be explained by the 'field cancerization' theory: premalignant epithelial changes can occur due to chronic local exposure to common carcinogens, such as alcohol and tobacco, which contributes to the development of syn- and metachronous SPTs.[6] An important risk factor in Western countries for the development of both ESCC and SPTs is alcohol.[7, 8]

Head and neck second primary tumors (HNSPTs) in patients with primary ESCC are reported up to 7% in retrospective studies.[4, 5] The prognosis and survival of patients with esophageal cancer (EC) is poor because most ECs are diagnosed in advanced stages, when definitive cure is most often not achievable.[9] The long-term prognosis is even worse in patients with an additional HNSPT compared to ESCC alone (5-year survival rate of 9.2% vs. 21.0%).[10] This poor prognosis makes early detection of HNSPTs vitally important, especially for ESCC patients with low-stage tumors that could be treated endoscopically, since they have a considerably higher 5-year survival rate.[11]

Different endoscopic techniques for HN cancer screening have been studied. Although Lugol chromoendoscopy is often used in the esophagus to detect dysplastic mucosal lesions, it is known to cause side effects in the HN region such as chest pain and aspiration.[12] Narrow-band imaging (NBI) seems to be the best technique for the detection of HNSPTs in patients with primary ESCC.[13] The HNSPT detection rate is significantly higher using NBI (sensitivity 100%, specificity 97.5%) compared to only white light endoscopy (WL).[13] The sensitivity of FDG-PET/CT for the detection of HNSPTs is 61.5%, more HNSPTs were detected by endoscopy.[14]

The European ESMO Clinical Practice Guideline for EC recommends endoscopic screening of the HN region and trachea-bronchoscopy to detect SPTs in the upper aerodigestive tract in all ESCC patients with chronic tobacco and alcohol consumption.[15] However, no Western screening studies have been published to date. The Japanese EC guideline recommends appropriate diagnostic measures of other organs (HN, stomach, large intestine) after treatment of ESCC due to the risk of developing SPTs.[16] However, no specific screening recommendations (*i.e.* diagnostic method and the time of screening) are mentioned.[16]

We have performed a systematic review and meta-analysis of studies that investigated the use of endoscopic screening for the detection of HNSPTs in patients with primary ESCC. Our primary objective was to investigate the yield of endoscopic screening for HNSPTs in patients with primary ESCC. Our secondary objectives were to investigate whether there is evidence to justify endoscopic HN screening in primary ESCC patients in the Western world, and to investigate whether screening should be performed synchronously or metachronously.

Materials and Methods

Literature search and selection criteria

A systematic literature search was performed in collaboration with the Medical Library of the Erasmus University Rotterdam, the Netherlands, in February 2019 with no limit on publication date. The search was performed in PubMed, Embase, Medline, Cochrane Central, Google Scholar and Web of Science databases. The full electronic search strategy for the Embase database is provided in Supplementary Appendix 1. The search was limited to English studies performed on humans. After removing duplicate citations, the remaining articles were reviewed based on title and abstract by two independent reviewers (SV and OB). Subsequently, the full text of the remaining articles was screened by the same authors and discrepancies were discussed mutually. If there was no agreement, a third party was involved (AK). Studies were included if patients with primary ESCC were endoscopically screened for HNSPTs. Studies were excluded if patients with primary head and neck squamous cell carcinoma (HNSCC) were screened for esophageal SPTs, since we investigated the yield of HNSPT screening in patients with primary ESCC. Moreover, these studies are already included in a systematic review about screening for esophageal SPT in patients with primary HNSCC.[17] Studies without full-text, case reports, reviews, and studies where only imaging techniques were used to detect HNSPTs were excluded. References of the retrieved studies were manually screened to locate additional studies.

Table 1. Relevance criteria

Criteria	Score		
	0	1	2
Text clarity	Low	Medium	High
Sub-location	No	-	Yes
Impact factor	< 2	2-3.9	≥ 4

Study quality

The Methodological Index for Non Randomized Studies (MINORS) was used to test the risk of bias and the methodological quality of the selected studies.[18] The study relevance

was determined using a checklist. This checklist includes: (1) impact factor of publishing journal (indication of the peer-review quality), (2) data of the HNSPT sub-location, and (3) text clarity (Table 1). The total quality score of the studies was the sum of the MINORS and relevance criteria score. The total scores were classified as low (≤ 10 points), medium (11–14 points) or high (≥ 15 points). Medium and high classified studies were included.

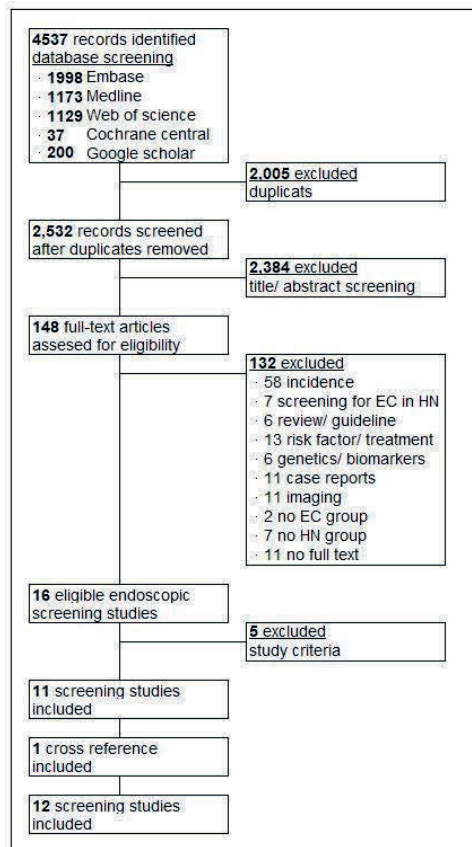


Figure 1. Study selection process. EC = esophageal cancer, HN= head and neck cancer.

Data extraction and outcome parameters

Data from included studies were summarized as Preferred Reporting Items for Systematic Reviews and Meta-Analyses (PRISMA) checklist and flow chart.[19] The primary outcome was the prevalence of diagnosed HNSPTs. A HNSPT was defined as a lesion in the HN region classified as carcinoma in situ or carcinoma. With NBI, these lesions can be described as well-demarcated brownish areas without magnification, irregular microvascular patterns, and increased intraepithelial papillary capillary loops.[20] Secondary outcomes were

recorded when possible: (1) HNSPT prevalence per sub-location (upper, middle and lower esophagus) and per tumor stage (0 to IV according to the Vienna classification of gastrointestinal epithelial neoplasia) of the primary ESCC, (2) synchronously (≤ 6 months after diagnosis of primary ESCC) or metachronously (> 6 months after diagnosis of primary ESCC) diagnosed HNSPTs, and (3) the tumor stage and sub-location of HNSPTs.[21] Other characteristics of the studies were also recorded: first author, publication year, study design, size and country of the study population.

Statistical analysis

For each study, the HNSPT prevalence was calculated (total number of HNSPTs divided by the total population that was screened). The standard error (SE) was calculated from the prevalence using the following formula: $SE = \sqrt{p \cdot (1 - p) / n}$, p = prevalence and n = total number of patients with ESCC that were screened. Estimation of the prevalence was carried out with the aid of a random-effects meta-analysis. Combined estimates and 95% confidence intervals (CIs) for the HNSPT prevalence rates were calculated. The heterogeneity among studies was measured by calculating the inconsistency index (I^2), with values from 0% to 100% (maximum heterogeneity). Categories of low, moderate and high were assigned to I^2 values of 25%, 50% and 75%, respectively.[22] When $I^2 \geq 50\%$, there was evidence of moderate or high heterogeneity.

Results

Study selection and quality assessment

The study selection process and eligibility assessment are outlined in Figure 1. Literature search identified 4537 citations. After screening, 148 articles were examined by full-text review for their eligibility by two reviewers (SV and OB). Discrepancies were discussed mutually without any final disagreements. One additional study was included after screening the references. Twelve studies were included in our systematic review.[7, 10, 13, 20, 23-30] Exclusion reasons are shown in Figure 1. All twelve included studies were qualified as medium or high (Table 2). The relevance criteria score ranged between 0 and 5 points (maximum possible score is 6). The MINORS-criteria score ranged from 9 to 23 points (maximum possible score of 24).

Study characteristics

The study characteristics are reported in Table 2. All studies were performed in Japan and published between 2002 and 2018. Nine of the twelve studies (75%) collected their data prospectively [7, 10, 13, 20, 24, 25, 27, 28, 30], and three (25%) retrospectively.[23, 26, 29] The total number of included patients was 6483 (median 313, range 71-1674). In two studies Lugol iodine was used for screening of the HN region.[24, 28] In five other studies both WL

Table 2. Study characteristics and quality score of all 12 studies

Author	Year	Design	N	Method	Quality Score			Quality Screening sites	
					MINORS	Rel.	Total		
Abiko et al.[7]	2018	Pro	158	WL	18	3	21	High	Larynx
Onochi et al.[29]	2018	Retro	285	WL	10	3	13	Medium	Oro- hypopharynx
Morimoto et al.[23]	2017	Retro	307	WL + NBI	18	5	23	High	Oro- hypopharynx Larynx
Kaneko et al.[26]	2013	Retro	348	WL + NBI	9	4	13	Medium	Oral cavity Pharynx
Katada et al.[30]	2012	Pro	71	WL + NBI	16	5	21	High	Head and neck region*
Muto et al.[20]	2010	Pro	320	WL + NBI	23	4	27	High	Oro- hypopharynx
Nonaka et al.[13]	2009	Pro	424	WL + NBI	19	5	24	High	Pharynx
Lo et al.[10]	2008	Pro	1675	WL	18	3	21	High	Head neck region*
Watanabe et al.[28]	2007	Pro	1118	Lugol	10	3	13	Medium	Head neck region*
Shimizu et al.[24]	2003	Pro	99	Lugol	18	5	22	High	Hypopharynx Larynx
Kagei et al.[27]	2002	Pro	1479	WL	10	2	12	Medium	Head neck region*
Motoyama et al.[25]	2003	Pro	200	WL	13	4	17	High	Larynx

* Nasal cavity, oral cavity, naso-, oro-, and hypopharynx and larynx. Pro = prospective, Retro = retrospective, WL = white light endoscopy, NBI = narrow-band imaging, Rel = relevance.

and NBI were used for screening.[13, 20, 23, 26, 30] In the remaining five studies, only WL was used for screening.[7, 10, 25, 27, 29] In only four studies, the entire HN region was screened.[10, 20, 27, 28, 30] Screening was limited to the pharynx and larynx, sub-locations known to be at an increased risk, in most other studies. Eleven of the twelve studies only screened patients with ESCC.[7, 10, 13, 20, 23-26, 28-30] One study screened both patients with ESCC (93%) and esophageal adenocarcinoma (7%).[27] In total, 98% of the esophageal tumors were squamous cell carcinomas and 2% adenocarcinomas. Screening was performed by an otolaryngologist or head and neck surgeon in 5/12 included studies.[7, 24, 25, 27, 28] Screening was performed by a gastroenterologist in 2/12 studies.[20, 29] In these two studies, only the oropharynx and hypopharynx were screened. In 5/12 included studies, however, it was not clearly reported who performed the screening endoscopy of the head and neck region (otolaryngologist or gastroenterologist).[10, 13, 23, 26, 30]

Pooled SPT prevalence

The prevalence of HNSPTs in patients with ESCC is shown for each study in Figure 2. In total, 353/6483 patients were diagnosed with HNSPT. Meta-analysis with a random-effect model was used to calculate the pooled prevalence since the I^2 was 89.0%. The pooled prevalence for HNSPTs of the twelve included studies was 6.7% (95% CI: 4.9-8.4%) (Figure 2).

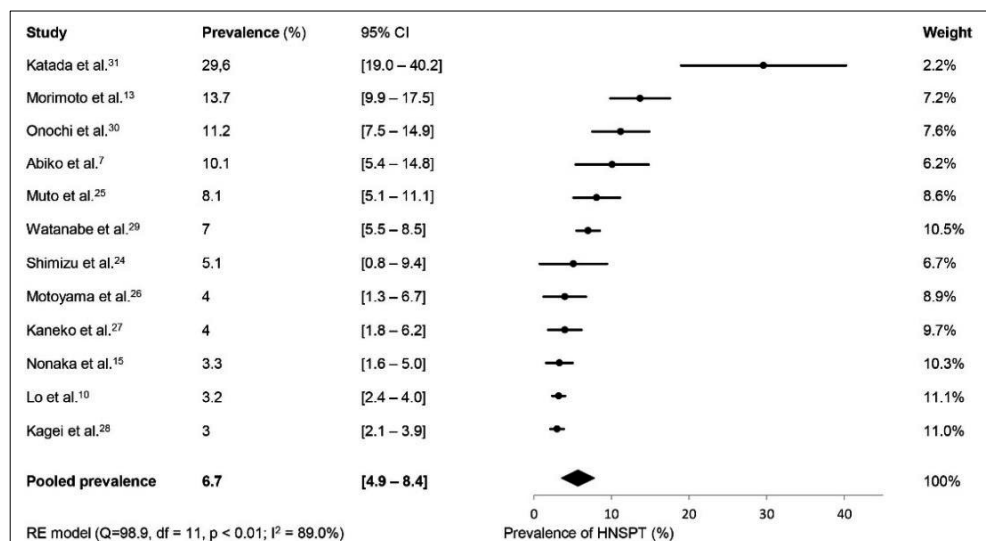


Figure 2. Forest plot of prevalence of head and neck second primary tumors in patients with esophageal squamous cell carcinoma. HNSPT = Head and neck second primary tumor

Sub-location of HNSPT and tumor stage

The sub-location of the HNSPTs was reported in eight of the twelve studies, for a total of 288 SPTs.[10, 13, 23-26, 28, 30]. In one study the sub-location was reported together for primary HN tumors and HNSPTs. Therefore, we excluded the study for this sub-analysis.[10] A total of 234 HNSPTs remained. The combined data showed that 60% (141/234) of all HNSPTs were located in the hypopharynx, 18% (41/234) in the oropharynx, 11% (26/234) in the oral cavity, 9% (22/234) in the larynx and 2% (4/234) in other sub-locations. In total, 405 HNSPTs were detected in 353 patients. Tumor stage of HNSPTs were reported in eight of the twelve studies.[13, 20, 23, 24, 26-28, 30] Morimoto et al. only reported tumor characteristics of metachronous HNSPTs.[23] Combined data showed that tumor stage was available for 62% of the HNSPTs (251/405). Overall, HNSPTs were classified as low-stage (stage 0, I and II) in 85% (214/251) and high-stage (stage III and IV) in 15% (37/251).

Time to diagnosis

Eight studies performed both syn- and metachronous endoscopic screening of the HN region [10, 20, 23-25, 28-30] and six studies adequately reported the percentage of detected synchronous and metachronous HNSPTs (Table 3).[10, 23-25, 28, 29] The median time to metachronous HNSPT diagnosis of these six studies ranged from 12 to 48 months. The time to SPT diagnosis in ESCC patients was reported for all SPTs together in Motoyama et al., not separately for HNSPTs.[25]

Table 3. Percentages synchronous and metachronous HNSPT

Authors	Total SPTs	Synchronous HNSPTs (%)	Metachronous HNSPTs (%)	Median time to diagnosis (months) (range)
Morimoto et al.[23]	67	14 (21%)	53 (79%)	31 (7-107)
Shimizu et al.[24]	5	0	5 (100%)	37 (15-61)
Motoyama et al.[25]	8	0	8 (100%)	Not reported
Watanabe et al.[28]	85	37 (44%)	48 (56%)	48 (12-103)
Onochi et al.[29]	32	23 (72%)	9 (28%)	Not reported
Lo et al.[10]	54	47 (87%)	7 (13%)	12 (8-110)
Total	251	121 (48%)	130 (52%)	

HNSPT = head and neck second primary tumor

Two studies, only performed HN screening synchronously, [26, 27] and two only metachronously.[7, 13] The HNSPT prevalence in the study by Nonaka et al. was 3.3% (14/424) with a median detection period of 27.6 months (range 7.1-143.5) in patients screened with NBI and 101.0 months (range 11.0-134.5) in patients screened with WL.

Primary ESCC tumor characteristics

Only four studies reported the sub-location of the index esophageal tumor.[10, 24, 25, 27] One study only included patients who underwent esophagectomy for thoracic ESCC.[25] The prevalence of HNSPTs in this study was 4.0%. The average percentages of index upper, middle, and lower ESCC of the other three studies were 17.0%, 57.7%, and 25.3% respectively.[10, 24, 27] However, they did not report the prevalence of HNSPT per ESCC sub-location. The tumor stage of the primary ESCC was reported in nine studies (75%).[7, 10, 20, 23-25, 27, 29, 30] On average, most esophageal lesions were stage I (29.0%) and stage 3 (29.8%). Other tumor stages were 0 (high grade dysplasia) (7.3%), 2 (20.2%), and stage 4 (13.6%). The HNSPT prevalence per tumor stage of the primary ESCC was reported in three studies, where only superficial ESCCs (stage 0 and I) were screened.[7, 29, 30]

Discussion

To our knowledge, this is the first systematic review on endoscopic screening for HNSPTs in patients with primary ESCC. Worldwide, the incidence of HN cancer is more than 550,000 cases annually.[2] We found a HNSPT (pooled) prevalence of 6.7%. Most HNSPTs were located in the hypopharynx (60.3%), and classified as low-stage (85.3%). The proportion of synchronous and metachronous HNSPTs was comparable. Although the worldwide incidence cannot be compared directly with the pooled prevalence from this meta-analysis, the concept of endoscopic screening in patients with ESCC bares promise.

An increase in early detection of HNSPTs could potentially improve the overall survival of ESCC patients.

Screening in Western countries will possibly show a different HNSPT prevalence because the etiology partly differs among these continents and ESCC and HNSCC have a higher prevalence in Asia.[3, 31] The etiology of ESCC in Asia is, besides smoking and alcohol intake, clearly linked to a lowered fruit and vegetables intake.[32] The overall incidence of HN cancer in Japan was increasing, whereas the incidence in the United States was decreasing.[31, 33] Since the included studies were performed in Japan, it is unlikely that these results can be applied to the contemporary Western population.

Non-screening Asian studies have reported HNSPT prevalence up to 7% in patients with primary ESCC.[4, 5] This is lower than the prevalence of the included studies (3.0%-29.6%). This might indicate that active screening of ESCC patients increase the number of detected HNSPTs.[23] Early diagnosis and treatment of both tumors can increase the survival rate.[23, 34]

Eighty-five percent of the HNSPTs were classified as low-stage, which is higher than in the general HN cancer population.[35] Morimoto et al. reported a higher percentage of low-stage HNSPTs in patients with primary ESCC who were actively screened, and 83% of these HNSPTs could be treated with ER.[23] Furthermore, survival was better in ESCC patients with HNSPTs who were actively screened.[23] ESCC patients could benefit from HN screening because this could result in an increased detection of superficial HN cancer, which can be treated with curative intent.

There is lack of standardization in HN examination protocols among the included studies, since different screening techniques are used (WVL, NBI and Lugol). Studies that compared NBI with WVL described a significantly higher detection rate of HNSPTs and a higher sensitivity and accuracy when using NBI.[13, 20, 23, 26] It would therefore be useful to always perform HN screening with WVL and NBI. Lugol chromoendoscopy is not recommended in the HN region, since this has to be performed under general anesthesia due to possible side effects.[28]

The average percentage synchronous and metachronous HNSPTs of all studies together is comparable. This could indicate that HN screening in patients with ESCC should be performed during work-up and follow-up. The median detection time of metachronous HNSPTs ranged from 12-101 months.[10, 13, 23, 24, 28] However, the optimal moment for screening during follow-up has yet to be defined.

Our systematic review showed that 78% of the HNSPTs were located in the pharynx, which suggest that the pharynx has the highest risk of developing SPTs. Moreover, patients with pharyngeal cancer also showed the highest prevalence of esophageal SPTs.[17] The pharynx is the head and neck region which should be definitely screened in patients with primary ESCC. Although ten of the twelve included studies performed screening of the pharynx, only four studies screened the whole HN region. We are aware of the fact that, of these four studies, only two studies reported the HNSPT sub-location.[28, 30] It was not possible to state if there was a correlation between ESCC tumor stage and the occurrence of HNSPTs since this information was only reported in three studies.[7, 29, 30] In these studies, only superficial ESCCs (stage 0 and I) were screened, which could underestimate the true HNSPT prevalence per ESCC tumor stage.

Some potential limitations about the methodology of the included studies need to be discussed; 1) different screening techniques (*i.e.* WL, NBI, Lugol chromoendoscopy) were used. The combination of WL and NBI has the highest HNSPT detection rate, potential HNSPTs could be missed when using only WL ; 2) One study performed screening with endoscopy and CT-scan.[27] It was not clearly described which proportion of HNSPTs were detected by endoscopic screening. The proportion of HNSPTs detected by endoscopic screening could be lower than reported; 3) a different definition of metachronous and synchronous was used in three studies, whereby the comparison of the different studies was more difficult and the proportion of metachronous SPTs could be higher than reported [7, 27, 28]; 4) only four studies screened the whole HN region. Therefore, we could not easily determine which HN sub-location was at increased risk of developing HNSPTs; 5) this meta-analysis contained both prospective and retrospective data, a significant bias may be present.

In conclusion, the pooled prevalence of HNSPTs in patients with primary ESCC is 6.7%. Most HNSPTs were classified as low-stage. Patients with low-stage HN tumors can be treated curatively with an excellent prognosis. Screening for HNSPTs could therefore be useful in ESCC patients. More screening studies are needed to investigate which type of ESCC (*i.e.*, tumor stage and sub-location) increases the risk of HNSPTs and to report on risk factors associated with HNSPTs. More importantly, it is necessary to perform Western screening studies to assess the HNSPT prevalence since it is unclear whether the results of Asian studies can be extrapolated into the Western population. Head and Neck examination protocols should be standardized in Japan; screening should be performed during work-up and follow-up with WL in combination with NBI. The pharynx is the head and neck region which should always be screened.

References

1. Ferlay J, et al. - Cancer incidence and mortality worldwide: sources, methods and major patterns in GLOBOCAN 2012. - *Int J Cancer* 2015.
2. Global Burden of Disease Cancer C, et al. - Global, Regional, and National Cancer Incidence, Mortality, Years of Life Lost, Years Lived With Disability, and Disability-Adjusted Life-years for 32 Cancer Groups, 1990 to 2015: A Systematic Analysis for the Global Burden of Disease Study. - *JAMA Oncol* 2017.
3. Arnold M, et al. - Global incidence of oesophageal cancer by histological subtype in 2012. - *Gut* 2015.
4. Poon RT, et al. - Multiple primary cancers in esophageal squamous cell carcinoma: incidence and implications. - *Ann Thorac Surg* 1998.
5. Chuang SC, et al. - Risk of second primary cancer among esophageal cancer patients: A pooled analysis of 13 cancer registries. - *Cancer Epidemiol Biomarkers Prev* 2008.
6. Slaughter DP, et al. - Field cancerization in oral stratified squamous epithelium; clinical implications of multicentric origin. - *Cancer* 1953.
7. Abiko S, et al. - Risk assessment of metachronous squamous cell carcinoma after endoscopic resection for esophageal carcinoma based on the genetic polymorphisms of alcoholdehydrogenase-1B aldehyde dehydrogenase-2: temperance reduces the risk. - *J Gastroenterol* 2018.
8. Henry MACA, et al. - Outcome of superficial squamous cell carcinoma of the esophagus. A clinicopathological study. - *Acta Cir Bras* 2013.
9. Alsop BR, et al. - Esophageal Cancer. - *Gastroenterol Clin North Am* 2016.
10. Lo OSH, et al. - Esophageal cancers with synchronous or antecedent head and neck cancers: A more formidable challenge? - *Ann Surg Oncol* 2008.
11. Berger A, et al. - Long-term follow-up after endoscopic resection for superficial esophageal squamous cell carcinoma: a multicenter Western study. - *Endoscopy* 2018.
12. Kondo H, et al. - Sodium thiosulfate solution spray for relief of irritation caused by Lugol's stain in chromoendoscopy. - *Gastrointest Endosc* 2001.
13. Nonaka S, et al. - Narrow-band imaging endoscopy with magnification is useful for detecting metachronous superficial pharyngeal cancer in patients with esophageal squamous cell carcinoma. - *J Gastroenterol Hepatol* 2010.
14. Miyazaki T, et al. - Effectiveness of FDG-PET in screening of synchronous cancer of other organs in patients with esophageal cancer. - *Anticancer Res* 2014.
15. Lordick F, et al. - Oesophageal cancer: ESMO Clinical Practice Guidelines for diagnosis, treatment and follow-up. - *Ann Oncol* 2016.
16. Kuwano H, et al. - Guidelines for Diagnosis and Treatment of Carcinoma of the Esophagus April 2012 edited by the Japan Esophageal Society. - *Esophagus* 2015.
17. Bugter O, et al. - Early detection of esophageal second primary tumors using Lugol chromoendoscopy in patients with head and neck cancer: A systematic review and meta-analysis. - *Head Neck* 2018.
18. Slim K, et al. - Methodological index for non-randomized studies (minors): development and validation of a new instrument. - *ANZ J Surg* 2003.
19. Moher D, et al. - Preferred reporting items for systematic reviews and meta-analyses: the PRISMA statement. - *J Clin Epidemiol* 2009.
20. Muto M, et al. - Early detection of superficial squamous cell carcinoma in the head and neck region and esophagus by narrow band imaging: a multicenter randomized controlled trial. - *Journal of Clinical ...* 2010.
21. Schlemper RJ, et al. - The Vienna classification of gastrointestinal epithelial neoplasia. - *Gut* 2000.
22. Higgins JP, et al. - Measuring inconsistency in meta-analyses. - *Bmj* 2003.
23. Morimoto H, et al. - Clinical impact of surveillance for head and neck cancer in patients with esophageal squamous cell carcinoma. - *World J Gastroenterol* 2017.
24. Shimizu Y, et al. - Head and neck cancer arising after endoscopic mucosal resection for squamous cell carcinoma of the esophagus. - *Endoscopy* 2003.
25. Motoyama S, et al. - Outcomes of active operation during intensive followup for second primary malignancy after esophagectomy for thoracic squamous cell esophageal carcinoma. - *J Am Coll Surg* 2003.
26. Kaneko K, et al. - Treatment strategy for superficial pharyngeal squamous cell carcinoma synchronously combined with esophageal cancer. - *Oncology* 2013.
27. Kagei K, et al. - Efficacy of intense screening and treatment for synchronous second primary cancers in patients with esophageal cancer. - *Jpn J Clin Oncol* 2002.
28. Watanabe A, et al. - Head and neck cancer associated with esophageal cancer. - *Auris Nasus Larynx* 2007.

29. Onochi K, et al. - Risk Factors Linking Esophageal Squamous Cell Carcinoma With Head and Neck Cancer or Gastric Cancer. - 2018.
30. Katada C, et al. - Risk of superficial squamous cell carcinoma developing in the head and neck region in patients with esophageal squamous cell carcinoma. - *Laryngoscope* 2012.
31. Ioka A, et al. - Trends in head and neck cancer incidence in Japan during 1965-1999. - *Jpn J Clin Oncol* 2005.
32. Yokokawa Y, et al. - Ecological study on the risks of esophageal cancer in Ci-Xian, China: the importance of nutritional status and the use of well water. - *Int J Cancer* 1999.
33. Mourad M, et al. - Epidemiological Trends of Head and Neck Cancer in the United States: A SEER Population Study. - *J Oral Maxillofac Surg* 2017.
34. Hiroshi Saeki, et al. - The treatment outcomes of synchronous and metachronous esophageal squamous cell carcinoma and head and neck squamous cell carcinoma. - *Esophagus* 2012.
35. Amar A, et al. - Evolution of patients with squamous cell carcinoma of upper aerodigestive tract. - *Sao Paulo Med J* 2003.

Chapter 6

LIGHT study

Detecting head and neck lymph node metastases with light reflectance spectroscopy: a pilot study

Oisín Bugter; Yassine Aaboubout; Mahesh Algoe; Henriëtte de Bruijn; Stijn Keereweer;
Aniel Sewnaik; Dominiek Monserez; Senada Koljenović; Jose Hardillo; Dominic Robinson;
Robert Baatenburg de Jong

Under review at Oral Oncology, May 2021

Abstract

Background. A challenge in the treatment of patients with head and neck cancer is the management of occult cervical lymph node (LN) metastases. This pilot study aimed to investigate whether single-fiber reflectance (SFR) spectroscopy could serve as an alternative or additional technique to detect cervical lymph node metastases.

Methods. We performed intraoperative SFR spectroscopy measurements of LNs with and without malignancies. We analyzed if physiological and scattering parameters were significantly altered in positive LNs. Nine patients with a total of nineteen LNs were included.

Results. Three parameters, blood volume fraction (BVF), microvascular saturation (StO_2), and Rayleigh amplitude, were combined into one optical parameter 'delta'. Delta had a high diagnostic accuracy where the sensitivity, specificity, PPV, and NPV were 90.0%, 88.9%, 90.0%, and 88.9%, respectively. The area under the ROC curve was 96.7% (95% confidence interval 89.7-100.0%).

Conclusions. This proof of principle study is a first step in the development of an SFR spectroscopy technique to detect LN metastases in real time. A next step towards this goal is replicating these results in LNs with smaller metastases and in a larger cohort of patients. This future study will combine SFR spectroscopy with fine-needle aspiration to perform preoperative *in vivo* measurements.

Introduction

Regional lymph node (LN) metastasis often occurs in head and neck squamous cell carcinomas (HNSCC).[1, 2] Regional LN metastasis at the time of diagnosis is among the most important negative prognostic factors.[3] Lymph node metastases (i.e., ‘positive neck’ or cN+) require treatment by surgery with or without adjuvant (chemo)radiation or by primary radiotherapy.[1]

The management of HNSCC patients without LN metastases (i.e., ‘negative neck or cN-’) is still a topic of controversy.[2] Because detection of LN metastases can be challenging, a high percentage of HNSCC patients have occult LN metastases.[1, 2] Two main policies are in practice when the treatment of the primary tumor is surgical. The first is to perform an elective neck dissection (ND) on all patients with clinical negative necks and a high risk of occult metastases. These elective NDs are performed to properly treat the group of “negative neck” patients with occult metastasis; patients who actually have a positive neck. However, a consequence of this strategy is that 60-70% of the patients that did not have occult LN metastasis will receive unnecessary surgery. This could cause morbidity, among other negative consequences.[2] The alternative policy is ‘watchful waiting’. In this strategy, the clinician carefully monitors the patients’ necks and only performs NDs in patients that develop manifest LN metastases. However, the existing techniques to monitor the neck all have limitations in detecting metastatic deposits in LN at the earliest stage.[1, 2, 4]

A solution for this issue in clinically negative necks is a more accurate staging of the neck to personalize treatment. Sentinel lymph node (SLN) biopsy in HNSCC diagnostics is an intra-operative technique that is used to assess whether the primary tumor has metastasized to the LN(s). The SLN(s) is/are the first LN(s) likely to harbor metastasis and they provide information on the rest of the nodal basin. The SLN biopsy is performed during surgery of the primary tumor and meticulously examined by the histopathologist. This SLN examination has a promising reported sensitivity of 86% and negative predictive values (NPV) of 95% in patients with early-stage oral cavity tumors.[4] When a SLN harbors metastatic cells, a ND is recommended. However, this needs to be performed in a second stage, due to the time needed for the pathologic examination of the sentinel LN. This is undesirable, because it could cause distress for the recovering patient and lead to OR-, or postoperative radiotherapy-planning difficulties.[2, 5, 6] Other disadvantages could be an increased risk of injury of the marginal mandibular branch of the facial nerve and a higher risk of morbidity and possibly infection associated with second-stage surgery.

Single-fiber reflectance (SFR) spectroscopy has the potential to serve as an additional technique, or ‘companion diagnostic’, for the SLN biopsy. Several researchers have reported

physiological tissue changes in LNs harboring metastases.[7-9] These changes indicate a compromised vascular network within the center of the LN, which affects microvascular blood oxygen saturation (StO_2) and blood volume fraction (BVF). Furthermore, these changes occur throughout the entire LN and not just in the part of the metastasis. Our group has previously shown that SFR spectroscopy measurements can be used to measure and quantify physiological and scattering properties of *in vivo* tissue.[10-12] Consequently, SFR might be useful to differentiate between metastatic and non-metastatic LNs in head and neck cancer.[13] Diagnosing LN metastases with SFR spectroscopy could give the head and neck surgeon an intraoperative tool to detect a (sentinel) LN metastasis in real-time. In this approach, a potential therapeutic ND could be performed in the same session, since the SLN would not have to be excised to be diagnosed by a histopathologist.

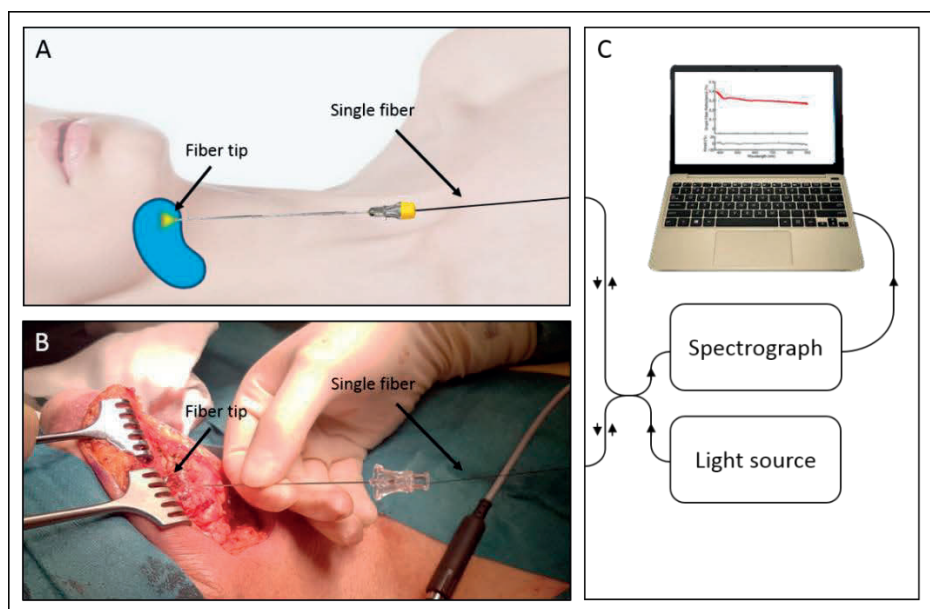


Figure 1. Schematic (a) and real life (b) representation of a single fiber reflectance spectroscopy measurement of a cervical lymph node. Patient consent was giving to take and use this intraoperative picture for scientific purposes

Another potential advantageous use of SFR spectroscopy is to combine it with (preoperative) ultrasound-guided fine-needle aspiration (FNA).[14, 15] Fine-needle aspiration is widely used in the diagnostic workup of HNSCC to acquire material for cytology of lymphatic tissue. Although the diagnostic accuracy of FNA is high, false negatives do occur.[16] This could be explained by the needle 'missing' the metastasis in the LN and only extracting normal tissue. Single-fiber reflectance spectroscopy might not have this problem, since its aim is to detect physiological changes that occur in the entire LN. The

SFR spectroscopy measurement could be performed through the same needle as used for the FNA.

Kanick et al. investigated this hypothesis in a study of ten patients with lung cancer.[13] They performed SFR measurements in 7 malignant and 7 non-malignant mediastinal LNs and found significant ($p < 0.01$) differences in StO_2 and BVF of the LNs. By combining these two parameters it was possible to predict a malignant LN with high accuracy. A recent study, using a similar technique, showed that at least one point measurement per LN is enough to accurately estimate the tissue properties of the entire LN.[17]

In this proof of principle study, we took the first step towards the use of SFR spectroscopy to detect cervical LN metastases. We aimed to investigate whether SFR spectroscopy measurements could differentiate cervical LNs harboring metastases from healthy LNs.[13] For this purpose, intraoperative SFR measurements of LN with and without metastases were performed. It was analyzed whether the optical properties of the metastatic LNs were altered compared to the non-metastatic LNs.

Materials and Methods

This prospective study was approved by the Medical Ethics Committee of the Erasmus MC (MEC-2017-551) and performed in accordance with the ethical standards of the Helsinki Declaration.

Subjects

Patients were recruited from the Department of Otorhinolaryngology and Head and Neck Surgery of the Erasmus MC Cancer Institute. Adult patients with a primary mucosal head and neck tumor (all subsites and stages) who had an indication for a neck dissection and at least 1 preoperatively diagnosed positive LN were included in this study. Patients with prior tumor treatment ([chemo]radiation or surgery) or another illness that could affect the anatomy of their LNs were excluded. All patients signed an informed consent form before enrollment in this study. Patient and tumor specific data such as age, sex, and tumor stage were collected using the electronic medical patient records.

SFR spectroscopy device

The measurements were performed with a SFR spectroscopy device, which has been described in detail previously (Figure 1).[18] In summary, the setup utilizes a sterilized single-use optical fiber (Light Guide Optics International, Latvia) had a core diameter of 230 μm , an outer diameter of 400 μm , an SMA905 connector, a distal polished fiber for wide-angle beam, a numerical aperture of 0.22, and a length of 3 m (± 0.2 m). Its sampling depth is

approximately 165 μm , which is the same as half the core diameter of the fiber. This optical fiber is connected to a bifurcated optical fiber, of which one arm delivers light from a halogen light source (HL-2000-FHSA, Ocean Optics, the Netherlands) to the tissue and the other arm collects light from the tissue to a spectrometer (SD-2000, Ocean Optics, the Netherlands) to measure white light reflectance. A calibration procedure to account for internal reflections, variability in lamp-specific output and in fiber-specific transmission properties has been described in detail in a previous paper.[19]

Examination procedure

The optical LN measurements were performed during neck dissection surgery with the patient under general anesthesia. They were performed in an *in vivo* environment after the surgeon had exposed the cervical lymph nodes. The LNs were chosen based on their likeliness to harbor metastases by visual and manual examination and preoperative clinical and radiologic information. Per patient, measurements of a positive and negative LNs were performed. Measurements were performed on both sides of the neck in patients with probable bilateral metastatic disease. We aimed to perform a peripheral and a central measurement of each LNs. For the measurements, a 'Spinocan' needle (Braun, Germany) (20 Gauge, outer diameter 0.91 mm, inner diameter 0.60 mm) was first inserted in the peripheral part of the lymph node. The surgeon aimed to place the tip of the needle approximately 1 mm inside the LN. The SFR fiber was then guided through the needle until it was in contact with the LN tissue. Finally 5 repeated SFR measurements were performed with a total duration time of approximately 10 seconds. This procedure was respectively repeated for the central part of the LN to ensure a peripheral and center measurement per LN. All measured LNs were individually marked to assure accurate correlation with final histopathologic assessment. After obtaining the SFR measurements, the surgeon continued the procedure including excision of the cervical LNs. All measurement were led by an investigator (OB, DR) and performed by experienced head and neck surgeons (JH, SKe, AS).

Analysis of Spectra

The SFR spectra were analyzed using a previously described analytical model to describe the wavelength-dependent optical properties, with the goal to extract physiological (absorption) and morphological (scattering) information from the sampled tissue.[18, 20]

The four physiological parameters extracted were: 1) microvascular blood oxygen saturation (StO_2 [%]), the fraction of oxygen-saturated hemoglobin relative to total hemoglobin in the blood; 2) blood volume fraction (BVF [%]), which is the percentage of blood in the measured volume; 3) mean vessel diameter (VD [mm]), which is the mean estimated mean of the vessel diameters; and 4) tissue bilirubin concentration ($[\text{BIL}]_{\text{tis}}$ [$\mu\text{mol/L}$]).

Part of the model is the background scattering model that is a combination of Mie and Rayleigh scattering, given by wavelength-dependent power law functions with fitted parameters specifying the Mie amplitude (S1), Mie slope (S2), and Rayleigh amplitude (S3).

Histopathologic assessment of LNs

All the measured LNs underwent histopathologic examination. To start, the LNs were visually and manually examined and any irregularities were described. Representative tissue samples were fixed by formalin 4% and embedded in paraffin. Thin 4 μm slices are examined by confocal microscopy. All LNs were examined by a single experienced head and neck histopathologist (SKo). The stage of differentiation of the metastasis, the presence of keratin deposits and the presence of fat cells were determined.

Statistical analysis

Confidence intervals on optical parameter estimates were calculated from the square root of the diagonal of the covariance matrix.[21] Parameter values were averaged over five repeated measurements, weighted by the confidence interval of individual spectral fits. Spectra that showed evidence of a blood pool within the detection volume (blood volume fraction > 40%) were excluded from the analysis. Seven parameters were analyzed: StO₂, BVF, VD, [BIL]_{tis}, Mie amplitude, Mie slope, and Rayleigh amplitude. Continuous data was reported as median value and interquartile range (IQR) (non-normally distributed data and $n < 30$ per group). Categorical data was reported as counts and percentages. Differences in the continuous data (parameters obtained from the spectral analysis) between the two groups were analyzed using the Mann-Whitney U test. We standardized our data to a standard normal distribution ($x_{\text{new}} = (x - \mu) / \text{sd}$) where μ is the mean and sd is the standard deviation of parameter x to compute a biomarker, delta, to identify positive LNs. A discriminant analysis of the significantly different parameters was performed to create a combined biomarker 'X'. A ROC-curve of delta was created to test its diagnostic accuracy. There were no missing data. Statistical analysis was performed using SPSS version 21 (IBM Co., USA) and the cut off point for significance was $p < 0.05$.

Results

Nine patients with a total of 22 LNs were included in this study (Table 1). Seven of them were males (77.8%) and two females. Their mean age was 67.9 years (IQR 59.0-74.7). The primary HNSCC tumors were located in the oral cavity (5), larynx (1), and hypopharynx (1). Two patients had an unknown primary tumor. All tumors had metastasized to regional LNs. In two patients (study ID 5 and 6), both sides of the neck (4 LNs) were measured.

The histopathologic assessment of the LNs did not confirm our preoperative assessment (based on physical examination and imaging techniques) in two patients (study ID 6 and 8). In patient 6 all four measured LNs turned out to be negative (without metastasis) and in patient 8 both measured LNs turned to be positive (with metastasis). In total 10/22 LNs showed metastases: four LNs showed well differentiated metastases with keratinization, two LNs showed mild differentiation, and the last four were poorly differentiated of which two were cystic. Fat absorption was observed in 12 out of 22 LNs of which 8 were normal LNs.

Table 1. Patients (n = 9), index tumor, and lymph node (n = 22) baseline characteristics

Patient	Patient		Index tumor			Lymph nodes						
	Sex	Age	Location	cT	cN	Pathology	Side	Level	Size (mm)*	Diff.	Keratin	Fat
1	Male	64.1	Oral cavity	3	2b	Positive	Left	2a	29	Well	Yes	Yes
						Negative	Left	1a				No
2	Female	77.7	Oral cavity	0	I	Positive	Right	2	25	Poor	No	Yes
						Negative	Right	4				No
3	Male	67.9	Unknown pr.	0	2a	Positive	Right	3	55	Poor	No	No
						Negative	Right	1a				Yes
4	Female	70.4	Oral cavity	3	I	Positive	Left	2a	20	Well	Yes	No
						Negative	Left	4				No
5†	Male	72.4	Larynx	3	2c	Positive	Right	3	40	Mild	No	No
						Negative	Right	5				Yes
						Positive	Left	2a	37	Mild	No	No
						Negative	Left	1a				Yes
6†	Male	59.7	Oral cavity	3	2b	X Negative	Right	2b				Yes
						X Negative	Right	4				Yes
						X Negative	Left	2a				Yes
						Negative	Left	4				Yes
7	Male	77.0	Hypopharynx	2	3b	Positive	Left	2a	20	Poor	No	Yes
						Negative	Left	1b				No
8	Male	58.2	Oral Cavity	3	3b	Positive	Right	1b	14	Well	Yes	No
						Positive	Right	3				Yes
9	Male	45.8	Unknown pr.	0	2a	Positive	Left	2a	44	Poor	No	No
						Negative	Left	1b				Yes

Diff. = stage of differentiation of the LN metastasis, Keratin = the presence of keratin deposits in the metastasis, Fat = the presence of fat cells in the LN, Unknown pr. = unknown primary tumor. * All negative lymph nodes were < 15 mm; † Both sides of the neck were measured in these patients.

The measurements of three LNs of patient 6 had to be excluded prior to the analysis of potential differences in optical properties between the LNs with and without metastases (LNs are marked with an 'X' in Table 1). The results from our spectroscopy measurements, together with histopathological examination of the tissue, showed that these measurements were not performed in lymphatic tissue, but in surrounding fat tissue. After exclusion of

those three LNs, statistical analysis was performed on nine patients with a total of ten positive LNs and nine negative LNs.

The LN optical properties of the central measurements were best predictive of the presence of a LN metastasis. Three parameters, BVF, StO₂, and Rayleigh amplitude, were significantly different between the negative and positive LNs (Table 2). The BVF was lower in the positive LNs (0.920 [IQR 0.780-4.720]) than in the negative ones (4.835 [IQR 2.035-18.480], $p = 0.022$). The StO₂ was also decreased in positive LNs, $p = 0.034$. Finally, the median Rayleigh amplitude was lower in the positive LNs (0.140 [IQR 0.035-0.235]) than in the negative LNs (0.305 [IQR 0.235-0.435], $p = 0.011$). The parameters VD, [BIL]_{tis}, Mie amplitude, and Mie slope were not significantly different between the two groups of LNs. The peripheral measurements, while not significantly different from the central measurements, were not able to discriminate between positive and negative LNs.

Table 2. Values of Rayleigh amplitude, blood volume fraction, and blood oxygen saturation values in 10 positive and 9 negative lymph nodes

		Median	25th %	75th %
S3 (-)	Pos	0,140	0,035	0,235
	Neg	0,305	0,235	0,435
BVF (%)	Pos	0,920	0,780	4,720
	Neg	4,835	2,035	18,480
StO2 (%)	Pos	40.0	15.8	53.8
	Neg	62.9	43.7	85.8

S3 = Rayleigh amplitude, BVF = blood volume fraction, StO2 = blood oxygen saturation, Pos = positive, Neg = negative.

The three significantly different parameters, BVF, StO₂, and Rayleigh amplitude were combined into one optical parameter 'delta', using a discriminant analysis. This resulted in an optical parameter that was significantly lower in positive LNs, $p = 0.00061$. It had a high diagnostic accuracy. The sensitivity, specificity, positive predictive value, and negative predictive value of delta were 90.0%, 88.9%, 90.0%, and 88.9%, respectively. The area under curve was 96.7% (95% confidence interval 89.7-100.0%).

Discussion

With the technique described in this paper, it could be possible to detect positive LNs by looking into the physiological changes caused by the malignant cells, instead of the malignant cells themselves. We analyzed whether SFR spectroscopy measurements were able to detect these tissue changes in cervical LNs of HNSCC patients. For this purpose, we performed intraoperative SFR measurements of positive and negative LNs.

Our measurements showed that the BVF was decreased in positive LN. This finding is in accordance with the study from Kanick et. al. in mediastinal LNs of lung cancer patients. This study used the same SFR spectroscopy technique. Interestingly, the BVF values of the cervical LNs in the present study were approximately a 2-fold lower than those of the mediastinal LNs. This might be because mediastinal LNs are better vascularized. However, we found no literature to support this hypothesis. An explanation might be that central region/organs are more vascularized than peripheral ones. Another similarity with both studies is that we both found a decreased blood oxygen saturation in LNs harboring a metastasis. Moreover, it is surprising that both the lower BVF and StO_2 were also seen in our 'Optical Screening' study in the measurement of the field cancerization (in the buccal mucosa) of laryngeal cancer patients.[22]

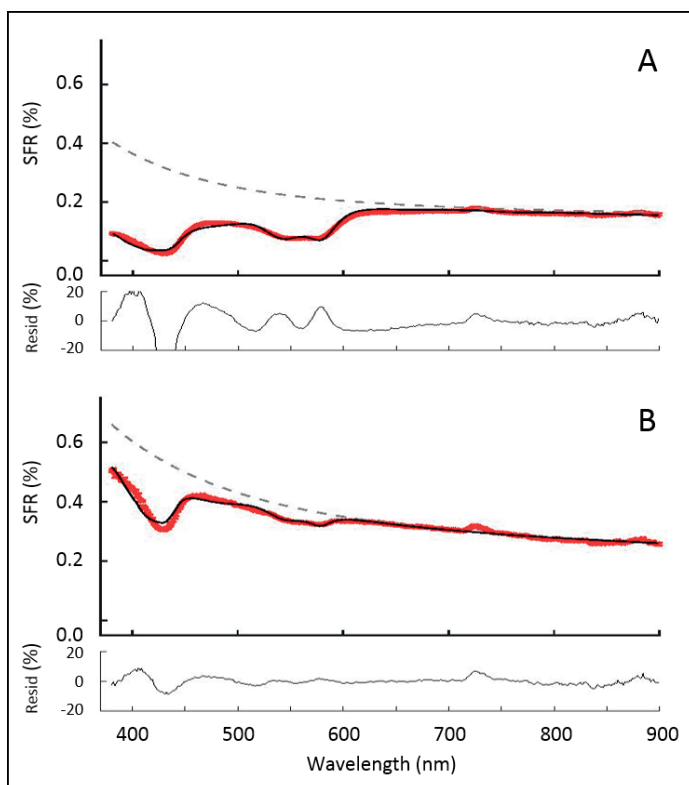


Figure 2. Spectra of the (a) negative and (b) positive lymph node of patient 9. Patient A features a higher absorption coefficient in the wavelength region from 500 to 600 nm. The spectrum from patient A correlates with a higher blood oxygen saturation and blood volume than patient B.

The scattering parameter Rayleigh amplitude was also decreased in positive LNs. This finding is not in line with the two previous studies from our group. However, it does confirm our pre-study hypothesis that LNs with metastases undergo ultrastructural tissue changes.

Liu et. al. also found spectroscopic changes, in the higher infrared wavelengths, in positive cervical lymph nodes of patients with thyroid cancer.[23] These changes were caused by alterations of nucleic acids, proteins, lipids and carbohydrates. Their *ex vivo* measurements of 68 metastatic and 123 non-metastatic LNs provided a sensitivity of 80.3% and a specificity of 91.9%.

During the execution and analysis phase of this pilot-study we encountered some challenges we did not account for in the design phase. This provided us with very useful information to design a future study.

Our study design was to perform the measurements on LNs in an “as *in vivo* as possible” environment: during surgery, when visible for the surgeon. During the measurements we noticed the LNs were not as *in vivo* as we initially thought they would be. In attempt to visualize the LNs, the surgeons had to remove a considerable amount of surrounding tissue. Although attempts were made not to disturb the LN’s vasculature, it is very plausible that this was not achieved. This may have had an influence on the physiological parameters of the measured LNs compared to a real *in vivo* measurement.

It also proved to be difficult to take SFR spectroscopy measurements from the periphery and center of each LN, without additional radiological guidance, which our study design dictated. This was especially the case for the, small, negative LNs. Despite efforts to carefully insert the needle in the desired locations in the LNs, the surgeons found it cumbersome to determine the exact position of needle tip (and thus the measurement point of the fiber tip). In our analyses we even had to conclude that some measurements were not performed inside an actual LN. In these cases, fat tissue might have been misclassified as LNs. With the use of ultrasound guidance, it is possible to overcome this challenge. Radiologists already widely use this technique of ultrasound-guided needle placement for fine-needle aspiration cytology. It is also possible to adjust our SFR spectroscopy device to also detect fat tissue, by increasing the wavelength range.

LNs with cysts bring another challenge. In the present study, the positive LNs of two patients (study ID 2 and 3) were cystic. Insertion of the needle into the cyst for an SFR spectroscopy measurement will unfortunately result in a non-reliable measurement. The fluid inside of the cyst will have a completely different “optical signature” than lymphatic or metastatic tissue. This should be avoided by either measuring the wall of the cyst or a non-

cystic part of the LN. Again, ultrasound guidance could assist in the needle placement in these types of LNs. Another option is to not use this method on LNs suspected to have cystic metastases.

This pilot study had a modest number of included patients and lymph nodes. This prevented us from making definitive statements. On the other hand, finding significant differences given the number of patients is promising. A future study will show whether these differences will remain in larger groups as this might increase the discriminative power of the method. It will also allow to cross-validate our test.

For this pilot study we chose patients with a high susceptibility of harboring malignant LNs (physical examination, imaging) or proven metastases (cytology). The real clinical value lies in detecting smaller, or even micro-, metastases. In this proof of concept study our primary goal was to determine if SFR spectroscopy measurements could discriminate positive LNs from negative. Future research should focus on detecting physiological LN changes caused by smaller metastatic deposits.

Conclusions

This proof of principle study showed that SFR spectroscopy of cervical LN has the ability to differentiate between positive and negative LNs. This may lead to a useful tool to detect LN metastases. It might eliminate the need for a two-stage surgery by analyzing the SLN in real-time. Another potential use is to implement SFR spectroscopy as an addition to FNA cytology. We aim to perform a future study in which we will perform the SFR spectroscopy measurements during, or just prior to, the FNA procedure, using the same needle, thus taking another step towards the implementation of this technique in clinical practice.

References

1. de Bree R, et al. - Advances in diagnostic modalities to detect occult lymph node metastases in head and neck squamous cell carcinoma. - Head Neck 2015.
2. Leusink FK, et al. - Novel diagnostic modalities for assessment of the clinically node-negative neck in oral squamous-cell carcinoma. - Lancet Oncol 2012.
3. Ferlito A, et al. - Elective management of the neck in oral cavity squamous carcinoma: current concepts supported by prospective studies. - Br J Oral Maxillofac Surg 2009.
4. Schilling C, et al. - Sentinel European Node Trial (SENT): 3-year results of sentinel node biopsy in oral cancer. - Eur J Cancer 2015.
5. Flach GB, et al. - Sentinel lymph node biopsy in clinically N0 T1-T2 staged oral cancer: the Dutch multicenter trial. - Oral Oncol 2014.
6. Govers TM, et al. - Sentinel node biopsy for squamous cell carcinoma of the oral cavity and oropharynx: a diagnostic meta-analysis. - Oral Oncol 2013.
7. Ahuja AT, et al. - Ultrasound of malignant cervical lymph nodes. - Cancer Imaging 2008.
8. Chikui T, et al. - Change of angiostructure and hemodynamics in lymph node metastases in rabbits. - Oral Surg Oral Med Oral Pathol Oral Radiol Endod 2002.
9. Tschammler A, et al. - Vascular patterns in reactive and malignant lymphadenopathy. - Eur Radiol 1996.
10. Brooks S, et al. - Sources of variability in the quantification of tissue optical properties by multidiameter single-fiber reflectance and fluorescence spectroscopy. - J Biomed Opt 2015.
11. Kanick SC, et al. - Method to quantitate absorption coefficients from single fiber reflectance spectra without knowledge of the scattering properties. - Opt Lett 2011.
12. Kanick SC, et al. - Measurement of the reduced scattering coefficient of turbid media using single fiber reflectance spectroscopy: fiber diameter and phase function dependence. - Biomed Opt Express 2011.
13. Kanick SC, et al. - Characterization of mediastinal lymph node physiology in vivo by optical spectroscopy during endoscopic ultrasound-guided fine needle aspiration. - J Thorac Oncol 2010.
14. Baatenburg de Jong RJ, et al. - Assessment of cervical metastatic disease. - ORL J Otorhinolaryngol Relat Spec 1993.
15. Baatenburg de Jong RJ, et al. - Ultrasound-guided fine-needle aspiration biopsy of neck nodes. - Arch Otolaryngol Head Neck Surg 1991.
16. Rammeh S, et al. - Accuracy of fine-needle aspiration cytology of head and neck masses. - Diagn Cytopathol 2019.
17. Horsnell JD, et al. - Raman spectroscopy--a potential new method for the intra-operative assessment of axillary lymph nodes. - Surgeon 2012.
18. Stegehuis PL, et al. - Toward optical guidance during endoscopic ultrasound-guided fine needle aspirations of pancreatic masses using single fiber reflectance spectroscopy: a feasibility study. - J Biomed Opt 2017.
19. Hoy CL, et al. - Method for rapid multidiameter single-fiber reflectance and fluorescence spectroscopy through a fiber bundle. - J Biomed Opt 2013.
20. Kanick SC, et al. - Integration of single-fiber reflectance spectroscopy into ultrasound-guided endoscopic lung cancer staging of mediastinal lymph nodes. - J Biomed Opt 2010.
21. Amelink A, et al. - Confidence intervals on fit parameters derived from optical reflectance spectroscopy measurements. - J Biomed Opt 2008.
22. Bugter O, et al. - Optical pre-screening for laryngeal cancer using reflectance spectroscopy of the buccal mucosa. - Biomed Opt Express 2018.
23. Liu Y, et al. - Detection of cervical metastatic lymph nodes in papillary thyroid carcinoma by Fourier transform infrared spectroscopy. - Br J Surg 2011.

Chapter 7

General discussion

Detection of field cancerization

Cumulative evidence indicates that a significant part of cancer evolution may occur before the development of histological abnormalities. Slaughter et al. named these changes FC almost 70 years ago.[1] Since then the term has been used to describe multiple patches of pre-malignant disease leading to a higher-than-expected prevalence of SPTs.

Numerous detectable biomarkers of FC have been identified in the epithelium and connective tissue. Among them are loss of heterozygosity, micro satellite alterations, chromosomal instability, mutations in TP53 gene and telomerase activity.[2-5] An extensive review by Simple et al. even identified markers of cancer stem cells in FC.[2]

These FC biomarkers are also correlated with structural changes of the mucosal cells, and specifically the cell nuclei. In this thesis we have tried to identify these structural changes in Chapter 3 and 4 with the use of electron microscopy image analysis and reflectance spectroscopy, respectively. Electron microscopy image analysis showed that the nuclei of the epithelial buccal mucosa cells of UADT cancer patients had a less organized chromatin packing. A logic hypothesis that follows this finding is that we would find an altered pattern of light scattering during spectroscopic measurements. Since the patients from the EM study were also the same patients included in the Optical Screening study, we were able to compare the results of both.

We indeed saw a tendency of the scattering parameters to be more altered in cancer patients. This was however not the case for all cancer subgroups or all scattering parameters. The reduced scattering coefficient, μ_s' , at 800 nm was the parameter that had the best ability to discriminate between cancer patients and controls. It was significantly increased in esophageal cancer patients ($p = 0.029$) and lung cancer patients (compared to COPD patients, $p = 0.072$ [n.s.] and compared to non-COPD patients 0.015). Contradictory, μ_s' at 800 nm was decreased in laryngeal cancer patients. However, this difference was not significant ($p = 0.398$). We also found a tendency for the scattering power of μ_s' to be higher for cancer patients. Finally, the average of the phase function parameter, γ , was slightly increased in esophageal and lung cancers, but decreased in head and neck cancer patients.

An explanation for the less pronounced difference in our spectroscopy study compared to our EM study could be that, although the measured patients were the same, the measured tissue volumes were not. In the EM study the cell nuclei were segmented and isolated, while in the *in vivo* spectroscopic studies the optical properties of all the cells (entire cell) of the mucosal top layers (not just the cell nuclei) were averaged.

Abnormalities in nuclear organization are one of the most definitive markers of dysplasia and malignancy and have been universally used by pathologists.[6] In a relatively large number of cells, we have shown that similar alterations develop in the chromatin structure of normal appearing buccal mucosa cells of UADT patients. With this finding we provided (additional) evidence that ultrastructural nuclear disorganization is a hallmark of early pre-dysplastic carcinogenesis (*i.e.*, FC). Cherkezyan et al. came to the same conclusion in a group of patients with colorectal adenomas.[7] They discussed that proper higher-order organization of chromatin is crucial for normal cell function. Disruptive organization negatively influencing gene expression and DNA replication and repair: well-known detectable biomarkers of FC.

The department of biomedical engineering at Northwestern University has produced several promising articles in which they identify altered chromatin organization as a marker of FC in patients with esophageal and lung cancer, but also in a range of other organs. They utilized partial wave spectroscopy (PWS), in which measurements are performed on tissue monolayers that are primarily comprised of cells in which the nucleus occupies > 80% of the cytology. This is similar to our EM study, but different than the *in vivo* MDSFR measurements described in Chapter 3 of this thesis.

The use of field cancerization in UADT cancer screening and diagnostics

Numerous researchers have utilized FC to screen for (pre-)malignancies. While the focus of this thesis lies on the UADT, other organs such as the mucosal lined stomach, small and large intestine and female reproductive organs as well as the non-mucosal skin, liver, pancreas and prostate have also been studied. However, the use of FC detection has not been widely adapted in early detection of cancer.

Head and neck

Inspection of the head and neck region is less invasive than that of the esophagus or lungs, especially for the oral cavity. Even inspection of the pharynx and larynx with a flexible fiberscope is easily performed without any (local) anesthesia in the outpatient clinic setting with only minor discomfort for the patient. This might be a reason why little effort has been put towards the detection of less invasive surrogate markers (*e.g.*, biomarkers of FC) for HNSCC. This is the complete opposite for esophageal and lung cancer. It seems like HNSCC research emphasis has been on enhancing the visualization of early malignancies and surgical margins with techniques such as narrow band imaging (NBI) and (auto)fluorescence.[8, 9]

Because of the diffuse presence of FC, it is suggested that additional removal of normally appearing mucosa adjacent to the tumor could lead to a decrease in local recurrence. This is because the FC around tumor is also seen as pre-malignant.[10] This suggestion might seem to be in conflict with the general goal of performing 'radical excisions', but at the same time, excising as little normal tissue as *possible*. Anatomic boundaries might also limit the clinician in following this advice. At present, the clinical utilization of FC detection and monitoring in HNSCC patients lie primarily in the prediction and monitoring of multiple primary tumors after treatment of the index tumor.

Contradictory to our hypothesis, we did not find significant differences in light scattering between HNSCC patients and controls. The differences we did find, were physiological parameters derived from the absorption of light: specifically the microvascular blood oxygen saturation (StO₂) and blood volume fraction (BVF). We combined them into an optical parameter to distinguish laryngeal cancer patients from 'tobacco use-matched' controls. Our parameter had a sensitivity of 78.3 % and a specificity of 73.9%. In Chapter 4a we discussed three hypotheses that could explain our findings. Two were based on a regional effect of hemolysis that occurs in the tumor itself and one was an increased thickness of the non-vascularized epithelial layer of the mucosa. We tested this last hypothesis on the subselection of patients who were also included in the EM study (which was chronologically performed later). However, this hypothesis was not confirmed as the epithelial thickness did not differ between the cancer and control group. It remains unclear why scattering differences in the buccal mucosa were found in esophageal and lung cancer patients, but not in patients with laryngeal cancer.

In a prospective study by Roesch-Ely et al. protein profiles of normal appearing mucosa of the oral cavity, pharynx, and esophagus were analyzed in patients with and without HNSCC.[11] In the normal mucosa of patients with tumors, they found similar protein profiles to those of the tumors self. Also, all cancer patients that developed local recurrences or SPTs were correctly predicted by altered mucosal protein profiles ($p = 0.007$). A downside of the method described in this study is the need to take tissue from the patient and analyze in *ex vivo*. Unfortunately we are not able to analyze the correlation between our MDSFR data and the occurrence of recurrent tumors or SPTs because this study was not designed with a follow-up. However, it might still be possible to do this retrospectively.

Esophagus

Chapter 4b of this thesis provided evidence of structural differences in the FC of esophageal squamous cell carcinomas (ESCC). So far, FC of ESCC was only identified by genetic

mutations, epigenetic markers, and telomerase activity.[12-14] The structural FC changes were not detected in the esophagus, but in the oral cavity: an easy reachable location for non-invasive tissue measurements. In contrast to the group of HNSCC patients, we did find scattering differences in the ESCC group. μ_s' at two different wavelengths was significantly increased in cancer patients. This correlates well with the results from our EM study (Chapter 3) and our hypothesis that disorganized chromatin results in more scattering of light. The discriminative power of our μ_s' biomarker showed a modest ability to discriminate cancer patients from controls: a sensitivity of 66.7% and a specificity of 70.8%. These rates of sensitivity and specificity are probably not sufficient to warrant a screening programme for ESCC.[15] However, it might be of aid as a risk stratification method, reducing the number of high-risk persons that need to undergo conventional cancer screening. For this, a higher negative predictive value of the test is needed. This could, to a certain degree, be achieved by adjusting the threshold of our biomarker.

The majority of esophageal cancer screening studies have focused on the detection of esophageal adenocarcinomas (EAC) in Barrett's esophagus (BE). Barrett's esophagus is characterized by the replacement of the normal squamous epithelium with the columnar epithelium, as seen in the stomach.[16] Although, BE has a small risk of progression to EAC, many countries implemented endoscopic surveillance on a routine basis.[10] Field cancerization is found to be detectable in the columnar epithelium around lesions and also in the cardia and the squamous mucosa around or above the BE mucosa.[17] This finding is important due to the difficulty in recognizing subtle lesions containing high grade dysplasia (HGD) or EAC in patients with BE. A more diffusely present biomarker might overcome this challenge.

In this we found no significant optical differences in the buccal mucosa of EAC patients. It seems like we performed our measurements outside of the field the EAC developed in. This might be explained by the fact that the main risk factor (gastric reflux) for EAC originates distal from the tumor site (EAC are mostly seen in the distal esophagus) and that the FC does not extend all the way proximal to the oral cavity: the location where we performed the measurements. Konda et al. quantitatively assessed non-dysplastic esophageal cells for nanostructural pre-malignant changes in a slightly more distal anatomically location.[18] They utilized partial wave spectroscopy (PWS) analysis of cells from the proximal esophagus of patients diagnosed with non-dysplastic and dysplastic BE and patients with EAC. Their optical parameter (disorder strength) was 1.79 times higher in EAC patients than in controls. Patients with dysplastic BE also had a disorder strength 1.63-times higher than controls. However, PWS did not resolve differences between cases with LGD and HGD or BE and EAC. Although interesting, the direct clinical applicability is ambiguous. Single fiber reflectance (SFR) spectroscopy, which we utilized in Chapter 6, might also be

complementary to the conventional esophageal cancer screening by detecting FC tissue changes. Future research will have to prove this hypothesis.

All the above-mentioned methods demonstrate that a field effect is present and detectable in EAC. Detection of the field effect in the clinical setting may increase the detection of HGD and EAC. However, detecting methods should prove to be valid and cost-effective and will probably be complementary to the current histopathological gold standard.[17]

Lung

In Chapter 4a we presented the results of our Optical Screening study in which we tried to discriminate between lung cancer patients and controls with and without chronic obstructive pulmonary disease (COPD). Again, we hypothesized that the field of pre-dysplastic mucosal tissue changes extended outside of the organ harboring the tumor, in this case the lungs.

We found that the power law of μ_s' , μ_s' at 800 nm, and the average were all higher in lung cancer patients than COPD. The only scattering parameter that was significantly different was μ_s' at 800 nm. μ_s' at 800 nm could identify lung cancer patients with a sensitivity of 73.9%, a specificity of 62.5%. As discussed in Chapter 4b, our results were in line with those from a similar study by Radosevich et al.[19] Both studies confirm the findings from our EM study.

Evidence that the field of lung cancer biomarkers encompasses the entire UADT is presented in reviews review by Billatos et al. and Saba et al.[20, 21] They discuss that gene expression biomarkers for lung cancer diagnostics have been found in the large bronchi, but also in the cytological normal bronchial epithelial cells of the nasal and oral cavity.[22-25] These findings support the hypothesis that there is a common gene expression signature (this could also be called FC) of lung cancer that extends from the bronchial epithelium into nose and mouth. Locations that are considerably easier reachable for non-invasive measurements than the trachea or bronchi.[25] Future research will have to confirm that gene-expressions profiles outside of the lungs have comparable diagnostic accuracy to the bronchi. It would also be interesting to combine a gene expression classifier with MDSFR spectroscopy, both in the oral or nasal cavity. If their combined accuracy is high enough it might even serve as a substitute for invasive bronchoscopy. Although interesting, this is still a far-fetched idea with multiple limitations to overcome.

The results from a recently published high-quality population-based, randomized study (NELSON trial) might lead to the first national screening programme for lung cancer.[26] The referral rate for suspicious lesions found with 22.600 CT-scans was 2.6% (467 patients).

About half of those referred patients (43.5%) were eventually diagnosed with lung cancer. The authors report that lung-cancer mortality was significantly lower among the high-risk persons who underwent screening. MDSFR FC screening of the buccal mucosa might aid as a risk stratification or pre-screening method to reduce to number of patients eligible for screening under the NELSON criteria (50-75 years old, current smoker or, smoking cessation < 10 years ago). This might also increase the relative referral rate of the screening programme. However, this would also increase the entire screening programme from a 2-step to a 3-step system and whether MDSFR screening is significantly less invasive than low-dose CT is debatable.

Field cancerization and multiple primary tumors in the upper aerodigestive tract

The occurrence of multiple primary tumors (patients that develop not one, but two or more individual tumors, *i.e.*, no recurrences or malignancies) has been explained by the occurrence of field cancerization. Field cancerization is defined by Angadi et al. as “an altered field in which the epithelium has multiple independent foci of abnormal tissue that can subsequently give rise to (pre-)malignant lesions”. [5] Field cancerization is a tissue field that may give rise to (pre-)malignancies. To simplify this definition even further: “FC is a pre-malignant tissue field”. The differences with conventional, extensively studied pre-malignant lesions is that FC is below the optical diffraction limit, and thus not visible for researchers in decades of progressing in oncologic knowledge. Field cancerization must be seen as the very first step in carcinogens; a step before the histopathological visible dysplasia. Another difference with dysplasia is the area the pre-malignant lesions extend to. It is thought that the risk of malignancy increases with each step in the carcinogenic process (e.g., high-grade dysplasia has a higher risk than low-grade dysplasia) and that each step occurs in more isolated local tissue areas. These steps ultimately lead to only one tumor in most patients, but, as just mentioned, in a minority of cancer patients also in more.

A review of the literature presented in chapter 5a to try to discover how many HNSCC patients develop esophageal SPTs. We included studies that screened for esophageal lesions with endoscopy enhanced with NBI and Lugol’s dye and found an average SPT yield of 12%. However, most studies were conducted on an Asian population. We started a new study (Van der Ven et al., not in this thesis) to investigate the true prevalence of esophageal SPTs in a Western HNSCC population. Preliminary results show that 5.9% of high-risk HNSCC patients have synchronous esophageal SPTs (high-grade dysplasia or invasive carcinoma. Several other were diagnosed with low grade dysplasia. These results indicate a lower prevalence of esophageal SPTs in the Western world than in Asia. The final results of the

study have to be collected before decisions can be made on the usefulness of esophageal SPT screening in a Western HNSCC population. A similar study was recently published with results from a Taiwanese population.[27] In a population of 501 HNSCC patients they found 60 (12%) esophageal SPTs. It is debated whether this type of screening also provides a survival benefit for the included patients. Future research with a long follow-up will have to be performed to answer this question.

Chapter 5a was basically repeated in Chapter 5b, but this time the other way around. We investigated how many esophageal carcinoma patients have HN SPTs by reviewing the available (Asian) literature. The pooled prevalence of HNSPTs we found was 5.4%. As expected, most HN SPTs were located in the hypopharynx (59%). According to our results, the prevalence HN SPTs in esophageal cancer patients was about half of esophageal SPTs in HN cancer patients. If we extrapolate the preliminary results from Van der Ven et al. the Western prevalence would be around 1.5%. However, this estimate is too uncertain to draw any conclusions on. It is safe to say that GE clinicians should be more aware of HN SPTs in their esophageal cancer patients. Special attention should be given to patients that were diagnosed with esophageal at a younger age.[28] Kato et al. also suggest that the hypopharynx (the most common site for HN SPTs should undergo careful inspection during endoscopy.[29] Methods to open the hypopharyngeal space, such as the Valsalva maneuver, should always be employed to maximize SPT (or proximal esophageal tumor expansion) detection.

Detecting lymph node metastases with light reflectance spectroscopy (LIGHT)

In the Chapter 6 we investigated whether positive cervical lymph nodes (LN) could be identified with SFR measurements. A proof of principle study was conducted with nine patients and nineteen LNs included. The results were very promising. An optical parameter 'delta', a combination of BVF, StO₂, and Rayleigh scattering amplitude, had a high diagnostic accuracy where the sensitivity, specificity, PPV, and NPV were 90,0%, 88.9%, 90,0%, and 88.9%, respectively.

This diagnostic accuracy is encouraging enough to continue this work towards the goal of clinical implementation of this method. Steps are made to conduct a new study in which we aim to overcome some of the challenges we encountered in this pilot study. In this new study we aim to replicate our present results in a larger group of patients and with a different approach method: transdermal measurements during regular fine needle aspiration (FNA) in the diagnostic work up of HNSCC. In this method the LNs remain in their *in vivo*

environment. One important finding of this study was that the per-operative measurements were in a more disrupted *in vivo* environment than we initially envisioned.

Once this technique has proven its clinical applicability, it has a great potential to be transferred to other fields of medicine/ other organs. Accurate, and preferably fast, diagnostics of potential LN metastases is something many clinicians can benefit from in the treatment of patients with, e.g., breast, skin, or colon cancer.

Clinical implications and future perspectives

An important clinical issue that remains in the study of FC is that of accurately determining the risk of malignant transformation.[30] As stated by Curtius et al., this risk might still be relatively small. Assuming all areas of FC (pre-malignant fields) eventually develop a malignancy, could lead to overtreatment with potential associated morbidities.[30] Biomarkers are needed to distinguish cancerized fields that will remain indolent for a long time from those that will rapidly become malignant.[5, 30] I believe that FC is a gradual process from the first chromosomal disorganization that influences gene transcription to high-grade dysplasia and all the small steps in between. Cumulative exposure to carcinogens results in an increase of carcinogenic steps the affected tissue undergoes. Research has shown that this carcinogenic process leads to changes in the light scattering. Since FC is not a static phenomenon, but yet an ongoing process, it would be interesting to find out if spectroscopic devices could also differentiate between ‘early’ FC and FC that developed almost to the stage of dysplasia. If proven possible, optical spectroscopy (or other techniques) could also aid in cancer risk predictions of early carcinogenic tissue changes.[31]

Now that we are gathering more knowledge on the early, pre-dysplastic carcinogenic tissue changes, it is being deliberated if FC will have a similar impact on both research and clinical practice as other oncologic discoveries from the last centuries (the relationships between cancer and inflammation, the discovery of epigenetic, cancer stem cells, or tumor heterogeneity) have had.[32, 33]

Adequate long term follow-up of patients after treatment of the index UADT tumor is paramount to increase early detection of SPTs.[4] Clinicians should not solely focus on their ‘own organ’ (HN region, esophagus, or lungs), but be aware of entire UADT of potentially one pre-malignant field. Patients should be persuaded to limit tobacco and alcohol (ab)use. Sathiasekar et al. and Van Oijen et al. point out that the continued exposure to carcinogens will induce more genetic mutations to the already present pre-malignant fields.[4, 34]

Definite therapy or excision of excision of an entire pre-malignant tissue field seems impossible due to the associated morbidity this would bring. Angadi et al. discuss that, because genetic alteration is one of the key aspects of FC, possible treatment strategies should be targeted for genetically ablation of altered clonal population, repair of genetic damage in affected cells, or continuous treatment with chemo-preventive agents.[5] However, they also note that extensive research is warranted in this area.

Researchers have investigated the use chemo-preventive agents have been performed to tackle the problem of recurrent tumors.[5, 30, 35, 36] Chemoprevention of cancer is a means of cancer control with a use of drugs or natural agents in order to hinder or delay the cancer development.[37] It can be utilized as a mean to restrict the progression of pre-malignancies or to prevent recurrent disease or SPT.[36] Such therapies could make the mucosal area around the tumor less sensitive to DNA alterations.[5] Several compounds have been utilized, of which retinoid is most promising.[5] Retinoids are known to play a role in the differentiation, development, and growth of epithelial cells.[36] No effective chemo-preventive agents have been applied to the clinical setting yet. The main challenges researchers are facing are low effectiveness, high toxicity, and a lack of highly specificity biomarkers for therapy monitoring.[37]

Cherkezyan et al. hypothesize that optical spectroscopy might be able to address the third challenge just presented.[7] A reverse of carcinogenesis, the goal of chemoprevention, should also change the nano-architecture of tissue. As extensively discussed in this thesis, optical spectroscopy is a very suitable method to detect such alterations. The same research group even provided a first proof of concept monitoring a chemo-preventive agent for carcinoma of the colon.[38]

I believe optical spectroscopy has a bright future in cancer diagnostics. It is easy to use, non-invasive, and fast. It gives information on tissue in a way clinicians are not used to. Most tissue information is still acquired by palpation and vision, whether plain eye vision or microscopic vision by the histopathologist. Many researchers are working towards clinical implementation of optical spectroscopy techniques. A (very) quick search of PubMed teaches that last year alone 4,050 papers have been published with the keywords 'optical' and 'spectroscopy'. Their scientific efforts will most likely result into the development of reliable and useful techniques. Well executed studies showing high diagnostic accuracies of their techniques are of course needed. I am confident it is just a matter of time before they will be widely embraced by surgeons to assist them in the diagnosis, excision and follow-up of tumors. With that, helping patients with correct and early tumor diagnosis, complete removal of tumors (and possibly pre-malignant adjacent tissue), and optimal follow-up.

References

1. Slaughter DP, et al. - Field cancerization in oral stratified squamous epithelium; clinical implications of multicentric origin. - *Cancer* 1953.
2. Simple M, et al. - Cancer stem cells and field cancerization of oral squamous cell carcinoma. - *Oral Oncol* 2015.
3. Mohan M, et al. - Oral field cancerization: an update on current concepts. - *Oncol Rev* 2014.
4. Sathisekar AC, et al. - Oral Field Cancerization and Its Clinical Implications in the Management in Potentially Malignant Disorders. - *J Pharm Bioallied Sci* 2017.
5. Angadi PV, et al. - Oral field cancerization: current evidence and future perspectives. - *Oral Maxillofac Surg* 2012.
6. Bauer GM, et al. - The transformation of the nuclear nanoarchitecture in human field carcinogenesis. - *Future Sci OA* 2017.
7. Cherkezyan L, et al. - Nanoscale changes in chromatin organization represent the initial steps of tumorigenesis: a transmission electron microscopy study. - *BMC Cancer* 2014.
8. Zhou H, et al. - The value of narrow band imaging in diagnosis of head and neck cancer: a meta-analysis. - *Sci Rep* 2018.
9. Atallah I, et al. - Role of near-infrared fluorescence imaging in head and neck cancer surgery: from animal models to humans. - *Eur Arch Otorhinolaryngol* 2015.
10. Zeki SS, et al. - Field cancerization in Barrett's esophagus. - *Discov Med* 2011.
11. Roesch-Ely M, et al. - Proteomic analysis of field cancerization in pharynx and oesophagus: a prospective pilot study. - *J Pathol* 2010.
12. Lee YC, et al. - Revisit of field cancerization in squamous cell carcinoma of upper aerodigestive tract: better risk assessment with epigenetic markers. - *Cancer Prev Res (Phila)* 2011.
13. Kammori M, et al. - Squamous cell carcinomas of the esophagus arise from a telomere-shortened epithelial field. - *Int J Mol Med* 2007.
14. Ito S, et al. - p53 mutation profiling of multiple esophageal carcinoma using laser capture microdissection to demonstrate field carcinogenesis. - *Int J Cancer* 2005.
15. Maxim LD, et al. - Screening tests: a review with examples. - *Inhal Toxicol* 2014.
16. Gindea C, et al. - Barrett esophagus: history, definition and etiopathogeny. - *J Med Life* 2014.
17. DeWard AD, et al. - Signatures of field cancerization: a step towards earlier detection of esophageal adenocarcinoma. - *Transl Cancer Res* 2017.
18. Konda VJ, et al. - Nanoscale markers of esophageal field carcinogenesis: potential implications for esophageal cancer screening. - *Endoscopy* 2013.
19. Radosevich AJ, et al. - Buccal spectral markers for lung cancer risk stratification. - *PLoS One* 2014.
20. Billatos E, et al. - The Airway Transcriptome as a Biomarker for Early Lung Cancer Detection. - *Clin Cancer Res* 2018.
21. Saba R, et al. - Buccal Epithelium, Cigarette Smoking, and Lung Cancer: Review of the Literature. - *Oncology* 2017.
22. Perez-Rogers JF, et al. - Shared Gene Expression Alterations in Nasal and Bronchial Epithelium for Lung Cancer Detection. - *J Natl Cancer Inst* 2017.
23. Sridhar S, et al. - Smoking-induced gene expression changes in the bronchial airway are reflected in nasal and buccal epithelium. - *BMC Genomics* 2008.
24. Zhang X, et al. - Similarities and differences between smoking-related gene expression in nasal and bronchial epithelium. - *Physiol Genomics* 2010.
25. Steiling K, et al. - The field of tissue injury in the lung and airway. - *Cancer Prev Res (Phila)* 2008.
26. de Koning HJ, et al. - Reduced Lung-Cancer Mortality with Volume CT Screening in a Randomized Trial. - *N Engl J Med* 2020.
27. Chung CS, et al. - Clinical benefits from endoscopy screening of esophageal second primary tumor for head and neck cancer patients: Analysis of a hospital-based registry. - *Oral Oncol* 2019.
28. Maekawa A, et al. - High incidence of head and neck cancers after endoscopic resection for esophageal cancer in younger patients. - *J Gastroenterol* 2020.
29. Kato M, et al. - Endoscopic surveillance of head and neck cancer in patients with esophageal squamous cell carcinoma. - *Endosc Int Open* 2016.
30. Curtius K, et al. - An evolutionary perspective on field cancerization. - *Nat Rev Cancer* 2018.
31. Fernandez PJ, et al. - Could field cancerization be interpreted as a biochemical anomaly amplification due to transformed cells? - *Med Hypotheses* 2016.
32. Gabusi A, et al. - Oral field cancerization: history and future perspectives. - *Pathologica* 2017.
33. Ha PK, et al. - The molecular biology of mucosal field cancerization of the head and neck. - *Crit Rev Oral Biol Med* 2003.

34. van Oijen MG, et al. - Oral field cancerization: carcinogen-induced independent events or micrometastatic deposits? - *Cancer Epidemiol Biomarkers Prev* 2000.
35. Kadara H, et al. - Field cancerization in non-small cell lung cancer: implications in disease pathogenesis. - *Proc Am Thorac Soc* 2012.
36. Smith W, et al. - Retinoids as chemoprevention for head and neck cancer: where do we go from here? - *Crit Rev Oncol Hematol* 2005.
37. Siemianowicz K, et al. - Chemoprevention of Head and Neck Cancers: Does It Have Only One Face? - *Biomed Res Int* 2018.
38. Roy HK, et al. - Spectral biomarkers for chemoprevention of colonic neoplasia: a placebo-controlled double-blinded trial with aspirin. - *Gut* 2017.

Chapter 8a

Short version: English summary

Chapter 1. Introduction

Tumors in the head and neck region, esophagus and lungs share similarities and are often referred to with the umbrella term upper aerodigestive tract tumors (UADT). UADT tumors are relatively common, especially lung cancer, and to lesser degrees head and neck and esophageal cancer. Risk factors include tobacco and alcohol use.

In general, patients with tumors detected at an early stage of development have a significant better survival rate than patients with advanced tumors. Unfortunately, UADT tumors are often diagnosed at a late stage. This highlights the need of a reliable detection method to facilitate early tumor detection. Luckily, UADT tumors appear well suited to population screening.

A new line in cancer screening research is focused on field cancerization (FC). Field cancerization is described as an altered field in which the epithelium has multiple independent foci of abnormal tissue that can subsequently give rise to (pre-)malignant lesions. There is evidence that FC of UADT tumors occurs throughout the upper aerodigestive tract, including the oral cavity.

These FC tissue changes might be detectable with biomedical optics. Biomedical optics is a study of the interaction between light and (human) tissue. Light possesses energy and is capable of interacting with biological cells, tissues, and organs. Medical optics applications use this interaction, which is determined by the optical properties of the tissue: absorption and scattering. The technique reflectance spectroscopy enables the measurement of both the absorption and scattering of light. In this thesis we use single-fiber reflectance spectroscopy and multidiameter single-fiber reflectance spectroscopy.

Chapter 2. Multiple primary tumors

The objective of **Chapter 2** was to get a better understanding of the incidence, survival rate and risk factors of multiple primary tumors (MPT) (i.e., patients with more than one primary tumor) in patients with head and neck squamous cell carcinoma (HNSCC). The ‘first multiple primary tumor’ is often referred to as the second primary tumor (SPT). The most frequent locations for such tumors were analyzed: the head and neck region, lungs and esophagus.

Chapter 2a focused on incidence and survival rate. Patient and tumor specific data of 1372 patients with HNSCC were collected from both the national cancer registry and patient records to ensure high-quality double-checked data. The total incidence of MPTs in the head

and neck region, lungs, and esophagus in patients with HNSCC was 11% (149/1372). Patients with lung MPTs and esophageal MPTs had a significant worse 5-year survival than patients with HN-MPTs (29%, 14%, and 67%, respectively, $P < 0.001$). The 5-year survival rate for synchronous HN MPTs was only 25%, whereas it was surprisingly high for patients with metachronous HN MPT (85%, $P < 0.001$).

Chapter 2b focused on risk factors for the development of SPTs. Data from 1581 patients were collected for this study. A cause specific Cox model for the development of an SPT was fitted, accounting for the competing risks residual/recurrent tumor and mortality. Of all patients, 246 (15.6%) developed SPTs. Analysis showed that tobacco and alcohol use, comorbidity and the oral cavity subsite were risk factors for SPTs. The C-index, the discriminative accuracy, of the model for SPTs was 0.65 (95% CI 0.61 – 0.68). These results show that there is potential to identify patients that have an increased risk to develop an SPT.

Chapter 3. Electron microscopy and field cancerization

In **Chapter 3**, we took a literal closer look at field cancerization. A profound characteristic of FC is alterations in chromatin packing. We aimed to quantify these alterations using electron microscopy image analysis of buccal mucosa cells of laryngeal, esophageal, and lung cancer patients. Analysis was done on normal-appearing mucosa, believed to be within the cancerization field, and not tumor itself. Large-scale electron microscopy (nanotomy) images were acquired of cancer patients and controls. Within the nuclei, the chromatin packing of euchromatin and heterochromatin was characterized. Further, the chromatin organization was quantified through chromatin packing density scaling. A significant difference was found between the cancer and control groups in the chromatin packing density scaling parameter for length scales below the optical diffraction limit (200 nm) in both the euchromatin ($p = 0.002$) and the heterochromatin ($p = 0.006$). The chromatin packing scaling analysis also indicated that the chromatin organization of cancer patients deviated significantly from the control group. These findings confirm that the ultrastructural field effect changes of the nuclear organization are a hallmark of early carcinogenesis. They might allow for novel strategies for cancer risk stratification and diagnosis with high sensitivity. This could aid clinicians in personalizing screening strategies for high-risk patients and follow-up strategies for treated cancer patients.

Chapter 4. Optical Screening study

In *Chapter 4* we investigated a potential new optical method, multidiameter single-fiber reflectance (MDSFR) spectroscopy, to detect FC in the buccal mucosa of cancer patients.

The novelty of this approach is that not the tumor, but the pre-malignant field it is thought to be part of, is detected. It is hypothesized that detection of this field could lead to a sufficient accuracy for the detection of the tumor itself. Optical measurements were performed in vivo with MDSFR spectroscopy. MDSFR spectra were acquired by a handheld probe incorporating three fiber diameters. Multiple absorption and scattering parameters that are related to the physiological and ultrastructural properties of the buccal mucosa were derived from these spectra. A linear discriminant analysis of the parameters was performed to create a combined biomarker to discriminate oncologic from non-oncologic patients. We investigated this method in patients with head and neck, lung, and esophageal cancer

In **Chapter 4a** the optical properties of the buccal mucosa of patients with laryngeal cancer were measured with MDSFR spectroscopy. The blood oxygen saturation and blood volume fraction were significantly lower in the buccal mucosa of laryngeal cancer patients than in non-oncologic controls. The data of these two parameters were combined to form a single 'biomarker α ', which optimally discriminates these two groups. Alpha was lower in the laryngeal cancer group (0.28) than the control group (0.30, $p = 0.007$). Alpha could identify oncologic patients with a sensitivity of 78% and a specificity of 74%.

In **Chapter 4b** the same method was used on patients with esophageal squamous cell carcinoma (ESCC) and esophageal adenocarcinoma (EAC). Twelve ESCC, 12 EAC and 24 control patients were included in the study. The median value of our biomarker σ , a combination of μ_s' at 450 nm and μ_s' at 800 nm, was significantly higher in patients with ESCC (2.07 [1.93-2.10]) than control patients (1.86 [1.73-1.95], $p = 0.022$). After cross-validation σ was able to identify ESCC patients with a sensitivity of 66.7% and a specificity of 70.8%. There were no significant differences between the EAC group and the control group.

In **Chapter 4c** the same method was used on 23 lung cancer patients, 24 chronic obstructive pulmonary disease (COPD) control patients, and 36 non-COPD controls. The majority of tumors were non-small-cell lung carcinomas (96%) and classified as stage I (48%). The tissue scattering properties μ_s' and γ at 800 nm and the tissue bilirubin concentration were all near-significantly different ($p = 0.072$, 0.058, and 0.060, respectively) between the lung cancer and COPD group. μ_s' at 800 nm had a sensitivity of 74% and a specificity of 63%. The microvascular blood oxygen saturation of the lung cancer patients was also higher than the COPD patients (78% vs. 62%, $p = 0.002$), this is probably a consequence of the systemic effect of COPD.

Chapter 5. Endoscopic screening; two systematic reviews

In **Chapter 5**, we took the results from previous chapters and studied the literature to check whether there was sufficient evidence to screen head and neck cancer patients for unknown second primary tumors in the esophagus using modern endoscopic techniques. This study was also repeated vice versa: screening esophageal cancer patients for second primary head and neck tumors. Two systematic reviews of all available databases were performed to find all Lugol chromoendoscopy screening studies (**Chapter 5a**) and all studies that endoscopically screened ESCC patients for head and neck SPTs (**Chapter 5b**). The primary outcome was the pooled prevalence of SPTs.

Fifteen studies with a total of 3386 patients were included in **Chapter 5a**. The average yield of esophageal-SPTs in HNSCC patients was 15%. The prevalence was the highest for patients with an index hypopharyngeal (28%) or oropharyngeal (14%) tumor. The esophageal-SPTs were classified as high-grade dysplasia in 49% of the cases and as invasive carcinoma's in 51%. Based on these results, we concluded that there is enough evidence to perform Lugol chromoendoscopy, especially in an Asian patient population. A new study (SCOPE) was started to investigate whether this is also the case for a Western population.

Chapter 5b included twelve studies, all performed in Japan, with a total of 6483 patients. The pooled prevalence of HNSPTs was 6.7% (95% CI: 4.9-8.4). This is lower than in the previous study. The overall heterogeneity was high across the studies ($I^2 = 89.0\%$, $p < 0.001$). Most HNSPTs were low-stage (85.3%) and located in the hypopharynx (60.3%). The proportion of synchronous (48.2%) and metachronous (51.8%) HNSPTs was comparable. Based on these results, there seems to be a lower need to screen ESCC patients for head and neck SPTs than the other way around.

Chapter 6. LIGHT study

A challenge in the treatment of patients with head and neck cancer is the management of occult cervical lymph node (LN) metastases. In **Chapter 7** we aimed to investigate whether single-fiber reflectance (SFR) spectroscopy could serve as an alternative or additional technique to detect cervical lymph node metastases. We performed intraoperative SFR spectroscopy measurements of LNs with and without malignancies. We analyzed if physiological and scattering parameters were significantly altered in positive LNs. Nine patients with a total of nineteen LNs were included. Three parameters, blood volume fraction (BVF), microvascular saturation (StO_2), and Rayleigh amplitude, were combined into one optical parameter 'delta'. Delta had a high diagnostic accuracy where the sensitivity, specificity, PPV, and NPV were 90.0%, 88.9%, 90.0%, and 88.9%, respectively. The area under

the ROC curve was 96.7% (95% confidence interval 89.7-100.0%). This proof of principle study is a first step in the development of an SFR spectroscopy technique to detect LN metastases in real time.

Chapter 7. Discussion

This core of this thesis is field cancerization. How to define, detect, and quantify it. But also how to use it to explain the occurrence of multiple primary tumors, to screen for unknown UADT tumors, and to detect lymph node metastases. The presented results are promising. I believe optical spectroscopy has a bright future in cancer diagnostics. It is easy to use, non-invasive, and fast. It gives information on tissue in a way clinicians are not yet used to. I am confident it is just a matter of time before spectroscopy will be widely embraced by surgeons to assist them in the diagnosis, excision and follow-up of tumors. With that, helping patients with correct and early tumor diagnosis, complete removal of tumors, and optimal follow-up.

Chapter 8b

Short version: Nederlandse samenvatting

Hoofdstuk 1. Introductie

Tumoren in het hoofd-halsgebied, de slokdarm en de longen hebben meerdere overeenkomsten en liggen relatief dicht bij elkaar in het lichaam. Het zijn relatief veelvoorkomende tumoren, met name longtumoren en in mindere mate hoofd-hals-, en slokdarmtumoren. Risicofactoren voor hun ontwikkeling zijn onder andere roken en alcoholgebruik.

In het algemeen geldt dat patiënten met tumoren die in een vroeger stadium van ontwikkeling ontdekt worden een betere overlevingskans hebben dan wanneer de tumor later wordt ontdekt. Dit benadrukt de nood voor een betrouwbare methode om tumoren in een vroeg stadium op te sporen. Gelukkig lenen hoofd-hals-, slokdarm- en longtumoren zich in principe goed voor een bevolkingsonderzoek.

Een nieuwe ontwikkeling in kankerscreening richt zich op het aantonen van ‘field cancerization’, ook wel veldeffect genoemd. Het veldeffect wordt beschreven als een weefselgebied dat er nog normaal uitziet, maar waarin er wel een verhoogde kans is dat zich een tumor ontwikkelt. Voor hoofd-hals-, slokdarm- en longtumoren wordt aangenomen dat het veldeffect zich ook in de mondholte bevindt.

De aanwezigheid van het veldeffect is mogelijk aan te tonen met optische technieken. Bij zulke technieken wordt de interactie tussen licht en (menselijk) weefsel gemeten. Licht bevat energie die in staat is een interactie aan te gaan met weefsel zoals cellen, weefsel en organen. Deze interactie wordt bepaald door de optische eigenschappen van weefsel: absorptie en verstrooiing. Reflectiespectroscopie is een techniek die deze optische eigenschappen kan detecteren en kwantificeren. In dit proefschrift wordt er gebruik gemaakt van single-fiber reflectiespectroscopie en multidiameter single-fiber reflectiespectroscopie.

Hoofdstuk 2. Multipale primaire tumoren

Het doel van **Hoofdstuk 2** was om een beter begrip te krijgen van de incidentie, overleving en risicofactoren van multipale primaire tumoren (MPT) (i.e., patiënten die niet één, maar meerdere tumoren ontwikkelen) bij patiënten met hoofd-halskanker. De term tweede primaire tumor (SPT) wordt vaak gebruikt om de eerste ‘multipale primaire tumor’ aan te duiden. De meest voorkomende locaties voor zulke tumoren werden geanalyseerd: het hoofd-halsgebied, de longen en de slokdarm.

Hoofdstuk 2a richt zich op de incidentie en overlevingskans. Data over 1372 patiënten met hoofd-halskanker en hun tumoren werd verzameld vanuit het Integraal Kankercentrum

Nederland en de patiëntendossiers. Hierdoor was er sprake van hoogkwalitatieve, dubbel gecontroleerde data. Elf procent van de onderzochte patiënten bleek meer dan één tumor te ontwikkelen. Patiënten waarbij de 2^e (of 3^e of 4^e) tumor zich ontwikkelde in de longen of slokdarm, hadden een slechtere overlevingskans dan wanneer deze zich ontwikkelde in het hoofd-halsgebied (5-jaarsoverleving 29%, 14%, en 67%, respectievelijk). De overlevingskans van patiënten met vervolgtumoren die zich ontwikkelden in het hoofd-halsgebied hadden een betere overlevingskans wanneer deze tumor zich na enkele maanden ontwikkelde, dan wanneer deze zich snel na de eerste tumor ontwikkelde (5-jaarsoverleving 85% vs 25%).

Hoofdstuk 2b richt zich op de risicofactoren voor de ontwikkeling van de tweede primaire tumor (SPT). Voor deze studie werd data van 1581 patiënten gebruikt. Er werd een specifieke analyse gebruikt die rekening hield met ‘concurrerende gebeurtenissen’ voor het ontstaan van een tweede primaire tumor (e.g., na het overlijden van een patiënt kan er zich geen nieuwe tumor ontwikkelen). Van alle patiënten ontwikkelde er ruim 15% een SPT. Analyse liet zien dat roken en alcoholgebruik, comorbiditeit en de sublocatie ‘mondholte’ van de eerste primaire tumor risicofactoren waren voor de ontwikkeling van een SPT. De mate waarin het model het ontstaan van SPTs kon voorspellen werd geduïd al 0.65. Dit is lager dan we hadden gehoopt, maar hoger dan ‘het opgooien van een munt’. Deze resultaten laten zien dat er potentie is om hoofd-halskankerpatiënten te identificeren die een verhoogd risico hebben op de ontwikkeling van een SPT.

Hoofdstuk 3. Elektronenmicroscopie en het veldeffect

In **Hoofdstuk 3** namen we het veldeffect letterlijk onder de loep. Een van de kenmerken van het veldeffect is een verandering in de structuur van het DNA. Ons doel was dit te kwantificeren met behulp van analyses van elektronenmicroscopiebeelden van het wangslijmvlies van patiënten met keel-, long- en slokdarmkanker en controlepatiënten zonder kanker. Deze analyses werden verricht op beelden van normaal uitzien wangslijmvlies, waarvan gedacht werd dat het onderdeel was van het veldeffect. De tumor zelf werd niet onderzocht. Grootschalige elektronenmicroscopiebeelden (nanotom) werden verkregen van zowel de kanker-, als controlepatiënten. Binnenin de celkern werd naar verschillende aspecten van de structuur van het DNA gekeken. Hierbij werden er significante verschillen gevonden tussen patiënten met en zonder kanker. Deze structuurverschillen waren zo subtiel dat ze met een normale microscoop niet zichtbaar zouden zijn. Deze bevindingen bevestigen dat deze ultrastructurele DNA-veranderingen in het veldeffect een vroeg teken zijn van de ontwikkeling van een mogelijke tumor. Mogelijk kunnen deze bevindingen in de toekomst bijdragen aan methodes om bepaalde tumoren eerder op te sporen. Ook zou het specialisten kunnen helpen bij het personaliseren van screenings-, en controlestrategieën van reeds behandelde kankerpatiënten.

Hoofdstuk 4. Optical Screening studie

In **Hoofdstuk 4** onderzoeken we een potentieel nieuwe methode, multidiameter single-fiber reflectance (MDSFR) spectroscopie, om het veldeffect op te sporen in het wangslimvlies van kankerpatiënten. Het innovatieve van deze methode is dat niet de tumor zelf, maar het veldeffect waarin deze zich bevindt aangetoond wordt. Wij hoopten dat detectie van dit veld voldoende discriminerend zou blijken om de aanwezigheid van een tumor elders in het veld waarschijnlijk te maken. Optische MDSFR spectroscopiemetingen werden *in vivo* verricht. Meerdere optische parameters werden gemeten die geassocieerd zijn met fysiologische en ultrastructurele eigenschappen van het onderzochte weefsel, in dit geval het wangslimvlies. Er werden analyses verricht om een optimale optische biomarker te bepalen die onderscheid kon maken tussen patiënten met en zonder kanker. In **Hoofdstuk 4a-c** onderzochten wij deze methode in patiënten met hoofd-hals-, long-, en slokdarmkanker.

In **Hoofdstuk 4a** werden de optische eigenschappen van het wangslimvlies van patiënten met keelkanker bepaald met behulp van MDSFR spectroscopie. Het zuurstofgehalte van het bloed en het volume van het bloed waren beide significant verlaagd in patiënten met keelkanker. De data van deze twee parameters werden gecombineerd tot een optische biomarker α . Alpha was lager in de keelkankergroep (0.28) dan de controlegroep (0.30, $p = 0.007$). Alpha was in staat de oncologische patiënten te voorspellen met een sensitiviteit van 78% en een specificiteit van 74%.

In **Hoofdstuk 4b** werd de dezelfde methode toegepast op patiënten met twee types slokdarmkanker (plaveiselcelcarcinomen (ESCC) en adenocarcinomen (EAC)). Twaalf ESCC, 12 EAC en 24 controlepatiënten werden geïncludeerd in de studie. De optische biomarker σ , een combinatie van twee verstrooiingsparameters, was significant hoger in ESCC patiënten (2.07 [1.93-2.10]) dan in de controlepatiënten (1.86 [1.73-1.95], $p = 0.022$). Sigma bleek ESCC patiënten te kunnen identificeren met een sensitiviteit van 66.7% en een specificiteit van 70.8%. Er waren geen significante verschillen tussen de EAC en de controlegroep.

In **Hoofdstuk 4c** werd dezelfde methode nogmaals gebruikt op 23 longkankerpatiënten, 24 patiënten met chronische obstructieve longziekte (COPD) en 36 controlepatiënten zonder COPD. De meerderheid van de tumoren waren niet-kleincellige longcarcinomen (96%) en geclassificeerd als stadium I (48%). Twee verstrooiingsparameters en de bilirubineconcentratie waren alle net niet significant verschillend tussen de longkanker-, en COPD-groep ($p = 0.072$, 0.058 , en 0.060 , respectievelijk). De best onderscheidende parameter had een sensitiviteit van 74% en een specificiteit van 63%. De zuurstofsaturatie

van het bloed in het wangslijmvlies van de longkankerpatiënten bleek significant hoger te zijn dan die van de COPD groep (78% vs. 62%, $p = 0.002$). Dit kwam waarschijnlijk door het systemische effect van COPD.

Hoofdstuk 5. Endoscopische screening: twee systematische reviews

In **Hoofdstuk 5** werd er in de bestaande literatuur onderzocht of er voldoende bewijs was om bij patiënten met hoofd-halskanker actief op zoek te gaan (screenen) naar tweede primaire tumoren (SPT) in de slokdarm. Ook onderzochten we of het zinvol was slokdarmkankerpatiënten te screenen op hoofd-hals SPTs. Twee systematische reviews werden verricht van alle studies die geavanceerde endoscopietechnieken gebruikten om de slokdarm te onderzoeken bij hoofd-halskankerpatiënten (**Hoofdstuk 5a**) en alle studies die slokdarmkankerpatiënten endoscopisch screenen voor de aanwezigheid van hoofd-hals SPTs (**Hoofdstuk 5b**).

Vijftien studies met een totaal van 3386 patiënten werden geïncludeerd in **Hoofdstuk 5a**. Bij 15% van de hoofd-halskankerpatiënten werd een slokdarm SPT gevonden. Deze prevalentie was het hoogst bij patiënten met een hypopharynx- (28%) of oropharynx tumor (14%). Deze sublocaties liggen het dichtst bij de slokdarm. De gedetecteerde SPTs werden geclassificeerd als hooggradige dysplasie in 49% van de casussen en als invasief carcinoom in de overige 51%. Gebaseerd op deze resultaten, werd er geconcludeerd dat er voldoende bewijs is om slokdarmscreening te verrichten bij hoofd-halskankerpatiënten. Een nieuwe studie (SCOPE) is gestart om te onderzoeken wat de daadwerkelijke prevalentie van slokdarm SPTs is in een Westerse populatie.

In **Hoofdstuk 5b** werden twaalf studies geïncludeerd, allen Japans, met een totaal van 6483 patiënten. De samengevoegde prevalentie was 6.7%. Dit was lager dan de 15% uit **Hoofdstuk 5a**. De heterogeniteit van de geïncludeerde studies was hoog ($I^2 = 89.0\%$, $p < 0.001$). Dit betekent dat ze moeilijk met elkaar te vergelijken waren. De meeste hoofd-hals SPTs waren in een laag stadium (85.3%) en gelokaliseerd in de hypopharynx (60.3%). Gebaseerd op deze resultaten lijkt het screenen van slokdarmkankerpatiënten op hoofd-hals SPTs minder noodzakelijk.

Hoofdstuk 6. LIGHT studie

Een uitdaging in de behandeling van hoofd-halskankerpatiënten is de benadering van patiënten die mogelijk verborgen uitzaaiingen in de lymfeklieren in de hals hebben. In

Hoofdstuk 7 onderzochten we of single-fiber reflectie (SFR) spectroscopie zou kunnen dienen als een alternatieve of aanvullende techniek om lymfeklieruitzaaiingen te detecteren. Er werden voor dit doel tijdens operaties SFR spectroscopiemetingen verricht van klieren met en zonder uitzaaiingen. Er werd vervolgens onderzocht of fysiologische en ultrastructurele eigenschappen van de positieve lymfeklieren veranderd waren ten opzichte van de normale lymfeklieren. Negen patiënten, met een totaal van negentien lymfeklieren, werden geïnccludeerd in deze studie. Drie optische parameters, het volume van het bloed, het zuurstofgehalte van het bloed en de 'Rayleigh amplitude' werden gecombineerd in een optische biomarker 'delta'. Delta had een hoge diagnostische nauwkeurigheid met een sensitiviteit, specificiteit, positief en negatief voorspellende waarde van 90,0%, 88,9%, 90,0%, en 88,9%, respectievelijk. Deze resultaten zijn de eerste stap richting de ontwikkeling van een SFR-spectroscopietechniek waarmee lymfeklieruitzaaiingen direct gediagnosticeerd kunnen worden.

Hoofdstuk 7. Discussie

De kern van dit proefschrift is het veldeffect. Hoe moet dit gedefinieerd, gedetecteerd en gekwantificeerd worden? Maar ook: hoe kan het gebruikt worden om het ontstaan van multiple primaire tumoren te verklaren, om te screenen voor tumoren en om lymfeklieruitzaaiingen te detecteren? De gepresenteerde resultaten zijn veelbelovend. Ik ben ervan overtuigd dat optische spectroscopie een toekomst heeft in kankerdiagnostiek. Het is een gemakkelijk te gebruiken, niet-invasieve en snelle methode die specialisten weefselinformatie geeft die nu nog niet benut wordt. Spectroscopie zal in de toekomst omarmd worden door artsen als hulpmiddel voor diagnose, verwijdering en controles van tumoren. Patiënten zullen hiervan profiteren door correcte en snelle diagnostiek, complete verwijdering van tumoren en optimale controlestrategieën.

Addendum

List of abbreviations and acronyms

Affiliations of contributing authors

PhD portfolio

List of publications

Dankwoord

About the author

List of abbreviations and acronyms

α_1	Mie amplitude
α_2	Mie slope
A_ρ	density fluctuation amplitude
AbsRisk	absolute risk
ACE-27	adult comorbidity evaluation-27
ACF	autocorrelation function
BE	Barrett's esophagus
$[\text{BIL}]_{\text{tis}}$	tissue bilirubin concentration
BMI	body mass index
BVF	blood volume fraction
CI	confidence interval
C-index	concordance probability
CIS	carcinoma in situ
CNN	convolutional neural network
COPD	chronic obstructive pulmonary disease
CRT	chemoradiotherapy
CT	computed tomography
CT	chemotherapy
D	fractal dimension
DC	desmosome cluster
desm	desmosomes
DNA	deoxyribonucleic aci
EAC	esophageal adenocarcinoma
EC	esophageal cancer
EM	electron microscopy
ery	erythrocyte
ESCC	esophageal squamous cell carcinoma
euCh	euchromatin
F	Fourier transform
F^{-1}	inverse Fourier
FC	field cancerization
FNA	fine needle aspiration
γ	phase function parameter
HB	deoxygenated hemoglobin

HBO ₂	oxygenated hemoglobin
HGD	high grade dysplasia
HN	head and neck
HNSSC	head and neck squamous cell carcinoma
HPV	human papillomavirus
HR	hazard ratio
htCh	heterochromotin
IKNL	Netherlands comprehensive cancer organization
IQR	interquartile range
IF	intermediate filaments
K-S	Kolmogorov-Smirnov
l_n	correlation length
LDCT	low-dose computed tomography
LEBS	low-coherence enhanced backscattering spectroscopy
LED	light-emitting diode
LN	lymph node
$\langle L_{\text{SFR}} \rangle$	effective photon path length for SFR
μ_a	absorption coefficient
MDSFR	multidiameter single-fiber reflectance
MPT	multiple primary tumor
MRI	magnetic resonance imaging
μ_s	scattering coefficient
μ_s'	reduced scattering coefficient
n	number
NBI	narrow band imaging
ND	neck dissection
η_{lim}	collection efficiency at the diffusion limit
nm	nanometer
NPC	nuclear pore complexes
NPV	negative predictive value
NSCLC	non-small cell lung cancer
PET	positron emission tomography
PF	phase function
PPV	positive predictive value
pro	prospective
PWS	partial wave spectroscopy

PY	pack year
ReLU	rectified linear unit
retro	retrospective
RNA	ribonucleic acid
ROC curve	receiver operating characteristic curve
RONCDOC	Rotterdam oncology documentary
R_{SF}^0	collected SFR in the absence of absorption
RT	radiotherapy
SCLC	small cell lung cancer
SD	standard deviation
SE	standard error
SFR	single-fiber reflectance
SLN	sentinel lymph node
SPT	second primary tumor
STEM	scanning transmission electron microscopy
StO ₂	blood oxygen saturation
STROBE	strengthening the reporting of observational studies in epidemiology
surg	surgery
TEM	transmission electron microscopy
TNM	tumor site, lymph node, metastatic spread
U/W	units per week
UADT	upper aerodigestive tract
VD	vessel diameter
WL	white light
WM	Whittle-Matérn
yr	year

Affiliations of contributing authors

Erasmus MC Cancer Institute

Department of Otorhinolaryngology and Head and Neck Surgery.

Robert Baatenburg de Jong	Henriëtte de Bruijn
Emilie Dronkers	José Hardillo
Martine de Herdt	Dirk van Iwaarden
Stijn Keereweer	Dominiek Monserez
Dominic Robinson	Aniel Sewnaik
Marjan Wieringa	

Department of Gastroenterology and Hepatology

Marco Bruno	Arjun Koch
Manon Spaander	Steffi van de Ven

Department of Pathology

Yassine Aaboubout	Mahesh Algoe
Senada Koljenović	

Department of Public Health (Center for Medical Decision Making)

Nikki van Leeuwen	Daan Nieboer
-------------------	--------------

Department of Pulmonology

Joachim Aerts

Department of Cardiothoracic Surgery

Alexander Maat

Department of Radiation Oncology

Gerda Verduijn

Department of Plastic and Reconstructive Surgery

Marc Mureau

Department of Oral & Maxillofacial Surgery, Special Dental Care, and Orthodontics

Ivo ten Hove

Department of Medical Oncology
Esther van Meerten

Northwestern University

Department of Biomedical Engineering
Vasundhara Agrawal
Andrew Chang

Vadim Backman
Yue Li

Department of Electrical Engineering and Computer Science
Amil Dravid

University of Groningen

Department of Biomedical sciences of cells and systems
Ben Giepmans

Anouk Wolters

The Netherlands Organization for Applied Scientific Research (TNO)

Department of Optics
Arjen Amelink

Fransiscus Gasthuis & Vlietland

Department of Pulmonology
Sigrid van Brummelen

Amphia

Department of Pulmonology
Cor van der Leest

PhD portfolio

Name PhD student: Oisín Bugter

Erasmus MC Cancer Institute

Department: Otorhinolaryngology and Head and Neck Surgery

PhD period: 2015-2021

PhD training	Year
General academic courses	
EndNote, Pubmed and other databases	2015
BROK (Basiscursus Regelgeving Klinisch Onderzoek)	2015
Research Integrity	2016
Biomedical English Writing and Communication	2016-17
Biostatistical Methods I: Basic Principles Part A	2018
Other ENT-related courses	
Head and Neck Anatomy (dissection)	2016
ABCDE	2019
Other thesis-related courses	
Basic and Translational Oncology	2017
Nederlandse Vereniging van Oncologie Basiscursus Oncologie	2018
(Inter) national conferences and presentations	
Phototonics Event, Eindhoven (attendee)	2015
Joint MC and WGs meeting in Confocal Reflectance Microscopy and Optical Imaging, Croatia (oral presentation)	2015
Health Tech Event, Eindhoven (oral presentation)	2015
Science day ENT dept., Rotterdam (oral presentation '15 '17 '19, attendee)	2015-19
3-monthly CODT meetings, EMC Rotterdam (oral presentation '15 (2x) '17, multiple attendee)	2015-17
Biannual National ENT-meeting, Nieuwegein (oral presentation '15 '16, '18, multiple attendee)	2015-19
Nederlandse Werkgroep voor Hoofd-Hals Tumoren congres, Utrecht (attendee)	2016

KWF-volunteers meetings, Rijswijk and Den Haag (oral presentation '16 '17)	2016-17
Molmed Day, Rotterdam (oral presentation)	2017
Daniel den Hoed Day, Rotterdam (attendee)	2017
World of Photonics Congress, Germany (oral presentation)	2017
52nd meeting of the European Society for Surgical Research (oral presentation)	2017
Jonge-Onderzoekersdag NWHHT, Rotterdam and Den Haag (oral presentation '18, attendee)	2017-18
Symposium Experimenteel Onderzoek Heelkundige Specialismen, Rotterdam (oral presentation)	2018
World Congress of the International Federation of Head and Neck Oncologic Societies, Buenos Aires (poster presentation (3x))	2018

Lecturing

Anesthesiologist assistants in training	2016-19
ER nurses in training	2016-19
Surgery assistants in training	2016-19
Supervising workgroups for medical students	2016-19

Supervision

Master thesis Rens van Iwaarden	2017
---------------------------------	------

Awards

Rotsbeendissectieprijs (1e jaars) - 1e prijs	2019
--	------

List of publications

1. van Zijl F, Monserez D, Korevaar T, **Bugter O**, Wieringa M, et al. - Postoperative value of serum squamous cell carcinoma antigen as a predictor of recurrence in sinonasal inverted papilloma. - Clin Otolaryngol 2017.
2. **Bugter O**, Monserez D, van Zijl F, Baatenburg de Jong R, Hardillo J - Surgical management of inverted papilloma; a single-center analysis of 247 patients with long follow-up. - J Otolaryngol Head Neck Surg 2017.
3. **Bugter O**, Spaander M, Bruno M, Baatenburg de Jong R, Amelink A, et al. - Optical detection of field cancerization in the buccal mucosa of patients with esophageal cancer. - Clin Transl Gastroenterol 2018.
4. **Bugter O**, Hardillo J, Baatenburg de Jong R, Amelink A, Robinson D - Optical pre-screening for laryngeal cancer using reflectance spectroscopy of the buccal mucosa. - Biomed Opt Express 2018.
5. **Bugter O**, van de Ven S, Hardillo J, Bruno M, Koch A, et al. - Early detection of esophageal second primary tumors using Lugol chromoendoscopy in patients with head and neck cancer: a systematic review and meta-analysis. - Head Neck 2019.
6. **Bugter O**, van Iwaarden D, Dronkers E, de Herdt M, Wieringa M, et al. - Survival of patients with head and neck cancer with metachronous multiple primary tumors is surprisingly favorable. - Head Neck 2019.
7. **Bugter O**, van Brummelen S, van der Leest K, Aerts J, Maat A, et al. - Towards the Optical Detection of Field Cancerization in the Buccal Mucosa of Patients with Lung Cancer. - Transl Oncol 2019.
8. van de Ven S, **Bugter O**, Hardillo J, Bruno M, Baatenburg de Jong R, et al. - Screening for head and neck second primary tumors in patients with esophageal squamous cell cancer: a systematic review and meta-analysis. - United European Gastroenterol J 2019.
9. **Bugter O** & van Iwaarden D, van Leeuwen N, Nieboer D, Dronkers E, et al. - A cause-specific Cox model for second primary tumors in head and neck cancer patients: a RONCDOC study. - Head Neck 2021.

10. van de Ven S, de Graaf W, **Bugter O**, Spaander M, Nikkessen S, et al. - Screening for synchronous esophageal second primary tumors in patients with head and neck cancer. – accepted at Diseases of the Esophagus 2021.
11. **Bugter O** & Yu L, Wolters A, Agrawal V, Dravid A, et al. - Early upper aerodigestive tract cancer detection using electron microscopy to reveal chromatin packing alterations in buccal mucosa cells. – accepted at Microsc Microanal 2021.
12. **Bugter O**, Aaboubout Y, Algae M, de Bruijn H, Keereweer S, et al. - Detecting head and neck lymph node metastases with light reflectance spectroscopy; a pilot study. – under review at Oral Oncology 2021

Dankwoord

Graag wil ik beginnen met het bedanken van de proefpersonen die allen zonder eigenbelang deelgenomen hebben aan de studies van dit proefschrift. Zonder hen had dit werk uiteraard nooit tot stand kunnen komen.

Geachte prof. dr. R.J. Baatenburg de Jong, beste Rob, bedankt voor de mogelijkheid die je mij hebt geboden om dit proefschrift te maken. Met veel plezier heb ik onder jouw leiding mijn eerste stappen in de wetenschap gezet. Jouw adviezen en innovatieve ideeën zijn van grote waarde geweest. Ik heb altijd veel bewondering gehad voor jouw wetenschappelijke en organisatorische inzichten en hoe je dit tezamen met je vele andere werkzaamheden weet te combineren.

Geachte dr. D.J. Robinson, beste Dom, ik heb het als zeer fijn ervaren om jou als co-promotor te hebben. Mede doordat je niet ook als arts werkte, kon ik altijd bij je binnen lopen voor een vraag of overleg. Dank voor de tijd die je hebt genomen om mij de techniek en theorie achter optische spectroscopie uit te leggen, ook op de momenten dat het voor mij soms lastig te volgen was.

Geachte dr. J.A.U. Hardillo, beste Jose, al voor de start van mijn proefschrift heb ik je leren kennen als een zeer kundige en rustige begeleider van mijn eerste wetenschappelijke publicatie. Ik vond het erg fijn dat jij ook de klinische kant van mijn promotietraject begeleidt. Ik houd mezelf aanbevolen voor ube-snoepjes als je weer eens naar de Filipijnen mag reizen.

Geachte prof. dr. S. Sleijfer, prof. dr. C. Verhoef en prof. dr. A.M. Rijs, hartelijk dank voor de tijd die jullie hebben genomen om mijn proefschrift kritisch te beoordelen. Mijn dank gaat ook uit naar de overige leden van de promotiecommissie.

Geachte prof. dr. A. Amelink, beste Arjen, je bent toch wel een beetje mijn derde co-promotor, met name in de eerste fase, en mede-initiator van mijn proefschrift. Dank voor je kritische blik, je scherpe vragen en de leuke gesprekken. Ik kijk met plezier terug op mijn eerste wetenschappelijke presentatie op het Phototonics Event in Eindhoven, waar jij me voor had uitgenodigd.

Geachte dr. B.N.G. Giepmans en A.H.G. Wolters, beste Ben en Anouk, ik heb onze samenwerking, ondanks de afstand tussen ons in, als heel fijn ervaren. Dank voor het verwerken van alle bipten. Deze hebben tot een mooi hoofdstuk in, en een mooie omslag om dit proefschrift geleid.

Beste Rens, dank voor jouw bijdrage aan dit proefschrift. Wat begon als een supervisor/student-relatie eindigde als bevriende collega's. Ik heb je ervaren als een zeer gedreven, leergierige en sociale onderzoeker. Ik heb genoten van onze gesprekken en jouw culinaire creaties. Op naar jouw boekje.

Dear Yue, despite the fact that we've never met in person, I have enjoyed our collaboration. I still find it remarkable to work on a scientific study together with colleges from the other side of the Atlantic Ocean. I wish you all the best with the completion of your PhD.

Beste Steffi, fijn dat wij onze interesses en vakgebieden hebben kunnen verenigen in een vruchtbare samenwerking, die weer het begin was van jouw SCOPE-studie. Veel succes met het afronden van jouw proefschrift.

Alle overige co-auteurs van dit proefschrift wil ik ook enorm bedanken. Ik zie dit boekje als een echte teaminspanning. 36 auteurs, verdeeld over 16 afdelingen, verdeeld over 6 instituten. Zonder jullie samenwerking was dit proefschrift er niet.

Beste paranimfen, beste Quinten en Sjoerd, het doet me goed jullie schuin achter me te hebben staan tijdens de verdediging van dit boekje. Q, jouw pure, persoonlijke interesse in gezondheid en wetenschap, en Sjoerd, jouw observerende en explorerende stylo werken altijd inspirerend.

Beste Wei, PhD roomie, ik heb een leuke tijd gehad met jou als kamergenoot. We hebben veel met elkaar gelachen als compensatie voor het serieuze werk. Helaas heeft onze olijfboom het niet gered, maar de blauwe bank wordt nog steeds gebruikt.

Beste kno-onderzoekers en –assistenten, dank voor de leuke tijd die ik met jullie heb gehad. Ik denk met plezier terug aan de vele lunches, borrels, fietstochten, weekenden, ski-reizen en congressen. Simone, je staat er goed op in Hoofdstuk 4.

Beste Jochem en Kasia, bored pandas, jullie waren altijd altijd een fijne afleiding tijdens de soms wat minder enerverende onderzoeksdagen (ook die zaten ertussen). Ik heb genoten van onze koffie-pauzes (thee mag ook) en etentjes bij elkaar thuis. Jochem, bijzonder dat wij op hetzelfde huisartsenpad terecht gekomen zijn en sinds kort ook nog eens burens zijn. Kasia, dank voor je hulp met de planning, het is dan toch goed gekomen. Succes met jouw proefschriftverdediging en je opleiding tot internist in deze heftige tijden.

Geachte dr. F.E.E. van der Does en C.H. Baar-Poort, beste Fer en Corine, wat een geluk heb ik met jullie als mijn opleiders. Dank voor de fijne leeromgeving en voor de ruimte die jullie me hebben gegeven om mijn proefschrift af te ronden naast mijn andere werkzaamheden. Joost, jij ook bedankt voor je bijdrage aan mijn opleiding.

Lieve Ann en Ben, heel erg bedankt voor jullie onvoorwaardelijke vertrouwen en liefde die jullie me vanaf jongs af aan hebben gegeven. Ondanks dat jullie niet alles helemaal begrepen waren jullie bij elke publicatie zo trots.

Lieve Lisanne, je bent een grote steun geweest bij het afronden van dit boekje. In lockdown aan tafel typen onder het muzikaal genot van klophamers en betonboren naast ons was een stuk dragelijker samen met jou. Dank voor het motiveren en relativeren. De kopjes koffie en thee die jij inschonk waren altijd iets lekkerder.

About the author



Oisín Bugter werd geboren op 22 oktober 1986 in Amsterdam. Dat hij later dokter wilde worden stond al op jonge leeftijd vast. Via de 5^e Amsterdamse montessorischool (De Zilvermeeuw) en de 1^e Almeerse montessorischool kwam hij terecht op het Oostvaarders College te Almere. Hier behaalde hij in 2005 zijn Gymnasium diploma. De studie Geneeskunde werd gevolgd aan de Universiteit van Amsterdam. In 2013 werd het artsexamen behaald. Gedurende zijn school- en studententijd werd er ook veel tijd besteed aan sport (o.a. wielrennen, hardlopen) en muziek (viool in orkesten en liefhebberij).

Na het afronden van de studie begon Oisín met werken als arts-assistent thoraxchirurgie in het Erasmus MC te Rotterdam. Al gauw werd er ook begonnen met wetenschappelijk onderzoek bij de kno-afdeling onder supervisie van Jose Hardillo. Dit leidde in 2015 tot de start van dit promotie-onderzoek met Robert Baatenburg de Jong, Dominic Robinson en Jose Hardillo als (co)promotoren. Het onderzoek werd voor een klein deel gecombineerd met klinische werkzaamheden en in 2019 werd er ook voor een korte periode gestart met de opleiding tot kno-arts.

In 2020 werd de overstap gemaakt naar de opleiding tot huisarts (verbonden aan het Erasmus MC). Deze volgt Oisín nu met veel plezier in Rotterdam Kralingen met Ferdinand van der Does en Corine Baar als zijn 1^e-jaar opleiders. Naar verwachting zal hij in 2023 zijn opleiding tot huisarts afronden.

